Planning and Optimisation Methods for Lunar In-Situ Resource Utilisation

Author:
Pelech, Timothy

Publication Date:
2023

DOI:

License:

Planning and Optimisation Methods for Lunar In-Situ Resource Utilisation

Timothy Michael Pelech

A thesis in fulfilment of the requirements for the degree of

Doctor of Philosophy

School of Minerals and Energy Resources Engineering

Faculty of Engineering

The University of New South Wales

February 2023

UNSW is supportive of candidates publishing their research results during their candidature as detailed in the UNSW Thesis Examination Procedure.

Publications can be used in the candidate's thesis in lieu of a Chapter provided:

- The candidate contributed **greater than 50%** of the content in the publication and are the "primary author", i.e. they were responsible primarily for the planning, execution and preparation of the work for publication.
- The candidate has obtained approval to include the publication in their thesis in lieu of a Chapter from their Supervisor and Postgraduate Coordinator.
- The publication is not subject to any obligations or contractual agreements with a third party that would constrain its inclusion in the thesis.

☑ The candidate has declared that **some of the work described in their thesis has been published and has been documented in the relevant Chapters with acknowledgement**.

A short statement on where this work appears in the thesis and how this work is acknowledged within chapter/s:

> The published works are acknowledged in the Publications section in the front matter of the thesis. All co-authors and resources have also been acknowledged in the Acknowledgement section. The publications used in the thesis have been used, modified, re-arranged or expanded within all of chapters to ensure a cohesive thesis is developed.

Candidate's Declaration

✓ I declare that I have complied with the Thesis Examination Procedure.

Abstract

Lunar water resources are expected to be used for space exploration and development in the future. These resources can be used for life support and rocket fuel to reduce the risks and costs associated with lunar settlement. There is a notable gap in literature relating to the planning and optimisation of lunar resource extraction. This thesis aims to address the problem by developing tools for planning and optimisation of In-Situ Resource Utilisation (ISRU) on the Moon, with a focus on H_2O resources.

The multidisciplinary tools currently used in the terrestrial mining industry are examined as possible solutions to fill the gap. However, several issues are identified with the direct transfer of these methods to ISRU. Four foundational areas of mining engineering are then expanded for off-Earth applications. These are geomechanics and modelling, mining system selection, extraction sequence optimisation and project valuation.

For geomechanics, the Discrete Element Method (DEM) is used to determine the stability of regolith excavations on the Moon. This method is also extended to the development of ground engaging tools under lunar gravity. Conceptual proofs are shown for two novel mining systems using DEM, the Impact Excavator and Drill and Pull method. With further development, these new rock breakage systems can improve ISRU planning and optimisation by enabling the access of harder, higher grade icy regolith. Within literature, there are also numerous off-Earth mining systems described. A procedure is developed to objectively select a mining system for a range of possible space resource deposit types. The procedure utilises principles of Axiomatic Design to estimate the reliability of systems in the absence of experimental data. These system reliabilities assist in making selections that can be used as inputs for subsequent planning and optimisation activities.

Traditional optimisation algorithms, such the Lerchs-Grossman pit optimisation method and other graph-based methods are next examined for their applicability to off-Earth mining. They are found to be incompatible when directly applied to ISRU and a new paradigm is developed based on Reinforcement Learning. This method has advantages over the traditional mine optimisation algorithms and solves many of the issues identified for ISRU. For example, it does not require uncertain financial inputs such as cost estimations or price forecasting. This particular weakness in financial inputs for off-Earth mine planning is also addressed for project valuations. An opportunity cost measure, the Propellant Payback Ratio, is shown to overcome many of the difficult input requirements of the traditional

method for the purpose of ISRU project appraisal. It enables ISRU project appraisals to be conducted completely independent of the uncertain financial inputs mentioned.

Overall, the thesis contributes to the expansion of the mining engineering discipline into the ISRU domain. Four interconnected areas of mining engineering are developed including: geomechanics, mining system selection, sequence optimisation and project appraisal. These are all part of a multidisciplinary approach to ISRU planning and optimisation. Although ISRU has so far not begun, the methods and tools developed here can be used to improve the future prospect of resource utilisation on the Moon.

Acknowledgement

Publications

Peer-reviewed journal papers, conference papers and a NASA design competition submission have been used in all chapters except for the Introduction and Conclusion. Some of the published text has been used, modified, re-arranged or expanded within the chapters to ensure a cohesive thesis is developed.

It has been important to expose these published works to a diverse range of peer reviews and inputs due to the multidisciplinary nature of the thesis. This is shown by the various types of journals and conferences that have been chosen to publish, peer-review and discuss these works. The commonality between all of these publications is the space resources related theme.

Four of the published papers are in the peer-reviewed journal *Acta Astronautica* with a CiteScore in the top 15% (Aerospace Engineering); SNIP in the top 17% (Aerospace Engineering); SJR in the top 13% (Aerospace Engineering) and; JIF in the top 16% (Engineering, Aerospace Engineering).

I am the primary author of all the following publications included in this thesis and have contributed greater than 50% to each of these items. Other contributions include conceptual discussions, reviews, writing, editing and supervision.

Peer-reviewed journals

- T.M. Pelech, G. Roesler, and S. Saydam, 2019. Technical evaluation of Off-Earth ice mining scenarios through an opportunity cost approach. *Acta Astronautica*, 162.

- T.M. Pelech, L. Sibille, A. Dempster and S. Saydam, 2021. A framework for Off-Earth mining method selection. *Acta Astronautica*, 181.

- T. Pelech, L. Yao, and S. Saydam, 2022. Planning lunar In-Situ Resource Utilisation with a reinforcement learning agent. *Acta Astronautica*, 201.

- T. Pelech, N. Barnett, M. Dello-Iacovo, J. Oh, and S. Saydam, 2022. Analysis of the stability of micro-tunnels in lunar regolith with the Discrete Element Method. *Acta Astronautica*, 196.

Other publications and works

- T.M. Pelech, A. Dempster, and S. Saydam, 2019, Developing the case for mining resources on the Moon, in: *Proceedings of the Fourth International Future Mining Conference 2019*, AusIMM, Sydney.

- T. Pelech, N. Barnett, M. Dello-Iacovo, J. Oh, and S. Saydam, 2022. Analysis of horizontal opening stability in lunar regolith, in: *Proceedings of the Australasian Ground Control Conference An ISRM Regional Symposium 2022 (AusRock 2022)*, AusIMM, Melbourne.

- T. Pelech, N. Barnett, N. Bennet, J. Sciortino, B. Deng, N. Adams, S. Cannard and others, 2020. The Regolith Tunneller. *Part of the DUExT team submission to the NASA Break the Ice Challenge Phase 1, 2020.*

Contents

List of Figures

List of Tables

Definition of Terms

The following abbreviations are used throughout the thesis.

ΔV – Change in velocity or change in velocity requirement, usually of a spacecraft in orbit of another body such as the Earth or Sun.

DEM – Discrete Element Method. A numerical modelling technique that involves numerous individual particles that can move and interact to transfer physical forces and motions.

GEO – Geosynchronous Earth Orbit. The orbital altitude above the Earth where a satellite orbits at the same angular velocity as the Earth's rotation, approximately 36 000 km above the Earth's surface [172].

ISRU – In-Situ Resource Utilisation. The generation of consumables from raw materials found on the Moon or other planetary bodies [55] for use in autonomous or human activities at or nearby the same location.

ISWS – In-Situ Water Sublimation. A mining system that involves directly heating icy regolith or another volatile resource to sublimate and collect water vapour.

LEO – Low Earth Orbit. The orbital zone around the Earth that is closest to the atmosphere with an altitude ranging from 200 km to 1600 km [257].

NEO – Near-Earth Object. Asteroids or comets in a solar orbit within 1.3 Astronomical Units (AU) from the Sun, where the Earth orbits at 1.0 AU from the Sun [119].

NPV – Net Present Value. A project evaluation tool designed to guide investment decisions by discounting the value of future revenues and costs by assigning a time-dependant discount factor [305].

PSRs – Permanently Shadowed Regions. Areas on the lunar surface that are never lit by the Sun. These are usually found in craters on the poles, where the angle of incidence of sunlight causes the depths of the craters to be in permanent shadow. These areas exhibit very low and stable temperatures compared to other areas on the lunar surface, and have been shown to contain volatiles in mineral deposits [17, 117, 273].

RL – Reinforcement Learning. An optimisation algorithm that makes use of an agent, capable of taking actions and receiving rewards in an environment. The agent progressively learns to maximise rewards and converges to an optimal solution.

SRU – Space Resource Utilisation. The use of natural resources from the Moon, Mars and other bodies for use in-situ or elsewhere in the Solar System [114]. This is a broader term to In-Situ Resource Utilisation, where resources are not necessarily used at the same location.

TRL – Technology Readiness Level. A ranking that describes the state of a given technology and provides a baseline from which maturity is gauged and advancement pathways can be defined [137].

UCS – Uniaxial Compressive Strength. An experimentally derived measure of material strength. The maximum stress a standard rock sample withstands under compression prior to failure when no confining pressure is applied.

The following technical terms are used for describing the novelty in this thesis.

Mine Planning – The engineering process required to extract a mineral resource. The mine plan includes aspects of geomechanics, economics, scheduling and various types of engineering such as mechanical, electrical and more.

Mine Optimisation – The process of improving a mine plan towards an optimal outcome. Various methods and algorithms can be used for this process.

Mining System – A set of tools or equipment that can be used in combination to access and extract mineral resources.

Mining Method – A specific technique used to apply a *mining system*. The difference between a *mining method* and a *mining system* is based on how the equipment is applied in different geology and geometry. For example, a truck and shovel is a *mining system*. Strip mining and open pit mining are two *mining methods* used to apply a truck and shovel. Strip mining is the act of removing long strips of waste material to progressively uncover a continuous, shallow seam of ore. Open pit mining requires the removal of waste and ore via benching and pushbacks for an ore body that extends downwards rather than laterally.

Off-Earth Mining – An broad term referring to ISRU, SRU and any mineral extraction not on the Earth. This also includes mining asteroids, for example, to sell commodities at a profit into terrestrial markets and more.

The following technical terms used in the terrestrial mining industry are also employed in this thesis.

In-situ stress – Stress in a rock in its original in-ground state, prior to any excavation.

Mineral Resource/Resource – A geologically significant concentration of a mineral that has potential to be considered as *ore* after further engineering studies [134].

Ore Reserve/Ore – The portion of a *mineral resource* that has a viable market and positive economic value to extract with known systems [134]. In this thesis and the ISRU sense, the term refers to a *mineral resource* that will be utilised off-Earth with known engineering solutions. It should not be considered waste after applying a *cut-off grade.*

Grade – The concentration of a desired mineral inside the surrounding material. In this thesis *grade* is measured in units of kg H_2O per of kg lunar regolith or % by mass.

Cut-off Grade – The boundary grade between *ore* and waste. As shown in Chapter 6 it is defined by a method of iterative resource extraction modelling taking into account the ISRU system capabilities, size and distribution of the *mineral resource,* extraction sequence and equipment reliability.

Ultimate Pit Limit – The largest possible economically extractable open pit, using traditional mine planning methods [204].

Pushback – A temporal open pit expansion aimed at achieving access to covered *ore* while minimising the waste movement requirements.

Some important terms used in the field of reinforcement learning are also defined below.

Agent – A series of computational functions, usually including a neural network that learn to observe, take actions and maximise rewards from an environment.

Training – For Reinforcement Learning, the process in which an agent repeatedly acts through and experiences environments (takes actions, makes observations and receives rewards) in order to improve future actions.

Hyperparameter – A high-level parameter that controls the machine learning process.

Episode – A full trajectory of agent actions, observations and rewards between the initial state and terminal state of an environment.

Generalisation – The ability of an agent to adapt to a range of problems wider than the training experiences provided.

Architecture – A unique formulation of a Reinforcement Learning algorithm including any optional pre-processing or post-processing steps as used by Sutton [286].

Chapter 1

Introduction

1.1 Motivation and Research Gap

Space exploration is considered important to the future development of our civilisation [54, 211]. One of the main limitations to this is the significant cost of transporting terrestrial resources to the desired location in space. Fortunately, it has been shown that finding and extracting resources in space can significantly reduce the costs and risks associated with space activities [54, 233]. Utilisation of off-Earth resources is therefore expected to act as a catalyst to further advancement of the space economy [54, 109, 254]. The earliest form of off-Earth mining is likely to be in the form of In-Situ Resource Utilisation (ISRU), where resources are extracted and used at, or very near to a base of operations.

The ISRU paradigm poses some new challenges for traditional mine planning and optimisation methods. The majority of terrestrial mining operations are planned and optimised with a multidisciplinary set of tools [62, 116], ranging from economics to geology to mechanical engineering and more. Examples can be given such as the determination of excavation stability using numerical modelling [79], selection of equipment based on proven mechanical capabilities in the appropriate style of geological deposit [213], and optimisation of extraction sequences using *cut-off grades* and system specific practical constraints [116].

The problem for ISRU is that the traditional methods used for planning and optimisation are not directly transferable from terrestrial mining engineering. The transfer issues include the very little geological, geotechnical and economic data or modelling available for space resources. This deficiency means it is illegitimate to begin a resource optimisation study of a particular deposit with traditional methods. Furthermore, there are no proven examples of a working ISRU operation or equipment, making selection of an optimal mining system difficult. Almost no literature has been written on the means to plan and optimise such an operation either. As ISRU operations are most likely to be autonomous or remotely operated, this unleashes various new technological possibilities for the new planning and optimisation methods required. Possibly the most important difference between ISRU and terrestrial mining engineering is that the optimisation goal of ISRU is not necessarily to make a profit, but instead to reduce risks and costs for other space activities such as lunar settlement.

Due to these broad issues, there is a significant gap between terrestrial mining engineering tools and the requirements of ISRU planning and optimisation studies.

1.2 Aim and Objectives

The aim of this thesis is to develop methods and tools to enable the planning and optimisation of In-Situ Resource Utilisation (ISRU) operations on the Moon. In doing so, the thesis will expand the mining engineering discipline to the domain of off-Earth In-situ Resource Utilisation. This thesis focuses on volatile water resource extraction but the methods and concepts developed can be applied to any type of resource. The problem is complex and multidisciplinary, not all aspects can be completely addressed within this thesis. The limitations of PhD research, and the effects of laboratory facility closures during the pandemic have encouraged a multifaceted approach to the problem, similar to terrestrial mining engineering. The broad approach will yield many recommendations for future research on topics that are necessarily placed outside this work. Hence, the following objectives are set to rationalise the scope of this thesis.

1. Develop a rapid and low-cost technique to demonstrate ISRU equipment designs and show proof-of-concept.

2. Collate and develop conceptual equipment designs that can be used for subsequent planning and optimisation.

3. Identify areas of deficiency or improvement when applying traditional mine planning methods to ISRU.

4. Resolve any deficiencies for ISRU planning and optimisation.

5. Demonstrate usage of the novel ISRU planning and optimisation methods.

1.3 Thesis Outline

This thesis has been arranged into the *Introduction*, *Background*, five technical chapters and a final discussion and conclusion chapter. The research objectives are tabulated against each relevant chapter in Table 1.1. A conceptual map of the thesis can be found in Figure 1.1. Each chapter progressively builds on the interdisciplinary capabilities needed in later chapters. The map shows how some Interdisciplinary Enablers are closely related to traditional mine planning and optimisation, while others are further afield from the discipline.

Table 1.1: Objectives by chapter.

Chapter	Short Title	Target Objectives
Chapter 2	Background	#3
Chapter 3	Modelling Geomechanics and Excavation	#1 & #5
Chapter 4	Off-Earth Mining System Concepts	#5 & #2
Chapter 5	Off-Earth Mining System Selection	#3, #4 & #5
Chapter 6	Extraction Sequence Optimisation	#3, #4 & #5
Chapter 7	ISRU Project Appraisal	#3, #4 & #5
Chapter 8	Conclusion and Future Work	All

Chapter 2 – Background defines the domain of the thesis and the current state of knowledge. This chapter will be used to *identify areas of improvement or deficiency when applying traditional mine planning methods to ISRU*. Each of the following technical chapters

3
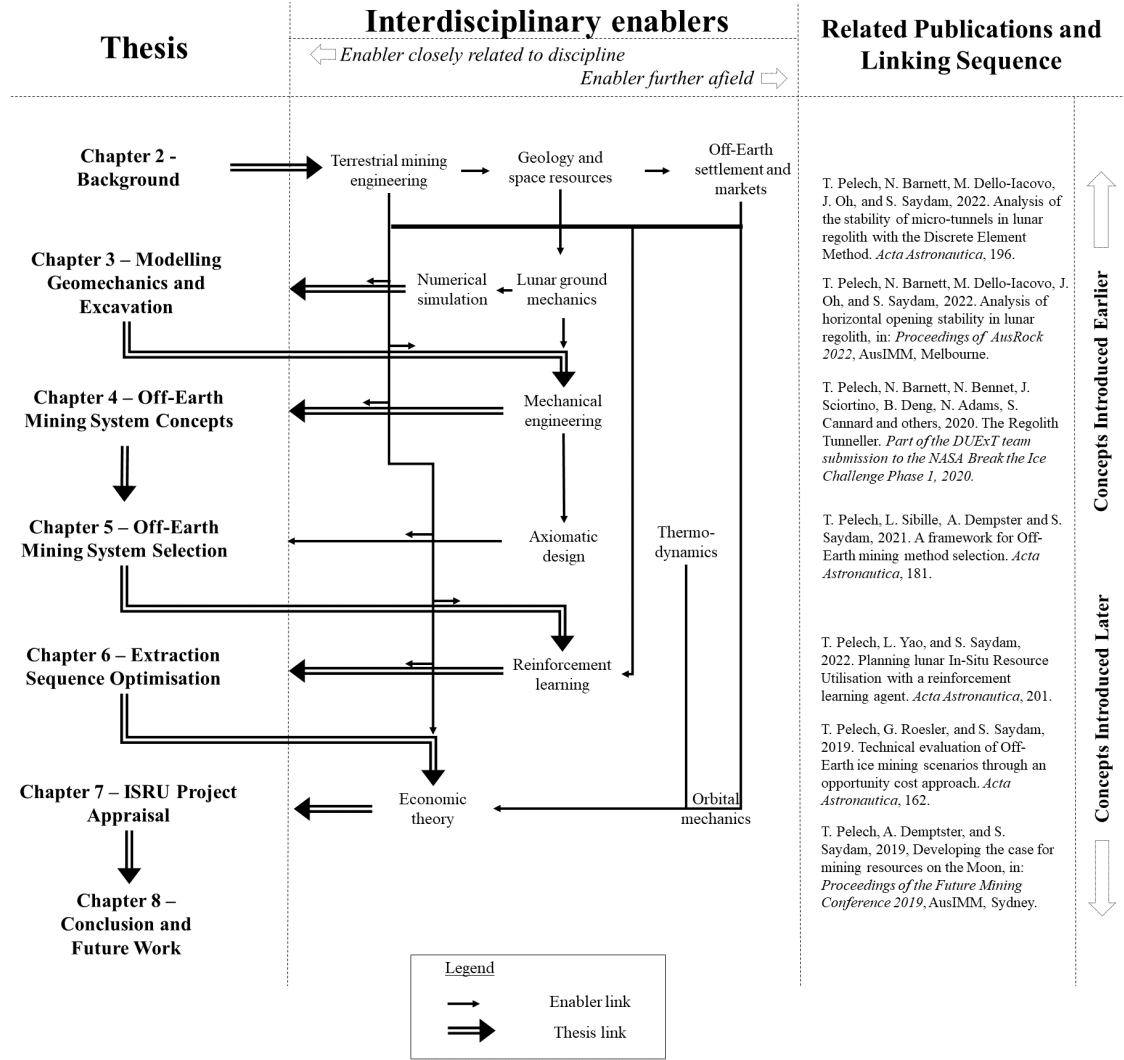
Figure 1.1: Thesis chapters and enablers map.

has its own specific literature reviews relevant to the contributions of that chapter. The *Background* chapter aims to appropriately situate the thesis as an addition to the limited off-Earth resource extraction planning and optimisation literature, and as an expansion of the mining engineering discipline into the Space Resource Utilisation domain.

Chapter 3 – Modelling Geomechanics and the Excavation of Lunar Regolith introduces the usage of the Discrete Element Method (DEM) in lunar regolith *as a rapid and low-cost technique to demonstrate equipment designs and show proof-of-concept.* This chapter is relevant to the following chapters and the thesis, as it demonstrates a method for

assessing excavation in lunar gravity and ground conditions. This can be used to define equipment capability constraints for system selection and extraction sequencing methods proposed in later chapters.

Chapter 4 – Lunar Mining System Concepts describes some *equipment designs that can be used for subsequent planning and optimisation.* The excavation modelling introduced in Chapter 3 is applied to show proof-of-concept for these designs. Various other mining systems have been collated from literature which will be used in the subsequent chapters.

Chapter 5 – Off-Earth Mining System Selection develops a procedure for categorising and selecting the preferred mining system from Chapter 4 for an array of possible geological deposit types. Mining systems will have differing capabilities and constraints and the selection of a system is critical to any further analysis and optimisation. By selecting an appropriate unique mining system, this procedure can also help to define extraction sequencing constraints for the following two chapters.

The method in *Chapter 6 – Extraction Sequence Optimisation with a Reinforcement Learning Agent* is also one of the key theoretical contributions of this thesis. Traditional *cut-off grade* theory, used in terrestrial mining, is advanced in this chapter. The techniques, data and systems developed in the previous chapters can also be used in conjunction with this method to achieve optimal efficiency in desired aspects of resource extraction. The proposed method is specifically designed to *resolve issues identified when transferring traditional mine planning methods to ISRU.*

Chapter 7 – ISRU Project Appraisal with Uncertain Inputs demonstrates how to assess an ISRU project with significant financial uncertainties that are common for space activities. The required inputs for this chapter are related to the works in previous chapters including appropriate mining systems, the use of an extraction sequence and various physical parameters such as excavation forces in regolith.

Finally, *Chapter 8 – Conclusions and Future Work* is framed as the thesis discussion and conclusion. It consolidates the broad, multidisciplinary contributions in terms of existing

ISRU literature and highlights the implications for the mining engineering discipline. It also proposes further areas for research related to planning and optimisation of off-Earth In-Situ Resource Utilisation.

1.4 Original Contributions

The main contributions within the thesis are the new methodologies proposed for off-Earth mine planning and optimisation. Chapter 3 outlines the calibration and use of the Discrete Element Method for lunar regolith excavation. This method can also be used to demonstrate the effectiveness of new ground engaging tools under lunar gravity as shown in Chapter 4. Chapter 5 develops an ISRU equipment selection procedure based on system complexity, Axiomatic Design [282] and expected reliability. A collection of lunar mining systems from literature are also assessed using this new procedure. Chapter 6 applies Reinforcement Learning (RL) techniques to the optimisation problem of resource extraction sequencing. This resource extraction optimisation method can also be applied in terrestrial mine planning scenarios. Finally, Chapter 7 demonstrates a process for economic appraisal of off-Earth resource extraction projects without the need for making assumptions on highly uncertain costs and market prices.

Empirical contributions are made in Chapters 3 and 4 in the form of results of calibration and modelling of dry lunar regolith for different styles of excavation.

Some theoretical contributions are also made in this thesis. Chapter 4 develops some novel excavation and rock breakage concepts in addition to supporting experiments and modelling. Chapter 5 proposes mining strategies for when H_2O extraction is limited by the energy intensive water sublimation or vaporisation stage. This has implications for Chapter 6 and 7 where optimal extraction sequences and *cut-off grades* are demonstrated to greatly improve the economic competitiveness of an operation. Chapter 6 also develops traditional resource *cut-off grade* theory by enabling rapid scenario testing with trained RL agents. Finally, Chapter 7 proposes that the opportunity cost, in the form of various

Propellant Payback Ratios can be used as a primary indicator of economic competitiveness for ISRU operations when there are significant financial uncertainties.

This is the first substantial piece of work done in the field of ISRU planning and optimisation. There are several original multidisciplinary contributions throughout this work. When taken as a whole, the thesis is intended to expand the mining engineering discipline into the space resource domain.

Chapter 2

Background

2.1 Context

There has been a renewed interest in lunar exploration in recent times as the International Space Station nears the end of its life [41]. The Artemis program is an example of NASA's latest plan for developing a sustainable presence on the Moon, with the goal to develop space resource utilisation technologies for exploring Mars and beyond [13, 270]. This chapter will provide background information and justification for the use of space resources. It will also define the state of off-Earth mining related research and begin to identify areas of improvement when applying traditional mine planning methods to ISRU according to Objective 3 of the thesis.

Several international contributions to the Artemis program are planned from Japan, Korea, Canada, Australia and the European Space Agency to name a few [56]. In-Situ Resource Utilisation is a priority for the Artemis program, and the strategy explicitly includes the demonstration of an ISRU system [246]. The Volatiles Investigating Polar Exploration Rover (VIPER) is an example of an Artemis mission planned in 2024 to map potential volatile resources sites on the lunar South Pole for future use [48, 56].

The European Space Agency (ESA) itself has released a strategy on space resources to

2030, with the specific goals to map out resource deposits on the Moon and demonstrate the production of water or oxygen on the Moon from local resources [91]. China also has plans to increase space-related research and exploration activities. The planned construction of the International Lunar Research Station on the lunar South Pole in partnership with Russia [131] and research into space based solar power satellites [100, 223] are evidence of this. In terms of space resource utilisation, China is planning to send experimental ISRU equipment to the Moon prior to 2030 [167, 313] and has also identified asteroids as a future target for resource extraction [109].

There is an element of strategic competition between these nations which has echoes of the space race from the 1960s [109]. During the previous space race, an extreme level of government investment was made with the goal of being the first country to put people on the Moon. Reportedly $25.8 billion USD was spent on Project Apollo, more than half of NASA's budget at the time. Adjusted for inflation, the Apollo program averaged $31 billion 2020 USD per year, greater than the entire NASA budget at any other point in history [76]. It is believed that even more was spent on the Soviet space program [88].

The parallel between the 1960s space race and the present may not be any more than strategic rhetoric [165]. But, there is clear evidence of another type of space race currently underway. Private enterprises such as Elon Musk's SpaceX and Jeff Bezos's Blue Origin have their own plans for development of the Moon and Mars. This has been called the billionaire's space race by some [93], which is supported by space technology privatisation strategies at NASA, in Luxembourg and elsewhere [297]. Furthermore, these two companies are not the only participants. Numerous other private companies have also stated intentions to develop space access or space resource utilisation technology or both. Notable mentions include United Launch Alliance [19], Boeing, Lockheed Martin, iSpace [154] and Richard Branson's Virgin Galactic [166].

Table 2.1 is a combined summary of the expected timeline of resource utilisation outlined in strategies published by NASA [175, 245, 246], ESA [91] and the Luxembourg Space Agency (LSA) [182]. It has been mentioned in presentations by NASA personnel [175, 245, 246] that oxygen derived from regolith minerals will be the first example of ISRU in space. This

is mainly due to the low comparative risk in locating and collecting appropriate regolith resources on the Moon. The process is energy intensive however, and once polar volatile deposits are unlocked and infrastructure is built nearby, they will become the favoured type of mineralisation for resource utilisation. It is agreed by all of the reports that production of both O_2 and H_2 will be initially valuable. This is to reduce the costs and risks of providing rocket propellant and life support systems on the Moon. The second obvious trend across all of the reports is that certain types of resource only become available after the mining, processing and utilisation technologies mature sufficiently, hence the delay in some of these applications and the importance of early government investment.

Table 2.1: Expected timeline of Space Resource Utilisation collated from NASA [175, 245, 246], LSA [182] and ESA [91].

Time Horizon	Resource	Source	Applications
5-10 years	Oxygen bound in Regolith	Moon	Rocket Fuel, Life Support
10 years	Water	Moon	Rocket Fuel, Life Support
15-20 years	Water	Asteroids	Rocket Fuel, Life Support
15-20 years	Raw Regolith	Moon, Mars	Infrastructure
>20 years	Metals	Moon, Asteroids Mars	Infrastructure, Equipment
>20 years	Precious Metals	Asteroids	Sale in terrestrial market

2.2 Geology

2.2.1 Solar System and Comet Formation

This thesis will intentionally omit much of the detail around off-Earth geological formations and modelling as there is currently not enough data to make certain conclusions. The important geological inputs required for mine planning tasks in this thesis will be replaced by assumptions. It is therefore important for readers to have a brief overview and understanding of space and lunar geology which form the basis of these assumptions.

The prevailing theory on the origin of the solar system is based on the observation that all the planets and main belt asteroids have low inclination orbits from 0° to 35° and orbit in

the same direction around the Sun [157]. The theory proposes that during the formation of the solar system a proto-planetary disk of dust particles and gas surrounded the Sun. These particles accumulated in a process called nucleation [72] into progressively larger pieces called planetesimals and eventually the asteroids, moons and planets themselves [3, 314].

Comets are formed from the accumulation of icy planetesimals, mostly consisting of small fragments of amorphous water ice [3] in the outer solar system. An analysis of the comet Hale-Bopp suggests the nucleus consists of around 35% water, with 7% CO_2, 13% CO and 45% dust [27]. This analysis was conducted from observing the tail spectrum versus distance from the Sun. Other sources indicate the abundance of H_2O to be around 80% of the mass of a comet [89]. Figure 2.1 illustrates the structure of a comet nucleus which has been developed from the planetesimal nucleation theory [27, 314]. It is supported by observations of surface emissions and structures from spacecraft flybys, the Deep Impact probe [224] and long range observations [271]. DeMeo and Binzel [67] survey the near-Earth asteroid population and highlight potential candidates for dormant comets, covered in an insulative dust layer which have made their way into the inner solar system through gravitational perturbations.
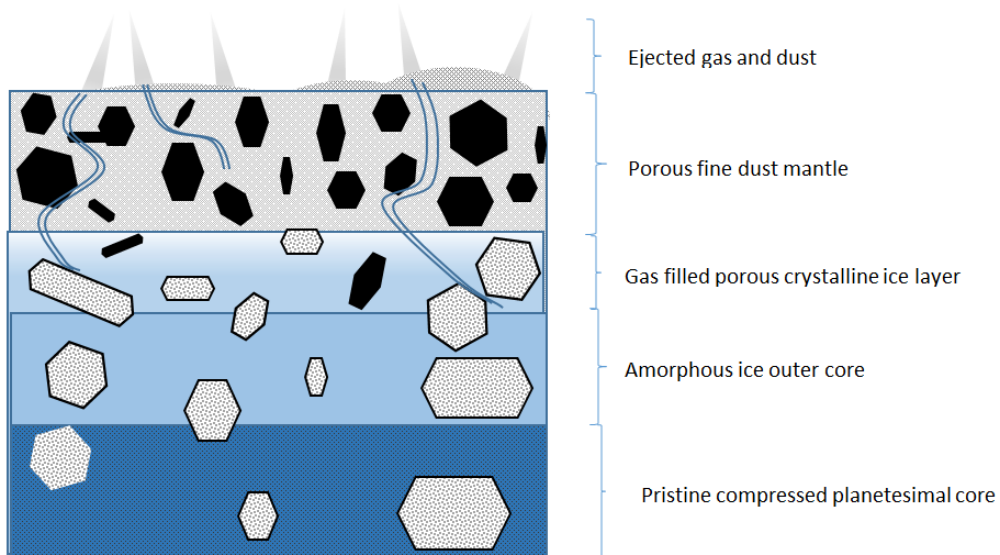
Figure 2.1: Structure of a comet nucleus after Brandt and Chapman [30].

2.2.2 Geology of The Moon

Currently the most plausible explanation for the formation of the Moon, is a giant collision of two planetesimals early in the history of the solar system. The proto-Earth and another Mars-sized object collided to form the present masses of the Earth and Moon system [16]. Modelling of this event has been carried out by several authors to match observations of the mass, mineralogy, isotopic composition and orbital properties of the Moon in support of the theory [8, 16, 37]. Over time, the Moon has undergone several stages of geological change including volcanism [274] and asteroid bombardment [241], although without the atmospheric weathering conditions important on Earth. This leads to the present-day lunar surface characterised by the highland crust and mare basins of basaltic regolith [111] marked by varying degrees of impact cratering and volcanic features. In some of these darker craters at the poles, volatile ices have been detected [11].

The LCROSS mission utilised an impactor probe which strongly suggests the presence of water ice in a southern polar crater named Cabeus. Analysis of the impact dust plume suggests the concentration of water in the upper layers of this crater's regolith to be 5.9% $\pm$ 2.9% by volume [17, 117]. Independent evidence of lunar polar ice in Permanently Shadowed Regions (PSRs) has been detected by using combinations of the Diviner radiometer, a Laser Altimeter (LOLA) [96] and the LAMP ultraviolet reflectance detector [120] on the Lunar Reconnaissance Orbiter and the Moon Mineralogy Mapper (M^3) near-infrared spectroscopy instrument on the Chandrayaan-1 lunar orbiter [171].

Three main geological processes are postulated to have delivered ice to the surface of the Moon. There is still some debate about the relative importance of each of these items [36], These delivery mechanisms are:

- ongoing impacts from asteroids, comets and micro meteoroids [240, 275];

- previous volcanic out-gassing during the Moons geological history [36]; and

- ongoing implantation of hydrogen from the solar wind [11].

Evidence of similar polar crater ice deposits are found on both Mercury [240] and the dwarf planet Ceres [159]. These are likely to have been deposited by the same geological processes to those evident on the Moon.

Lunar regolith covers a large portion of the surface of the Moon. Seismic measurements taken at the Apollo landing sites show that the soil there ranges in depth from 3.7 m to 12.2 m in depth [174]. This depth is expected to greatly increase within a crater basin due to gardening and slumping effects [277], as shown in Figure 2.2. Lunar regolith is created by impact gardening, when meteoroids break the crust of the Moon and redeposit it over geological time [17].
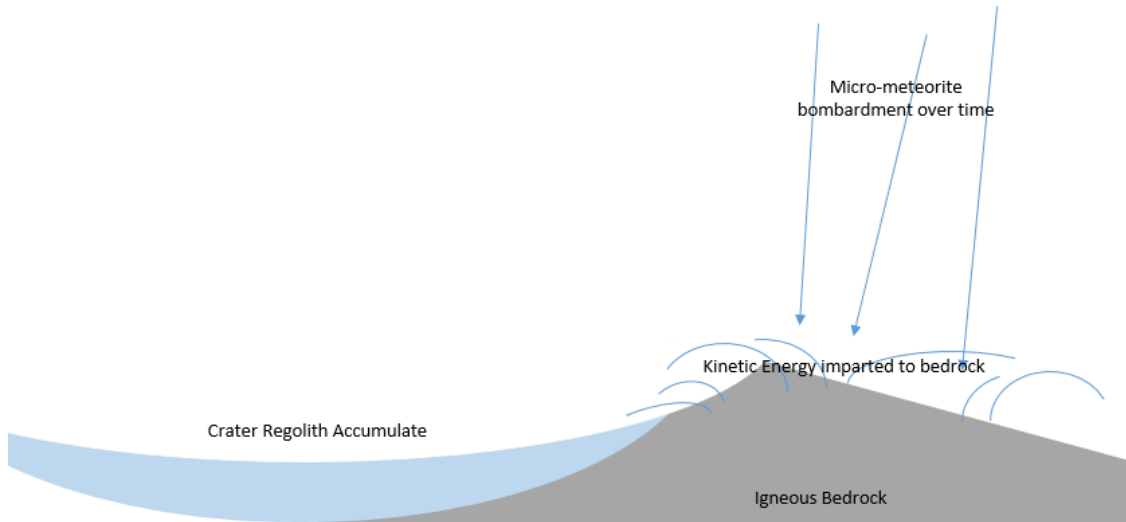
Figure 2.2: Sedimentary effect in crater basins after Lindsay [174].

These geological paradigms will be used in subsequent chapters to postulate potential H_2O *Mineral Resources* on the Moon that could be available for utilisation.

2.3   Lunar Resources

Various material resources available on the Moon have been detailed in a broad review by Crawford [54] and in other works [11, 233]. In the near term, ISRU operations supplying

a nearby settlement are expected to dominate rather than mining operations aimed at selling a product into another market. This is described in Table 2.1. ISRU operations will aim to extract useful materials for life support and basic construction nearby such as:

- volatiles including water;

- ilmenite in regolith; and

- regolith itself.

These three resources can be used to provide oxygen for life-support and rocket propellant. Ilmenite ($FeTiO_3$) can be reduced by a hydrogen reduction process to produce water, which in turn can be electrolysed to recover hydrogen and oxygen useful for both life support and rocket fuel [54]. Regolith can also be used to produce oxygen from molten electrolysis [260], although this is very energy intensive. If ilmenite and regolith are the only available ISRU resources, a stock of hydrogen must be transported from Earth or elsewhere to enable its use as propellant [11]. It will likely be more energy efficient to recover the H_2O directly from icy deposits, however these are thought to be only located in cold traps such as the PSRs mentioned above. Raw lunar regolith can also be used for radiation and micrometeoroid shielding [11] and construction of protection bunds for launch pads.

Other resource types will become accessible after off-Earth mining technology is further developed. These more advanced resources are in line with what is considered mining on Earth today. These materials of potentially longer term economic interest on the Moon according to Crawford [54] include:

- nanophase iron in regolith;

- meteoritic siderophile metals such as nickel, gold and Platinum Group Metals;

- industrial metals such as aluminium and titanium;

- important technology manufacturing feedstocks such silicon and Rare Earth Elements;

- nuclear energy minerals such as uranium; or

- Helium-3 depending on nuclear fusion technology advancements; and

- other possibilities yet to be discovered.

These advanced manufacturing materials are found in varying concentrations in different locations on the lunar surface due to geological process. For example, it is postulated that previous and ongoing impacts of metallic asteroids on the lunar surface have created localised areas of enriched metal concentration. These can be identified by magnetic signatures from higher concentrations of iron in the regolith as shown by Wieczorek [307].

It is important to realise that all of the elements available naturally on Earth are also available on the Moon due to their similar origins in the solar system. However, differing geological processes occur on the Earth and Moon. Therefore, the quantity, concentration and the type of *mineral resources* are different [54].

2.4 Mine Planning and Optimisation

2.4.1 Fundamentals of Mine Planning

Terrestrial mine planning and optimisation is founded on multidisciplinary technical tools outlined in the SME Mining Engineering Handbook [62] and more. Some of the most important are itemised below. A short discussion on each item with respect to this thesis is included in this section. The order of these items has been arranged into a commonly used flow for terrestrial mining feasibility studies shown below.

1. Commodity market price forecasting.

2. Geological exploration and resource estimation.

3. Geomechanics and modelling.

4. Mining method selection.

5. Infrastructure and services design and construction.

6. Mineral processing.

7. Economic decision making including extraction sequencing.

8. Protection of the environment, societal issues, health and safety.

9. Project valuation and appraisal.

A feasibility study addresses each of these items as part of an iterative assessment of a mining project prior to investment [62]. The same flow has been used as the blueprint for structuring this thesis. These terrestrial mine planning tools can be developed for use in space resources, although some are too broad or too uncertain to detail in subsequent chapters here. This thesis's objectives target items 3, 4, 7 and 9 as areas that can be advanced specifically for off-Earth In-Situ Resource Utilisation, expanding the foundations of mining engineering into the space resources domain.

2.4.2 Market Price Forecasting

Market price forecasting is risky and prone to error in the best of circumstances. The price-time series of a globally significant commodity such as oil for example, is characterised with high levels of periodic volatility [115]. Extensive efforts are made in industry and academia to accurately forecast commodity prices, however the success of each individual technique varies depending on the commodity and the selected input data [115]. Mining feasibility studies proceed nonetheless, usually with some form of sensitivity or options analysis at the end to demonstrate the risks of price forecasting [70]. One factor working in the favour of terrestrial mining companies over the last few decades has been the general

decline in production costs due to technology improvements. It is observed that due to this and increasing commodity scarcity in terms of lower-grade deposits being mined, even sub-economic resources should eventually become valuable [62]. The space economy is different at this point in time. Without any previous examples or existing market data, it is not currently possible to predict off-Earth commodity prices with any degree of accuracy. Since price assumptions are key inputs into mine planning, these methods will not work for ISRU. For this reason, this thesis offers alternative planning methods in Chapters 6 and 7 that do not require market price forecasting.

2.4.3   Geological Resource Estimation

Geological exploration and resource estimation forms the base input into any physical mine plan. A well informed resource model allows engineers to identify and prioritise target areas for economic extraction. The methods used in resource modelling are well developed for terrestrial mining, involving various data inputs, geostatistics, specialised model parameters for each deposit, and a regular validation process [239]. All of these methods are easily transferable to space resources. The main limitation is the current availability of input data, although this has been recognised in the space resource strategies outlined by NASA [175, 245, 246] and ESA [91]. Terrestrial mine versions of these models typically require hundreds, if not thousands of data samples from the deposit and an educated interpretation of the structure and size of the mineralisation.

Lunar resource modelling using modified terrestrial resource estimation techniques has recently been shown by Cannon and Britt [36]. A novel Ice Favourability index was implemented in this work to improve results, albeit with very limited geospatial data. Geological modelling is a large area of study and will continue to be developed as long as there are more deposits and data to model. As there is currently not enough data available to produce any realistic and useful models for ISRU planning and optimisation, this area will not be further developed in this thesis. Random or fictitious geological models based on current understanding and assumptions will be used instead to demonstrate the

planning and optimisation methods in the following chapters.

2.4.4 Geomechanics and Modelling

During the mining process it is necessary to understand and control the stability of excavations, waste storage dumps and stockpiles. Ground control reduces unplanned operational delays and damages to equipment from rockfalls or collapses. It is also crucial to understand rock breakage and excavation properties of the *mineral resource* and surrounds to plan a mining project. All this information can be used in mining method selections, and hence place constraints on feasibility studies and optimisations.

There are mature modelling methods available for geomechanics studies in the mining industry today, including variations of the Finite Element Method (FEM), the Discrete Element Method (DEM) and hybrids of both. The Finite Element Method is a continuum-based method, where a network interconnected nodes is used to represent a continuous rock mass. Adjacent nodes are used to pass stress and displacement calculations throughout the network and resolve a solution. This method is unable to model larger displacements, for example when nodes may change their relative arrangements. It is also not ideal for highly fractured materials, although there are more advanced variations of FEM which enables this [79].

In the Discrete Element Method, the material is represented by numerous discrete shapes that can move and change location under certain conditions. Interactions based on proximity at each time-step are identified between discrete elements to pass forces and motions throughout the simulation. The Discrete Element Method and its variations are used in the terrestrial mining industry for complex dynamic problems, including block caving, pit wall toppling and mechanical optimisations [79, 101, 279]. DEM has advantages for use in modelling mechanics of space mining scenarios, as the excavation systems can be modelled dynamically for proof-of-concept and optimisation. The use of DEM for modelling ISRU excavation, rock breakage and stability will be shown in Chapter 3 and 4.

2.4.5   Mining Method Selection

Terrestrial mining method selection is usually undertaken by engineers with experience in several different mines and methods. Selections are made during the iterative feasibility study process depending on deposit geometry, geomechanics, and economics. There are also mining method selection procedures specified in literature [192,212,212] which can be used to make a less subjective selection. These are rarely used in practice. Currently, there is no such procedure or experience available for selection of mining systems for off-Earth mineral resources. Instead, non-exhaustive, subjective selections based on an author's limited knowledge, preference or personal works are made as in Kornuta *et al.* [146].

The term *mining method* has not been used to describe the equivalent space resources term in this thesis, instead opting for the term *mining system* selection. A mining method can vary even when using the same equipment, for example an underground stoping mine and block cave mine will utilise approximately the same equipment, but with different geometry, geology and means to break and extract rock [62]. The different means of managing these aspects results in a different *mining method.*

The current state of the art in space resources has not advanced far enough to describe *mining methods* based on extraction geometry. Instead, a mining system selection procedure is proposed in Chapter 5 of this thesis. It is more useful to the current state of the art where the focus is on different types of equipment rather than different types of deposit geometry and geomechanics. These items are still considered in Chapter 5, but in a more generalised manner. Eventually, similar to terrestrial mining, variations of *mining methods* will develop based on geology and geometry. This is touched on in the novel concepts shown in Chapter 4 but more operational demonstrations and analyses are required before establishing *mining method* selection as the norm.

2.4.6 Infrastructure and Services

Various types of infrastructure and services are specifically built for terrestrial mining operations. In many, if not most examples, the remoteness of mine sites from population centres means that everything from roads, railways and power stations to water bores, medical facilities, airstrips and in some cases even ports may need to be constructed to enable the extraction of the deposit. The costs of building or the availability of pre-existing infrastructure can have a significant impact on the final valuation of a project, especially in certain jurisdictions or geographies where difficulty building such infrastructure may turn out to be a fatal flaw [62, 217]. Terrestrial mining infrastructure requirements are somewhat specific to the chosen mining method. For example, underground drilling equipment usually requires provision of compressed air and water while many open pit style drills do not require this support.

Off-Earth mining infrastructure requirements will also be specific depending on the mining system selected. In particular for ISRU operations, a nearby settlement or base would likely share much of the required infrastructure such as power, transport and communications equipment. Infrastructure requirements have been touched upon in Chapter 7 of this thesis and literature [146]. Much more detailed designs would be developed when carrying out the next iteration of a feasibility study or in future research.

2.4.7 Economic Decision Making in Mining

For terrestrial mining operations, medium to long-term (greater than one year) decision making is usually based on an analysis of Discounted Cash Flows (DCF) and related indicators such as the Net Present Value (NPV) and Internal Rate of Return (IRR). Advanced methods are also available for managing the various uncertainties with longer term decision making, such as geological risk and commodity price risk. These methods involve stochastic simulations using a distribution of possible inputs to better understand the risk and expected returns of particular decisions [70, 116].

Shorter term decisions on the time horizon of several days up to twelve months are usually made with specific system optimisation objectives in mind. For these types of decisions, the assumption is made that the mining system and capacity is set. Costs and market prices will also be stable over that period. With these assumptions it is usually beneficial to aim for maximising production within the available resources [62]. Care must be taken when using this system simplification. Decisions should not be made that affect longer term value without consideration [116]. Types of decisions that may be made to optimise operations in the short term include extraction sequence changes and mine design changes perhaps due to economic or geotechnical factors.

With the present low Technology Readiness Level of off-Earth mining systems and the high-level of market price and geological uncertainty, none of the traditional or advanced terrestrial mine decision making methods are applicable. This will be discussed further in Chapter 6 where a new method is proposed for making short and long term economic decisions for ISRU.

2.4.8   Mineral Processing

Mineral processing or beneficiation techniques can be generally divided into two categories: comminution and concentration. Comminution includes rock breakage, crushing and grinding to liberate valuable minerals from waste material. Concentration aims to accumulate the valuable minerals in an output stream by separating the waste particles into another stream [113]. The mechanical and chemical methods used to achieve these aims are specific to each mineral.

Many, or perhaps most of the terrestrial mineral processing techniques will not be applicable to space resources. This is not only due to the different minerals targeted as shown in Table 2.1, but also due to the ubiquity of liquid water in terrestrial processing systems. Almost all terrestrial mineral beneficiation techniques require the use of water at some stage, even if only to control dust [77]. This will likely be impossible for space missions due to the scarcity of water and the difficulty using it in the low temperatures and vac-

uum of space. It is therefore necessary to invent entirely new systems for off-Earth mineral processing. The focus on volatile H_2O resources in this thesis enables a significant simplification of this problem. To achieve the desired product from icy regolith, it is assumed that thermodynamic equations can be used without equipment design. These equations are used as input into the appraisal and demonstration models shown in Chapter 5 and 7. The intricate details of mechanical handling and processing have been left to resolve with future research and development. Here, mineral processing is assumed to simply involve the handling and heating of regolith in order to liberate volatile H_2O gas in near vacuum conditions.

2.4.9   Environment, Society, Health and Safety

All modern terrestrial mining operations must manage environmental and societal issues. Mining is now seen by many people as a dirty, damaging activity that benefits a few people while many others suffer negative externalities [62]. There are numerous examples of mining operations failing to obtain or maintain their social license to operate, leading to disruptive conflict with surrounding communities [40, 215, 217].

Environmental and societal issues related to off-Earth mining have been partially covered in Dallas' thesis [59] and other works [84]. Some societal and environmental issues with space resource utilisation are listed below including:

- terrestrial environmental damage due to chemical rocket launches and landings [60];

- terrestrial environmental or property damage due to re-entry of space junk;

- destruction of areas of potential scientific significance in space, for example geological records;

- destruction of common human heritage in space, for example the visible face of the Moon;

- unequal distribution of returns from space resource extraction ventures [61]; and

- long-term sustainability of use for scarce off-Earth resources [84].

It has been proposed that a method of linking off-Earth mining operations to the UN's Sustainable Development Goals be employed [61]. This ensures the value extracted from space resources is shared with all people, not just those who reach the location first. Other societal and heritage concerns can be addressed in a similar way as done for advanced terrestrial mining operations on Earth, through study, discussion, negotiation and mitigation with stakeholders [61].

Health and safety are also integral components to modern mining operations. Many of the activities undertaken involve some form of physical hazards that require mitigation. The quality and quantity of these hazards are specific to each mine and activity. The scope and detail required to assess the broad range of ISRU hazards requires a depth of technical analysis that must be placed outside the scope of this thesis. However, it is expected that hazards will be risk assessed as per current standards as written in the NASA System Engineering Handbook [137] or practiced at any advanced mining operation around the world [112, 294].

2.4.10   Project Valuation

Finally, the most important output of the terrestrial mine feasibility study is the project valuation. Usually this is reported as discussed in Section 2.4.7 as NPV. A table of annual Discounted Cash Flows and sensitivity analyses can also be used to show more detail.

It is critically important for a mining company to use the same methods and global assumptions across all appraisals when undertaking multiple assessments for potential investments [62]. The end goal is to compare the value of different investment options on equal footing. It is therefore detrimental to have any variance in the methods or assumptions used. This requirement is sometimes hard to achieve within large companies as the individual studies must be divided between different people, with inherent bias.

NPV and other traditional economic decision-making tools are not applicable to ISRU at this stage, due to the uncertainty of financial inputs such as operational costs and market prices. This thesis develops a new method to evaluate relative project values and commence the feasibility study process.

2.5   Key Literature on ISRU Planning and Optimisation

In comparison to the advanced methods available for terrestrial mine planning discussed in Section 2.4, there are not many equivalent methods or even relevant research papers available for space resources or ISRU. A couple of early examples exist, which will be discussed in this section to highlight the research gap.

The Commercial Lunar Propellant Architecture [147] is one of the most detailed papers available describing off-Earth mining. It also follows a structure comparable to a terrestrial mine feasibility study, including many of the points mentioned in Section 2.4.1. There are a few points not detailed in this study, such as economic decision making, extraction sequencing and geomechanics which will be discussed now.

With respect to geomechanics, it is implied that the proposed drilling systems have been tested in appropriate conditions. This is not possible to be certain, as those ground conditions are not yet known and there is still some debate about the level of consolidation of different types of icy regolith on the Moon [36]. It should be noted that even with all the knowledge of ground conditions we have of the Earth, geotechnical assessment is still a critical part of every mine feasibility study. Sometimes poor ground conditions can be the fatal flaw in a project. As it is such an important facet of mining engineering, the modelling of lunar ground conditions will be a focus of Chapter 3 and 4 in this thesis.

The selection of mining systems in this paper is also somewhat subjective, with only three systems considered and the authors referencing their own previous works, the Mobile In-Situ Water Extractor (MISWE) [319], the Planetary Volatiles Extractor (PVEx) [320] and the thermal tent [273]. A more objective mining system selection procedure is required to

attain the best results for a project. This will be the focus of Chapter 5 in this thesis.

It is mentioned in the Kornuta paper [147] that the MISWE [319] and PVEx [320] drilling mechanism are able to undertake a selective mining strategy. This means they have the capability to identify higher concentrations of H_2O using onboard sensors and prioritise those areas. There is no more detail written about the results of those sequence optimisations or how that would be achieved subject to physical and time constraints. This should be included in a terrestrial mining study in the form of scheduling scenarios. Chapter 6 in this thesis proposes a method to enable this type of real-time autonomous sequence optimisation using Reinforcement Learning.

Several important cost and price assumptions are also made to enable the project valuation or business case using the discounted cash flow (DCF) method in the Kornuta paper [147]. The use of DCF weakens credibility of the paper because of the highly uncertain input price and cost assumptions. An alternative method for project appraisal will be shown in Chapter 7 of this thesis, to eliminate the errors that will come when using these assumptions.

Blair *et al.* [26] propose a similar method for analysing lunar ISRU operations including engineering design, market price forecasting, cost modelling and sensitivity analysis. There is also a section describing scenario optimisation. However, like many other papers available on ISRU [19, 135, 147, 176], the focus of the optimisation is on system design and orbital transfers. There is very little detail on the tasks that would be considered mining engineering in the sense of terrestrial extractive industry. The introduction and translation of terrestrial mine planning and optimisation principles to be demonstrated in this thesis will bring another dimension to ISRU research, enabling even further optimisations and value extraction.

There have been few papers written on space resources by people with terrestrial mining backgrounds. Gertsch and Gertsch [105] contributed a conference paper that describes a lunar regolith mining operation using several terrestrial mining paradigms. Equipment selection is briefly discussed, synonymous with *mining system* selection described in this

thesis. Optimisation of the mine plan through production scheduling, mine design and economic decision making is also shown in this paper, albeit with limited detail.

Cox [51] describes the geological data that should be collected prior to planning the mine, then also goes on to discuss options for mining system selection, excavation design and extraction sequencing. This is a short paper that touches lightly on some of the aspects that will be detailed in this thesis.

These four pieces of literature [26, 51, 105, 147] are examples taking similar perspectives to a mining engineer. Many of the authors of the above referenced works have backgrounds in mining, which are reflected in the specific angles they take on the ISRU problem. In contrast, other researchers tend to focus on mission architectures and orbital mechanics [19, 135], mechanical systems design [144, 200, 263] and economic models [259] rather than planning and optimisation of a lunar mine. All these areas of research are important and valuable, but miss a significant opportunity to improve the feasibility of ISRU as done by terrestrial mining engineers. To bridge this gap, much of the work in this thesis builds upon traditional mine planning techniques as described in the SME Mining Engineering Handbook [62] and yields some specialised methods for the particular problem of ISRU planning and optimisation.

Chapter 3

Modelling Geomechanics and the Excavation of Lunar Regolith

3.1 Introduction

Along with geology and economics, geomechanics is one of the fundamental technical components of mining operations. Modelling the stability of excavations is necessary to ensure that resource extraction can be undertaken safely and without delays or losses due to a collapse. Numerical modelling is used extensively in the terrestrial mining industry to determine the stability of various excavations, dumps, dams and stockpiles [79].

One of the potential methods of extracting resources on the Moon is via tunnelling. The basic principles of tunnel design require penetration and removal of a material while maintaining tunnel stability throughout the entire required lifecycle from initial drilling through to abandonment [248]. For off-Earth environments, tunnelling poses additional risks due to the limited available information on regolith and rock formations. Developing an understanding of the potential challenges in lunar tunnelling is also important so that appropriate mining system selections can be made in the future. This will be discussed further in Chapter 5.

This chapter proposes the use of the Discrete Element Method (DEM) as a modelling tool for excavation systems and geomechanical stability on the Moon. As tunnelling is a potentially important part of future ISRU, a tunnel stability case study is used here to demonstrate DEM for this purpose. The case study will demonstrate the utility of DEM under static and dynamic (seismic) conditions and provide some quantitative results in the form of a lunar regolith tunnel stability chart. Importantly, the model in this chapter will be calibrated to various lunar regolith samples from the Apollo missions [39]. This chapter builds towards Objective 1 of the thesis, to develop a rapid and low-cost method to demonstrate ISRU equipment designs. The usage of this method is shown which also complies with Objective 5. The calibrated model will be used in the following Chapter 4 to demonstrate novel excavator designs.

3.2   Literature Review

Tunnel stability is related to the forces acting on particles of rock inducing stresses and movements. When a particle is removed from the rock strata, the mechanical properties and stress state will determine the magnitude of the rock deformation surrounding the void. In cases where the stress is evenly distributed or small compared to the strength of the rock such as isotropic loading, the hole will deform evenly and retain its original shape. However, if the magnitude of the major principal stress is significantly higher than the minor stresses, anisotropic loading, the hole may become unstable and collapse [185, 189].

The Discrete Element Method (DEM) has been developed for modelling granular materials where Newtonian calculations are carried out on discrete particles in each iterative timestep [325]. This can be used as an alternative to continuum-based methods such as Finite Element Method (FEM) [302]. Several programs and codes are available for implementing the Discrete Element Method, including Itasca PFC [128], EDEM and YADE [268]. The open source YADE code has been used in this research.

Aboul Hosn *et al.* [2] have implemented YADE software to model loose soil particles and

validated this against laboratory triaxial compression tests. YADE has been applied to many other material behaviour setups such as impacting cohesive, frictional geomaterials [73] and triaxial tests of sand using various particle shapes and parameters [149].

The calibration and practical implementation of DEM models has been investigated extensively by numerous researchers [47, 63, 149, 295]. The research shows that accurate predictions coming from DEM can only be made if the input parameters are calibrated and validated. There is no standard process for calibration. A common approach, and the method used in this chapter, is an iterative tuning of the particle parameters until a target bulk sample response is met [47].

DEM has been favoured for off-Earth soil mechanics modelling due to the difficulty in obtaining realistic samples and experimental setups on Earth. Lane, Metzger and Wilkinson [160] conducted a review of the appropriate DEM particle shapes and size distributions for simulating lunar regolith. Jiang, Shen and Thornton [130] have further developed a contact model used in DEM for lunar regolith which includes the van der Waals force originating from a very thin layer of adsorbed gas on the particles in the vacuum of space. It has been found that the van der Waals force is an important component of cohesion in lunar conditions. More practical examples include the work done by Nakashima *et al.* [209] who investigated the cutting resistance of lunar regolith using DEM. Cui *et al.* [57] conducted a DEM analysis of regolith excavation cutting resistance in low gravity to determine heat transfer from a rotary drill in the lunar environment. A lunar regolith excavation or sampling tool has also been tested by Liu *et al.* [178] using DEM. They have calibrated their regolith samples using triaxial tests with lunar regolith data similar to the method applied in this chapter.

Tunnel stability has been investigated with YADE DEM in a terrestrial context by Boon, Houlsby and Utili [28]. Their research focussed on terrestrial hardrock tunnelling and ground support with failure caused by discontinuities in the rock, gravitational forces, and *in-situ stresses*. Similar techniques can also be applied for analysing tunnel stability in shallow regolith on the Moon with our current knowledge of lunar material parameters [39]. The following work in this chapter demonstrates this.

3.3 Methodology

3.3.1 Physical Data and Model Inputs

3.3.1.1 Depth Stress and Porosity Model

The *in-situ stress* for lunar regolith has been measured and reported by Carrier, Olhoeft
and Mendell [39] as shown in Equation 3.1. The porosity for lunar regolith samples from
0 cm to 60 cm in depth has been shown to be in the range of 54%-42% [39]. For samples
at greater depth an empirical calculation can be used following Equation 3.1. Porosity,
bulk density, and particle density are physically defined by the following equation in dry
soil.

$$Bulk\ Density = Particle\ Density \times (1 - Porosity) \tag{3.1}$$

The samples are created and checked to ensure that the simulated porosity is close to the
calculated porosity shown in Table 3.1. The modelled empirical equation for the density
of the lunar soil based on observations made by Carrier, Olhoeft and Mendell [39] is shown
in Equation 3.2.

$$Bulk\ Density = 1.92\frac{(z + 12.2)}{(z + 18)} \tag{3.2}$$

Where z is the depth below surface on the Moon.

This is transcribed into Table 3.1 for each respective depth (m). The calculated porosity
is then derived from Equation 3.1. The Column Density is a weighted average of the
Modelled Bulk Density for each incremental depth in the column.

This is then translated to Applied Vertical Stress at the respective depth by applying
lunar gravity (1.62 m/s^2) to a 1 m^2 column of regolith. The Applied Vertical Stress will be
utilised as a parameter in the DEM model as the pressure applied to the top of the sample.

The Expected Horizontal Stress is derived by multiplying vertical stress by the assumed ($K_0 = 0.7$) for lunar regolith as recommended by Carrier, Olhoeft and Mendell [39]. The assumption has been made as it has not been measured previously *in-situ* [49]. This value is an indicator only and will not be directly used in the experiments.

Table 3.1: In-situ stress and porosity model.

Depth (m)	Modelled Bulk Density [39, 266] (kg/m³)	Calculated Porosity (%)	Column Density (kg/m³)	Applied Vertical Stress (Pa)	Expected Horizontal Stress (Pa)
0.6	1777	43%	1777	1727	1209
1.2	1839	41%	1819	3535	2475
2	1869	40%	1845	5978	4185
3	1885	39%	1863	9053	6337
4	1893	39%	1874	12144	8501

3.3.1.2   Target Physical Parameters

Physical parameters for lunar regolith are found in the works done by Slyuta [266] and Carrier, Olhoeft and Mendell [39]. The numerical values used in this research are shown in Table 3.2. Young's modulus has been chosen based on data from lunar simulant JSC-1 testing, the value recorded varies depending on experimental parameters such as Relative Density of the sample and confinement pressure [145]. An upper bound value from these experimental results has been chosen for Young's Modulus for regolith particles in this research. It is known that the friction angle and cohesion values increase with depth and compaction as more closely packed particles have more frictional-cohesive contacts. It is also shown that the van der Waals force from adsorbed volatiles on regolith particles will increase cohesion with increased compaction [130]. For simplicity, however, the range of cohesion and friction angles are taken as the mean recorded value between 30-60 cm for the purpose of this experimental setup as shown in Table 3.3.

Table 3.2: Physical parameters of lunar regolith used in DEM for this research.

Particle Density	3100 kg/m^3 [266]
Cohesion	3000 Pa [39]
Friction Angle	54° [39]
Young's Modulus	90 MPa [145]
Poisson's Ratio	0.25 [266]
Lunar Gravity	1.62m^2/s

Table 3.3: Typical values of the cohesion and internal friction angle for lunar regolith [39].

Depth Interval (cm)	Cohesion (Pa)		Friction angle (°)	
	mean	interval	mean	interval
0-15	520	440-620	42	41-43
0-30	900	740-1100	46	44-47
30-60	3000	2400-3800	54	52-55
0-60	1600	1300-1900	49	48-51

3.3.2 Calibration Method

Experimental parameters have been investigated using a triaxial calibration test to determine their independent effect on the result and carry out fine-tuning of the parameter. The parameters tested for calibration include, mean particle radius, damping factor, friction angle and cohesion. The procedure for selection of each of the material parameters is outlined in this section.

3.3.2.1 Mean Particle Radius

The mean particle size influences output results and the time required to compute. An efficient balance is desired between fidelity of results and computing time. The number of regolith particles simulated by one sphere and hence computational time reduction is approximately proportional to the cube of the particle radius as shown by Equation 3.3 [276].

$$Particles\ packed\ in\ sphere \approx \frac{\pi r_{upscaled}^3}{3\sqrt{2}r_0{}^3} \qquad (3.3)$$

Where $r_{upscaled}$ is the mean radius of the simulated sphere and r_0 is the true regolith distribution mean radius. Scaling from a mean radius around 0.1 mm in true regolith [39] to 12.5 mm reduces the number of particles and computations per timestep by a factor of approximately 1.4 million.

Coetzee [46] has shown that the selection of a particle upscaling factor is dependent on the application and should be chosen carefully as part of the calibration process. The mean particle radius parameter for these experiments has been tested across a range between 2.5 mm and 25 mm using triaxial calibration tests. Table 3.4 shows the macro test results for triaxial test on samples with varying particle sizes in which most of the tests correlate fairly closely to the input parameters. However, it can be seen as the particle size increases the error in the macro cohesion increases. Larger particle sizes reduce the number of stress paths available in the simulation and changes the bulk sample response in the triaxial test, despite all other parameters being held the same [295]. It has been found that 12.5 mm mean particle radius is the maximum that can be used without modifying other experimental parameters for this setup. The particle size chosen for each trial is also dependant on the diameter of the tunnel being tested, where the boundary of the tunnel should have sufficient discrete particles to allow for failures to propagate. A minimum of ten particles across the diameter of the tunnel has been used in this work and has been further outlined in Section 3.3.2.4.

Table 3.4: Calibration sensitivity to particle radius.

Mean Radius (mm)	Damping Coefficient	Input (micro param.)		Output (macro result)		Cohesion Error (Pa)
		Cohesion (Pa)	Friction Angle (°)	Cohesion (Pa)	Friction Angle (°)	
2.5	0.25	3 000	54	3 000	54	0
5	0.2	3 000	50	3 000	54	0
10	0.2	3 000	54	5 000	58	2 000
12.5	0.2	3 000	54	8 000	56	5 000
25	0.3	3 000	54	20 000	56	17 000

Particle clouds were generated using random densely packed positions with a nominal mean radius. The actual radius of each individual particle is taken from a uniform random

distribution +/- 20% of the nominal mean radius. This random distribution ensures that
artificial patterns of particle packing are not developed that could affect the results.

3.3.2.2 Damping Coefficient

When simulating quasi-static samples, it is desirable to dissipate kinetic energy of particles
to counter the introduction of numerical errors and rapidly achieve a steady state [268,325].
The damping coefficient is used for this purpose. It is an artificial modelling tool without
any direct analogue in nature. In some cases, damping has been used to model certain
energy dissipation modes such as plastic deformation [31]. However, it is difficult to
calibrate to an observable phenomenon [325]. A calibration validation of the damping
factor has been conducted by Coetzee [46] showing the results are not sensitive to the
damping factor for static tests. A detailed study of the effect of the damping coefficient on
kinetic energy of the sample has also been conducted by Kozicki, Tejchman and Mühlhaus
[149].

The damping coefficient reduces force transfer between particles via a percentage factor
on each force according to the generalised Equation 3.4 [268]. This is an artificial method
of simulating losses of force transfer in the sample via means such as particle breakage,
friction heat loss and acoustic losses. The factor influences calibration results, effectively
increasing the strength of material as pressure waves are not transmitted as easily, reducing
the number of cohesive and frictional bond breakages.

$$\frac{(\Delta F)_{dw}}{F_w} = -\lambda_d sgn(F_w \dot{u}_w^\ominus) \tag{3.4}$$

Where F_w is the sum of forces that increase particle velocity, $\dot{u}_w^\ominus$ is the mid-step particle
velocity and λ_d is the damping coefficient for particle w and $w \in [x, y, z]$.

The damping coefficient has been used in this research to achieve a steady state for sample
preparation. A damping factor close to zero does not allow the sample to achieve equi-
librium and instead, residual waves propagate throughout the sample and break the weak

cohesive bonds prior to excavation tests taking place. An appropriate damping coefficient has been iteratively determined through triaxial testing to avoid this problem. The lowest, yet still effective damping coefficient for this experimental setup is 0.2.

Figure 3.1 shows the results of a comparative triaxial test damping coefficient of 0.1 on Figure 3.1a, compared to 0.2 on Figure 3.1b. All other parameters are held constant. The chosen damping coefficient is correlates with the 0.08-0.4 values used by other YADE authors [28, 63, 110, 250].
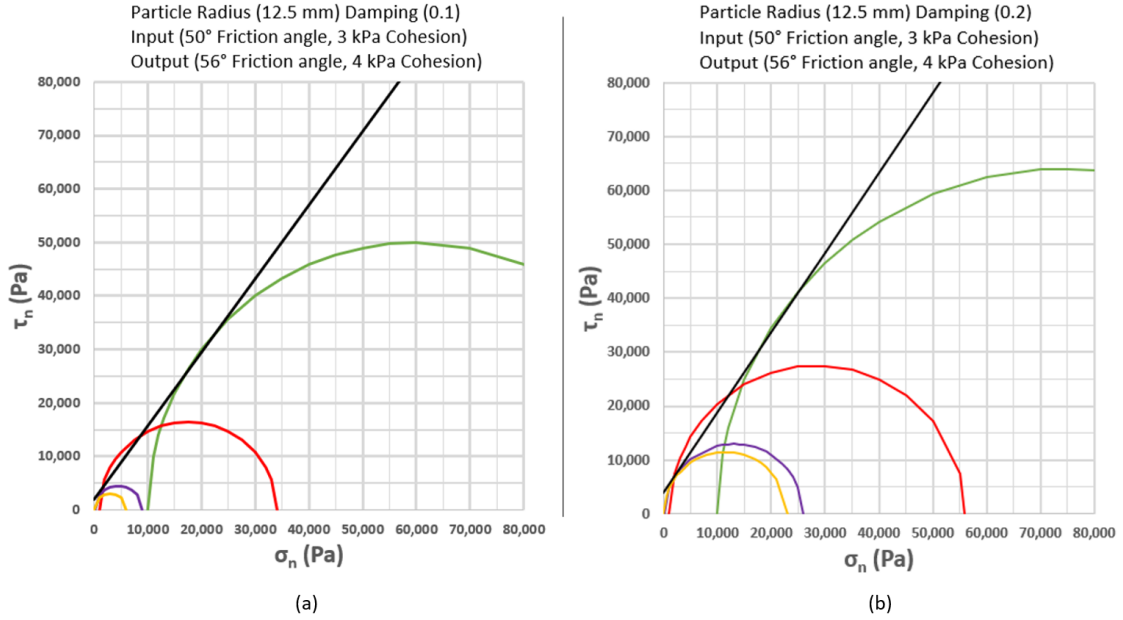
Figure 3.1: Comparison of triaxial test results with damping coefficient 0.1 (a) and 0.2 (b).

3.3.2.3 Physical Laws and Interactions

The YADE discrete element program runs an iterative loop carrying out interaction detection and physics integration along with other supplementary functions on each timestep. The loop used for the simulations in this work is shown in Figure 3.2.

Further details on the working of each of the functions in this loop are available in the YADE Documentation [268].
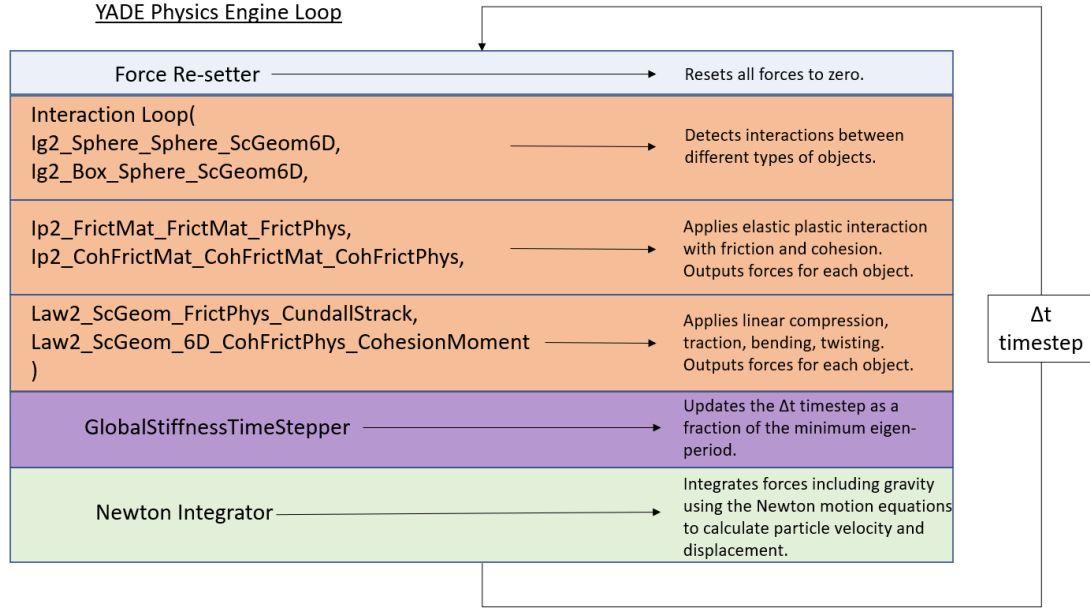
Figure 3.2: YADE interaction and physics loop used in this research.

To ensure the physics and interaction loop is working as desired, some checks should
be conducted prior to beginning calibration and experimental trials. Confirmation of
successful interactions and cohesive laws can be made by counting the number of cohesive
interactions at the start of the simulation compared to the end of the simulation. The
experiment will only run until initial failure of the tunnel begins, or a steady state is
reached. At this time, there will not be enough kinetic energy developed in the sample to
break 100% of all cohesion bonds. Results showing otherwise indicate problems with the
interaction or cohesive laws.

The frictional laws are easily checked via triaxial test, applying zero confining pressure
to a test sample shows a weak sample and the same test conducted at a higher confining
pressure should show a stronger sample. This demonstrates the functioning of the frictional
bonds.

3.3.2.4   Material Parameter Calibration

The Mohr-Coulomb Failure Criterion (Equation 3.5) is used to validate the model using a triaxial test setup. Figure 3.3 shows the conceptual experimental setup for a triaxial test and Figure 3.4 the corresponding Mohr-Coulomb Failure Envelope that is derived from several tests. Triaxial tests have been performed at four different confining stresses ($\sigma_{min} = 0\ Pa$, $100\ Pa$, $1\ 000\ Pa$, $10\ 000\ Pa$) to derive the macro-sample cohesion and friction angles. DEM parameters (mean particle size and damping coefficient) have been iteratively adjusted to reconcile the input friction angle and cohesion values derived from the Mohr Coulomb Failure Envelope.

$$\tau_f = c + \sigma_n tan\phi \tag{3.5}$$

Where τ_f and σ_n are the shear and normal stresses respectively. c is the cohesion value and $tan\phi$ is the friction angle.
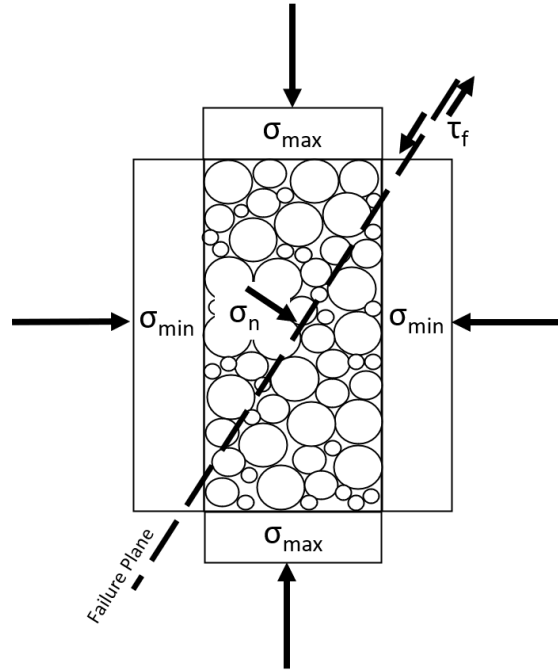
Figure 3.3: Triaxial experimental setup for derivation of Mohr's Circles and failure envelope after Puzrin [232].
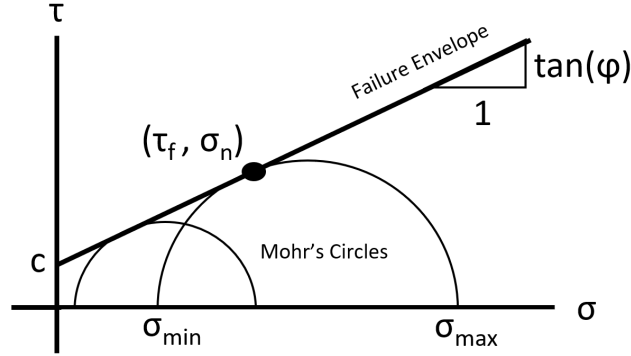
Figure 3.4: Plotting the Mohr-Coulomb Failure Envelope for a triaxial test after Puzrin
[232].

Figure 3.5 shows the YADE setup for the triaxial test. A cylindrical sample surrounded by
facets that provide confining pressure (σ_{min}). The green and the red spheres at each end
of the sample are constrained to move toward each other at a constant strain rate. The
stress-strain relationship for the sample is recorded and used to derive the Mohr-Coulomb
Failure Envelope. An example of the stress-strain curve for a range of confinement tests
is shown in Figure 3.6. These tests were carried out with a mean particle radius of 5
mm, internal friction angle of 50°, cohesion value of 3 kPa and confining pressures of 0
Pa, 100 Pa, 1 000 Pa and 10 kPa. The first 150 iterations with strain less than 0.01,
do not match what is expected from a physical triaxial test. All tests exhibit the exact
same exponential decrease in strength early in the simulation. The loss in strength is due
to many of the sample's weak cohesive bonds breaking from a small strain-pressure wave
until an equilibrium is reached. The sample results are invalid until an equilibrium between
newly created cohesive bonds and broken bonds is reached around 0.01 strain. Once this
equilibrium has been reached, the test can be considered analogous to a physical triaxial
test. The maximum value for stress (σ_{max}) after the cohesive equilibrium is reached (the
second peak) is therefore used in the derivation of the Mohr Coulomb failure envelope.

The overall results of DEM particle parameter calibration are shown in Table 3.5. A mean
particle radius of 5 mm has been chosen for tunnel diameters greater than 50 mm and
less than 250 mm. A mean radius of 12.5 mm for is used for tunnel diameters larger
than 250 mm and a mean radius of 2.5 mm for tunnel diameters less than 50 mm. These

particle radii selections ensure at least 10 particles and corresponding contacts represent the unsupported span of the tunnel and have been validated as per Section 3.3.2.1. Figure 3.7, 3.8 and 3.1(b) show the Mohr Coulomb Failure Envelopes for the trials with particles of 2.5 mm, 5 mm and 12.5 mm mean radii respectively. The Failure Envelope in these figures does not exactly match the edge of the Mohr's circles, as these are based on imperfect experimental data, with measurement errors included. The Failure Envelope is a best fit to the four experiments carried out for each figure.

Table 3.5: Final sample calibration results.

	Mean Particle Radius	Damping	Input	Target	Output
Cohesion	2.5 mm	0.25	3 kPa	3 kPa	3 kPa
	5 mm	0.2	3 kPa	3 kPa	3 kPa
	12.5 mm	0.2	3 kPa	3 kPa	4 kPa
Friction Angle	2.5 mm	0.25	54°	54°	54°
	5 mm	0.2	50°	54°	54°
	12.5 mm	0.2	50°	54°	56°
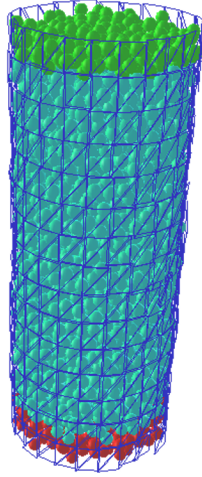
Figure 3.5: Triaxial test DEM setup.

Both 2D and 3D samples were tested for calibration, however, the 2D model did not perform well. Parameter calibration for 2D samples required input cohesion values 50 to 80 times higher than the output macro sample target in order to calibrate. 3D model calibration, on the other hand, has performed well, showing almost 1:1 calibration after tuning the damping coefficient to 0.2. Hence, all subsequent experimentation has been
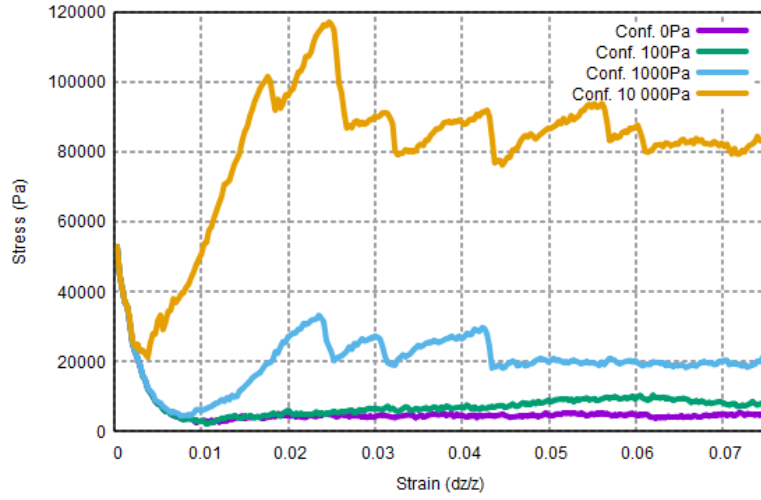
Figure 3.6: Normal stress-strain chart for triaxial tests on sample with 5 mm mean particle radius, 50° friction angle, 3 kPa cohesion.

conducted with 3D samples, contact laws and forces. Tunnel tests have been conducted

with the third depth dimension of 16x the mean particle radius.
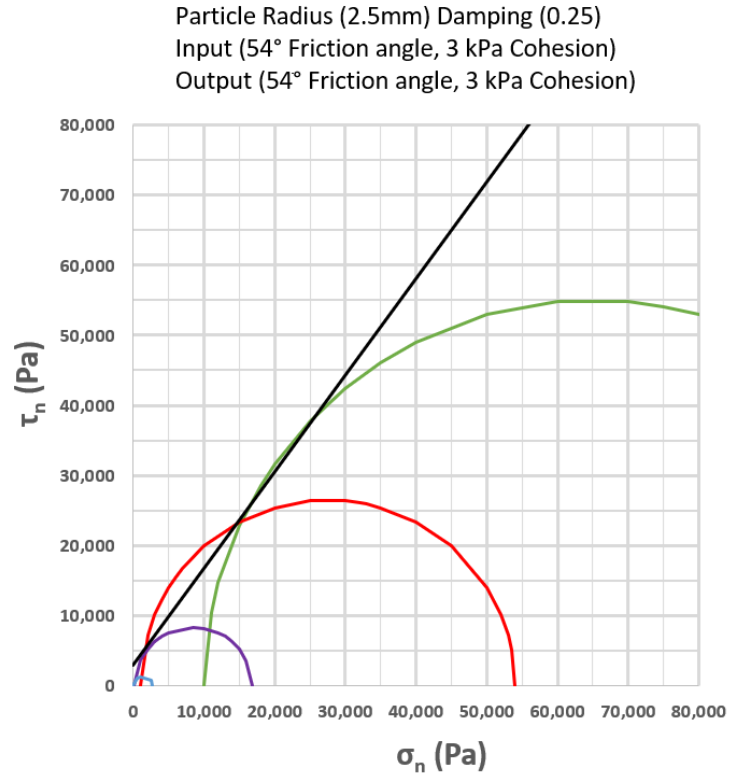
Figure 3.7: Calibration triaxial tests for 2.5 mm radius lunar regolith particles.

Particle Radius (5 mm) Damping (0.2)
Input (50° Friction angle, 3 kPa Cohesion)
Output (54° Friction angle, 3 kPa Cohesion)
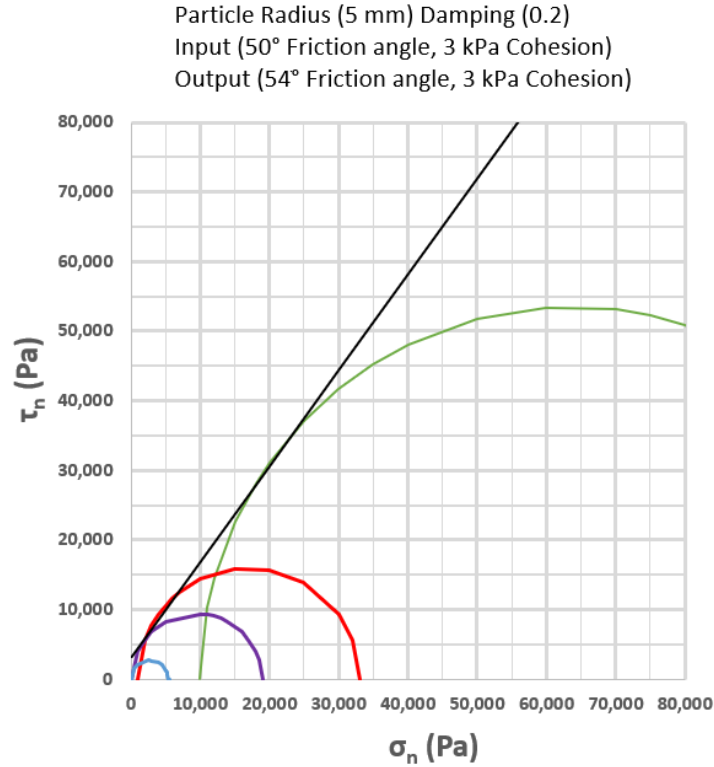
Figure 3.8: Calibration triaxial tests for 0.005m radius lunar regolith particles.

3.3.3   Experimental Method

3.3.3.1   Overview

The tunnel stability experimental procedure is summarised in Figure 3.9. The procedure has been divided into three parts, where the end of each part results in a saved sample and data outputs.

The first part, Sample Setup, is conducted for every parameter combination on the tunnel stability chart. Once the samples are prepared, they are individually run through the Excavation Test and observed for stability conditions such as visual collapse and the total kinetic energy in the sample. A "stable" tunnel is defined in terms of the kinetic energy (KE) [110, 149] as the initial sample has been intentionally created with negligible kinetic energy to represent a static equilibrium. A sample containing a stable tunnel will have a

41

stable sum of kinetic energy in all particles. An "unstable" tunnel will show increasing KE
in the sample as particle velocities begin to increase. The simulation is run for a period
of 30 000 iterations after the excavation is complete and the kinetic energy of the sample
recorded. Any conspicuous results, or apparently stable results are run for an additional
100 000 iterations until stable kinetic energy levels are confirmed. No external forces are
applied to the sample during the Excavation Test other than constant lunar gravity and
the compaction pressure via a rigid frame.

The largest diameter stable tunnel is then passed into the Seismic Test and qualitative
results are observed.
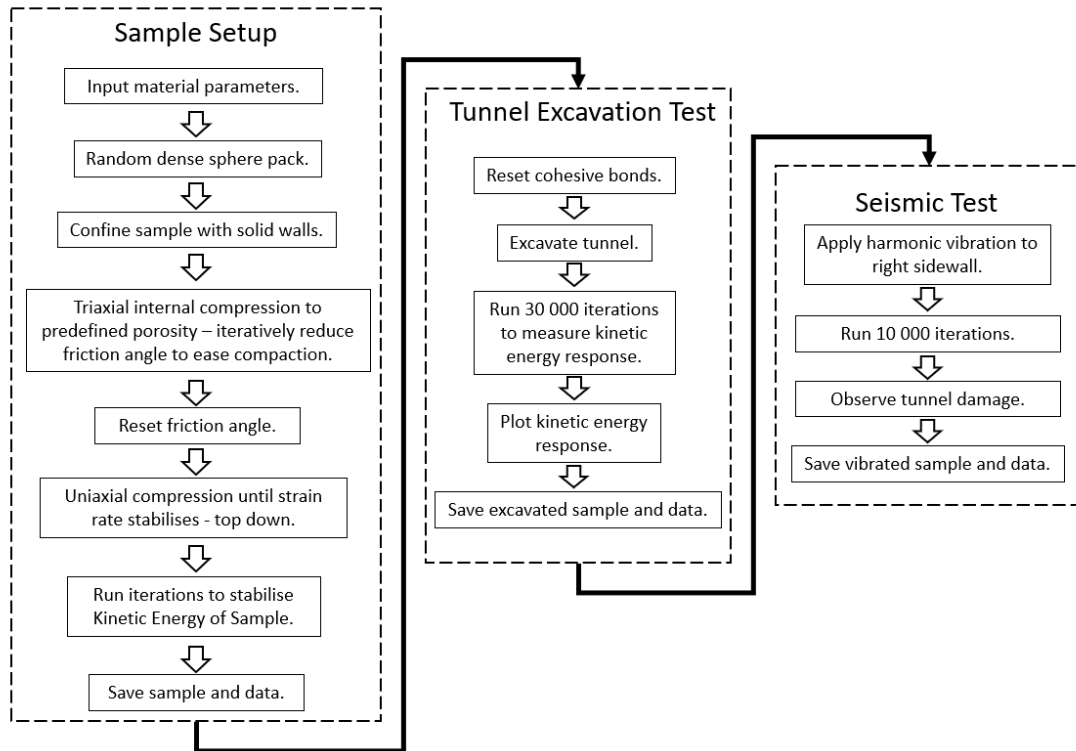
Figure 3.9: Tunnel stability experimental procedure.

3.3.3.2   Test Parameters

Excavation tests have been conducted with increasing tunnel diameters and compaction pressures. The tunnel diameters tested are shown in Table 3.6. They have been chosen to frame the study as an evenly spaced grid search, to produce a Stability Chart with various trials in a grid demonstrating success or failure of a tunnel. The diameters are not an exact evenly spaced grid as the available dimensions are limited by the size and number of the discrete particles making up the tunnel. Therefore, diameters have been chosen in a fashion that matches an integer number of particle diameters. For example, a test using the 25 mm diameter particles will fit 16 particles across a 400 mm diameter tunnel. This also minimises variance between experiments due to particle packing misalignment.

Table 3.6: Tunnel diameters for stability testing.

Excavation Diameter (mm)	Model Particle Diameter (mm)	Number of in span
50	5	10
100	10	10
160	10	16
250	25	10
300	25	12
400	25	16

The apparent depth of the tunnel will be modified by applying compaction pressure to the top layer of particles. The pressure applied follows the Depth Stress and Porosity Model in Table 3.1. A set of tunnel diameter experiments has been carried out for each depth and applied vertical stress in Table 3.1.

The experiments have been conducted using two different size samples as shown in Figure 3.10. The initial experiments were done with the 3R sample to save computational time and identify the appropriate search space for the stable-unstable transition. The small sample results were then confirmed with the same trials run on larger samples with a wall thickness of 6R, where R is the radius of the tunnel excavation.

The stability results with respect to tunnel diameter and depth were then plotted on 2D axis to create a tunnel stability chart.
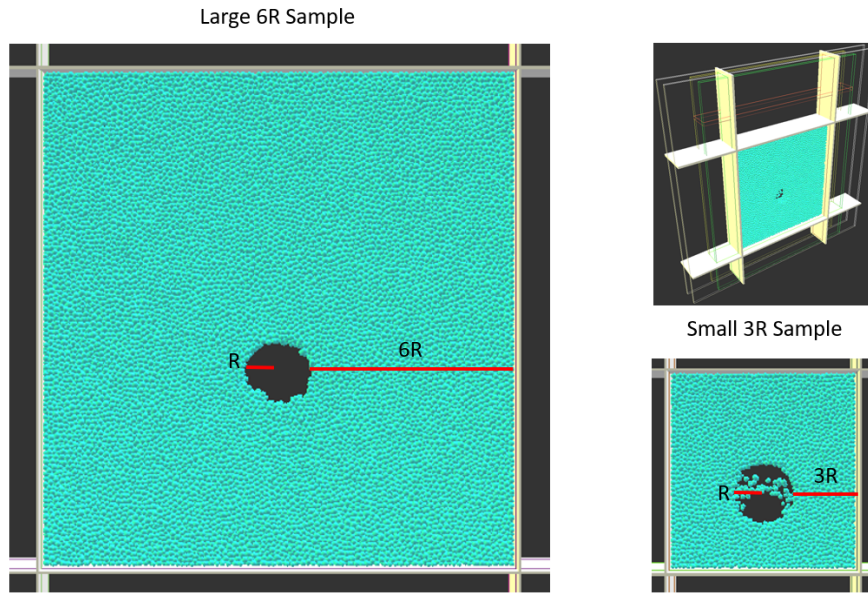
Figure 3.10: Sample and wall size comparison.

3.4 Results

The results from the tunnel stability trials are shown in Table 3.7. Representative samples have been reported with visuals and kinetic energy charts in Table 3.8. These samples have been labelled with an index that can be used to reference their location on Table 3.7 and the tunnel stability chart in Figure 3.11. Some of the trials did not reach an appropriate terminal condition in a reasonable timeframe and were terminated manually, yielding No Data as shown in Table 3.7. Some of the tests are not required as they are known to be within the stable region of the grid-search. Sufficient data is available around the transition zone between "stable" and "unstable" meaning this missing data has not affected the analysis. The tunnel stability chart shows a pattern of stability, where stability increases with depth or confinement pressure/compaction and decreases significantly with an increase in tunnel diameter.

The shear stress pattern for the stable tunnel in index D is shown in Figure 3.12. The predicted shear stress pattern around the excavation is typical of an unsupported tunnel excavation [102]. This further supports the stable tunnel hypothesis as an unstable tunnel

44

is expected to be de-stressed around the tunnel diameter.

The stable tunnel at 4 m depth and 160 mm diameter (Index D), shown in Table 3.8, has been selected for an additional lunar seismic test in YADE. A vibration of amplitude 2 mm and frequency 10 Hz has been applied to the left side wall to observe the effects. The seismic p-wave translates horizontally from left to right and reflects back from the right-hand wall. All other conditions are the same as for the tunnelling tests. These seismicity parameters have been selected based on the reported lunar seismicity by Lammlein [158]. The strength and frequency of moonquakes depends on location and other factors such as diurnal cycle and tidal patterns. The data collected by Lammlein [158] show that multiple moonquakes occur each year in the amplitude range between 1 mm and 8 mm. The level of vibration tested in this study may not only originate from natural moonquakes, but also vibrations from machinery and rockets being used nearby on the Moon.
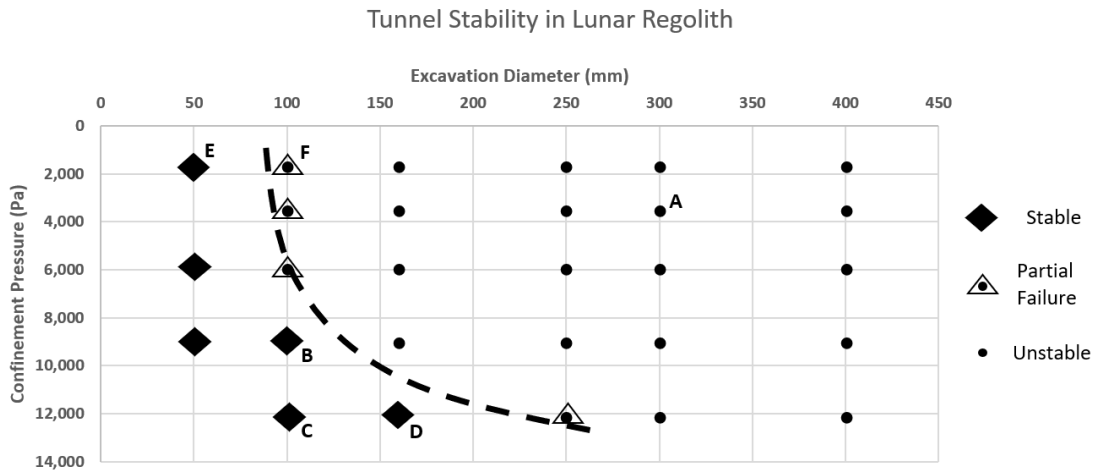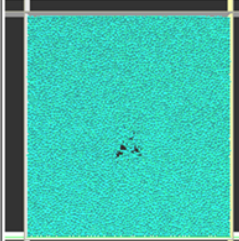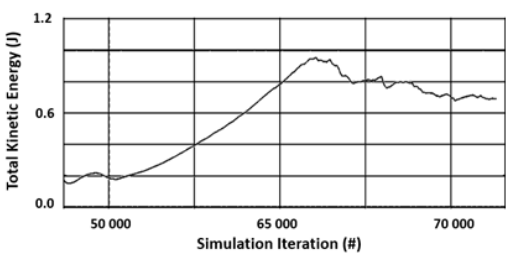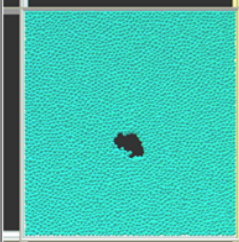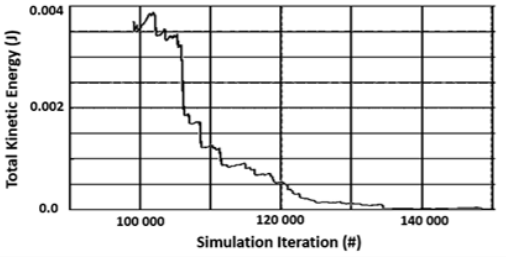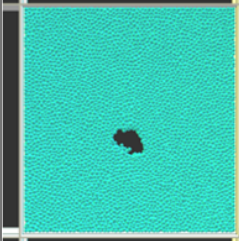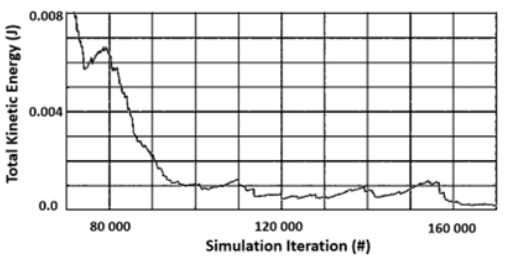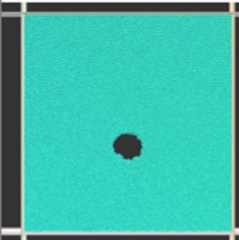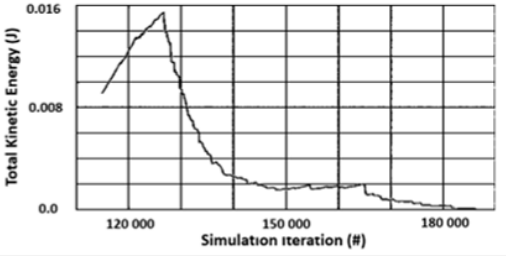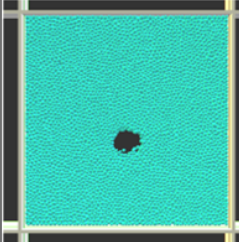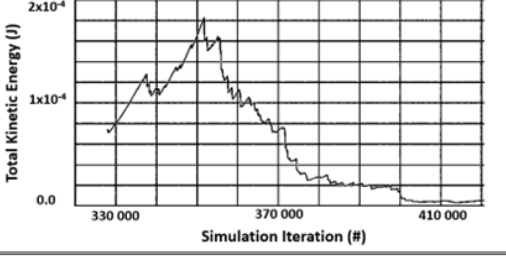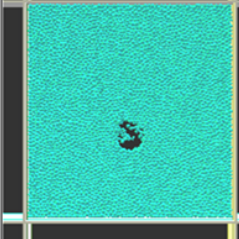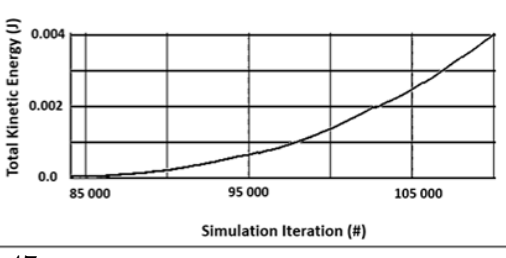
Figure 3.11: Tunnel stability chart for lunar regolith.

The results of seismicity tests are shown in Figure 3.13. The tunnel becomes unstable under the lower range of dynamic loading recorded on the lunar surface (under a 2 mm amplitude quake). This indicates that this tunnel in lunar regolith is unlikely to be stable over longer time periods and under non-static conditions. This finding raises issues for tunnel stability during excavation or with nearby vibrating machinery and rockets.

45

Table 3.7: Tunnel stability experiments qualitative results.

Index	Tunnel Diameter (mm)	Confinement (Pa)	6R sample - Failure?	3R sample - Failure?
E	50	1727	No	No Data
	50	3535	No Data	No Data
	50	5978	No	No Data
	50	9053	No	No Data
	50	12144	No Data	No Data
F	100	1727	Partial	Partial
	100	3535	Yes	No
	100	5978	Yes	No
B	100	9053	No Data	No
C	100	12144	Partial	No
	160	1727	No Data	Yes
	160	3535	Partial	No Data
	160	5978	No Data	Yes
	160	9053	Yes	Yes
D	160	12144	No	No
	250	1727	Yes	No Data
	250	3535	Yes	Yes
	250	5978	Yes	Yes
	250	9053	Yes	Partial
	250	12144	Yes	No
	300	1727	Yes	Yes
A	300	3535	Yes	Yes
	300	5978	Yes	Yes
	300	9053	Yes	Yes
	300	12144	Yes	Yes
	400	1727	Yes	Yes
	400	3535	No Data	Yes
	400	5978	Yes	Yes
	400	9053	Yes	Yes
	400	12144	Yes	No Data

Table 3.8: Tunnel excavation test visual results.

Index	Parameters	Visual Inspection	Kinetic Energy Record
A	Diameter - 300 mm Confinement - 3535 Pa Friction - 50°		
B	Diameter - 100 mm Confinement - 9053 Pa Friction - 50°		
C	Diameter - 100 mm Confinement - 12144 Pa Friction - 50°		
D	Diameter - 160 mm Confinement - 12144 Pa Friction - 50°		
E	Diameter - 50 mm Confinement - 1727 Pa Friction - 54°		
F	Diameter - 100 mm Confinement - 1727 Pa Friction - 50°		
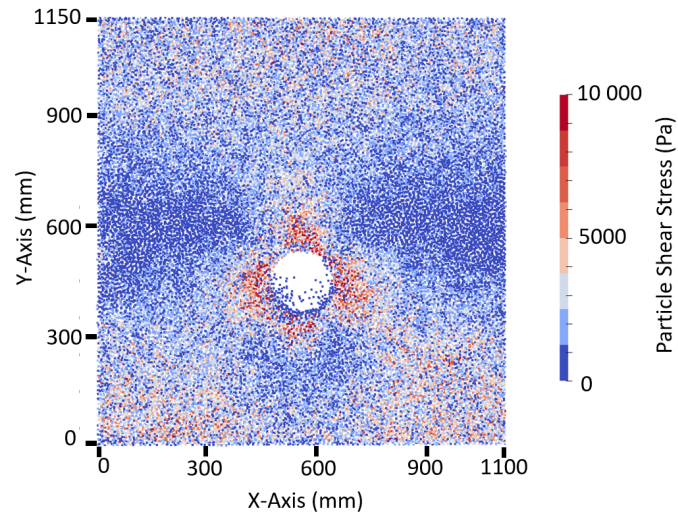
Figure 3.12: Stable excavation sample (Sample Index D) with shear stress legend.
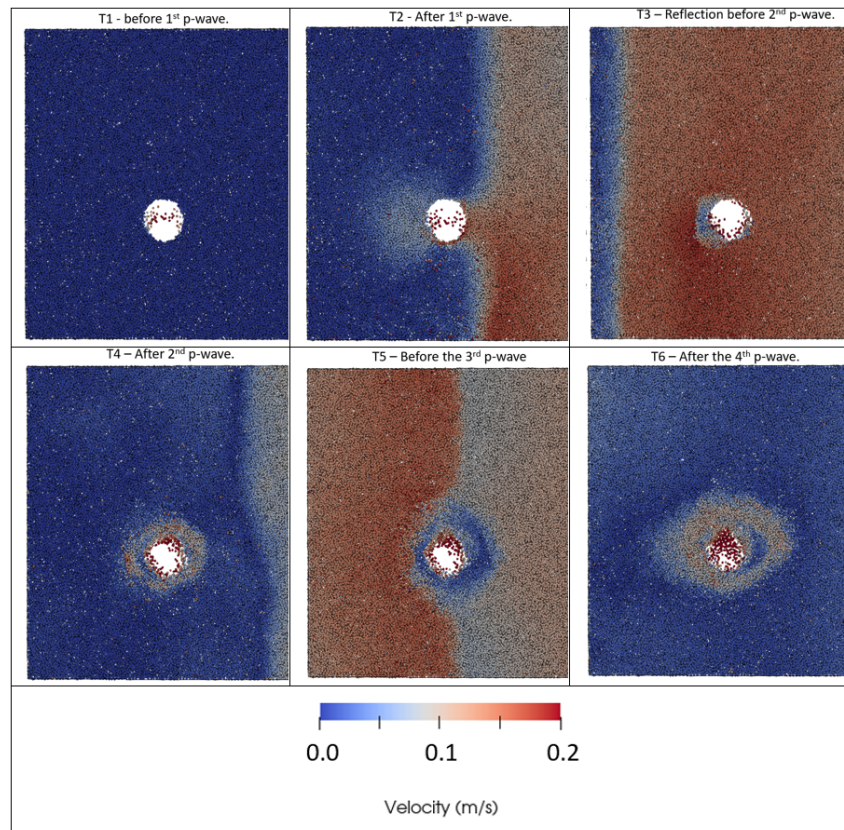
Figure 3.13: Velocity coloured snapshots of seismic test 10 Hz/2 mm amplitude on Index
D tunnel.

3.5 Discussion

The Discrete Element Method is limited by computational power. The number of simulated particles is proportional to the amount of time required for a simulation to finish. The simulations in this research are run with sufficient iterations to produce 1-2 seconds of real time data. To achieve this, particles have been scaled and calibrated to achieve computational reductions up to 1.4 million times according to Equation 3.3. The question is raised whether there is sufficient time or sample fidelity to determine tunnel stability. Certainty of the results in this chapter is provided by recording and inspecting the total kinetic energy and shear stresses in samples along with visual proof of instability. The bulk sample calibration procedure is chosen to allow particles to be scaled up and simplified, while still producing the same bulk sample response. Currently it is not possible to simulate the exact shapes and dimensions of lunar regolith particles for tunnel stability trials. However, the array of independent analysis techniques used in this chapter increases certainty in the result and enables shorter simulations to be run.

This research was conducted using an Intel Core i3 CPU with 4 processors. Individual simulations take between 2 and 13 hours once code prototyping was complete. Increasing the available cores for computation and using parallelisation techniques will enable more realistic simulations with more particles. Cluster CPU resources were investigated for running the simulations. However, these were disregarded as the available operating systems were not compatible with YADE software without modifications.

The effect of volatiles such as H_2O in regolith is of great interest to the researchers in the field of In-Situ Resource Utilization (ISRU) or off-Earth mining. A significant increase in the cohesiveness of regolith is expected with increased H_2O content. Unfortunately, geotechnical data for real icy lunar regolith is not currently available. Only laboratory tests on imperfect simulants and assumptions can be made such as the work done by Pitcher *et al.* [225]. Further research defining the cohesion and friction values of cryogenic icy regolith and applying those values to the DEM models outlined in this chapter would likely lead to increased lunar tunnel stability in those materials and will also be useful for

designing future lunar ISRU systems.

The stability of the tunnels under seismicity and dynamic conditions has been shown to
be low. This raises questions about the method of excavating the tunnel and if it would
be possible to do so without causing destructive vibrations. This is also a question for
further excavation systems research.

3.6 Conclusions

DEM can be applied to off-Earth mining scenarios which are difficult to simulate on Earth
due to different gravity and specific material properties. In this chapter, it has enabled
the production of a tunnel stability chart for shallow small diameter horizontal tunnels
and drillholes in lunar regolith and gravity.

The parameter study here has shown that the stable tunnel diameter is dependent on
the depth and compaction of the regolith, where higher compaction leads to larger stable
tunnel spans. The largest stable tunnel diameter found in this study was at a depth of ap-
proximately 4 m. The confining pressure and compaction levels at this depth are expected
around 12 kPa. This has yielded a maximum stable tunnel diameter of approximately 160
mm. The small diameter of stable tunnels in lunar regolith shows that they are unlikely to
be useful for practical purposes. Some form of ground support would be required to enable
greater diameters for uses such as habitation or access for machinery to extract resources.
There is potential to use icy regolith as a form of ground support as the cohesion values
are expected to be much higher, although more data is required for this modelling.

The stability of the tunnel is decreased significantly under seismic conditions which include
vibrations from machinery and nearby rockets. It is unlikely that the stable regolith
tunnels as described in static conditions in this chapter will survive the long term under
the surface of the Moon due to vibrations and seismicity. Ground support would be
required for most long-term tunnels in regolith for the purposes of exploration, scientific
analysis, habitation, infrastructure, or resource extraction. Examples may include fibrous

or metallic bolting of the tunnel walls, freezing regolith with an in-situ application of water, sintering the tunnel surface with microwave radiation or some form of chemical bonding of the surface layer. These possibilities can be explored in future work to determine the increase limits of tunnel stability with ground support, using the same DEM method outlined in this chapter.

The DEM method developed and calibrated in this chapter has shown to be a useful method for simulating lunar regolith and gravitational conditions. Future geomechanics studies in relation to off-Earth mining can benefit from this method and be used to derive excavation stability constraints for planning and optimising mining operations on the Moon. The lunar regolith tunnel stability chart and any future iterations of it can also be used to guide engineering decisions for future lunar ISRU equipment concepts. One of the major advantages of the DEM technique shown in this chapter, is that the same model, or new models with important variations in geomechanical or geological properties can also be used to test new ground engaging tools for ISRU equipment. This will be shown in the next chapter to reduce the costs and time of system development, and to rapidly demonstrate proof-of-concepts in a low-cost DEM simulation.

Chapter 4

Lunar Mining System Concepts

4.1 Introduction

Mining system design is currently one of the main focuses of ISRU research around the world. The development of mining systems for space applications faces a major issue though; testing prototypes in an appropriate environment that simulates all the required environmental properties. There are currently no known methods to physically simulate the temperatures, vacuum, radiation, gravity, dust and material hazards known on the Moon simultaneously.

Furthermore, mining equipment must be specifically designed for each type of geological deposit and environment. Important design decisions can be made depending on geomechanical and geological properties as well as environmental factors. For example, when the material is very hard, an excavator alone will be insufficient to mine a resource. Instead, a multi-step process of rock breakage, excavation, transport and beneficiation may be required.

According to Objective 2, this chapter investigates various mining systems in literature and categorises them according to their capabilities. As part of the categorisation, an assessment of the mining system's Technology Readiness Level (TRL) [137] is also undertaken.

Three novel off-Earth mining system concepts are proposed here that could be used to fill capability gaps in certain aspects of lunar ISRU. Modelling of these proposed systems is carried out with the Discrete Element Method (DEM) following from the calibrations and demonstrations in the previous chapter. The use of the DEM for this purpose shows how it can be applied to the design process for various resource utilisation systems as well as determining the stability of excavations, these demonstrations also follow Objective 1.

A subset of the mining systems collated in this chapter will be used in all subsequent chapters when mining system selection is required. These specific mining system selections allow the novel planning and optimisation methods proposed later in this thesis to be demonstrated.

4.2 Literature Review

Current state-of-the-art mining system designs for the Moon and Mars include diverse examples. The Mobile In-Situ Water Extractor (MISWE) system [319] utilises an auger and heating element to release volatiles from the regolith. The Regolith Advanced Surface Systems Operations Robot (RASSOR) [202] uses counter rotating bucket-drums to collect regolith with minimal mass required for reaction force. The PlanetVac pneumatic system [317] uses compressed gasses to agitate and collect regolith. Other designs generally fall into the categories of a loader [52], bucketwheel excavator [265], bucket drum excavator or in-situ water sublimation (ISWS) systems [32, 89]. Many of these systems, similar to excavators on Earth are only able to manage already broken materials or loosely consolidated soils such as regolith.

Mueller and Van Susante [200] completed a review of entrants into the annual Lunabotics competition over several years. The review shows that many designs are applicable to the specific problem of excavating lunar regolith and that system designs converge over successive years of trial and error for a single deposit type. The designs have been condensed into categories, and the convergence to a Bucket Ladder system is shown in Table 4.1.

This suggests there is an optimal system for a given geological deposit type.

Table 4.1: Regolith excavation categories in the Lunabotics Competition [200].

Excavator Category	Number of Entrants
Bucket Ladder	34
Bucket Belt	10
Bulldozer	10
Scraper	9
Auger	5
Backhoe	4
Bucket-wheel	4
Bucket drum	3
Claw scoop	2
Street Sweeper	2
Rotating tube	1

A collection of mining systems from literature are collated in Table 4.2. This table also includes the three novel systems proposed later in this chapter.

Table 4.2: Off-Earth mining equipment pool.

Equipment Description	Subclass	Stage of Development	Reference Examples
Impact Excavator	Excavation	Proof of Concept	Section 4.5
Drill and Pull	Rock Breakage	Proof of Concept	Section 4.6
Truck	Transport	Prototypes and Heritage Designs	[259, 264, 319]
Bucket Drum Excavator	Excavation, Transport	Prototypes	[201, 269]
Hammer Drill	Rock Breakage	Prototypes	[323]
Discrete Excavator	Excavation	Prototypes	[263, 264]
Continuous Excavator	Excavation	Prototypes	[263, 265]
LHD (Load-Haul-Dump Excavator)	Excavation, Transport	Prototypes	[264]
Oven	Processing	Prototypes	[184, 208]
Pneumatic Excavator	Excavation, Transport	Breadboard	[284, 317, 321]
Crusher Oven	Rock Breakage, Processing	Terrestrial Heritage Designs	[184, 208]
Micro Tunnel Borer	Rock Breakage, Excavation	Terrestrial Heritage Designs	Section 4.7 [20, 323]
Volatile Extraction Drill	Rock Breakage, Excavation, Transport, Processing	Breadboard	[319, 323]

4.3 Off-Earth Mining System Categorisation

The mining systems in literature and the additional three novel concepts proposed in this chapter are divided into four subclasses as shown by the mining flow chart in Figure 4.1. They are: Rock Breakage, Excavation, Transport and Processing. This categorisation enables logical matching of equipment to form a resource extraction system. The equipment list is shown in Table 4.2. The list has also been categorised by the level of development of each system. The least amount of development being the "Proof of Concept", and the most advanced stage in this table being when "Prototypes" have been built. "Terrestrial Heritage Designs" are based on similar systems that already exist in the terrestrial mining or other industries. "Breadboard" systems are where the unique components have been demonstrated in isolation in a laboratory. To classify the stage of development for an established system, the NASA Technology Readiness Level (TRL) classification can be used [137]. The definitions of each Technology Readiness Level are described in Table 4.3. All systems in Table 4.2 appear to be at TRL 4 except for the Impact Excavator and Drill and Pull Systems. These are only at a TRL of 3 and 2 respectively as successful laboratory tests have not been completed to a sufficient level. Although results are reported in this chapter, the Impact Excavator did not complete all planned tests due to manufacturing issues. The Drill and Pull mechanism also has not been physically tested. All equipment in Table 4.2 at or above TRL 4 will be used as input for works in the Chapter 5. These items have demonstrated a successful proof-of-concept and can be analysed at a functional level. The deficit of "Rock Breakage" equipment in Table 4.2 will be the focus of the remainder of this chapter. The new Drill and Pull, Impact Excavator and Regolith Tunneller designs will better enable rock breakage for optimisation of ISRU in conjunction with selective mining algorithms as demonstrated in Chapter 6.

Table 4.3: NASA System Engineering Handbook definition of the Technology Readiness Levels. [137]

TRL	Criteria
9	Actual system "flight proven" through successful mission operations.
8	Actual system completed and "flight qualified" through test and demonstration (ground or flight).
7	System prototype demonstration in a target/space environment.
6	System/subsystem model or prototype demonstration in a relevant environment (ground or space).
5	Component and/or breadboard validation in relevant environment.
4	Component and/or breadboard validation in laboratory environment.
3	Analytical and experimental critical function and/or characteristic proof-of-concept.
2	Technology concept and/or application formulated.
1	Basic principles observed and reported.
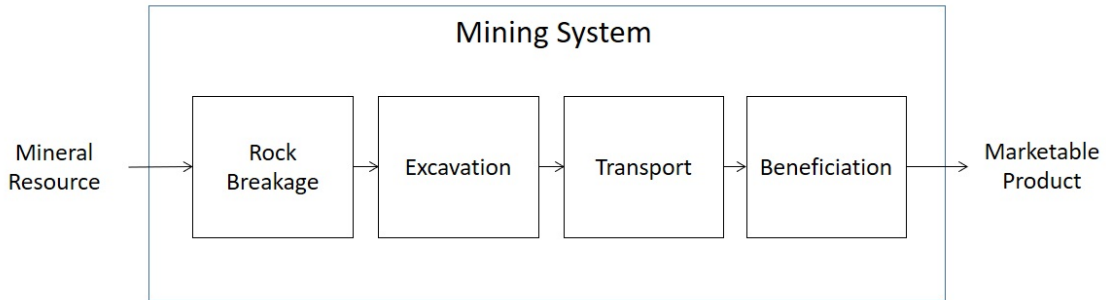
Figure 4.1: Flowchart through equipment subclasses of the mining system.

4.4 Rock Breakage Systems Gap

Lunar ISRU systems have mostly been designed on the premise that the target resource will be a loosely consolidated material with a near uniform concentration of valuable minerals [146]. Unfortunately, there is not yet enough data to describe lunar resources in this detail for certain [36]. Numerous physical data samples are required to define a *mineral resource* and then conduct subsequent engineering studies [134]. The current lack of available data for this purpose limits how we can proceed with equipment design. The equipment development done in this thesis is therefore limited to proof-of-concept works for hypothetical geological deposit styles.

Experiments by Atkinson and Zacny [9] show a 12% H_2O concentration icy regolith simulant (JSC-1a) has a UCS strength of around 35 MPa. Material of this hardness is similar to concrete, and will require rock breakage prior to excavation. The majority of the off-Earth mining equipment found in literature (see Table 4.2) are of the excavation class. Only the drilling mechanisms, crushers and tunnel borers are available for rock breakage. None of these items work in conjunction with an excavator. This result implies that many of the harder, compacted, icy deposits will not be accessible for bulk mining methods without developing new rock breakage methods. Inability to access higher grade minerals such as this 12% H_2O grade regolith is a significant limitation on ISRU planning and optimisation. To converge to an optimal system for harder ISRU deposits, new rock breakage mechanisms should be developed.

There are only some limited examples of research into rock breakage mechanisms for off-Earth mining. Systems that receive significant attention such as MISWE [319] and RASSOR [202] are designed for non-consolidated or loosely consolidated deposits. The use of microwave energy to assist rock breakage for off-Earth mining has been demonstrated by Satish *et al.* [247]. Percussive digging has also been demonstrated to reduce the reaction force required to excavate compacted material in experiments by Craft *et al.* [52]. These are however, energy intensive exercises.

For terrestrial mining, rock breakage is undertaken by several methods. Some are more common than others. They are listed as follows:

- drill and blast [62];

- mechanical picks and discs (e.g. tunnel boring or road-heading) [62];

- rock cutting [310];

- surface scraping [298];

- hydraulic means (e.g. pressure fracturing [296] or hydro-mining [62]); and

- heating and quenching (fire-setting) rock in ancient times [62].

Most of these methods require mechanical ground engaging tools for part or all of the rock breakage process. The steps involving explosives, heating, quenching and hydraulic fracturing differ in that they use chemical and mechanical means not derived from a ground engaging tool. Currently, explosives are the most important rock breakage tool on Earth. However, these chemical tools may need significant modifications to function in the cryogenic temperatures and vacuum of the Moon. There are currently no details available in literature on how explosives could be adapted. At the least, implementing an explosive manufacturing process in the lunar environment would need significant further research and development to become feasible. At worst it may not be feasible at all for ISRU, technically or economically. Many of the necessary feedstocks for explosive manufacturing such as hydrogen, oxygen and nitrogen are also the desired products of ISRU. Therefore, any process that would implement explosives would need to ensure the mass yield of ISRU product far exceeds the mass of explosive used.

The option of bulk excavation for hard minerals is an indispensable mine planning and optimisation tool. The importance of being able to access high grade material will be shown in Chapter 5, to reduce energy expenditure in heating regolith to extract volatiles. The same theory applies to all mining projects constrained by the beneficiation stage of operations [116, 161]. Chapter 6 will demonstrate the use of *cut-off grades* to optimise space resource utilisation using an excavator system. It is implied that this concept will require rock breakage for harder icy materials to be excavated. For the foreseeable future, mechanical ground engaging methods are the most favourable type for ISRU rock breakage due to the difficulties in implementing hydraulic or explosive methods in space. Three potential mechanical rock breakage candidates have been developed in this chapter to enable excavation systems to work with harder materials.

As will be shown in this chapter, some researchers are also combining and supporting their physical experimentation with DEM models and other numerical modelling techniques. Examples include Erarslan, Liang and Williams [86] and Kazerani, Yang and Zhao [140].

4.5 Impact Excavator

4.5.1 System Design

The Impact Excavator uses the principle of centrifugal acceleration to reduce the required reaction mass for excavation. Many traditional excavator designs involve pulling soil or regolith towards the vehicle with the raw mass of the equipment acting as an anchor or counterweight. This type of mass-dependent design can be undesirable for off-Earth mining systems due to the high cost of transporting mass to the site.

Figure 4.2 (a) shows the Computer Aided Design (CAD) prototype of the Impact Excavator full bench-top assembly. The adjustable frame allows the angle of incidence of the projectile to the target to be varied throughout experiments. Figure 4.2 (b) shows a detailed view of the electric motor attachment, a small DC electric motor is designed to fit into this slot and provide a rotational driver for the centrifugal wheel as seen in Figure 4.2 (c) and (d). Figure 4.2 (d) shows the intended trajectory of the projectile as it is accelerated and released. The projectile is inserted through a small slot located near the centre of the wheel, on the opposite side of the electric motor attachment. From this location, momentum exchange is at a minimum between the wheel and the projectile. This minimises the instantaneous forces applied to the structure during operation. An advantage of the central entry point and centrifugal acceleration design is that many projectiles can be released and accelerated in a short period. This enables a rapid incremental increase of the excavated volume as many projectiles can be released in a short period of time.

The experiments in this chapter are based on the early prototype to demonstrate a valid concept. No mobile chassis or regolith collection equipment has been designed yet. It is envisaged that the chassis would be a simple wheeled rover with an additional bucket to collect ejecta material from the impact craters.

The first iteration of the Impact Excavator was designed and built with 3D printed Polylactic Acid plastic and off-the-shelf electronic components, bearings and frame.
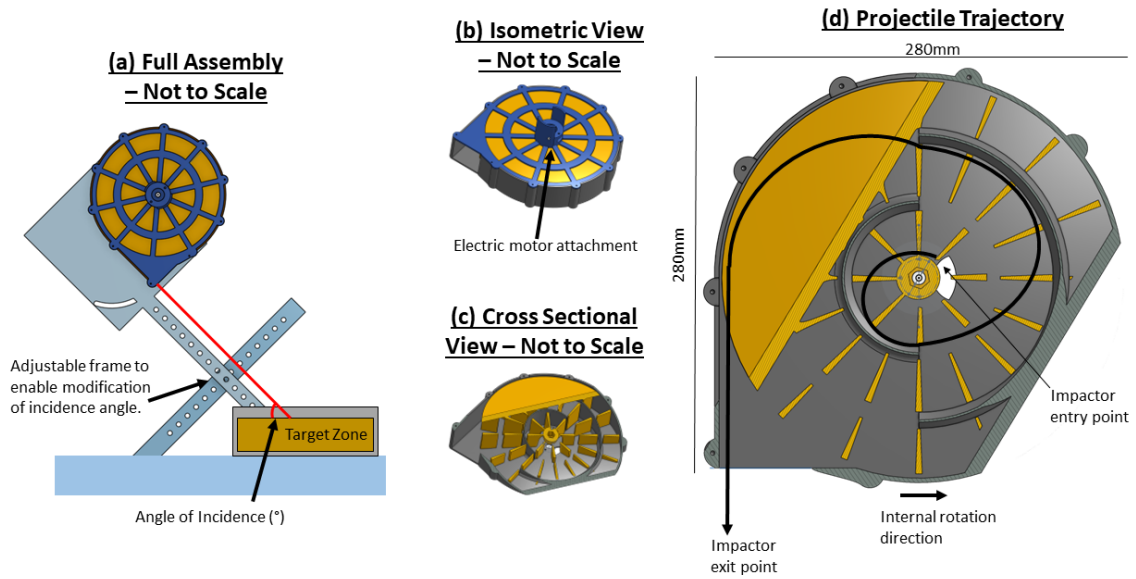
Figure 4.2: Impact Excavator CAD design and details.

4.5.2 Proof-Of-Concept Experiments

4.5.2.1 Aim

The aim of the prototype Impact Excavator laboratory experiment is to provide a baseline for calibration of the DEM model and also identify any reliability or design issues with the equipment.

A second objective, to determine the effectiveness of the Impact Excavator in harder icy conditions was planned. However, this was not completed due to several issues encountered throughout the experiment. These issues will be further detailed in the discussion, Section 4.5.5.

The aim of DEM Modelling of the Impact Excavator is to gain an understanding of the change in performance of the in lunar regolith and under lunar gravity conditions and demonstrate a proof-of-concept of the system.

4.5.2.2   Materials

The materials required for the laboratory testing are as follows:

- the Impact Excavator prototype;

- a protective sheath to cover the apparatus during testing;

- Personal Protective Equipment such as safety glasses, standard lab shoes and clothing;

- a target calibration material of dry beach sand from Sydney, NSW;

- a variable voltage power source to a maximum of 12 V;

- several 12 mm diameter 304 Stainless steel ball bearing impactors;

- a magnetic revolution counter (RPM meter) and magnet to be attached to the Excavator; and

- a calliper and ruler for measuring impact crater length, width and depth.

The materials required for the DEM model are as follows:

- a computer with a Linux operating system and minimum Intel Core i3-6100U processor;

- YADE software installed;

- at least 64GB of internal or external data storage for experiments; and

- Paraview data analysis software installed.

4.5.2.3   Laboratory Method

The laboratory experiments were conducted as follows:

1. Set the alignment of the Impact Excavator to a predetermined angle of incidence by sliding the foot along the bench.

2. Accelerate the wheel with a constant voltage until a stable angular velocity is reached.

3. Measure the angular velocity of the wheel using the magnetic RPM meter. This can be used to calculate the velocity and kinetic energy of the impactor.

4. Insert a projectile.

5. Measure the impact crater length and width with a calliper and note any qualitative effects. The length and width of the crater must be measured from peak to peak of the crater rim to ensure standard results as per Figure 4.3.

6. Measure the impact crater depth with a ruler. The crater must be measured from the highest part of the rim crest to the lowest part to ensure standard results as per the generic crater dimensions in Figure 4.3.

7. Repeat all steps for each impact angle and voltage.
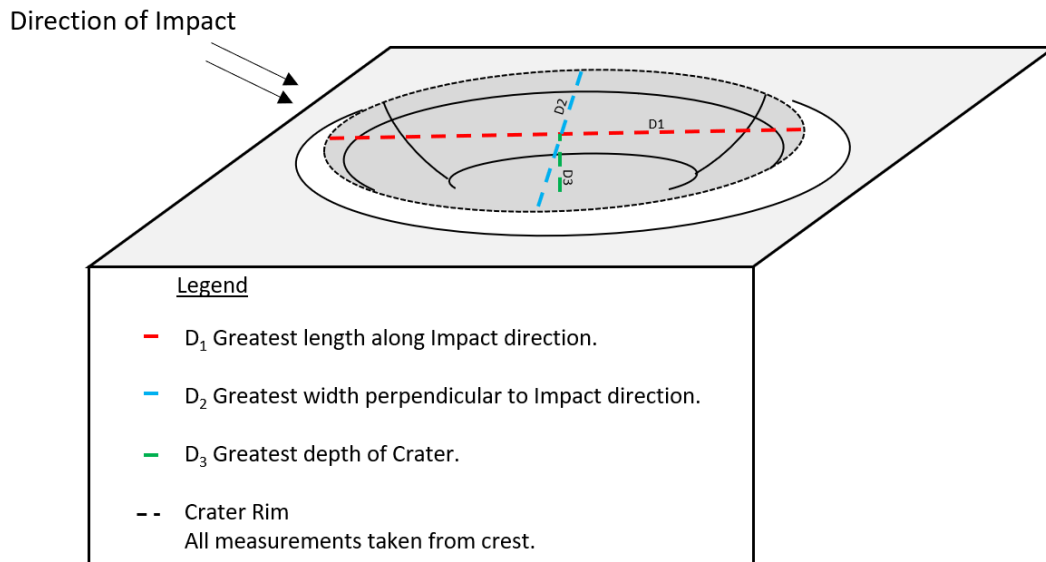
Figure 4.3: Impact Excavator experiment crater measurement standard for physical and DEM trials.

It was initially intended to repeat the impact and measure each setting at least three times to reduce uncertainty due to measurement errors, however the Impact Excavator was progressively damaged throughout the experiments due to weakness of the PLA plastic, 3D printing process and design. The prototype did not survive long enough to complete all the repeated measurements.

The experimental setup is shown in Figure 4.4. The target sample is shown under the protective sheath in Figure 4.5. The corresponding experimental setup for the DEM modelling is shown in Figure 4.6.

Figure 4.4: Impact Excavator laboratory testing facility setup.

Figure 4.5: Impact Excavator sand target zone setup.
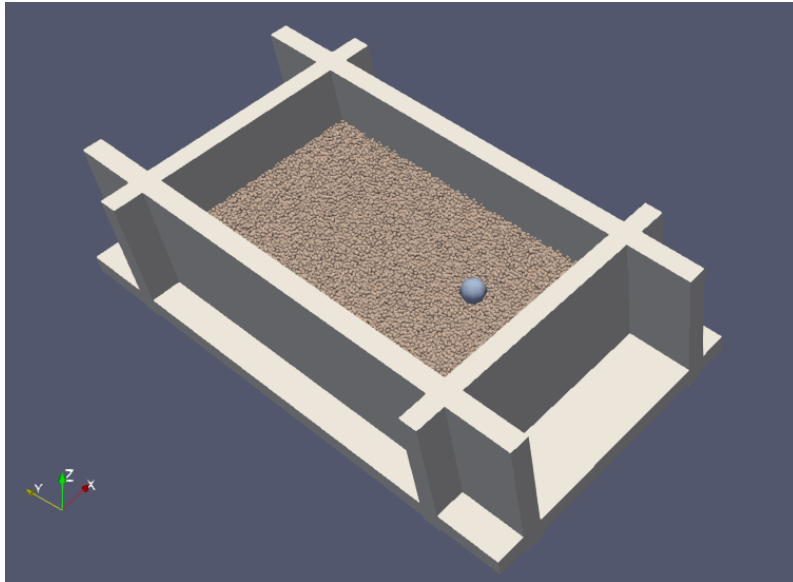
Figure 4.6: Impact Excavator DEM setup.

4.5.2.4 DEM Modelling

The parameters used for calibrating and modelling beach sand and lunar regolith for this experiment are the same as used for the model developed in Chapter 3. These model parameters have also been shown to be valid in literature [46, 47, 267]. The material properties targeted for calibration in this experiment are shown in Table 4.4 with relevant references.

Table 4.4: Material properties used for Impact Excavator DEM model with references.

	Dry Sydney Sand	Loose Lunar Regolith	Stainless Steel
Friction Angle (°)	34 [68]	54 [39]	29 [164]
Cohesion (Pa)	Not Used	1000 [39]	Not Used
Particle Density (kg/m^3)	2650 [68]	3100 [266]	7990 [164]
Poisson Ratio	0.2 [288]	0.25 [266]	0.3 [164]
Young's Modulus (Pa)	50×10^6 [68]	9×10^7 [145]	193×10^9 [164]
Particle Radius (mm)	0.86 +/- 0.17	0.86 +/- 0.17	6

The DEM experiments were conducted as follows:

1. Set up the DEM model using appropriate material properties as per Table 4.4.

2. Calibrate the DEM model by minimising the crater diameter error (DEM diameter minus physical diameter) for a set of four possible DEM damping factors.

3. Use the calibrated model to produce impact simulations of regolith under the Earth's gravity (9.81 m/s^2) and the Moon's gravity (1.62 m/s^2) for selected impact velocities and angles.

4. Measure the impact crater length, width and depth with Paraview software and note any qualitative effects. The length and width of the crater must be measured from peak to peak of the crater rim to ensure standard results as per the generic crater dimensions in Figure 4.3.

5. Quantitatively compare the crater volumes for tests in both the Earth's and the Moon's gravity.

6. Visualise the difference in crater formation for each gravitational environment.

The volume of the crater is approximated using the dimensions $\frac{D_1}{2}, \frac{D_2}{2}$ and D_3 as the radii of an ellipsoid. The equation for the volume of the half-ellipsoid is shown in Equation 4.1. This is an approximation only. The crater walls in reality are not perfectly ellipsoidal and the rim is not of equal height at all points. The crater volume is also not equal to the useful excavation volume of the Impact Excavator as much of the crater volume is due

to material excavated towards the rim of the crater. In reality much less material will be recoverable by the excavator. More experimentation and optimisation are required to determine the material recoverability, although lower lunar gravity is expected to allow higher recovery rates. The half-ellipsoid method is the most practical to achieve standard measurements and results across both physical and DEM experiments, hence its usage for this purpose.

$$Approximate\ Crater\ Ellipsoid\ Volume\ (mm^3) = \frac{2\pi D_1 D_2}{3} D_3 \qquad (4.1)$$

4.5.3 Discrete Element Model Calibration

The Discrete Element Model for the Impact Excavator has been calibrated by minimising the measurement error of D_1 and D_2 between DEM and physical experiments. These dimensions are measured from the DEM model and the physical experiment as shown in Figure 4.3. The error is calculated according to Equation 4.2. It is an average of the error between DEM and Physical diameters D_1 and D_2 at four different velocities. The error is minimised by repeating the test with varying damping factors until a minimum is identified.

$$Measurement\ Error\ for\ D\ (mm) = \frac{\sum_{t=1}^{n} (DEM_t - physical_t)}{4} \qquad (4.2)$$

Where t is the trial number, conducted at a specific velocity. n is the number of different velocity experiments used in the calibration. In the case of this calibration, n=4. DEM_t represents D_1 or D_2 measured from each Discrete Element Method output t, and $physical_t$ represents the equivalent measurements taken from a physical experiment t.

The minimised Measurement Error for both D_1 and D_2 comparisons is achieved with a damping factor of 0.07 for this model. The full results of the calibration process are shown in Figure 4.7.

The model is then compared against a broader set of physical experiments as shown in Figure 4.8. It can be seen from these results that the DEM model is appropriately estimating crater volumes depending on changes in impactor velocity and the angle of incidence.
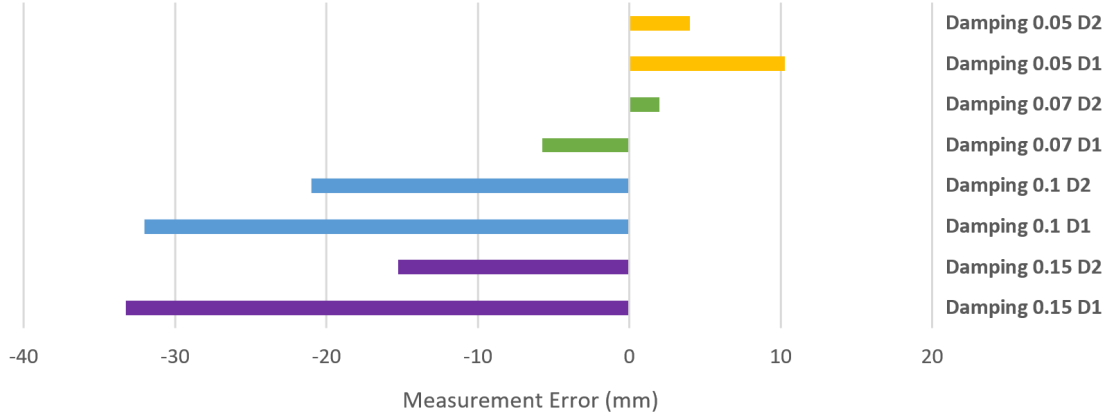
Figure 4.7: Calibration of Impact Excavator DEM model.
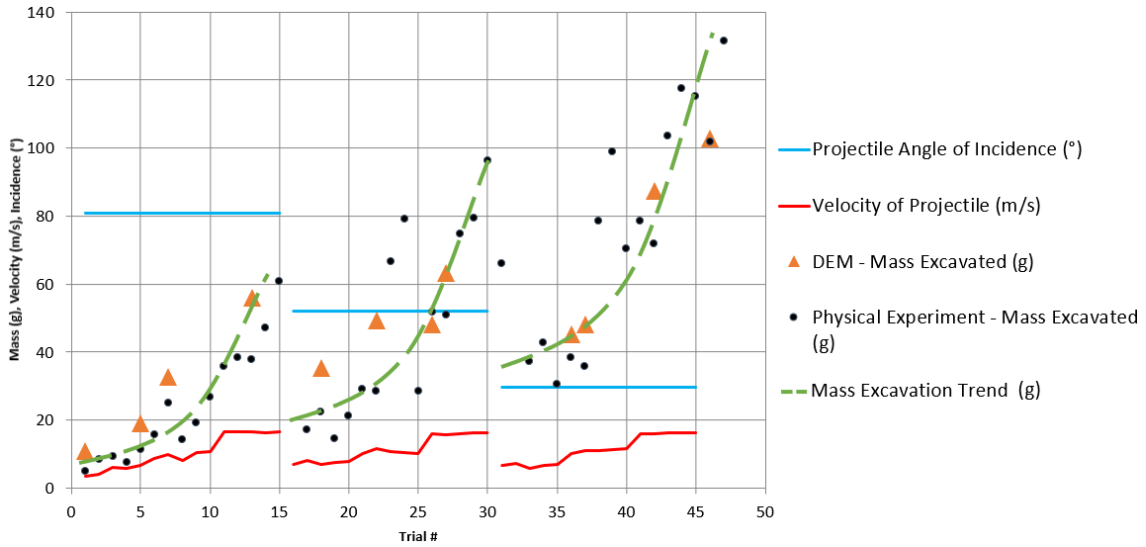
Figure 4.8: Calibration data for Impact Excavator DEM model compared to physical experiments.

4.5.4 Results

The lunar regolith DEM experiment has been used to demonstrate the functioning of the Impact Excavator in regolith on the Moon. It was hypothesised that the low lunar gravity would improve the efficiency of impact crater development and allow this novel excavation method to function more effectively than on Earth. Figure 4.9 shows the results of a comparative experiment conducted under both the Earth's gravity and lunar gravity. The increase in crater volume is shown for four separate impactor tests. There is a significant increase (greater than 40% in some cases) in the volume excavated on the Moon using the same equipment parameters.

Figure 4.10 visually shows the effects of the Impact Excavator under the Earth's surface gravity and lunar surface gravity in parallel. The visualisation shows many more particles outside of the crater are also lifted from the surface during the lunar test. These particles are not included in the crater volume calculation. This observation demonstrates how dust hazards may be created more easily on the Moon and also how the Impact Excavator may be able to take advantage with an optimised collection system.
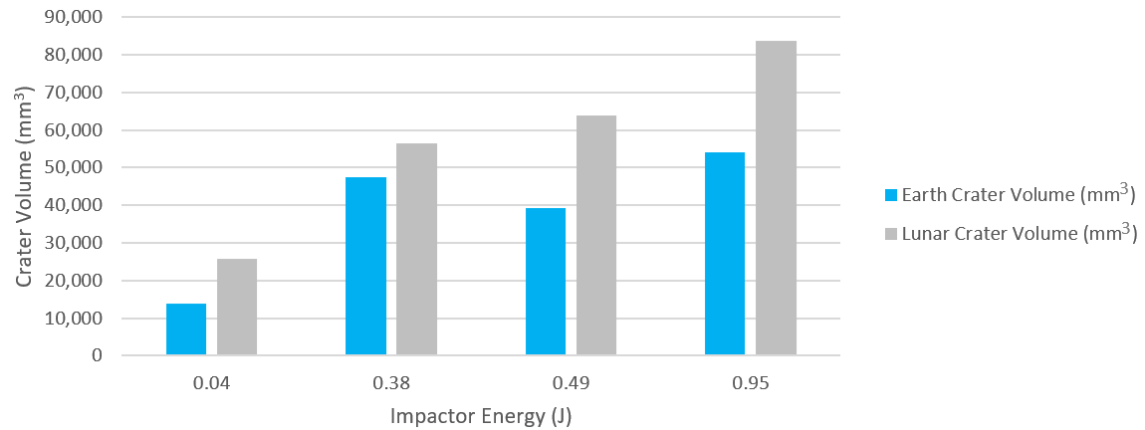
Figure 4.9: Results of the calibrated Impact Excavator DEM model compared under terrestrial and lunar gravity.
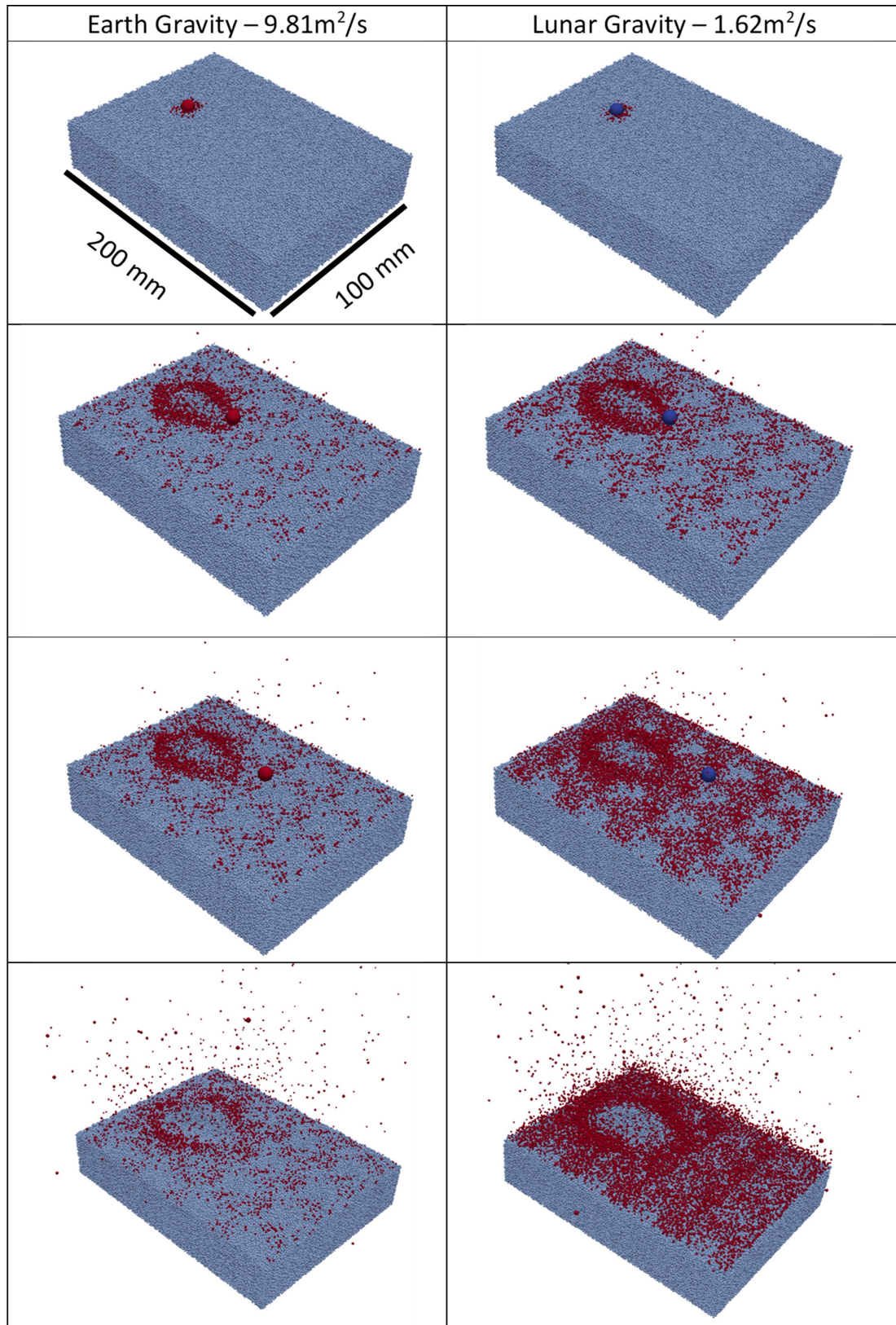
Figure 4.10: Visualisation of Impact Excavator DEM model in terrestrial and lunar gravity.

4.5.5   Discussion

The Impact Excavator worked as expected for unconsolidated material. Causing a crater to be excavated, with the size of the crater depending on the angle of incidence, impact velocity, material properties and gravitational field. More exotic effects such as the potential impacts of temperature variations, vacuum conditions, and static charges that may be present on the lunar surface have not been included in this study. More data is required to understand the effects of these conditions, if any.

There were issues encountered during the experiments with the toughness of the 3D printed mechanism. The vanes of the centrifugal wheel slowly deteriorated over the life of the experiment due to the high acceleration forces from the steel ball bearing impactor. This can be seen in Figure 4.11 as small red particles of PLA plastic break off progressively from the prototype. Future iterations of the design must aim to reduce these forces as much as possible. A stronger material and manufacturing process should also be used.

It is noted that the final projectile velocity is reduced by aerodynamic drag due to the presence of an air medium. This will not be the case in the vacuum of the Moon. It is suggested that the use of a dirty vacuum chamber could assist this investigation in the future to reduce the atmospheric effects experienced in this experiment.

The original experimental objectives included trialling the capabilities of the Impact Excavator on a harder icy regolith. These tests were initiated but unable to be completed due to several reasons. Mainly, the deterioration of the 3D printed parts of the Impact Excavator but also due to difficulties in maintaining constant target material temperatures during the experiment. A re-design of the experiment and a stronger prototype of the excavator will be required to complete these icy regolith tests. Construction of a second prototype was not feasible during this research due to pandemic related laboratory closures and uncertainties. However, some observations of the Impact Excavator's effectiveness on harder icy material were made before failure of the system. The following qualitative and anecdotal observations can be used for future system improvements.

The ice content appeared to have a significant effect on the strength of the target material and effectiveness of the Impact Excavator. Lower ice content and higher temperature materials were weaker and more susceptible to impacts. Higher ice concentrations and lower temperatures did not appear to be susceptible to the impact velocities trialled in this experiment. The temperature of the target samples increased rapidly after starting the experiment. This caused changes in the hardness of the material in the region directly in front of the Impact Excavator. The change in temperature of the target sample is shown in Figure 4.11. This was discovered to be caused by a constant flow of warm air exhausted from the acceleration wheel mechanism. This is shown in Figure 4.12. The soft melted region was far easier to excavate compared to the hard ice region. In future, and in order to properly validate these experiments, this melting needs to be controlled. This may be achieved by a thermal inertia sink (some larger mass of cold material) and operating inside a dirty vacuum chamber. This also raises the potential for a future improvement of the system; if lunar icy regolith can be warmed and its strength decreased in-situ on the Moon, that may enable easier excavation. The effectiveness of using this technique will depend on the availability of energy at the ISRU site on the Moon. A site with excess thermal energy, perhaps powered by a nuclear reactor could apply a heating technique to reduce the strength of icy regolith, enabling rock breakage with much less mechanical force.
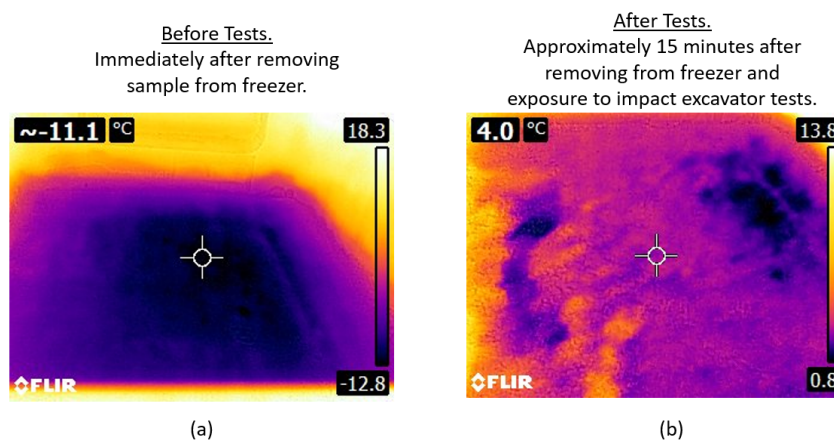
Figure 4.11: Temperature of target material before and after experimentation taken by FLIR thermal imaging camera.
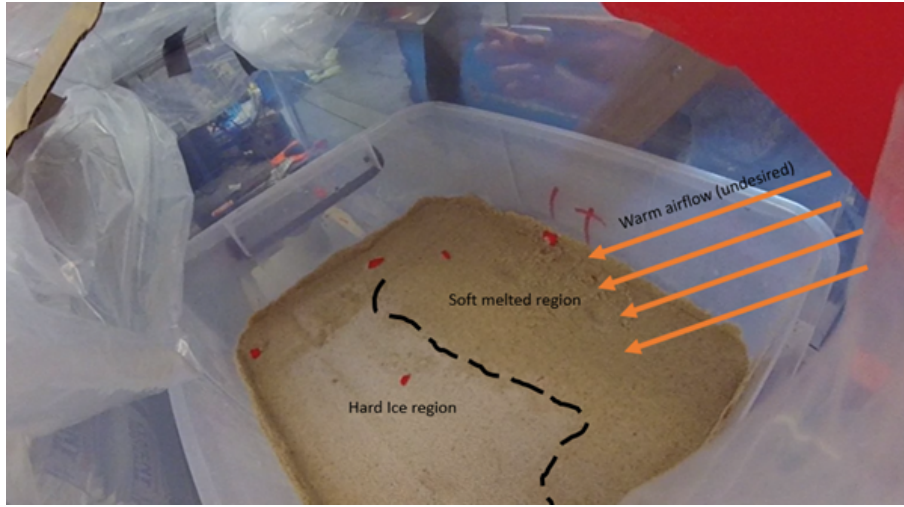
Figure 4.12: Variation in ice hardness due to warm airflow.

4.6   Drill and Pull System

4.6.1   System Design

It is widely known amongst rock mechanics professionals that rock breakage occurs most easily by propagating tensile fractures in rock [35]. The Griffith criterion [12] is used to explain why imperfect materials such as rocks break at far lower stresses than would be otherwise expected. It considers that flaws in the material allow stresses to be concentrated in small areas where tensile cracks can occur and propagate [12]. Previous rock mechanics studies look at different methods of measuring and quantifying the inherent flaws in rock as they play an important role in rock breakage and overall mining productivity. The tensile strength of rock is usually measured with an accepted standard called the Brazilian or indirect tensile strength test [127,168]. This test involves the application of a compressive force on a standard disc shaped sample to indirectly measure a tensile failure. In most cases for rock, the sample will break in tension prior to any compressive failure, demonstrating the lower tensile strength.

Currently there are only limited rock breakage mechanisms available in space resources literature as identified in Section 4.3. The Drill and Pull rock breakage concept aims to

improve that deficit. Figure 4.13 shows the concept visually. Firstly, the system requires a free face to maximise efficiency of breakage. The free face can be the original surface of the rock or a previously excavated face. It is expected, that as with terrestrial excavations the breakage and excavation efficiency will be increased with the assistance of gravity. Hence a vertical face is preferred to the original horizontal surface [62]. This system requires a hole to be drilled in a hard rock material, similar in strength to moderate UCS concrete, where the conical-ended Pull Rod is inserted. A hard crushing media, such as steel is used to fill the remaining void in the hole. A steel plate is placed on top of the hole to ensure the crushing media is confined and cannot escape when mechanical work is applied. The final step is to pull the rod to compress the crushing media and exert outwards force onto the free face causing tension cracks and eventual breakage.

The expected mode of failure is shown in Figure 4.13. It is expected to be a combination of tensile crack failure and crushing, however this must be carefully observed during the experiment and further work will be necessary to properly define the mechanism for optimisation. It is expected that the sample will fail slowly as increasing force is applied to the anchor and top surface. A limit may be reached where the sample has failed sufficiently to allow the anchor to be released yet the sample has not been completely broken for excavation.
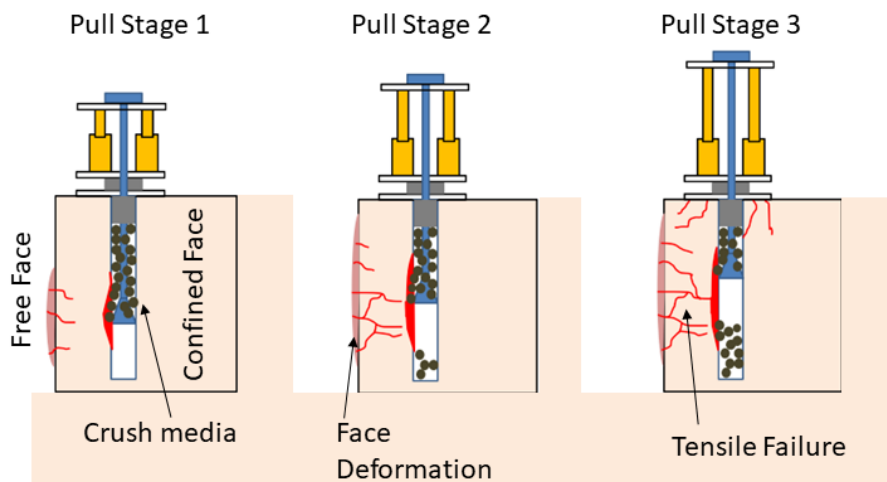
Figure 4.13: A conceptual drawing of the Drill and Pull rock breakage mechanism.

A free-body diagram of the system and its components can be seen in Figure 4.14. Newtonian steady state resolution of forces has been chosen here to communicate the working of this system, although in practice it is a dynamic system and better modelled with DEM.

It has been assumed that the crush media will be spherical, which is achievable if steel bearings are used. However, it is also desired to utilise different media such as drill cuttings and gravel which are easier to obtain on the surface of the Moon. The mechanism can be scaled-up or down depending on a later iteration system-mass optimisation study for lunar ISRU. An optimisation study such as this may use the Project Appraisal indicators developed in Chapter 7 as a basis.
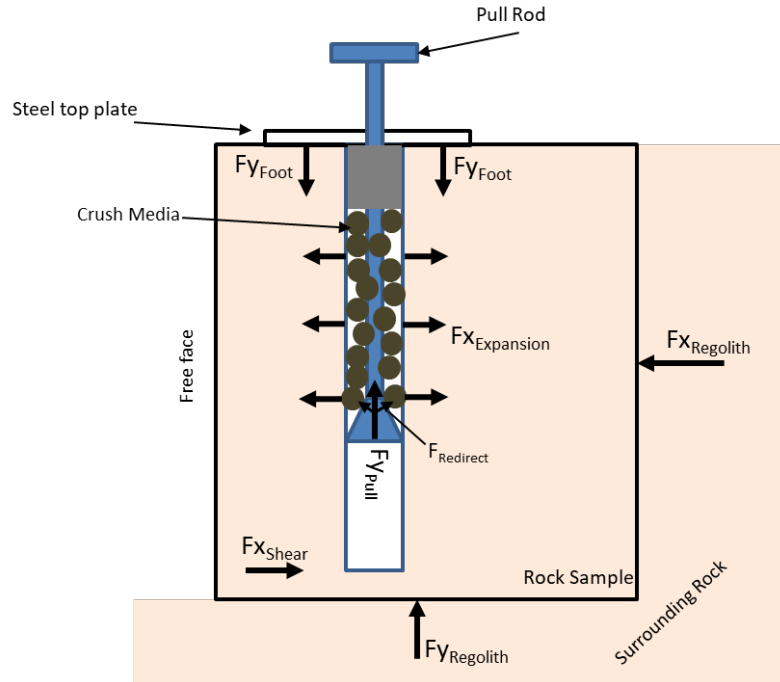
Figure 4.14: A rock mass free body diagram when applying the Drill and Pull rock breakage mechanism.

The Drill and Pull mechanism will be demonstrated here using the Discrete Element Method similar following the works in Chapter 3.

4.6.2   Proof-Of-Concept Experiments

4.6.2.1   Aim

The aim of the DEM testing for the Drill and Pull system is to demonstrate a proof-of-concept in lunar conditions. This will allow a recommendation to be made whether or not to proceed with a physical prototype. The DEM testing may also provide some insights into the ground engaging mechanism that can be used for early stage optimisation. A qualitative simulation of the Drill and Pull system will be carried out with DEM to achieve this objective.

For the purpose of Objective 1 of this thesis, these experiments also demonstrate the utility of the Discrete Element Method for off-Earth mining system development and optimisation.

4.6.2.2   Method

There are currently no available published DEM parameters for icy regolith. In fact, there is an ongoing debate about the level of consolidation of icy regolith expected in Permanently Shadowed Regions (PSRs) on the Moon. In some cases, it is believed that the material will be in an unconsolidated state due to constant impact gardening. In other cases, it may be in a harder consolidated form [36]. As there have been no geomechanical observations of ice on the Moon to date, the discussion is still open. As mentioned, experiments by Atkinson and Zacny [9] show a 12% H_2O concentration icy regolith simulant (JSC-1a) has a strength of around 35 MPa, similar to concrete [299]. Given the similar strength of concrete and icy regolith according to Atkinson and Zacny's [9] results, the Drill and Pull method will be trialled in a DEM model using concrete as the target material.

The method for conducting this experiment is as follows:

1. Setup the target material using the Concrete Particle Model (CPM) proposed and calibrated by Šmilauer [267].

2. Set up the DEM model with appropriate sized Pull Rod and steel ball bearing crushing media. Dimensions for the relevant particles are shown in Table 4.5.

3. Pull the rod through a stabilised sample while recording data.

4. Qualitatively analyse data with Paraview software to confirm the proof-of-concept.

Table 4.5: Setup dimensions in Drill and Pull experiment.

Dimension	Value (mm)
Crushing Media Diameter	10
Pull Rod Diameter	12
Hole-Rod Clearance	4
Top Plate Thickness	9
Sample length	110
Sample width	110
Sample height	100
Particle Diameter	1.83 +/- X, where $X \sim Uniform(0, 0.55)$

4.6.3 Concrete Particle Model Calibration

The Concrete Particle Model proposed by Šmilauer [267] will be used for this experiment. Šmilauer [267] outlines a calibration process for this model similar to the methods outlined by Wang [303] and Tran [293]. Alternative novel calibration techniques could also be used, such as the implementation of an optimisation algorithm based on genetic algorithms [71] or kriging [18] to determine the correct micro properties that correspond with desired macro properties. A detailed review of DEM calibration procedures has been completed by Coetzee [47] for reference.

The CPM is similar to the Bonded Particle Model (BPM) [229] used in the PFC2D and PFC3D software [128]. The CPM however, utilises an expanded interaction space for each discrete element in the setup of the model, which allows particles to interact which are

not in direct contact. This leads to more realistic ratio between compressive strength and tensile strength for brittle rock breakage [252]. The CPM also includes two macroscopic stress induced features of material breakage. Firstly, tensile cracking damage and secondly, the hardening of plasticity in compression. Rate dependant damage (viscosity) has also been investigated by Šmilauer [267]. However, it is not included in the baseline CPM model used here as it has been found to have minimal effect.

Šmilauer [267] has provided some recommended values for a calibrated concrete model. These values are used for the demonstration of the Drill and Pull method in concrete. They are shown in Table 4.6.

Table 4.6: Material parameters and references used for the Drill and Pull DEM Model.

CPM Parameter	Value
Particle Density	4 800 kg/m^3
Friction Angle	38°
Young's Modulus	24 GPa
Poisson's Ratio	0.2
Initial Cohesion (σ_T)	3.5 MPa
Relative Ductility $\epsilon_\mathrm{f}/\epsilon_0$	30
Strain Crack Onset ϵ_c	1×10^{-4}

A uniaxial compressive strength (UCS) test has been run with the parameter values shown in Table 4.6 to confirm the validity of the calibration. The sample tested has a height of 150 mm and a diameter of 75 mm, complying with standard concrete UCS testing procedures [299]. The results of the UCS test are shown in Figure 4.15. It can be seen that the UCS of this sample is approximately 34 MPa, marked with a red line. This corresponds with weak to moderate strength concrete from a range of UCS test data collated by Vu *et al.* [299]. This calibration also approximately matches the compressive strength of icy regolith observed in experiments by Atkinson and Zacny [9].

4.6.4   Results

The Drill and Pull experimental results can be seen in Figure 4.16. This shows a 3D projected view and cross-sectional view of the sample during the pulling process. Forces
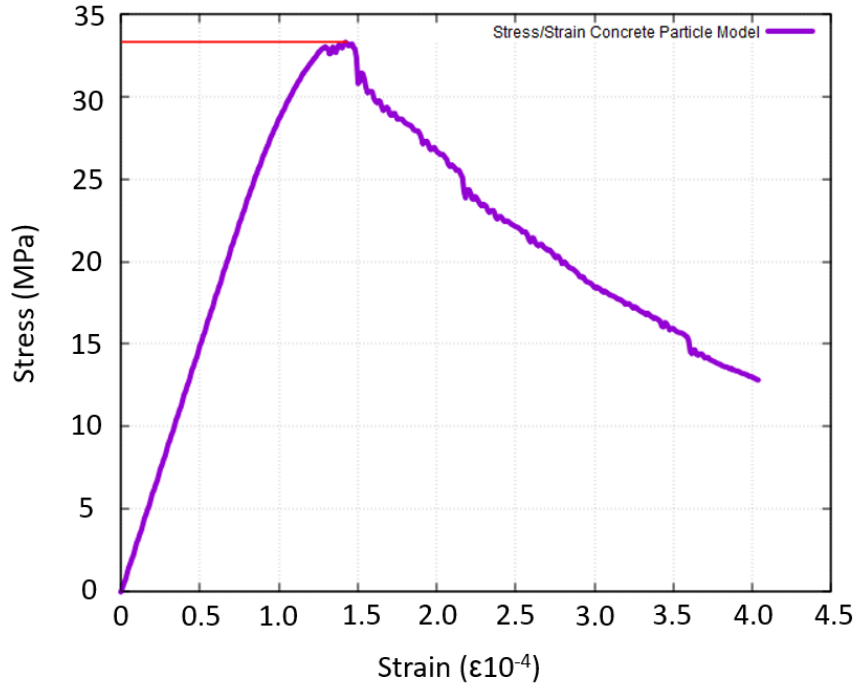
Figure 4.15: Calibrated Concrete Particle Model in a UCS test.

are redirected through the Pull Rod to the rock causing stress, damage, cracking and eventual failure in tension. Cracking recorded in the Concrete Particle Model is shown with the heat map in Figure 4.16. Cracked and weakened areas are indicated in red.

4.6.5 Discussion

The DEM experiment of the Drill and Pull method has shown that it is a physically viable concept and is worthwhile moving to a physical testing stage. This is a very simple conceptual design and there are many possible optimisations that may come about through a physical research and development cycle. For example, the use of different shaped or style pull rods could be trialled to increase efficiency of the system. As mentioned by Šmilauer [267], some aspects of concrete breakage are rate dependant, as cracks can only propagate at a certain speed. The use of a vibrating or percussive pull rod may be possible to optimise rate dependant breakage. Physical experiments were not carried out during the time of this research due to pandemic related laboratory closures and uncertainties.
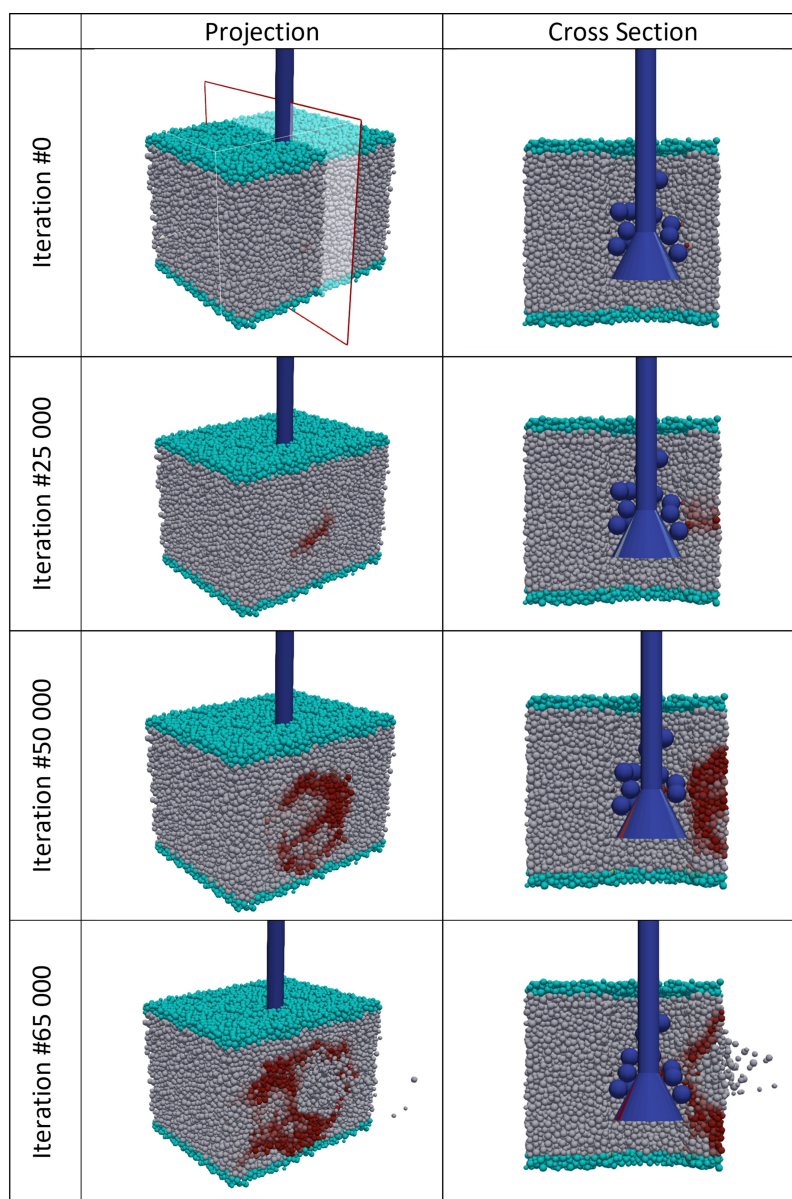
Figure 4.16: The results of the Drill and Pull DEM model showing accumulated crack intensity until failure.

One issue that has been foreseen with the physical implementation of the Drill and Pull system is the recovery of the crush media. Steel ball bearings have been suggested as they can be easily recovered using electro-magnetism. However, over time it is expected that the steel crush media will be progressively lost causing a long-term reliability issue. An

in-situ resource could be used instead to supply the crush media. For example, basaltic gravel or stones recovered from the target material. Modelling would need to be conducted to see the effectiveness of potentially weaker crush media and the impact this would have on productivity.

It has also been mentioned that the system requires a free face to enable rock breakage in tension and hence to work effectively. Almost all excavations will need to start without an available vertical free face. The ability of the Drill and Pull method to break rock via a horizontal free face also needs to be tested. This could possibly be done by drilling an inclined hole and breaking an initial "wedge" to achieve a more vertical free face.

There are many potential options to investigate with further modelling and physical experiments. This concept is theoretically functional for rocks with at least as strong as a moderate UCS concrete. It is expected to eventually be a useful addition to the off-Earth mining system inventory to remove the need for blasting H_2O regolith *ore* and the complex supply chain required for that activity.

4.7   Lunar Regolith Tunneller

4.7.1   System Design

The Lunar Regolith Tunneller shown in Figure 4.17 is an evolution of the terrestrial Continuous Miner [97]. It is also capable of pushing, bracing and anchoring against tunnel walls, picking rock faces, breaking hard material and loading granular material into the transport mechanism.

This rock cutting mechanism is a well-developed technology. Experimental data is available to assist with design optimisation and estimation of energy consumption. The power input has been calculated using this data in Equation 4.3 [14, 23].
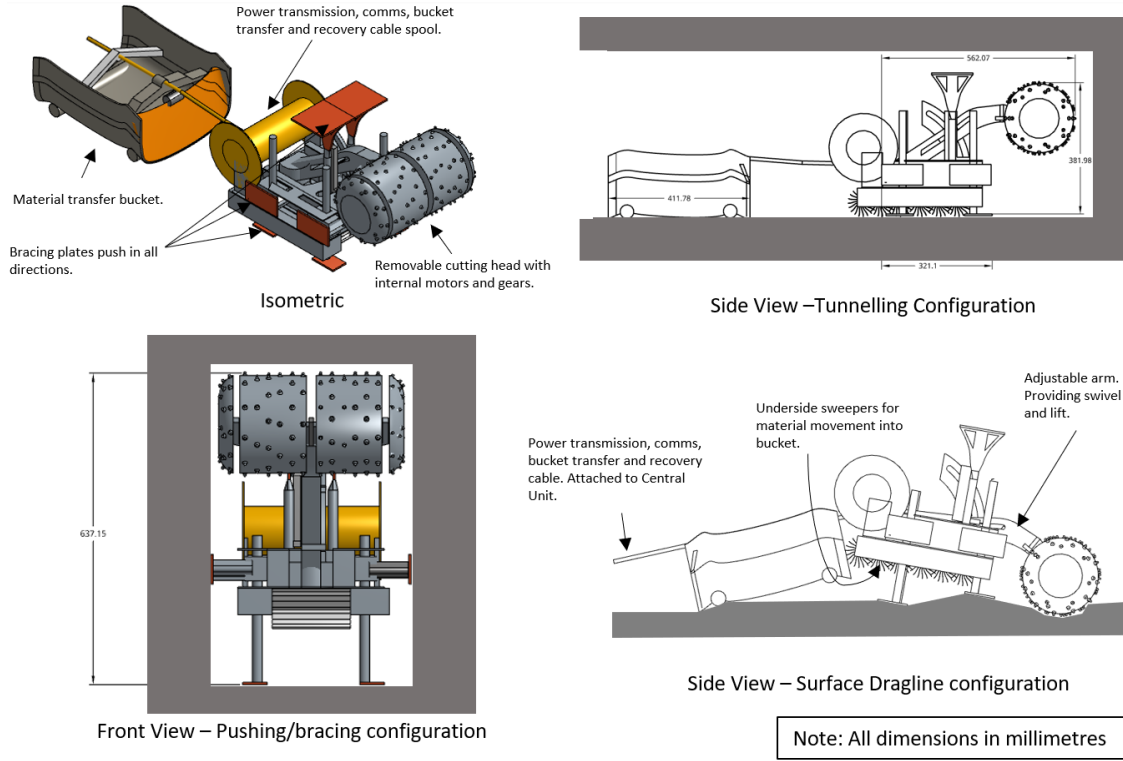
Figure 4.17: Concept design of the Regolith Tunneller and material transfer bucket.

$$Cutting\ Rate\ (m^3/s) = k\frac{P}{SE} \tag{4.3}$$

Where k is a breakage efficiency constant. Similar terrestrial Road Headers usually have a k value of 0.8 [324]. P is the input power in kW and SE is the Specific Energy (kWh/m^3) for 10% H$_2$O regolith. The expected SE for cutting 10% H$_2$O regolith is based on an expected UCS of icy regolith around 35 MPa [9], in line with concrete [299]. Data available from Balci *et al.* [14] and Bilgin emphet al. [23] show that the expected SE for this material is around 7.5 kWh/m^3.

Tungsten Carbide or diamond tipped cutting picks will be required to minimise wear and replacements of the cutter head.

One of the major strengths of the Regolith Tunneller is the ability to categorise material with additional sensors and select it's final destination. Undesirable material can be loaded

onto haulage equipment, not described as part of the Tunneller, and be sent via haulage equipment to a waste storage location. The waste disposal location is assumed to be a nearby area where both mine waste and process system waste are taken for final deposition. Conversely, the higher H_2O grade materials be selected to be transported to the energy intensive beneficiation process to heat and extract volatiles. Refer to Figure 4.1 for a representation of the material flow from Rock Breakage, to Excavation, to Transport, etc.

In a balanced system with surplus energy supply, almost all excavated material should go to the beneficiation process. Optimisation via a *cut-off grade* may be used to divert lower grade materials to the waste storage location to save energy for example. It is also possible that unplanned geological variances may lead to waste material being found in unexpected areas that must be mined to access more desirable material. The excavation system should be therefore intentionally sized larger than the capacity of any downstream process. This not only enables a stable production rate if maintenance issues are encountered, but also if geological issues are found. For example, if the mineral resource is found to be non-uniform and higher volumes of waste must be excavated.

An initial site survey and geological data collection during the excavation process will assist in selective mine optimisation. The application of *cut-off grades*, selective mining and the extraction sequence will be explored in much further detail in Chapter 6.

4.7.2 Excavation Planning and Improved Mining Methods

The Regolith Tunneller is a versatile piece of equipment. Variations in the excavation geometry and sequence are expected to yield higher productivity.

An example of increasing the excavation efficiency by utilising the bracing mechanism to push down pillars between pre-excavated voids is shown in Figure 4.18. This method ensures the rock will break in the weakest mode, tension, when pushing out the pillar. The Tunneller completes the excavation in sequence from #1 to #4, firstly excavating a central void (#1), then access tunnels (#2) to push the pillars for further extraction (#3).

The amount of energy expended for this breakage mode is expected to be less than for direct cutting. Optimising the thickness of pillars and maximising the volume extracted via this efficient breakage method can be done with DEM modelling once more calibration data is available for icy regolith.
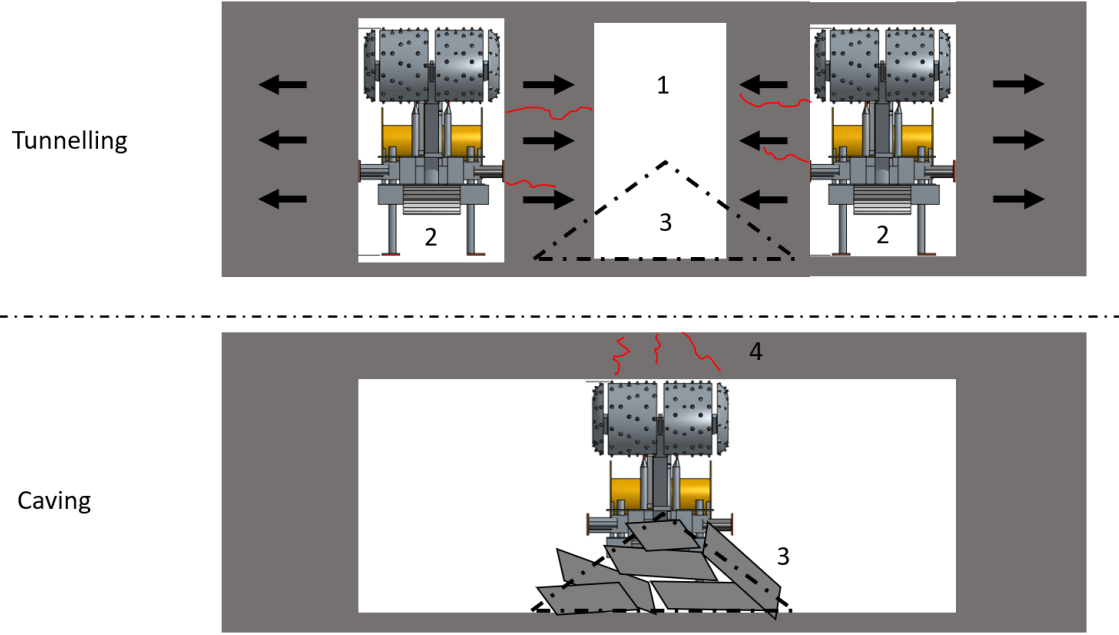
Figure 4.18: Regolith Tunnellers extracting wall pillars by pushing into open void.

Even further increases in excavation efficiency can be achieved by creating sufficiently wide spans without pillars and inducing collapse of the roof (#4) while the tunnellers are in a safe location. This caving method is expected to be the most energy efficient as gravitational energy is harnessed to do the majority of rock breakage. Further modelling is required with specific deposit geotechnical parameters, such as the natural fracture frequency and strength of the material to confirm the feasibility of this caving method. This caving method can be compared to block caving or sub-level caving in terrestrial underground mines [62].

The flexibility of the Regolith Tunneller gives rise to many contingent excavation plans. This can be used as a way to manage geological risks as the exact nature of the deposit will be unknown until excavation is complete. Modifications to excavation strategies can be made after the commencement of operations to carry out selective mining and optimise

production as more information is gathered.

4.7.3   Discussion

A significant risk for mining operations is that the *mineral resource* in reality is not as expected. This is more likely to be the case with extremely limited data as for lunar ISRU resources. The Regolith Tunneller manages this risk by having multiple contingency excavation plans available as mentioned in Section 4.7.2. The recovery of the *mineral resource* is therefore not entirely dependent on accuracy of the resource modelling or material parameters. Regolith strength, porosity, volatile permeability and uniformity of H_2O grade are examples of material parameters which have varying importance for each specific mining system. The Regolith Tunneller in comparison to others is flexible and does not depend on a high accuracy of any of these parameters.

A summary of the advantages of the Regolith Tunneller concept includes the following capabilities.

- Maximising the downstream processing output by selectively targeting higher H_2O grade areas.

- Minimising the dust creation by excavating consolidated regolith underground.

- Minimising the energy usage via gravity assisted excavation techniques such as caving.

- Providing the reaction forces by bracing against the tunnel walls.

- Including redundancy and flexibility with various excavation plan contingencies.

- Minimising the surface waste material movement and hence energy usage by directly accessing ore from underground.

- Utilising the weak tensile strength property of rock to break harder icy H_2O regolith.

The expected weaknesses are:

- the cutting heads may experience wear and need to be replaced;

- the excavation rate is limited by the material transfer bucket; and

- the material transfer bucket and transfer line may experience wear over long term.

The improved *mining methods* shown in Section 4.7.2 are an example of how a single *mining system* can be applied differently in various geological or geometric settings. This will be touched upon again in the next chapter, which specifically focuses on selecting *mining systems*. It is evident that with the current immature state of off-Earth mine planning that a high level of detail is not possible when describing *mining methods*. Although in practice and as is evident in terrestrial mining [62], improved *mining methods* will be an important tool in optimising future ISRU operations.

4.8 Conclusions

The Discrete Element Method has been shown to be useful when developing ISRU systems that physically interact with materials such as regolith or ice. It allows faster prototyping to bypass some traditional physical testing of ground engaging tools, especially for when it is difficult to simulate lunar conditions such as gravity.

The Impact Excavator aims to minimise reaction forces and equipment mass with a new excavation technique. However, it also creates a dust hazard that may be problematic for longer term reliability. The Impact Excavator works conceptually in low strength material but may struggle with harder ice and rock. The limits of its use need to be further explored within a better controlled environment. Increasing thermal inertia in the test sample and less atmospheric effects are desirable properties of future physical tests. The manufacturing process also needs to be improved to produce a more robust

acceleration mechanism. The results of this experiment can however, be used to optimise future iterations of the excavator.

Future research can be undertaken to investigate the effectiveness of the Impact Excavator on harder materials using repeated strikes. DEM and physical experiments can be used for this purpose.

The Drill and Pull system enables rock breakage via mechanical tension cracking with minimal equipment mass. This equipment is not standalone. It must be used in conjunction with another drill and excavator-type piece of equipment. Further mechanical design improvements can be made after some physical testing to identify reliability issues. As there are currently not many concepts available for off-Earth rock breakage, this system can be used to unlock harder, high grade deposits without the need for complex explosives manufacturing and delivery systems. The benefits of mining higher grade deposits will be further explored in Chapter 5 and 6.

The Lunar Regolith Tunneller enables targeting and selectively mining higher *ore grades* without wasting energy moving large amounts of waste. It creates reaction forces by bracing on tunnel walls, thereby minimising the gravity dependent reaction forces and equipment mass requirements for that purpose. It also efficiently combines the rock breakage and excavation tasks for harder icy resources. Tunnel stability modelling in Chapter 3 shows that tunnelling is unlikely to be feasible for equipment larger than around 10 cm diameter. However, tunnel stability will increase significantly in icy regolith. Further physical testing is required to determine reliability and operability of the Tunneller when working underground in icy regolith.

There are many examples in literature of lunar mining systems that could be applied to the ISRU task, which have been collated in Table 4.2. Three more concepts have been proposed in this chapter. All these mining systems have been categorised based on their function in the mining process and also their Technology Readiness Level. The criteria to achieve TRL 5 is "component/breadboard validation in a relevant environment". It can be implied from the number of systems that are currently at TRL 4 that there are difficulties in developing

these systems in environments relevant to the lunar surface. Discrete Element Method has been used in this chapter as a rapid and low-cost technique to assist in the development of the system without having access to relevant testing environments. Although, physical experiments in a relevant environment will still be required to increase the TRL according to the NASA criteria [137].

The next step of the mine planning and optimisation process is to select the best system combination for extracting a foreseeable lunar H_2O deposit type. The items collated in Table 4.2 with appropriate Technology Readiness Levels will be used in the following chapter for the task of mining system selection.

Chapter 5

Off-Earth Mining System Selection

5.1 Introduction

Mining system selection is an important early phase in the design and planning of mineral extraction. It is undertaken prior to a full economic feasibility study, which is used to confirm or reject the selection. Once a system has been confirmed and operations have begun, it is challenging and costly to change systems. The Nicholas Mining Method Selection procedure [213] is one of the more well-known frameworks for this task in terrestrial mining. It uses empirical data from example mines around the world to rank *mining methods* based on the characteristics of a given ore body.

The lack of operational data to represent off-Earth mines in this process is problematic. Currently, off-Earth mining system selection is undertaken subjectively. This may lead to authors favouring certain popular works or their own for ISRU project evaluations as discussed in Chapter 2. This chapter aims to develop a framework that can be objectively applied to off-Earth *mining system* selection by using the available knowledge detailed in Chapter 4, with a focus on conceptual systems engineering. This is in line with the thesis Objectives 3 and 4, related to identifying and resolving deficiencies in the currently available planning and optimisation methods for ISRU.

A logical selection framework is proposed and demonstrated in this chapter instead of the empirical ranking methods used for terrestrial *mining method* selection. Ranking in this chapter is based on the probability of success of the *mining system*, also known as the equipment reliability. The framework will be progressively disclosed due to the depth and complexity via partial demonstrations of the tools investigated throughout the chapter.

In the future, this new framework can assist selecting systems for the range of different geological settings that could be found on the Moon or other bodies. The process in this chapter primarily focuses on mining of H_2O resources, but can be expanded to other resources as well.

5.2 Literature Review

Mining method selection has been studied as an essential part of terrestrial mine design for several decades. The majority of researchers have built upon the Nicholas Mining Method Selection procedure [213]. The Nicholas procedure defines several key characteristics of an ore deposit that affect the suitability of each mining method. The deposit characteristics used for selecting mining methods are the ore body shape, thickness, dip angle, grade distribution and the rock strength of the ore zone and surrounding rock. These characteristics are assigned numerical scores (0-4) depending on how well each *mining method* will be suited. A score of -49 is also possible to completely discount a method due to a particular deposit characteristic. The method with the highest overall score should then be used in the next stage of mine design in a feasibility study.

The popular UBC (University of British Columbia) Mining Method Selection procedure [192] is a modified version of the Nicholas procedure. It applies new weightings to each of the deposit characteristics depending on their importance when selecting a *mining method*. The weightings are based on empirical data from the Canadian mining industry in 1994 with an intentional bias toward long hole stoping [192]. The bias is due to a large portion of underground mining in Canada being conducted by mechanised long-hole stoping, where

ore is extracted vertically between tunnels utilising drilling, blasting and gravity.

Descriptive language is used to define the boundaries between different characteristics in both the Nicholas procedure and the UBC procedure. For example, the Ore Thickness can be defined as "Narrow", "Intermediate", "Thick" or "Very Thick". Saydam, Mitra and Russell [249] improved the UBC method by defining this thickness variation and use Virtual Reality technology to visualize the deposit. This new tool is called ViMINE. However, ViMINE was developed only for teaching purposes.

More recently, other authors have built on these techniques by implementing fuzzy variables and pairwise decision-making techniques [24, 244, 311] to account for the uncertainty in the linguistic categories used previously.

Just *et al.* [136] have completed a review of current off-Earth mining equipment research, and have noted the difficulty in comparing various works on a common basis. The lack of operational data and under-developed *mining systems* makes it difficult to carry out pairwise comparisons based on the effectiveness of demonstrated systems as has been done with UBC and Nicholas procedures. This limits the ability to compare and select mining equipment. Hence, a framework for off-Earth *mining system* selection has not yet been attempted. A new selection procedure as shown in this chapter may aid technology developers and decision-makers in designing off-Earth mining missions with the highest probability of success.

5.3 Methodology

Several tools will be investigated to determine their applicability to off-Earth *mining system* selection. As this chapter is aimed at developing a new selection procedure, the investigation has been divided into detailed sections to demonstrate each of the potential tools. The following Sections 5.4 to 5.10 are designed to review available tools, develop new tools and analyse their effectiveness to provide demonstrative results in Section 5.11.

A review of literature has been completed to identify appropriate tools already available, or closely related tools which may be modified or developed for the purpose of this chapter. Where appropriate tools are available in previous literature, they have been detailed and applied in worked examples. Where there are no appropriate tools available, they have been evolved from closely related tools in other scientific works. Each of these tools is also demonstrated by an example application.

Not all of the tools investigated have proven useful for the final framework. However, the negative results and analysis are still important contributions and will be described in this chapter.

5.4 Axiomatic Design

The theory of axiomatic design proposed by Suh [280] can be applied to many different engineering design fields to enable a "top-down" functional approach to the design process [152, 237, 281–283]. This is in contrast to a "bottom-up" development processes based on experimental trial and error [219]. Terrestrial applications of this method are most commonly found in manufacturing engineering, software engineering and mechanical engineering domains [152, 219, 234] and can be extended to any engineering design process.

The axiomatic design process is based on fulfilling two primary axioms. Firstly, the Independence Axiom, which states *"An optimal design always maintains the independence of Functional Requirements (FRs)"* [219]. It means that when designing a system or product, each functional requirement should be mapped to an independent parameter called the design parameter (DP). The DP ideally will not affect any other FR. However, in many cases it inevitably does.

Mapping is carried out through matrix multiplication, as shown in Equations 5.1 and 5.2 for an independent design with two FRs. Note that when the mapping matrix "A" is a diagonal matrix, the design is considered uncoupled. FR1 and FR2 do not affect each other. This is the ideal situation according to the Independence Axiom [219].

$$F = AD \tag{5.1}$$

Where F is a vector of Functional Requirements, D a vector of Design Parameters and A is the mapping matrix. F and D contain respective lists of the system's FRs and DPs.

The independent, uncoupled design parameter mapping is shown in Equation 5.2.

$$\begin{bmatrix} FR1 \\ FR2 \end{bmatrix} = \begin{bmatrix} x_{11} & 0 \\ 0 & x_{22} \end{bmatrix} \begin{bmatrix} DP1 \\ DP2 \end{bmatrix} \tag{5.2}$$

Where x_{11}, x_{22}, x_{21} in Equation 5.3 and x_{12} in Equation 5.4 are FR:DP mapping variables. In the most common qualitative application of this process, they usually take the pseudo-value of one. It is acceptable to have a design where the "A" mapping matrix is triangular rather than diagonal as shown in Equation 5.3. This is called a decoupled design [219] as the DPs do affect each other. However, since the functions (FRs) are designed in a specific sequence allowing a triangular matrix, the dependent relationships between DPs are manageable as long as parameters are manipulated in the correct order. The decoupled design parameter mapping is shown in Equation 5.3.

$$\begin{bmatrix} FR1 \\ FR2 \end{bmatrix} = \begin{bmatrix} x_{11} & 0 \\ x_{21} & x_{22} \end{bmatrix} \begin{bmatrix} DP1 \\ DP2 \end{bmatrix} \tag{5.3}$$

The third possibility is a coupled design, as shown in Equation 5.4. This design has both FRs linked together in the design parameter space. An example of a coupled design is a shower temperature and flow control system with a separate hot and cold tap. It is impossible to change the temperature without a change in the flow rate [219]. This is a poor design according to the Independence Axiom as the user will require a substantial amount of information in order to achieve specific results for flow and temperature. The success of satisfying an FR also depends on the tolerance of the user. The coupled design parameter mapping is shown in Equation 5.4.

$$\begin{bmatrix} FR1 \\ FR2 \end{bmatrix} = \begin{bmatrix} x_{11} & x_{12} \\ x_{21} & x_{22} \end{bmatrix} \begin{bmatrix} DP1 \\ DP2 \end{bmatrix} \tag{5.4}$$

The second Axiom, the Information Axiom, is used to determine the best design from a set of designs that satisfy the Independence axiom. The Information axiom states that; *"the best design is a functionally uncoupled design that has the least Information Content"* [219]. Where Information Content is defined by an index of the probability that the DP settings will satisfy the FRs. The information content is zero when there is certainty of success (probability of success = 1). Conversely, the information content approaches infinity as the probability of success approaches zero. The information content index is represented numerically using Equation 5.6 [219] where p_s is the probability of success the DPs will satisfy the FRs. The probability of success can also be considered as equal to the reliability (R) as shown in Equation 5.5. Reliability can be altered by changing the acceptable operating tolerance (increasing or decreasing the threshold of success) for the FRs.

$$p_s = 1 - p_f = R \tag{5.5}$$

$$I = \log_2(\frac{1}{p_s}) \tag{5.6}$$

The information index proposed by Suh [280] in Equation 5.5 requires the precise measurement of all probabilities of success, or probability density functions of success for each DP. This includes DPs which are influenced by others in decoupled designs [219] where conditional probabilities must be applied. In practice, it may not be possible to obtain all the required information to determine conditional probabilities. Certainly for this application, it is not currently possible to determine the real probabilities of success for each *mining system* as they have not been trialled operationally. An alternative method must be employed.

A new measure of the Information content has been proposed by Kulak and Kahraman [153]. They utilise fuzzy numbers to deal with uncertainty around linguistic DPs. The fuzzy approach requires a fundamentally strong understanding of the DP tolerances and FRs for the design in order to convert the DPs into fuzzy linguistic variables. This is similar to the Nicholas and UBC Mining Method Selection procedures, in that linguistic criteria are used to categorise deposits but can be interpreted differently by various people. This has been acceptable in the past for mining method selection as experienced engineers have an excellent fundamental understanding of the different deposit types and the systems that may be applicable. The tolerance for error for terrestrial mining method selection is also large and the subsequent stages of optimisation allow confirmation of the initial selections through proven processes. This is not yet true for nascent off-Earth mining systems and it is necessary to rank systems with a more objective process to guide technology development efforts, without requiring large amounts of operational data.

Section 5.8 and Section 5.9 of this chapter will detail the assessment of system complexity measures for suitability to replace the Information Content. These measures include graphical complexity, measures of design connectivity, design problem solvability [199, 262, 290] and a novel Monte Carlo reliability method. Application of the novel method will allow the Information axiom to be used to rank systems objectively and maintain the axiomatic design principles. It will also be possible to directly substitute operational reliability data as it becomes available in the future.

5.5   Off-Earth Mining Systems

Conceptual mining system designs drawn from a range of off-Earth mining and engineering publications [20, 184, 201, 208, 259, 263–265, 269, 284, 317, 319, 321, 323] and some novel contributions are categorised in Chapter 4. Systems that have been identified with a Technology Readiness Level [137] of 4 or greater will be used for works going forward in this thesis. These items have been successfully demonstrated in a physical laboratory and can be analysed at a functional level to create the required Design Parameter Maps. This

filtered list of equipment is shown in Table 5.1 with a link to the Design Parameter Map in text or the Appendix. These systems will be used for the demonstration of off-Earth mining system selection procedure in this chapter. The Impact Excavator, Drill and Pull mechanism and Regolith Tunneller introduced in Chapter 4 do not have appropriate levels of development (TRLs) to create the necessary Design Parameter Maps at this stage. These technologies are therefore omitted from Table 5.1.

Table 5.1: Off-Earth mining equipment pool.

Equipment Description	Subclass	Reference Examples	Design Parameter Map
Truck	Transport	[259, 264, 319]	Table 5.2
Bucket Drum Excavator	Excavation, Transport	[201, 269]	Table A.1.
Hammer Drill	Rock Breakage	[323]	Table A.5.
Discrete Excavator	Excavation	[263, 264]	Table A.4.
Continuous Excavator	Excavation	[263, 265]	Table A.2.
Load-Haul-Dump Excavator	Excavation, Transport	[264]	Table A.6.
Oven	Processing	[184, 208]	Table A.8.
Pneumatic Excavator	Excavation, Transport	[284, 317, 321]	Table A.9.
Crusher Oven	Rock Breakage, Processing	[184, 208]	Table A.3.
Micro Tunnel Borer	Rock Breakage, Excavation	[20, 323]	Table A.7.
Volatile Extraction Drill	Rock Breakage, Excavation, Transport, Processing	[319, 323]	Table 5.3

Each mining equipment listed in Table 5.1 has been broken down into their "core" Functional Requirements, and each FR is mapped to a Design Parameter. For the purpose of objectiveness in this study, a "core" Functional Requirement needs an explicit definition. It is defined as follows; *a Core Functional Requirement enables mining operations for the defined ore body disregarding the presence of mitigable environmental hazards.* Mitigable environmental hazards include radiation, temperature, atmospheric conditions, etc. They do not include gravity which is an intrinsic part of mining system design. Mitigable hazards do not include geologic hazards such as rock strength or variability which are taken into account during the mining system selection procedure or a later stage of feasibility. The need for the explicit use of core and auxiliary Functional Requirements is discussed

further in Section 5.10.

The process of breaking down a system into its Core FRs and mapping design parameters is iterative. The process flowchart is shown in Figure 5.1.
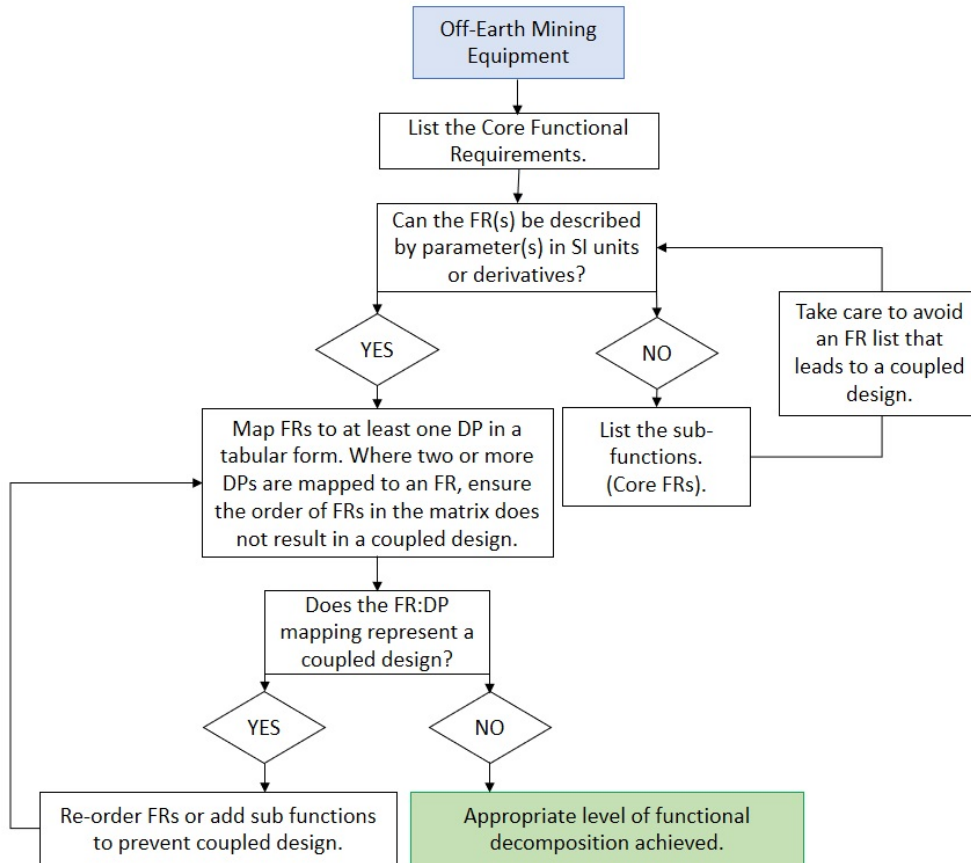
Figure 5.1: Process of Functional Requirement decomposition and Design Parameter mapping.

The aim is to achieve a level of decomposition that demonstrates a decoupled system where a triangular or diagonal mapping matrix is achieved. The level of FR decomposition carried out is also somewhat arbitrary unless additional rules are applied to ensure repeatability in the scientific method. This allows consistent comparisons of designs through axiomatic design principles. Consequently, this procedure requires that the decomposition of FRs be continued until all DPs can be measured with quantifiable SI units or derivatives. An example of FR-DP mapping is shown in Table 5.2 for the most straightforward design concept, the "Truck" [259, 264, 319].

Table 5.2: Design Parameter mapping for Tip Truck.

				DP			
				1	2	3	4
				Joules per second (J/s)	Tub volume (m³)	Wheel Diameter (m)	Actuator extension length (m)
FR		1	Provide energy	x			
		2	Store material		x		
		3	Transport with wheel torque	x	x	x	
		4	Unload material with actuator arm	x	x		x

One of the most intricate designs, the "Volatile Extraction Drill" [319, 323] is also shown in Table 5.3. All other designs are mapped in successive tables in the Appendix. An 'x' marked on the mapping matrix signifies a quantifiable relationship between the FR and DP on that row and column as per Equation 5.1.

5.6 Mass and Specific Energy Criteria

Equipment mass and energy efficiency have been investigated as criteria for off-Earth mining system selection. These factors are widely believed to be important to off-Earth mining system selection as they are major constraints for planetary surface missions. This section investigates the importance of mass and energy requirements through a parameter study and literature review.

Table 5.3: Design Parameter mapping for Volatile Extraction Drill.

FR			DP															
			1	2	3	4	5	6	7	8	9	10	11	12	13	14	15
			Joules per second (J/s)	Wheel diameter (m)	Extension distance (m)	Rotation velocity (rad/s)	Retraction distance (m)	Door gap distance (m)	Heat power (J/s)	Gas pressure (Pa)	Chamber-storage pressure differential (Pa)	Compressor Pressure (Pa)	Storage volume (m³)	Door gap distance (m)	Auger rotation velocity (rad/s)	Connection coordinates (m,m,m)	Pressure Differential (Pa)
	1	Provide energy	x														
	2	Transport to site with wheel torque	x	x													
	3	Extend drill through rock	x		x												
	4	Rotate drill to auger material	x		x	x											
	5	Retract drill into oven	x				x										
	6	Confine chamber	x					x									
	7	Transfer heat to material	x		x				x								
	8	Measure chamber Pressure			x					x							
	9	Remove volatiles at pre-set pressure	x								x						
	10	Pressurise volatiles	x						x			x					
	11	Store volatiles	x						x				x				
	12	Open heat chamber	x											x			
	13	Eject processed material	x		x									x	x		
	14	Connect to product depot	x													x	
	15	Unload volatiles	x										x	x		x	x

98

5.6.1   Specific Energy Model

The Specific Energy of mine production (energy expenditure per unit mass of product) is defined as in Equation 5.7.

$$Specific\ Energy\ (\frac{J}{kgH_2O}) = SE_{breakage} + SE_{excavation} + SE_{transport} + SE_{processing}\ (5.7)$$

A general model for calculating the components and total specific energy has been developed for mining of icy regolith resources on the Moon. Parameters utilized in this model have been outlined in Table 5.4. The chosen parameters are similar to those used in previously published models [220, 221]. The excavation tool parameters and soil mechanics components are derived from the Swick excavation model, previously used for estimating excavation forces for space missions [289, 308]. Rock breakage parameters come from experimental data published by Gertsch, Gustafson and Gertsch [104]. There are several other parameters in the model such as the concentration of ice in regolith (*ore grade*) and site specific Mine Design parameters that lack, or do not require published data to support them. These are considered as variable assumptions as shown in the reference column of Table 5.4. Sensitivity analysis is carried out on all parameters to show the effect of variations and inaccuracies in these assumptions.

Table 5.4: Mining model parameters and constants.

Description	Symbol	Default	Unit	Min	Max	Parameter Type	Reference
Ore grade	Gr_{H2O}	0.1	kg/kg	0.01	1	Geological	Variable assumption
Ore bulk density	γ	Eqn. 5.8		950	1900	Geological	Eqn. 5.8
Lunar gravity	g	1.6	m/s^2	-	-	Physical Constant	[308]

External friction angle	δ	10	°	-	-	Physical Constant	[289, 308]
Tool cutting angle	β	45	°	-	-	Physical Constant	[289, 308]
Failure plane angle	ρ	45	°	-	-	Physical Constant	[289, 308]
Internal friction angle	φ	47.6	°	-	-	Physical Constant	[289, 308]
Surcharge load on excavation	q	0	N	-	-	Physical Constant	[289, 308]
Regolith cohesion	c	860	Pa	-	-	Physical Constant	[289, 308]
Soil-tool adhesion	C_a	200	Pa	-	-	Physical Constant	[289, 308]
Tool velocity	v	0.01	m/s	0.005	0.05	Equipment Design	[289, 308]
Depth of cut	d	0.2	m	0.05	0.4	Equipment Design	[289]
Width of cut	w	0.2	m	0.1	0.4	Equipment Design	[289]
Length of cut	l	0.2	m	0.1	0.5	Equipment Design	Variable assumption
Average excavation height	Δh_e	0.6	m	0.1	1	Equipment Design	Variable assumption
Load ratio	LR	0.6	Ratio	0.3	1.2	Equipment Design	[306]
Transport vehicle weight	W_{rover}	450	N	225	675	Equipment Design	[306]

Rolling resistance (% of weight)	RR	0.1	Ratio	0.05	0.3	Mine Design	[38, 306]
Haulage $\Delta height$ (mine)	Δh_h	8	m	-30	30	Mine Design	Variable assumption
Haulage distance (mine)	$x_{MinePlant}$	450	m	50	1000	Mine Design	Variable assumption
Haulage $\Delta height$ (dump)	Δh_h	0	m	-2	2	Mine Design	Variable assumption
Haulage distance (dump)	$x_{PlantDump}$	50	m	30	100	Mine Design	Variable assumption
Specific heat capacity regolith	$c_{regolith}$	0.5	J/gK	-	-	Physical Constant	[121]
Specific heat capacity water-ice	c_{water}	1.36	J/gK	-	-	Physical Constant	[106]
$\Delta Temperature$ required to sublimate	ΔT	100	K	-	-	Physical Constant	[108]
Enthalpy of sublimation	H	2800	K	-	-	Physical Constant	[92, 106]
Breakage experimental precision	-	1	Ratio	0.8	1.2	Equipment Design	Variable assumption

Breakage heat loss to processing	-	0.6	Ratio	0.4	0.8	Mine Design	Variable assumption
Efficiency breakage	$\varepsilon_{breakage}$	1	Ratio	0.7	1.3	Equipment Design	Variable assumption
Efficiency excavation	$\varepsilon_{excavation}$	0.2	Ratio	0.01	0.3	Equipment Design	Variable assumption
Efficiency transport	$\varepsilon_{transport}$	0.2	Ratio	0.1	0.4	Equipment Design	Variable assumption
Efficiency processing	$\varepsilon_{processing}$	0.6	Ratio	0.4	0.9	Equipment Design	Variable assumption

It is assumed that the density of regolith and ice are not the same, and consequently different concentrations of ice in regolith will lead to different bulk densities of the mixtures. The exact relationship is not known, and will vary depending on compaction and mineralisation in the regolith. A simple assumption is to take the bulk density of regolith and the density of ice and interpolate between the two based on the ratio of regolith to ice. This assumption has been used in the specific energy mining model in this chapter. The relationship is described by Equation 5.8. The specific energy model components $SE_{breakage}$, $SE_{excavation}$, $SE_{transport}$ and $SE_{processing}$ are calculated according to the Equations 5.9 to 5.19.

$$Bulk \ Density \ (\frac{kg}{m^3}) = \gamma = 1900 \times (1 - Gr_{H2O}) + 950 \times (Gr_{H2O}) \qquad (5.8)$$

$$SE_{breakage} \ (\frac{J}{kgH_2O}) = \frac{k \times (27.075 \times Gr_{H2O} - 0.0957) \times 10^6}{\epsilon_{breakage} \times Gr_{H2O} \times \gamma} \qquad (5.9)$$

For $SE_{breakage}$, k is a parameter used for sensitivity analysis on the precision of the experiments conducted by Gertsch, Gustafson and Gertsch [104], the value for the base case

is 1 for control purposes. The base case Breakage Efficiency parameter is also set to one, as the indentation experiments internalise the inefficiencies in rock breakage and account for that in the regression formula. It is known that rock breakage energy conversion efficiency is always low due to system losses to friction and heat, usually less than 1% [126]. Interestingly, the goal of the processing equipment is to increase the temperature in order to liberate water ice. With good engineering design, some of the wasted energy in rock breakage can be used to reduce the energy requirement of the processing equipment. A variable parameter has been introduced into the model in order to capture this potential upside in the design (Breakage heat loss to processing).

$$
\begin{aligned}
F_{Total\ excavation} = (\frac{g\gamma d}{2}(\cot(\beta) + \cot(\rho))\sin(\varphi + \rho) + q(\cot(\beta) + \cot(\rho))sin(\varphi + \rho) + \\
\frac{c\cos\varphi}{\sin(\rho)} + \frac{-c_a\cos(\beta + \varphi + \rho)}{\sin(\beta)} + \\
\frac{\gamma v^2\sin(\beta)\cos(\varphi)}{\sin(\beta + \rho)}) \times (\frac{wd}{sin(\beta + \varphi + \rho + \delta)}) \quad (5.10)
\end{aligned}
$$

The Swick excavation model [289, 308] is applied to calculate the total excavation forces and subsequently, the work done by the excavator (Eqn. 5.10). The physical constants are stated in Table 5.4. To determine the work done by the excavator, only the horizontal forces will be considered to act on the motors (Eqn. 5.11).

$$
F_h = F_{Total\ excavation} \times sin(\beta + \delta) \quad (5.11)
$$

$$
\therefore\ SE_{excavation}\ (\frac{J}{kgH_2O}) = \frac{F_h l}{\gamma dwl \times Gr_{H2O}} \quad (5.12)
$$

The energy required for transport is calculated as in Equations 5.13-5.17. The model includes energy expended due to drive resistance and gradient resistance for uphill and downhill sections. The assumption is made that each haulage leg has a change in height in only one direction, and the exact opposite change is experienced in the return cycle.

However, the load carried by the transport equipment is significantly less on the return. The haulage energy is calculated for the average haulage distance and change in height from the mine to process plant and the process plant to waste dump, as there will not be sufficient space available near the plant for the life of mine tailings dump.

$$Transport\ Payload\ Weight\ (N) = LR \times W_{rover} \qquad (5.13)$$

$$Transport\ Payload\ Mass\ (kg) = \frac{Transport\ Payload\ Weight}{g} \qquad (5.14)$$

$$Haulage\ Drive\ Resistance\ (N) = R_{haulage} = \frac{\Delta h_h}{x} \times (W_{rover} + Transport\ Payload\ Weight) +$$
$$RR \times (W_{rover} + Transport\ Payload\ Weight) \quad (5.15)$$

Where x can be the haulage distance from mine to processing plant, or the distance from plant to waste dump depending on which haulage resistance is being calculated.

$$Drive\ Resistance\ Return\ (N) = R_{return} = \frac{-\Delta h_h}{x} \times W_{rover} + RR \times W_{rover} \qquad (5.16)$$

$$SE_{transport}\ (\frac{J}{kgH_2O}) =$$
$$\frac{x_{MinePlant} \times (R_{MinePlant} + R_{PlantMine}) + x_{PlantDump} \times (R_{PlantDump} + R_{DumpPlant})}{Transport\ Payload\ Mass} \times$$
$$\frac{\gamma}{\epsilon_{transport}}/(Gr_{H2O} \times \gamma) \quad (5.17)$$

$R_{MinePlant}$, $R_{PlantMine}$, $R_{PlantDump}$ and $R_{DumpPlant}$ are all calculated in Equations 5.15 and 5.16 with the parameters for each respective journey leg. For example, $R_{MinePlant}$ is the haulage distance calculated by Equation 5.15 which will use parameters from Table 5.4

for haulage from the mine to the processing plant and $R_{PlantMine}$ is the return distance calculated by Equation 5.16.

The energy required for processing is calculated as in Equations 5.18-5.20. It is assumed as in the work by Pelech, Roesler and Saydam [221] that the processing stage will involve heating regolith and ice equally in an oven.

$$Energy\ to\ phase\ change\ ice\ (\frac{J}{kgH_2O}) = 1000 \times (\Delta T \times c_{water} + H) \tag{5.18}$$

$$Energy\ to\ heat\ regolith\ (\frac{J}{kg\ regolith}) = 1000 \times (\Delta T \times c_{regolith}) \tag{5.19}$$

$$SE_{processing}\ (\frac{J}{kgH_2O}) = ((Gr_{H2O} \times Energy\ to\ phase\ change\ ice+$$
$$(1 - Gr_{H2O}) \times Energy\ to\ heat\ regolith) \times \frac{\gamma}{\epsilon_{processing}}) \times \frac{1}{Gr_{H2O} \times \gamma}$$

$$\text{-} (Breakage\ Heat\ loss\ to\ Processing \times SE_{breakage}) \tag{5.20}$$

5.6.2   Parameter Sensitivity and Importance

Calculating the specific energy with the model and base case parameters in Table 5.4 against ore grades between 1% and 100% produces the results in Figure 5.2. The results show that there is a large advantage of mining higher grade material, although the advantage becomes less important with ore grades higher than 30%. The single most important component of the Total Specific Energy is the Processing Energy, which is several orders of magnitude higher than the other components. It can be deduced that for the base case it is optimal to expend more energy in rock breakage, excavation and transport in order to

access higher grade ore and reduce the processing (and total) energy required to produce water. This result also justifies the importance of the new rock breakage mechanisms introduced in Chapter 4.
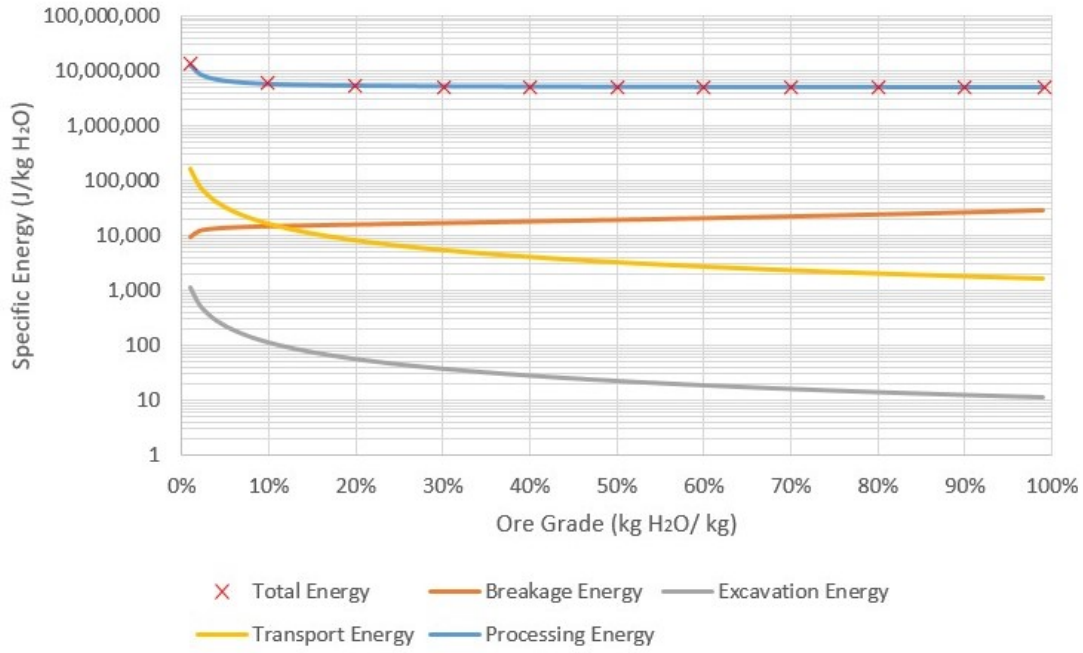
Figure 5.2: Specific energy consumption of system subclasses versus ore grade.

A sensitivity analysis was carried out in order to compare the relative importance of each parameter.

Equation 5.21 shows the calculation of the Relative Sensitivity which is used here to highlight the importance of various parameters. Features of statistical variance, approximation of partial differentiation and relative magnitude ratios have been utilized in devising this indicator.

$$Relative\ Sensitivity = \sqrt{\frac{(\delta SE/SE_{base\ case)}^2}{(\delta P/P_{base\ case)}^2}} = \sqrt{\frac{(\frac{SE_i - SE_{base\ case}}{SE_{base\ case}})^2}{(\frac{P_i - P_{base\ case}}{P_{base\ case}})^2}} \tag{5.21}$$

Where SE_i is the total specific energy as calculated by Equation 5.7 with a P_i independent parameter value, with other parameters held constant to the default value. The $SE_{base\ case}$

is calculated by Equation 5.7 with all parameters set to their default values from Table 5.4.

The relative sensitivity partial differential Equation 5.21 has been evaluated at five equally spaced points between the maximum and minimum feasibly expected values of the parameter as outlined in Table 5.4. The average of these five evaluations is shown in Figure 5.3.

The parameters have also been categorised into four groups, depending on how much control the mine operators will have over them. The categories have been assigned in Table 5.4. They are (i) physical constants over which engineers have no control; (ii) geological parameters over which engineers have no control but when understood in sufficient detail can be exploited to optimize the mine; (iii) equipment design parameters over which engineers have control during the research and development phase, but not after the equipment has been built; and (iv) mine design parameters which can be changed over the mine life in order to optimize production.

This parameter categorisation allows us to see at which stage they can be optimized in order to influence the specific energy. Some parameters may relate to more than one category, however, for simplicity they have been allocated only to their most important category. Figure 5.3 shows the parameters organized within the following categories: geology, equipment design and mine design. Sensitivity analysis was not carried out on physical constants as they cannot change.

The results of the Specific Energy Model sensitivity analysis show that the specific energy required to produce one kg of H_2O is strongly dependent on the ore grade between 1% and 10% and the efficiency of the processing stage. The processing stage here is assumed to be an oven heater that causes sublimation of vapour, although a pressurised oven system that causes melting of the ice is also possible with a different efficiency. The next most important factors: transport efficiency, transport distance, transport rolling resistance and the amount of breakage heat loss to processing are all around two orders of magnitude less important than ore grade and processing efficiency.
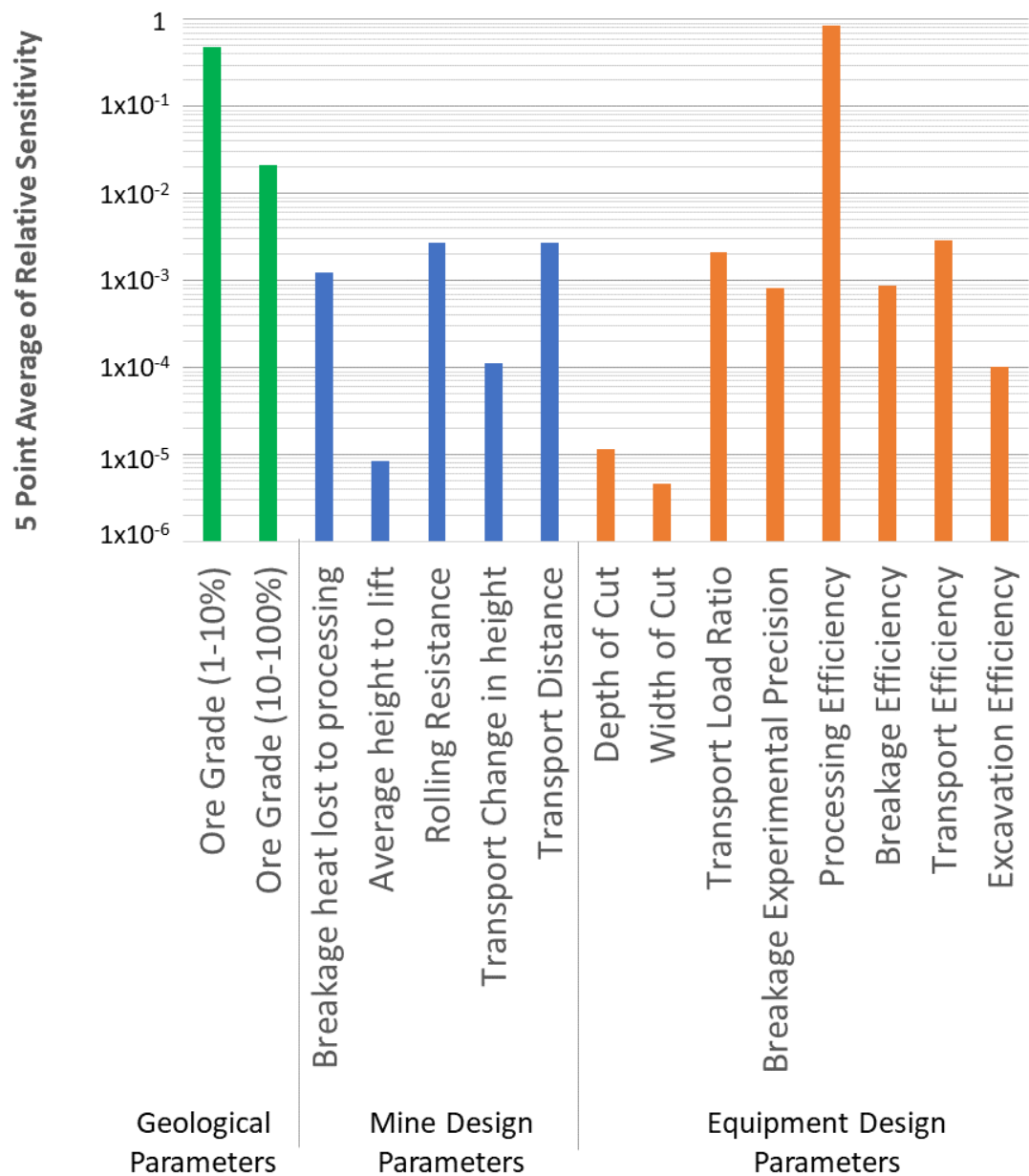
Figure 5.3: Relative Sensitivity to model parameters and parameter categories.

The equipment parameters related to excavation and rock breakage are mostly incon-sequential to the total system SE. The processing stage requires by far the most energy, and is currently limited to heating methods with comparable efficiencies. Since processing is the last stage in the mining system flowchart as shown in Figure 4.1, outputs of the

previous steps influence the amount of energy spent in this stage. It would be perilous to attempt to reduce the specific energy of $SE_{breakage}$, $SE_{excavation}$, and $SE_{transport}$ without considering the system as a whole. $SE_{breakage}$, $SE_{excavation}$, and $SE_{transport}$ are interesting measures to classify mining equipment, however they should not be used as criteria for mining system selection. The whole system including unknown geological parameters must be considered to carry out a fair optimization. This requires much more information around geology and system effectiveness which must be completed at a later stage of a feasibility study, once more data has been collected.

If SE was included as a selection criterion in this early stage, a suboptimal system will likely be chosen with a higher overall specific energy. For example, if the rock breakage stage is removed to save energy, only a low grade deposit that doesn't require breakage (Deposit ID#1 in Table 5.6) would be mined. If rock breakage were utilized, a higher grade ice deposit (Deposit ID#3 in Table 5.6) could be mined instead. The higher grade deposit would require much less energy to mine due to processing savings even with the energy intensive rock breakage stage.

It is important to note that the mining system selection procedure does not select a geological deposit, a deposit must be available and the procedure helps engineers to apply a mining system to that particular deposit prior to the economic assessment. The previous example has been used to illustrate what could happen if Specific Energy were a selection criterion. As a result, Specific Energy is not part of the mining system selection procedure proposed in this chapter.

5.6.3 Equipment Mass

In order to determine a confident estimate of the equipment mass, a geological model, mine plan, preliminary mining system selection and economic analysis are required. It is therefore premature to use mass as a criterion for the preliminary mining system selection as it pre-empts the outcome of the feasibility study. Note that these processes are iterative and the initial mining system choice does not need to be the final choice. It is also observed

that terrestrial mining method selection procedures [192, 213] do not use the capital and operating costs as a selection criterion for this same reason. This is despite these two parameters being of substantial interest to mine planners and investors.

A detailed off-Earth mining feasibility study focussing on equipment mass "opportunity costs" will be detailed in Chapter 7. The economic indicator to be used is the Propellant Payback Ratio (PPR). It links the economic return, equipment mass and the product delivered to market together. However, as will be shown in Chapter 7, a selection of the mining system should be made first, to enable the economic assessment to be carried out.

5.6.4 Terrestrial mining analogy and strategy

The revelations of the Specific Energy model for icy regolith show that *ore grade* is a most important parameter. The best mining strategy would be to undertake exploration or "grade control" activities during the mine life. Grade control is a mining industry term for improving a *mineral resource* model with higher resolution data to minimize unplanned waste mining, optimize extraction and de-risk the grade and tonnage production profile [34, 50]. This is done on the Earth and allows mine planners to optimise the mine with respect to operating cost. In that sense, the terrestrial mine operating cost and off-Earth mining Specific Energy are analogous.

Grade control may also prove to be critical in off-Earth operations as reliability and lifespans of equipment is likely to be low. This magnifies the value of undertaking grade control activities compared to terrestrial operations. Grade control should occur over time as the mine progresses, probably by sampling during the excavation stage or by conducting additional exploration drilling. It is important that the mining system continues to operate as expected so that sufficient time is given for new geological information to be applied and enable reductions in SE cost. Hence, there is an important indirect link between mining system reliability and the ability to minimise SE.

It will be more effective to have a reliable mining system that can survive until grade con-

trol optimization can pay off. This is true, even at the cost of a higher initial $SE_{breakage}$, $SE_{excavation}$, and $SE_{transport}$. This energy expenditure can be optimised effectively even after all equipment is committed and a mine has commenced as it heavily depends on geological and mine design parameters as described in Section 5.6.2 and shown in Figure 5.3. Prolonging equipment life is an effective strategy to optimise mass and specific energy costs. Therefore, system reliability is the key criterion for off-Earth mining method selection and the rest can be taken into account at a later stage. The review of specific energy and equipment mass criteria for mining system selection has shown that there is little benefit to their usage at this stage of the process. These criteria must be assessed later in a detailed economic study.

5.7 Logical Selection Framework

With reliability as the key selection criterion, mining system selection can be undertaken using axiomatic design principles. A large database will be logically filtered down to a small pool of applicable candidates for a given ore body. The logical filtering will depend on each equipment's FRs and capabilities in various geological settings. For example, it is logical that a pneumatic suction device designed to collect loose regolith particles does not have the function of mining ice deposits encased in consolidated soils at depth. Similarly, a hammer drill designed for the rock breakage function will not be required to mine a loose gypsum sand dune.

The deposit characteristics for the off-Earth mining system selection have been developed from similar attributes used in the terrestrial Nicholas classification [212] and the UBC Mining Method Selection Procedure [192]. The deposit characteristics are outlined in Table 5.5. They have been carefully named to ensure a combination exists for all the identified deposit examples in literature [45, 81, 138, 179, 193, 194, 226, 230, 277], and to provide enough classifications for filtering the mining equipment database as well. A comprehensive list of all combinations of characteristics is accompanied by a geological description and relevant example references in Table 5.6. It is noted that there may be

more geological examples that can fit each combination and therefore, the description column is non-exhaustive. Current literature contains a far greater number of papers describing the geology and physical characteristics of soils on Mars than papers providing similar information for the Moon. This clearly indicates the near-term need for space missions to a variety of lunar locations where ground assets will acquire sufficient usable data for mining system selection on the Moon.

Table 5.5: Deposit characteristics for classification.

Volatile	Ore Strength	Deposit Geometry
Yes	Unconsolidated	Layered
No	Partially Consolidated	Evenly Distributed
	Rock	Variable

Each mining system is input into the framework with predefined Boolean attributes of "Volatile, Unconsolidated, Partially Consolidated, Rock, Layered, Evenly Distributed, Unevenly Distributed", which encode whether or not (1/0) a particular system can work on a deposit with the given characteristic. Conditional logic is then used to filter down the original database of equipment from Table 5.1 to a small pool for a particular deposit.

The conditional logic is based on conceptual assessments of each system, and that each system can either work or not work (1/0) on a particular deposit type. It is anticipated that this framework will be evolved in the future once more operational data is collected on different systems. For preliminary off-Earth mining system selection, a conceptual assessment is currently the only means based on currently reported data and publications.

Once a deposit is defined, and the equipment list has been filtered down to the relevant parts, they are divided into four subclasses as shown by the mining flow chart in Figure 4.1. They are: Rock Breakage, Excavation, Transport and Processing. These four subclasses enable the mixing of equipment to best suit the ore body or additional engineering requirements (e.g. auxiliary FRs in Section 5.10) after ranking is complete. Boolean attributes for each subclass are also encoded in the equipment database.

In some cases, the Rock Breakage subclass is not required. The deposit could already be unconsolidated ready for the Excavation subclass. The Transport and Processing subclass

Table 5.6: Possible combinations for deposit characteristics and suggested descriptions.

Deposit ID	Material Geomechanics				Deposit Geometry			Description
	Volatile	Unconsolidated	Partially Consolidated	Rock	Layered	Evenly Distributed	Variable	
1	Yes	Yes			Yes			Loose icy regolith sediment. [45, 194, 277]
2	Yes		Yes		Yes			Compacted icy regolith. [45, 194, 277]
3	Yes			Yes	Yes			Pure ice layers. [138]
4	Yes	Yes				Yes		Icy/H_2O adsorbed regolith. [45]
5	Yes		Yes			Yes		Compacted Icy regolith/H_2O adsorbed regolith. [45, 277]
6	Yes			Yes		Yes		Pure massive ice. [138]
7	Yes	Yes					Yes	Glacial rill with pockets of ice. [138, 226]
8	Yes		Yes				Yes	Compacted lunar crater regolith with ice pockets. [45]
9	Yes			Yes			Yes	Compacted icy regolith. [45, 194, 277]
10		Yes			Yes			Eroded hydrated mineral sediment. [81, 179]
11			Yes		Yes			Hydrated mineral sediment. [81, 179]
12				Yes	Yes			Gypsum rocks with interbedded barren material. [193, 230]
13		Yes				Yes		Hydrated mineral regolith. [45, 95]
14			Yes			Yes		Compacted hydrated mineral regolith. [45]
15				Yes		Yes		Massive gypsum or epsomite rocks. [81, 230]
16		Yes					Yes	Eroded hydrated mineral mixed with barren material. [95, 193]
17			Yes				Yes	Eroded hydrated mineral mixed with barren material. [95, 193]
18				Yes			Yes	Hydrated mineral veins. [207]

may or may not be required depending on the capabilities of the chosen excavator. If the excavator is capable of extracting pure water and transporting it to a storage depot, then it will be the only equipment required for that system.

The proposed mining system selection algorithm has been based on a highly constrained brute force solution to the 0/1 Knapsack problem [124, 258]. The Knapsack problem can

be summarised by the optimisation problem of filling a finite-sized knapsack with tools for a hike. They must fit within the knapsack and provide the maximum utility to the user for the conditions on that hike.

The algorithm iterates through all possible combinations of the filtered system equipment and evaluates which combinations fit the deposit characteristics. Combinations are then ranked based on axiomatic design principles. The algorithm is constrained to fill all subclasses with an equipment, considering that some equipment fill more than one subclass. This is achieved by reading the Boolean attributes for each equipment and identifying the subclasses it can fill. The algorithm trials all combinations to check for the attributes (Rock Breakage, Excavation, Transport, Processing) = (1, 1, 1, 1) or the binary value 15.

Since not all deposits will require a Rock Breakage subclass, a placeholder called "Breakage Not Required" has been introduced into the mining equipment list. This will filter through to enable the Rock Breakage attribute to attain a 1 value even for unconsolidated deposits.

The output from this part of the algorithm will yield all the potential combinations from the equipment database that could be used to mine the specified deposit.

5.8 System Rankings

The majority of the terrestrial mining system selection techniques utilise a numerical ranking methodology for planners to identify which method is likely to be most applicable. As previously stated, employing a similar ranking methodology for off-Earth mining system selection is difficult due to the lack of operational data to compare and rank. Hence, a new comparison methodology is proposed based on the modelled Information Content from equipment reliability.

5.8.1   Series and Parallel System Reliability

The reliability of systems with components in series and parallel are important concepts utilised in this analysis [85]. Reliability (R) is defined as the probability a component completes its assigned task within a given period [205]. It can be calculated from the probability of failure (p_f) as shown in Equation 5.5. Reliability of a system with components in series (R_{series}) can be calculated as the product of each component's reliability as shown in Equation 5.22 and generalised for multiple components in series as in Equation 5.23. A system with components in parallel will fail only if all components connected in parallel fail, hence the reliability $R_{parallel}$ is calculated as in Equation 5.24. It has been shown by Myers [205] that redundant components in parallel improve system reliability while components in series do not, as shown in Figure 5.4 and Figure 5.5. The assumption is made with these equations that all components are probabilistically independent and the simplified probability laws are applied. In practice component independence is likely not the case and Bayes' conditional probability formula should be applied. Unfortunately, it is difficult and premature to define probabilistic relationships for system components where no data is available. An alternative assumption is applied in this chapter where components have known functional relationships from the axiomatic design assessment in Section 5.5.

$$R_{series} = R_1 R_2 \tag{5.22}$$

$$R_{series} = \prod_{i=1}^{n} R_i \tag{5.23}$$

$$R_{parallel} = 1 - \prod_{i=1}^{n} (1 - R_i) \tag{5.24}$$

To demonstrate the assumption and thought process, an illustrative example is given. It is known that a truck design requires a power supply component which itself has reliability.

The power supply component is linked in series to the truck tub storage and the drivetrain. It is also known that the drivetrain is dependent on the power supply to function. There exists a conditional probability relationship. Without operational data, the actual relationship cannot be deterministically evaluated. The drivetrain physically depends on the power supply, and so it can be assumed that the probability of success (reliability) of the drivetrain cannot be greater than the reliability of the power supply. This assumption is defined by Equation 5.25. Where known functional dependencies exist, the reliability of functions in series must be less than that of the primary function.

$$R(FR_{series}) \leq R(FR_{primary}) \tag{5.25}$$

The serial dependency assumption in Equation 5.25 is utilised to increase the amount of knowledge that is input into the complexity measure and allow for better differentiation between mining equipment for the ranking process. Note that this is only applicable if the functions are dependent in series, for example when the drivetrain is dependent on the power supply.
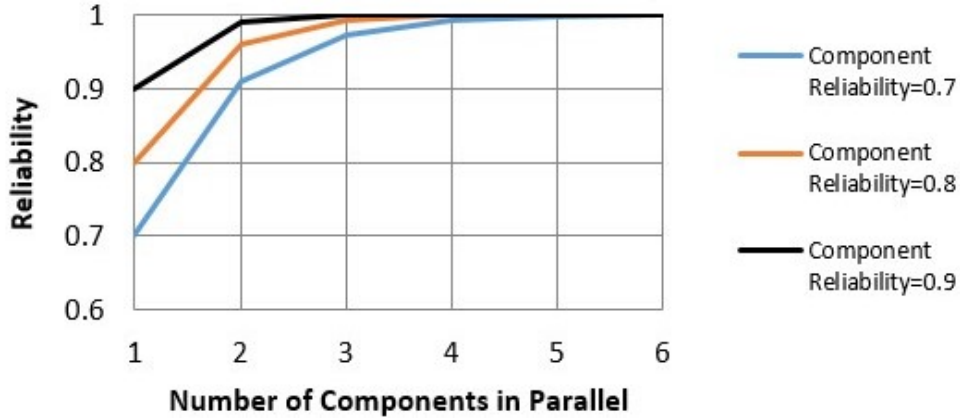
Figure 5.4: Reliability of components in parallel after Myers [205].
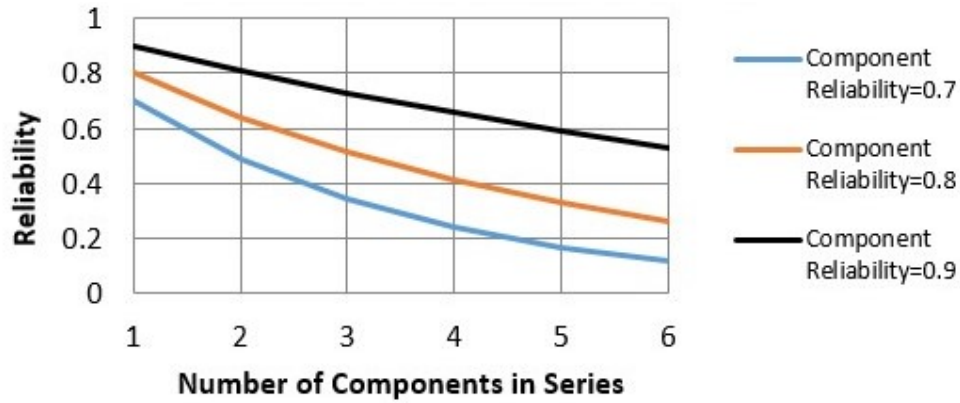
Figure 5.5: Reliability of components in series after Myers [205].

5.8.2   Complexity Measures and Information Content Ranking

Complexity in mechanical design is generally measured as a function of system size, component connectivity or design problem solvability [150, 199, 262, 290].

Graphical methods are sometimes used to determine the system size and connectivity, through mapping out the functional blocks of a system and counting the number of nodes and connections [143, 285]. Myers [205] describes the functional block diagram as presenting the relationships between system components in the purest form without losing information about the independent failure of components. The representation of a system through a functional block diagram is depicted as a group of interconnected "black boxes" each capable of a function and independent failure.

Efatmaneshnik and Ryan [80] observe that measurements of complexity have both a subjective and objective component. They have presented a method for measuring complexity through an objective size measure (number of parts) and also a subjective measure (number of additional functional blocks in comparison to a reference design). This methodology requires the use of functional block diagrams and a reference system block diagram.

The use of complexity measures to indicate system reliability, such as the block diagram, have been considered by Suh [283] and Stuart and Mattikalli [278]. The results show that complexity and reliability are not correlated. This is due to the existence of redundancy

in a system intended to increase reliability, while at the same time increasing system complexity [278] according to the above definitions.

Axiomatic design principles as outlined in Section 5.4 allow an alternative method for assessment and improvement of engineering designs by mapping how the Design Parameters relate to more than one Functional Requirement. Frey, Jahangir and Engelhardt [99] show that it is not correct to use independent probability laws when considering non-diagonal (coupled/decoupled) design mapping, as DPs are interlinked. They have instead utilised probability density functions and known tolerances on the DPs to accurately calculate the information content of the decoupled design. Based on their findings, the Information Axiom as described by Equations 5.5 and 5.6 has been chosen as the primary measure to rank off-Earth mining systems in this work. It is applicable to conceptual designs and has a correlative relationship with system reliability, a highly desirable trait for off-Earth mining systems.

Unfortunately, the reliability of system components is a significant unknown at present for off-Earth mining systems. They are also a critical input to the Information Content Equation 5.6. A Monte Carlo approach to system reliability has been utilised to differentiate and rank the systems and overcome this obstacle. The approach is outlined further in Section 5.9.

5.9   Monte Carlo Reliability Trials

Deterministic evaluation of the Information Content of the off-Earth mining systems is currently out of reach due to the lack of operational and manufacturing data. Instead, mapping of the Functional Requirements to the Design Parameters using axiomatic design principles has been applied to determine the level of complexity in each design. Each FR has been assumed to have a randomly distributed probability of success between the Lower Limit of 0.9700 and Upper Limit of 0.9999. It is assumed the highest level of reliability will be engineered into these systems. Subsequently, 5000 Monte Carlo trials have been

carried out for each FR to explore the total system reliability.

A uniform random distribution from MS Excel has been used for the trials, and a lower probability limit 0.9700 has been chosen to reduce pull-up of the distribution when dependencies are applied. Experimentation with probability limits revealed that elevated lower limit assumptions (e.g. 0.9900) led to many minimum values occurring and destruction of the random distribution.

The calculation of the overall reliability of the system assumes probabilistic independence of each FR, resulting in the linkage in series of each FR by default. In cases where dependencies exist according to the axiomatic design mapping matrix, the constraint in Equation 5.25 is applied instead of the conditional probability formula.

Table 5.7 demonstrates a single Monte Carlo trial on the "Truck" equipment parameter mapping in Table 5.2. Where p_s is the probability of success of a functional requirement (FR). Note where Equation 5.25 has been applied to calculate $p_{s(FR3)}$ and $p_{s(FR4)}$ as the requirement to "transport with wheel torque" and "unload material with actuator" both depend on the functioning of previous FRs "provide energy" and "store material". The upper limit on the reliabilities of FR3 and FR4 are hence limited by the success of FR1 and FR2 and their minimum reliability in each Monte Carlo trial. Also note that only a single minimum is used as an upper bound, and not the product of the $p_{s(FR1)}$ and $p_{s(FR2)}$. This is because only one failure mode can occur at any one time, or in any single Monte Carlo trial.

Table 5.7: Monte Carlo trial example for Tip Truck parameter mapping.

Evaluation Step	Serial DP Dependency	Calculation
$p_{s(FR1)}$	DP1	$= Randbetween(LowerLimit, UpperLimit)$
$p_{s(FR2)}$	DP2	$= Randbetween(LowerLimit, UpperLimit)$
$p_{s(FR3)}$	DP1, DP2, DP3	$= Randbetween(LowerLimit, min(p_{s(FR1)}, p_{s(FR2)}))$
$p_{s(FR4)}$	DP1, DP2, DP4	$= Randbetween(LowerLimit, min(p_{s(FR1)}, p_{s(FR2)}))$
Equipment Reliability (p_s)		$= \prod (p_{s(FR1)}, p_{s(FR2)}, p_{s(FR3)}, p_{s(FR4)})$
Information Content		$= log_2(\frac{1}{p_s})$

This trial is repeated 5000 times for each parameter map to obtain an average expected value and standard deviation for the Reliability and Information Content as shown in Figure 5.6 and Figure 5.7. Results show that the overall reliability of each system converges to an expected value and standard deviation dependent on the initial assumptions.
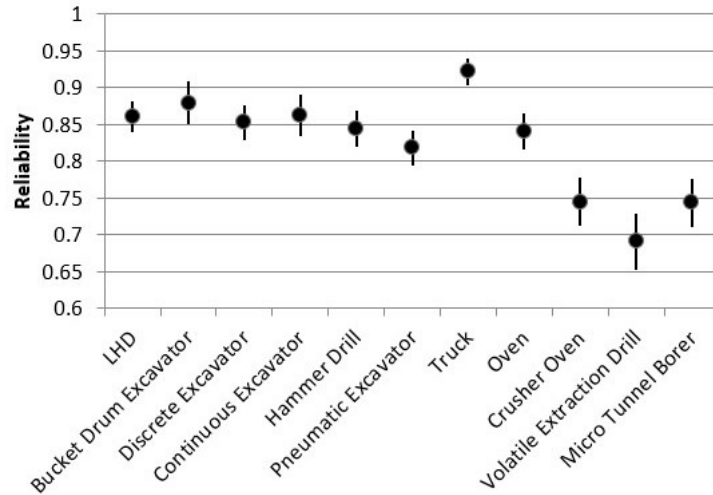
Figure 5.6: Distributions of reliability using Axiomatic Design Monte Carlo model.
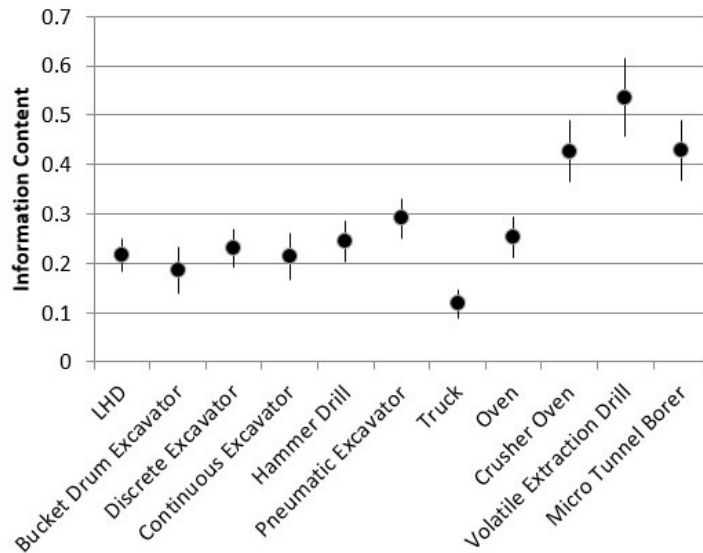
Figure 5.7: Distribution of Information Content using Axiomatic Design Monte Carlo model.

Sensitivity analysis presented in Table 5.8 indicates that the actual ranking of each design is not very responsive to changes in the assumptions, as long as the assumptions are

consistent across all designs. This is useful in the mining system selection process, as designs are compared against each other and not ranked for absolute effectiveness.

Table 5.8: Sensitivity to sample range analysis.

	Random Sample Assumption Range for Reliability			
Ranking	**0.99-0.9999**	**0.9-0.9999**	**0.85-0.95**	**0.8-0.95**
1	Truck	Truck	Truck	Truck
2	Bucket Drum Excavator	Bucket Drum Excavator	Bucket Drum Excavator	Bucket Drum Excavator
3	Hammer Drill	Hammer Drill	Hammer Drill	Hammer Drill
4	Discrete Excavator	Discrete Excavator	Discrete Excavator	Discrete Excavator
5	**Continuous Excavator**	**Continuous Excavator**	LHD (Load-Haul-Dump Excavator)	LHD (Load-Haul-Dump Excavator)
6	LHD (Load-Haul-Dump Excavator)	LHD (Load-Haul-Dump Excavator)	**Continuous Excavator**	**Continuous Excavator**
7	Oven	Oven	Oven	Oven
8	Pneumatic Excavator	Pneumatic Excavator	Pneumatic Excavator	Pneumatic Excavator
9	**Crusher Oven**	**Crusher Oven**	Micro Tunnel Borer	Micro Tunnel Borer
10	Micro Tunnel Borer	Micro Tunnel Borer	**Crusher Oven**	**Crusher Oven**
11	Volatile Extraction Drill	Volatile Extraction Drill	Volatile Extraction Drill	Volatile Extraction Drill

5.10   Auxiliary Functional Requirements

Auxiliary Functional Requirements can be added to the mining systems in order to mitigate the effects of environmental hazards common to all equipment such as radiation, temperature, dust, other atmospheric conditions, etc. They are not a core part of the mining system and do not affect the fundamental method of how the material will be broken, excavated, transported and processed according to the definition of the mining system in Figure 4.1. They have been left out of the design parameter maps in the analysis to enable easy comparison between equipment. This is possible as the Auxiliary FRs are

somewhat common to all designs. This leaves only the Core FRs used in the analysis.

In practice, Auxiliary FRs do affect the reliability of mining systems. Bayes' Conditional probability formula can be applied to the reliabilities of Auxiliary FRs and Core FRs as described in Table 5.9 and Figure 5.8. It can be inferred that; if all Auxiliary FRs are operating within their Design Parameters, the probability of success according to Equation 5.26 is maximised. In other words, engineering solutions to hazards should improve the reliability of the mining system if working correctly. This is visually depicted by the relatively large green area in the Venn diagram in Figure 5.8 where Pr(A|B)>Pr(B') and Pr(A|B)>Pr(A'). The probability of success is maximized given a working Auxiliary FR.

$$Pr(A|B) = \frac{Pr(A \cap B)}{Pr(B)} \tag{5.26}$$

Where A is the success of the mining system and B is the success of Auxiliary FRs, A' is probability of failure of the mining system and B' is the probability of failure of the auxiliary FR.

Table 5.9: Truck design mapping with auxiliary FRs to manage specific environmental hazards.

				DP						
			1	2	3	4	5	6	7
			Thickness of shield (m)	Joules per second (J/s)	Change in temperature (Δ°K)	Bearing electric field strength (V/m)	Tub volume (m³)	Wheel Diameter (m)	Actuator extension length (m)
FR	1	Shield circuitry from radiation	x						
	2	Provide energy	x	x					
	3	Balance severe thermal variations.	x	x	x				
	4	Protect bearings from electrostatic dust		x		x			
	5	Store material					x		
	6	Transport with wheel torque		x		x	x	x	
	7	Unload material with actuator		x		x	x		x
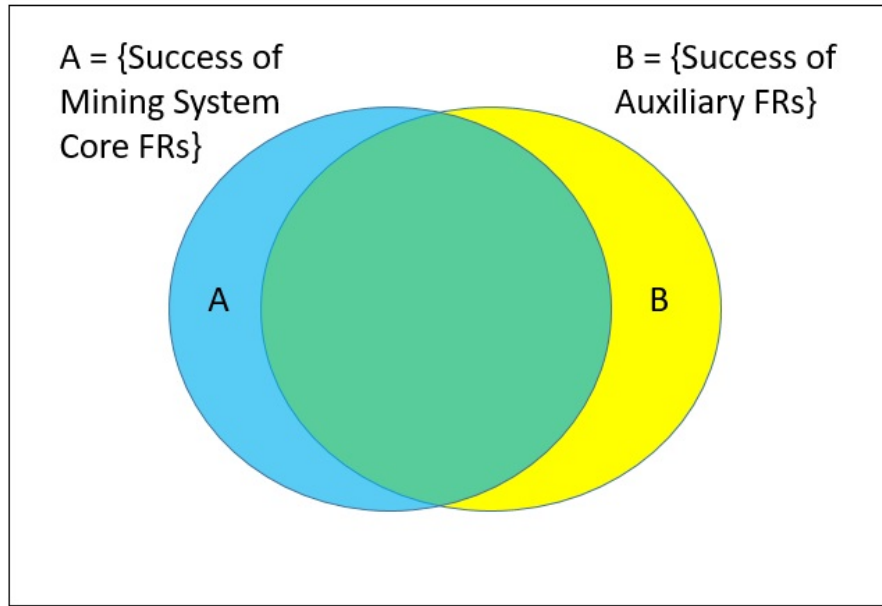
Figure 5.8: Reliability of mining systems with Core FRs and Auxiliary FRs.

It would be possible to extend the Monte Carlo approach that has been carried out for Core FRs to the Auxiliary FRs. However, a much greater knowledge of off-Earth mining environments is required to map Auxiliary FRs to mitigate the wide range of possible hazards. The range of potential FR:DP solutions is very large. Despite the existence of on-going testing of engineered solutions for dust mitigation and radiation in the literature [139], no attempt to map these auxiliary FRs was made in this research due to the increased complexity. This is also why it has been advantageous to separate the Core and Auxiliary FRs, enabling the mining system selection method discussed in this chapter to focus on Core FRs only.

The application of the Monte Carlo trials on Auxiliary FRs would be different than that of Core FRs. The serial dependency assumption (Equation 5.25) cannot be applied for Auxiliary FRs because the Core FRs are not dependent on them in series to be successful. An example of a Core FR serial dependency is between the power system and the wheel motors. The motor FR will not operate without the power system; it is serially dependent. An example of an Auxiliary FR is a wheel bearing dust protection on a rover. The rover will still function for some time without an FR to ensure they are protected from dust.

There is no serial dependency in this case and the FR serial dependency assumption (Equation 5.25) must be removed from the Monte Carlo trials on Auxiliary FRs.

The outcome where a Core FR is fulfilled despite the absence of the Auxiliary FR is represented by the smaller blue area in the Venn Diagram in Figure 5.8, Pr(A|B'). The probability of success of the system is smaller in this blue area, but it is not guaranteed to fail as would occur if a serial dependency existed.

The removal of the serial dependency assumption (Equation 5.25) for Auxiliary FRs will allow Monte Carlo reliability trials to occur above that limit and effectively increases the average long term reliability. The expected relationship is described by Equation 5.26 and reliability inference from Figure 5.8 is fulfilled. That is, if Auxiliary FRs are successfully applied, then the reliability of the system should increase.

5.11   Results and Discussion

5.11.1   Off-Earth Mining System Selection Framework

The resulting off-Earth mining system selection framework is shown in Figure 5.9. The main elements have been included as described in Section 5.5, 5.7, 5.8 and 5.9. The elements outlined in Section 5.6 and 5.10 relating to Equipment Mass, Specific Energy and Auxiliary Functional Requirements should be considered as extensions to the overall assessment of an off-Earth mine. The final step in the process, the Economic Assessment will include these factors and iteratively optimise the preliminary mining system selection for those parameters. An example of the Economic Assessment stage is shown in Chapter 7.

It is important to note the difference between the traditional Mining Method Selection done for terrestrial mining and the Mining System Selection procedure proposed in this chapter. A *mining system* is a set of tools or equipment that can be used in combination to access and extract *mineral resources*. Without more detail and operational examples for

off-Earth ISRU, mining system selection by functional analysis, as proposed is the most that can be reasonably be undertaken. A *mining method* is a specific approach to applying a *mining system*. The difference between a *mining method* and a *mining system* is based on how the equipment is applied in different geology and geometry. For a terrestrial mine example, a truck and shovel is a *mining system*. Strip mining and open pit mining are two *mining methods* used to apply a truck and shovel. Strip mining is the act of removing long strips of waste material to progressively uncover a continuous, shallow seam of ore. Open pit mining requires the removal of waste and ore via benching and pushbacks for an ore body that extends downwards rather than laterally. As mentioned, there are not currently enough baseline examples to formulate a mining method selection procedure for ISRU that takes into account the specific geometry of excavations.
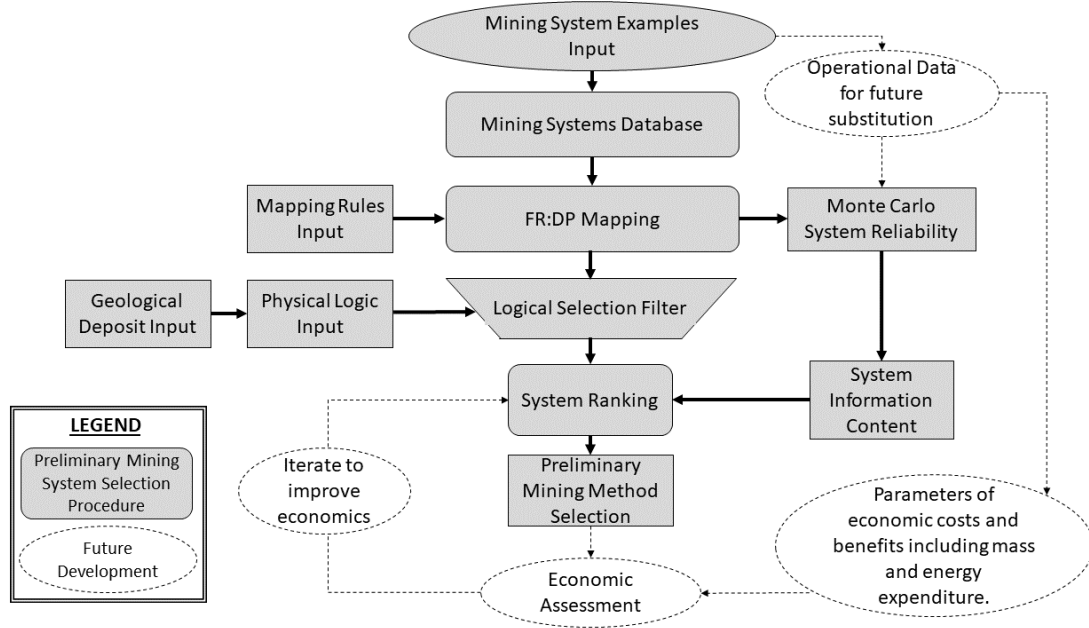
Figure 5.9: Mining system selection framework developed in this chapter.

5.11.2 Framework Application and Discussion

The preliminary Mining System Selection algorithm has been run on all of the 18 defined deposit types as described in Table 5.6. Selected results of the top 5 proposed mining systems are shown in Table 5.10 for loose icy regolith sediment, Table 5.11 for compacted

icy regolith sediment, Table 5.12 for eroded hydrated mineral sediment and Table 5.13 for hydrated mineral veins. The compacted icy regolith sediment has only yielded one option for the mining system, the volatile extraction drill, as no other proposed breakage systems are considered capable of this hard material [316].

Table 5.10: Deposit 1 loose icy regolith sediment top 5 mining systems.

Rank	Breakage	Excavation	Transport	Processing	Information Content
1	Breakage Not Required	Bucket Drum Excavator	Bucket Drum Excavator	Oven	0.4395
2	Breakage Not Required	LHD	LHD	Oven	0.4690
3	Breakage Not Required	Pneumatic Excavator	Pneumatic Excavator	Oven	0.5425
4	Breakage Not Required	Bucket Drum Excavator	Truck	Oven	0.5565
5	Breakage Not Required	Continuous Excavator	Truck	Oven	0.5830

Table 5.11: Deposit 9 compacted icy regolith sediment mining system.

Rank	Breakage	Excavation	Transport	Processing	Information Content
1	Volatile Extraction Drill	Volatile Extraction Drill	Volatile Extraction Drill	Volatile Extraction Drill	0.5360

Table 5.12: Deposit 10 eroded hydrated mineral sediment top 5 mining systems.

Rank	Breakage	Excavation	Transport	Processing	Information Content
1	Breakage Not Required	Bucket Drum Excavator	Bucket Drum Excavator	Oven	0.4395
2	Breakage Not Required	LHD	LHD	Oven	0.4690
3	Breakage Not Required	Pneumatic Excavator	Pneumatic Excavator	Oven	0.5425
4	Breakage Not Required	Bucket Drum Excavator	Truck	Oven	0.5565
5	Breakage Not Required	Continuous Excavator	Truck	Oven	0.5830

Table 5.13: Deposit 18 hydrated mineral veins top 5 mining systems.

Rank	Breakage	Excavation	Transport	Processing	Information Content
1	Hammer Drill	Bucket Drum Excavator	Bucket Drum Excavator	Oven	0.6830
2	Hammer Drill	LHD	LHD	Oven	0.7125
3	Hammer Drill	Bucket Drum Excavator	Truck	Oven	0.8000
4	Hammer Drill	Discrete Excavator	Truck	Oven	0.8215
5	Hammer Drill	LHD	Truck	Oven	0.8295

Table 5.14 shows a summary of all top 5 results, with mining systems information content averaged for comparison across deposits.

Table 5.14: Top 5 average results for all deposits.

Deposit ID	Deposit Description	Top 5 Average Information Content
1	Loose icy regolith sediment. [45, 194, 277]	0.5181
2	Layered compacted icy regolith. [45, 194, 277]	No solution
3	Layered pure ice layers. [138]	No solution
4	Icy/H_2O adsorbed regolith. [45]	0.5171
5	Compacted Icy regolith/H_2O adsorbed regolith. [45, 277]	0.7947
6	Pure massive ice. [138]	0.7947
7	Glacial rill with pockets of ice. [138, 226]	0.528
8	Compacted lunar crater regolith with ice pockets. [45]	0.5360
9	Compacted icy regolith. [45, 194, 277]	0.5360
10	Eroded hydrated mineral sediment.	0.5181
11	Layered hydrated mineral sediment. [81, 179]	No solution
12	Layered gypsum rocks with interbedded barren material. [193, 230]	No solution
13	Hydrated mineral regolith. [45, 95]	0.5171
14	Compacted hydrated mineral regolith. [45]	0.7562
15	Massive gypsum or epsomite rocks. [81, 230]	0.7562
16	Eroded hydrated mineral mixed with barren material. [95, 193]	0.5258
17	Eroded hydrated mineral mixed with barren material. [95, 193]	0.7693
18	Hydrated mineral veins. [207]	0.7693

No solution was found for the layered and consolidated/partially consolidated deposits as mining equipment in the current database are not capable to effectively break hard surface layers parallel to flat bedding planes and then allow selective excavation. Selective excavation is a requirement to mine this type of material without significant ore dilution. It is still possible to mine these deposits with components from the current database, but a change in the selective mining unit is required and internal dilution must be accepted. Hence, a reclassification of the ore body is needed. A selective mining unit is defined by Bozorgebrahimi, Hall and Blackwell [29] as *"the smallest block inside which ore and waste cannot be separated"*.

In order to reclassify the ore, the ice layering is ignored and larger selective mining units are considered. Figure 5.10 illustrates the change in selective mining unit and the effect of re-classification. The deposits could instead be considered lower grade and "evenly distributed". This change in selective mining unit enables the reclassification of deposits as shown in Table 5.15. The ore bodies would then be massive enough to apply bulk mining methods as the algorithm has suggested for the relevant re-classified deposits. The top 5 mining system suggestions for these re-classified deposits are shown respectively in Table 5.16, Table 5.17, Table 5.18 and Table 5.19. This type of mine planning process is usually considered after the preliminary mining system selection and instead as part of a feasibility study. It has been carried out simplistically here as a demonstration of the application of the Mining System Selection procedure.

Table 5.15: Potential reclassification of deposits with internal dilution to allow efficient mining.

Original Deposit Classification		Potential Reclassification	Consequence
Deposit Type #2	$\rightarrow$	Deposit Type #5	Internal Ore Dilution
Deposit Type #3	$\rightarrow$	Deposit Type #6	Internal Ore Dilution
Deposit Type #11	$\rightarrow$	Deposit Type #14	Internal Ore Dilution
Deposit Type #12	$\rightarrow$	Deposit Type #15	Internal Ore Dilution
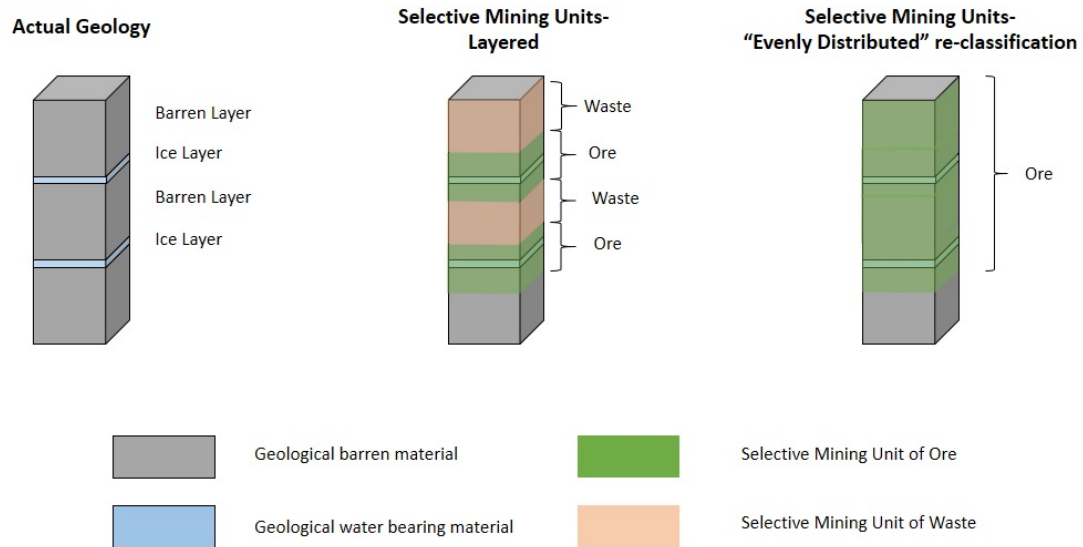
Figure 5.10: Selective mining units for layered deposit and re-classification.

Table 5.16: Top 5 mining systems for Deposit 5 (layered compacted icy regolith).

Rank	Breakage	Excavation	Transport	Processing	Information Content
1	Volatile Extraction Drill	Volatile Extraction Drill	Volatile Extraction Drill	Volatile Extraction Drill	0.5360
2	Micro Tunnel Boring	Micro Tunnel Boring	Truck	Oven	0.7995
3	Micro Tunnel Boring	Micro Tunnel Boring	Bucket Drum Excavator	Oven	0.8695
4	Micro Tunnel Boring	Bucket Drum Excavator	Bucket Drum Excavator	Oven	0.8695
5	Micro Tunnel Boring	LHD	LHD	Oven	0.8990

Table 5.17: Top 5 mining systems for Deposit 6 (layered pure ice layers).

Rank	Breakage	Excavation	Transport	Processing	Information Content
1	Volatile Extraction Drill	Volatile Extraction Drill	Volatile Extraction Drill	Volatile Extraction Drill	0.5360
2	Micro Tunnel Boring	Micro Tunnel Boring	Truck	Oven	0.7995
3	Micro Tunnel Boring	Micro Tunnel Boring	Bucket Drum Excavator	Oven	0.8695
4	Micro Tunnel Boring	Bucket Drum Excavator	Bucket Drum Excavator	Oven	0.8695
5	Micro Tunnel Boring	LHD	LHD	Oven	0.8990

Table 5.18: Top 5 mining systems for Deposit 14 (layered hydrated mineral sediment).

Rank	Breakage	Excavation	Transport	Processing	Information Content
1	Hammer Drill	Bucket Drum Excavator	Bucket Drum Excavator	Oven	0.6830
2	Hammer Drill	LHD	LHD	Oven	0.7125
3	Hammer Drill	Pneumatic Excavator	Pneumatic Excavator	Oven	0.7860
4	Micro Tunnel Boring	Micro Tunnel Boring	Truck	Oven	0.7995
5	Hammer Drill	Bucket Drum Excavator	Truck	Oven	0.8000

Table 5.19: Top 5 mining systems for Deposit 15 (layered gypsum rocks with interbedded barren material).

Rank	Breakage	Excavation	Transport	Processing	Information Content
1	Hammer Drill	Bucket Drum Excavator	Bucket Drum Excavator	Oven	0.6830
2	Hammer Drill	LHD	LHD	Oven	0.7125
3	Hammer Drill	Pneumatic Excavator	Pneumatic Excavator	Oven	0.7860
4	Micro Tunnel Boring	Micro Tunnel Boring	Truck	Oven	0.7995
5	Hammer Drill	Bucket Drum Excavator	Truck	Oven	0.8000

5.11.3   Limitations and Future Work

The preliminary Mining System Selection procedure for off-Earth mining proposed in this chapter has some notable limitations. Primarily, the accuracy in evaluating the Reliability and Information Content of potential designs is limited by the axiomatic design mapping process. In the absence of any real data on operational reliability the FR:DP mapping process can be inaccurate. However, the framework in this chapter has been deliberately chosen with a view to input real data into the algorithm in the future to remedy subjectiveness. The Monte Carlo reliability simulations can be directly substituted with real data once it is available and the FR:DP mappings have an intricate link to reliability that can be further developed in the future as described in Section 5.10. With these features, continuous improvement is anticipated and this procedure will not be easily replaced over time.

The issue of subjectivity was mentioned previously in Sections 5.2 and 5.4. It is noted that traditional mining system selection techniques have included subjective components in the past. The axiomatic design mapping process, as described in Section 5.4 is particularly likely to suffer from subjectivity. In order to minimise this weakness, rules that guide the level of decomposition of an equipment's Functional Requirements have been implemented to reduce disparity between users.

There also exists an issue with the ranking methodology based on reliability and information content. Productivity and effectiveness of the mining systems are not considered. For example, experiments by Craft et al. [52] have shown that a percussive excavation mechanism can reduce the amount of dig force required. This could potentially be a significant improvement on other excavation systems. However, there is no provision to quantify a productivity improvement within this mining selection procedure. Traditional mining system selection procedures do not consider productivity or cost at all so this issue is not new. Productivity and hazards management will be accounted for in later stages of the mine planning process as more information is made available, including the completion of preliminary mining system selection.

The results in this chapter should only be considered as a first step to deciding which systems are best applicable to off-Earth deposits and do not take productivity and hazard management into account. As with terrestrial mining, geological, environmental and operational data will be needed for a feasibility study to confirm the technical and economic viability of a particular mining system.

5.12 Conclusion

Mining method selection is a crucial part of the terrestrial mine planning process, and it has been identified that there is not an equivalent objective process for off-Earth mining. This chapter has outlined a novel mining system selection procedure for off-Earth resources. The results have demonstrated that the method can be applied to preliminary mining system selection, and provide useful, objective information to flow into follow up off-Earth mine planning and optimisation studies.

Although the current lack of operational data is a limitation of this research, the conceptual approach utilised here allows a process to be undertaken that was previously not possible. Collection of real operational data in the future will be easily fused into this algorithmic procedure to improve results.

Chapter 6

Extraction Sequence Optimisation with a Reinforcement Learning Agent

6.1 Introduction

ISRU is fundamentally different to terrestrial mining, it is the extraction and utilisation of materials, minerals or volatile chemicals in space, for space settlement and space mission-specific purposes. There are also many parallels with terrestrial mining, but as mentioned in Chapter 1 - *Introduction* it is incorrect to assume that the same objectives exist for ISRU that do for mining. The most important difference is that modern terrestrial mining operations are operated to make a profit. The planning processes and algorithms that guide modern mineral extraction systems are designed to maximise profit. However, profit is not the initial objective for ISRU. It has been identified as a requirement for future off-Earth missions and settlements [242] regardless of profit. Instead, it is cost saving and risk mitigation for the missions and settlements that creates value.

ISRU extraction planning has been shown in literature with some simple derivatives of

terrestrial mine planning [44, 51, 105, 147], which as mentioned above does not have the same objectives of ISRU. There has not been any focus on the extraction sequence or *cut-off grade* optimisation for ISRU. According to the thesis Objective 3, this chapter will examine the shortcomings of traditional mine planning algorithms when applied to ISRU. It firstly examines the difference between ISRU and terrestrial mining, identifying some deficiencies in established mine planning tools when applied to ISRU that must be resolved. A novel ISRU planning method is then presented that harnesses the problem-solving capability of Reinforcement Learning to optimise the extraction sequence and maximise the related benefits. This method resolves several issues with traditional methods when applied to ISRU, according to Objective 4 of the thesis. Reinforcement Learning algorithms are detailed and trialled for this specific task. Following Objective 5, an architecture is finally demonstrated which in some ways exceeds the capabilities of an expert human under test conditions.

6.2 Literature Review

6.2.1 Terrestrial Mine Planning

The goal of terrestrial mining is to extract the portion of a *mineral resource* which has positive economic value, otherwise known as the *ore reserve*, to make a profit. The definition of this *ore* described by Lane [161] depends on factors such as market prices and the costs of production. *Ore* can be categorised by a *cut-off grade* policy using Lane's formulae or other similar methods [116]. The chosen *cut-off grade* policy condenses a complex financial model into a single heuristic value for each discrete volume block of the *mineral resource*. This cut-off heuristic streamlines decision making for design and scheduling engineers.

In the special case of an open pit mine, there is naturally a requirement to uncover material prior to extracting it. An algorithm can be used in this case to determine the *ultimate pit limit*. This overburden removal constraint simplifies the problem sufficiently so a graphical algorithm such as Lerchs-Grossman or one of its descendants can be used to derive the

ultimate pit limit based on input cost and revenue parameters [204]. Advances on the speed of the Lerchs-Grossman algorithm have been made by implementing a pseudo flow algorithm [10] although the underlying graph relations remain similar.

The resulting *ultimate pit limit* is a mathematically optimal pit, albeit impractical to mine. It is used along with heuristic *cut-off grades* to assist engineers with further practical design and scheduling to provide a Net Present Value (NPV) business case [58]. The *cut-off grade* heuristic and the *ultimate pit limit* algorithms form the basis of modern terrestrial mine planning.

Hall [116] has also proposed a new paradigm for the derivation of *cut-off grades*. Instead of calculating the *cut-off grade* according to Lane's formulae [161], it could be derived from a numerical optimisation process. Hall [116] implements an iterative approach where a multi-dimensional NPV response is calculated from a parametric set of *cut-off grades* and other mine planning variables such as the extraction rate and processing rate. The most optimal parameter values are then selected for mining operations [15, 116, 300]. This new approach has yet to be widely adopted in industry.

6.2.2   Off-Earth ISRU Planning

ISRU is an enabler for off-Earth research, development, industry and settlement [191]. Although there are many analogies to terrestrial mining, ISRU is a distinct activity with distinct objectives. The value of ISRU can be measured by the cost savings in launch mass for these activities rather than the terrestrial analogy of profit [191, 221, 272]. This will be shown in more detail in Chapter 7. Another discrepancy is that mining requires an existing market [134], while ISRU aims to create its own market. Due to these discrepancies and more, a direct transfer of terrestrial mine planning tools to ISRU optimisation is ineffective.

For a detailed example, production cost and market price assumptions are not available for ISRU operations as no market or proven extraction technology currently exists. These inputs are required for terrestrial mine planning tools such as the Lerchs-Grossman algo-

rithm [204], Lane's formulae [161] and the parametric Hill of Value optimisation proposed by Hall [116]. Even in the terrestrial context, feasibility studies have significant issues in accurately determining production costs and market prices. Ongoing research is aimed at addressing this problem specifically for terrestrial mining [21, 66, 118].

Terrestrial mining feasibility studies also include equipment availability factors and cost items for maintenance and replacement in their assumptions. The longevity of equipment is not considered critical to the continuity of terrestrial mining operations as any equipment can be repaired or replaced while respecting the estimated parameters of cost and availability. In contrast, off-Earth ISRU operations will pause if enough equipment component failures occur, and the equipment could take months or years to replace. This is a major risk as resource extraction scheduled in the future may not be feasible at that time if the equipment has failed. In that case, the scheduled *resource* may not be considered *ore* in the terrestrial mining sense [134]. Another problem is that the timing of the equipment failure is unknown, adding significant uncertainty onto the classification of *ore* for ISRU. *Cut-off grade* policies based on Lane's theory [204] or other methods [116] contain the underlying assumptions that the equipment rates and costs are predetermined and equipment is perpetual or replaced without delay. The terrestrial mining algorithms and heuristics are therefore incompatible with ISRU as they do not account for uncertainties in those variables, or the finite and uncertain equipment lifespans.

The technology and engineering for ISRU operations are in the early stages. Capital costs for a range of engineering solutions are not yet known. ISRU feasibility is also constrained by the unknown capabilities of these engineering solutions. Examples include the infrastructure required to provide power to the site or the excavation equipment itself [222]. In the case of terrestrial mining, capital cost is one of the most important variables when determining physical constraints such as power and equipment capabilities. The capital cost can usually be benchmarked against a reference example which has already been carried out somewhere on Earth. This is not the case for off-Earth ISRU. The ISRU planning and optimisation process must account for these constraints at a more fundamental level compared to terrestrial mine optimisation. To enable this, ISRU financial costs need to

be decoupled from the assessment process so that cost assumptions can be updated as the engineering and technology are developed in the future. An example of de-coupling these assumptions is shown in the non-financial ISRU project assessment in Chapter 7.

Uncertainty in the geological environment has been a focus of research efforts to improve traditional mine planning methods [70]. The primary means to account for geological uncertainty in literature has been to run the Lerchs-Grossman algorithm with a distribution of geological inputs [170, 197]. This can be described as a Monte-Carlo method or stochastic simulation. Although the method allows better understanding of the effect of changes in the geological environment or other parameters, the probabilistic output creates an issue for mine design engineers. With stochastic simulation, there is a requirement to make subjective decisions based on a distribution of results and translate that into a practical mine design and schedule. With poor input data and even greater uncertainties for off-Earth ISRU, the input distributions and hence the Monte-Carlo Simulation results distribution broadens. Increasingly stochastic geological inputs and hence Monte-Carlo outputs make it difficult to select appropriate resource extraction plans that relate to the real *mineral resource*. Hence for off-Earth ISRU, the final extraction design using a Monte-Carlo approach is likely not much better than using a completely random design approach.

Finally, ISRU will likely be carried out via autonomous or remote operations and deliver a continuous stream of new sensor data. This data should be used to optimise extraction. The traditional heuristic mine planning approach is laborious. A continually changing dataset will cause process difficulties in maintaining an optimal mine design with limited human engineering resources. By moving beyond the traditional heuristic planning approach and towards methods that enable rapid data driven iteration, optimality in the design can be maintained with much less human effort.

6.2.3 ISRU Planning Requirements and Gaps

The previous section establishes reason for the incompatibilities between terrestrial algorithms and heuristics and off-Earth ISRU. Table 6.1 summarises the set of requirements identified for off-Earth ISRU planning techniques and the current analogous capabilities of terrestrial mine planning. There is a gap between the two that must be bridged to enable mine planning for ISRU and ensure maximum value is returned. In this chapter, a novel planning procedure for ISRU is developed to bridge these gaps.

Table 6.1: ISRU planning requirements and incompatibilities with traditional capabilities.

	ISRU planning requirement	Traditional mine planning capability
#1	Aim to maximise Resource Utilisation. Physical constraints such as power and equipment capabilities apply.	Aim to maximise Net Present Value. Cost, market price and equipment availability assumptions apply. These assumptions are incompatible with ISRU.
#2	Account for the risk of equipment failure and the effect on operations.	Assume that equipment can be easily replaced. Risk of termination of operations due to equipment failure not usually considered.
#3	A planning algorithm without inputs of production cost or market prices due to uncertainty of these assumptions.	Planning algorithms balance between input production costs and market revenue assumptions.
#4	Manage stochastic input assumptions for geology and equipment reliability.	Typically, Monte Carlo Simulation scenario analysis. This must be condensed to a final design by a subjective decision maker.
#5	Rapid iteration of designs with large volumes of new data.	Engineering design based on data. Rapid updates not possible with limited human resources.

6.2.4 Reinforcement Learning

Reinforcement Learning (RL) uses principles of dynamic programming to break complex multidimensional optimisation problems into smaller recurrent problems [6, 98]. The RL problem is framed as an interactive environment where an agent can take actions to transition through the environment and collect rewards or penalties for each transition. The environment is a Markov Decision Process (MDP) which can be deterministic and

only affected by the agent's actions or stochastic and include random elements. This framing of the problem is ideal for the ISRU extraction optimisation as it allows for random uncertainties in the environment to be considered, learning of optimum policies which can generalise to various environments, non-explicit programming of complex mining constraints and the continual update of the environment with new data. The capabilities of RL promise to bridge all the requirement gaps for ISRU planning identified in Table 6.1.

The RL agent learns underlying value distributions of the MDP environment and selects maximum value actions based on its neural network function approximation. The agent improves its actions closer to the optimal trajectory through exploration of the MDP.

There have been many new algorithms developed for Reinforcement Learning recently as function approximation via neural networks has become more practical. They can be divided into several classes of algorithm: value based or policy based [98], model based or model free [98], on-policy or off-policy [65], online or offline [253]. The details of all these categories of RL algorithm are beyond the scope of this chapter, but further information can be found in the reference books by Sutton and Barto [287] or François-Lavet *et al.* [98] and Beysolow II [22].

Three model-free experience sampling RL architectures from literature and contained in the Stable Baselines [122] python package are trialled for this research. The algorithms trialled include Deep Q-Learning (DQN) [196], Advantage Actor-Critic (A2C) [195,301] [33, 34] and Actor-Critic with Experience Replay (ACER) [304]. Their respective categories are outlined in Table 6.2.

Table 6.2: RL algorithm categorisation.

Algorithm	Abbrev.	Policy/Value	On/Off Policy
Deep Q-Learning [196]	DQN	Value Based	Off Policy (Experience Replay)
Advantage Actor-Critic [195]	A2C	Policy Based	On Policy (No Experience Replay)
Actor-Critic with Experience Replay [304]	ACER	Policy Based	Off Policy (Experience Replay)

The first potential algorithm is Deep Q-Learning [196]. This is a value iteration algorithm
which attempts to estimate the value of any potential action, and maximise the rewards
based on the estimated values. An iterative update of the Bellman Equation is utilised
for this purpose, the one-step Q-learning update [287] is shown in Equation 6.1.

$$Q\left(s_t, a_t\right) \leftarrow Q\left(s_t, a_t\right) + \alpha[r_{i+1} + \gamma \max_a Q\left(s_{i+1}, a\right) - Q\left(s_t, a_t\right)] \tag{6.1}$$

Where $Q(s_t, a_t)$ is the total expected future reward from iteration step (t) when following
the optimal Q value function action $\max_a(Q(s_t, a_t))$ for the current state s and action a.
The transition reward is r and the discount factor for future rewards is γ for a step size α.

Iteratively updating this equation with state-action-reward-state data will allow conver-
gence to the optimal value function Q^* as i approaches infinity [287]. The Q^* function or
a close approximation is then used to find the optimal trajectory.

The Deep Q-Learning algorithm will usually not perform well in environments with a
random element to the reward function or state transition (such as stochastic geological
environments) as the action selection depends on iterative update of previously received
deterministic rewards [301].

Instead of taking the maximum expected value action as with Q-learning, actions can be
chosen based on a parameterised policy $(\pi(a|s; \theta))$ [195]. Where π is a policy to determine
action a given state s. The policy has parameters θ, usually approximated by a neural
network. This policy is iteratively updated by gradient ascent to maximise the expected
reward. This policy gradient method can also be improved by reducing the variance of
rewards in the update step. This is done by quantifying and proportionately learning from
more surprising actions. Prioritising surprising experiences in the learning update process
is done by applying the Advantage function in Equation 6.2.

$$A^\pi(s, a) = Q^\pi(s, a) - V^\pi(s) \tag{6.2}$$

Where A^π is the advantage of taking action a in state s. Q^π is the expected reward for policy π in state s and action a. V^π is an estimate of the value of the state s.

Equation 6.2 is used in the Advantage Actor-Critic (A2C) algorithm [195,301]. It converges to the optimal policy by iteratively taking actions, receiving rewards and updating the parameters (θ) of policy ($\pi(a|s;\theta)$ as per Equation 6.3.

$$d\theta \leftarrow d\theta + A^\pi(s_{t,}a_t)\nabla_\theta \log \pi_\theta(a_t|s_t) \tag{6.3}$$

Where the $\nabla_\theta \log \pi_\theta(a_t|s_t)$ is the policy gradient approximation. The update parameters for the state value function $V(s;\theta_v)$ are accumulated using Equation 6.4.

$$d\theta_v \leftarrow d\theta_v + \frac{\partial A^\pi(a_t, s_t)^2}{\partial \theta_v} \tag{6.4}$$

The values of the parameters θ and θ_v are then updated synchronously (for A2C) or asynchronously (for A3C) using $d\theta$ and $d\theta_\mathrm{v}$.

The Advantage Actor-Critic methods are on-policy algorithms, meaning they only use the current trajectory to update policy parameters. For sparse environments where many actions are required to receive a single reward, the on-policy algorithms may take a long time to converge and can exhibit high variance.

The high variance and poor sample efficiency of Advantage Actor-Critic is improved by the Actor-Critic with Experience Replay (ACER) [304] algorithm. This algorithm implements experience replay, where state-action-rewards are stored in memory and can be re-used for learning multiple times and improve sample efficiency. Several innovations have been implemented to enable Actor-Critic with Experience Replay. These include a truncated importance sampling method called RETRACE proposed by Munos *et al.* [203]. The importance sampling ratio gives extra weight to behavioural policies that have provided a positive surprise in reward. These are more likely to be used for the policy update. The

second main innovation used in ACER is the policy update trust region after Schulman *et
al.* [255]. This limits the magnitude of policy parameter updates to reduce variance.

Another innovation that could be applied to improve any of these reinforcement learning
algorithms is pre-processing with a 3D Convolutional Neural Network (CNN) [163, 177].
In the case of the 3D geological environment a 3D CNN uses optimised data filters to
identify larger features that span across several blocks. For large geological environments,
pre-processing data with a 3D CNN could improve the speed and effectiveness of agent
training. The 3D CNN is an additional step of a data processing pipeline prior to the
trained neural networks. It requires neural network back-propagation to optimise the
filters and hence can also decrease computational efficiency depending on the complexity
of the problem itself.

Extensive experimentation and parameter tuning is required to determine the best archi-
tectures and parameter combinations for specific reinforcement learning problems.

6.2.5   Reinforcement Learning in Mine Planning

There are limited examples of research where reinforcement learning has been applied to
terrestrial mine planning and none for ISRU. Elevli [83] has proposed a combination of
the scheduling and pit optimisation problems through a dynamic programming approach.
This approach also applies a version of the Bellman Equation 6.1. It varies from RL, as a
graph of the geological environment is generated and an exhaustive search for the highest
reward trajectory is conducted. It is model-based and not computationally practical for
larger geological environments as the possible number of trajectories becomes very large.

Askari-Nasab and Awuah-Offei [7] apply Q-learning to open pit *pushback* selection in or-
der to maximise the Net Present Value of the long-term schedule. This algorithm has
been developed to easily fit with contemporary terrestrial mine planning methods and
was demonstrated on a full-scale iron ore deposit. The algorithm utilises *pushbacks* gen-
erated by the Lerchs-Grossman revenue factor method. It selects options for scheduling

the *pushback* to maximise NPV. However, since the Lerchs-Grossman algorithm requires costs and market prices as inputs, it is not applicable to ISRU. It is also constrained by the Lerchs-Grossman algorithm revenue factor step size and does not support short term decision making as with the block-by-block approach. Furthermore, the Q-learning approach does not allow generalisation to other geological environments as the state-values of each specific *pushback* are progressively learned.

Kumar and Dimitrakopoulos [156] have developed an algorithm that optimises the short term mine schedule using Monte Carlo Tree Search and an RL agent. The environment is regularly updated with incoming new data from blasthole drilling and equipment utilisation rates. This enables decisions to be made using the most up to date data, without engaging in the traditionally slow human mine planning decision process. It is designed specifically for terrestrial mine planning and utilises market prices and financial costs in the optimisation objective function, therefore not applicable to ISRU. Furthermore, the RL agent shown by Kumar and Dimitrakopoulos [156] uses a fixed extraction sequence from the long-term mine plan. Only the material destinations are modified by the agent. This is a form of short-term *cut-off grade* optimisation and not full scale mine planning.

RL has also been proposed for other terrestrial mining problems such as the optimisation of truck dispatching [216] whereas neural networks and broader machine learning algorithms can also be applied to problems such as geological modelling [129].

The key contribution of this chapter is a new method of extraction planning specifically for off-Earth ISRU and testing of various RL algorithms for this purpose. The proposed method includes a generalised mine sequencing agent. The generalisation allows the extraction sequence for various orebodies to be generated by a single agent. The short-term schedule becomes unnecessary due to the ease of re-generating a full long-term extraction sequence with a trained agent. Optimized *cut-off grades* can also be quickly derived by the agent and some post-processing of parameterised scenarios. The rapidly generated mining sequences can also be used to quantify various risks related to ISRU operations, including equipment failures and geological uncertainty. Although designed specifically for ISRU optimisation, the proposed method could also be used as an alternative for terrestrial

mine planning.

6.3 Methodology

6.3.1 ISRU Optimisation Objective and Constraints

This section will explore an optimisation objective for ISRU planning when traditional maximisation of financial objectives, such as NPV, are not applicable.

The intent of off-Earth ISRU is generally to maximise the "value" of the operation. The "value" can be measured by the amount of launch mass saved for other off-Earth activities [191, 221, 272]. These savings can be more directly measured by the quantity of in-situ resources utilised. This is a contrast to the financial objectives of terrestrial mining. An example of one non-financial measure, the Propellant Payback Ratio for ISRU will demonstrated in detail in Chapter 7. The Propellant Payback Ratio is a unitless indicator of an operation's long-term competitiveness compared to a terrestrial launch capability which can be calculated at an early stage. It can also be used for short term decision-making similar to Lane's theory [161]. However, it does not solve all the incompatibilities stated in Table 6.1. Much like traditional mine planning tools, it doesn't efficiently accept stochastic inputs and does not support rapid design iteration with continuous data streams.

Since "value" for an ISRU operation can be measured by the cost savings from launching the same mass from Earth, a non-financial ISRU optimisation objective is naturally *to maximise the quantity of resource utilisation*. This is subject to the following inputs and constraints.

1. Geological inputs and uncertainty – described by probability distributions.

The quantity of product in each block of a *resource* is limited and uncertain. Each block will be subject to a time and energy consuming process to extract the product before the

product value is realised. This means that uncertainty in the amount of contained product may lead to wasted time and energy (or a surprising gain).

2. Material precedence constraints – described by geometry.

The mining system is limited by its design parameters. It is unable to select any block of material at any time. In the case where the deposit is non-uniform and undercover, an open pit style system must move waste material to access the desired block. This is known as a precedence constraint [10]. The precedence constraint can be programmed into the reward function as a penalty to encourage the agent to take valid actions or explicitly coded as a limitation on the available actions. If only a penalty is applied for an incorrect action, the algorithm may find solutions by accepting a short-term penalty and breaking this constraint. To avoid this, all actions are checked for validity. Invalid actions are not allowed to make progress. During training, the agent will learn to avoid these invalid actions, as they cause a penalty and do not make any progress.

3. Equipment reliability and lifespan constraint – described by stochastic distribution.

The equipment lifespan is an uncertain length. It has a measurable dependency on the amount of work done by the equipment and the amount of preventative and corrective maintenance done. Equipment lifespan determines the time limit for product delivery and hence the value of the operation.

4. Equipment capability constraints – described by physical equations.

The number and type of equipment, including their power and any ancillary requirements limits the work that can be done. In this chapter, only a simple single-trajectory system is considered for demonstration of the planning algorithm. Systems with multiple units may require more advanced co-operative ISRU planning algorithms.

6.3.2 Resource Extraction Trajectory

RL can be applied to produce a near optimal trajectory for resource extraction subject to
the constraints for each system. This trajectory can be used as a sequence of extraction
that optimises resource utilisation subject to constraints. It serves a similar purpose to the
Lerchs-Grossman's ultimate pit limit methodology but solves several of the issues created
by that algorithm and traditional mine planning in general.

Firstly, an RL agent does not need to balance costs with revenue to determine an *ultimate
pit limit*. An *ultimate pit limit* is no longer valid due to uncertainty in equipment lifespans.
The reward function can instead be based on the product quantity generation alone, or
with penalties included for undesirable actions. The agent trajectory can be used instead
of an *ultimate pit limit* for value analysis.

Secondly, a resulting trajectory can be accurately discounted at each timestep to estimate
risk adjusted returns and be used for short term decision making. The Lerchs-Grossman
algorithm alone is not appropriate for short term decision making due to the additional
engineering required to translate the results of a mathematical optimum to a practical
design and sequence. In this way, it does not work well to apply discount factors on a
block-by-block resolution and is generally only used for largescale slices or *pushbacks* with
an estimated extraction timeframe [190].

Thirdly, the resource extraction trajectory can be truncated at any timestep depending
on the random occurrence of equipment failure. Varying the trajectory length based on
equipment lifespan expectations yields an expected quantity of resource utilisation. Hence
the ISRU operation's value can still be estimated if future blocks on the trajectory result
in being unviable.

Fourthly, a generalised RL agent can be used to provide ISRU trajectories and values for a
range of input geological environments and risk settings. This allows better understanding
of the mine design and sequence impacts of geological updates or chances in risk parameters
and reduces the need for subjective human decision making. The trajectory of a generalised

agent can also be easily re-run for any updated environmental data that may become available, allowing rapid design iteration.

6.3.3   Geological Environment

The geological environment used in this study is a voxelised estimation of the desired product *grades* in a defined area of lunar regolith. The product is H_2O to be used in rocket fuel manufacturing [19, 36] on the Moon. An array is generated in three geometric dimensions representing the relative physical location of each block of material. Each block is assigned two data channels. One for H_2O concentration and one for physical status. The physical status is a logical variable 1/0 representing the block being mined/unmined respectively. This results in a 4-dimensional array. Additional channels can be added to convey any desired information, although more concise environmental representations are easier for the RL agent to learn.

The environment is populated with a geological structure of varying H_2O concentrations. To automatically generate geological structures, a number of randomised H_2O seeds are placed in a blank 3D block environment. Interpolation using the inverse distance squared weighting method populates the remaining H_2O concentrations as shown in Equation 6.5.

$$H_2O_\mu = \frac{\sum_i^n \frac{H_2O_i}{d_i^2}}{\sum_i^n \frac{1}{d_i^2}} \tag{6.5}$$

Where H_2O_μ is the concentration or *grade* in a given block, i is the seed at distance d and n is the total number of seeds.

Figure 6.1 shows separate examples of the generated geological environment. The average H_2O concentration for each environment is taken as the visible cut-off value for improved images. Any of the visible blocks are coloured based on their H_2O *grade* relative to the sample average as shown in the legend.

Geological environment generation is simplified in this chapter compared to a practical
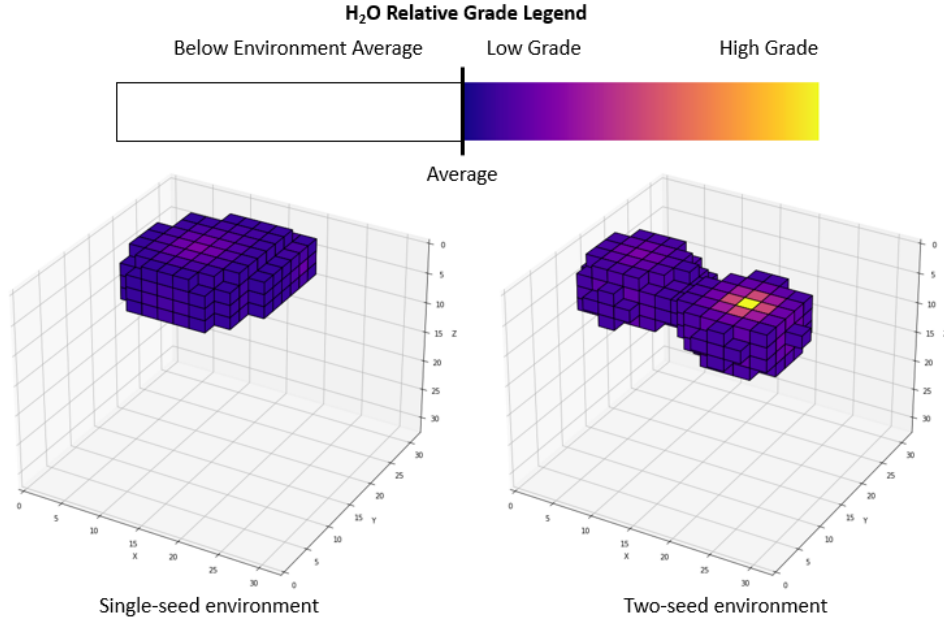
Figure 6.1: Geological environment examples.

method. The simplification enables research to proceed without data intensive geological
modelling techniques that add little value to the results presented here. In practice,
detailed lunar geological data should be collected, inferences made, and domains should
be identified to assist with environment modelling. The modelled environment should
then be tested against ground truth as mining progresses. Currently, geological model
validation is not possible for ISRU research. Cannon and Britt [36] have begun to examine
the modelling of geological environments for lunar H_2O resources in more detail.

6.3.4 Mining System Constraints and Reward Shaping

The number of available extraction sequences will be limited by the precedence constraints
of the mining system. Mining system examples such as the Volatile Extraction Drill and
Discrete Excavator can be taken from a generic equipment pool summarised in Chapter 4.
For example, a Volatile Extraction Drill will move around the surface and drill downwards
to reach a volatile block of *ore* and then heat it to remove the desired gaseous H_2O
product. This system will easily extract blocks aligned vertically but require additional

time to move to a new site and establish the hole. In contrast, a Discrete Excavator will dig regolith from the surface and then move outwards from that initial location. Downward cuts rather than horizontally advancing cuts will require slightly more time and energy due to gravitational force working against the excavator.

These mining system constraints can be implemented explicitly by limiting available actions for each step. Additionally, the system constraints can be included as penalties in the environment's reward function. A penalty can be applied to the transition (instead of a reward) where predetermined inefficient or impractical actions are taken. The RL agent will learn to avoid these actions where possible. In this chapter, to avoid learning from undesirable actions and wasting training time, a penalty is assigned for an invalid action and no progress will be allowed in the environment. This limits the number of invalid action-states that an agent can learn from. Other similar studies explicitly limit actions at each step based on precedence constraints [7, 83, 156].

The mining system chosen for demonstration in this chapter is based on the Discrete Excavator from Chapter 4. For simplicity, the assumption is made that no additional equipment is required for rock breakage. The reward function is modified with mining system penalties based on block precedence requirements such as overburden removal shown in Figure 6.2. Nine overlying blocks must be removed prior to the target block so that a penalty is not received. The RL agent learns the optimum policy of extraction while avoiding unnecessary penalties.

Other constraints such as safe working proximity and geotechnical stability constraints could also be included in the future.

The reward function in this chapter has also been used to encourage the agent to take actions that are considered efficient for an excavator-type system. Figure 6.3 shows the first block to be extracted from a level surface (red) will result in an inefficiency penalty while the adjacent blocks will not. This penalty aims to account for the additional time and energy required to take a downwards cut.
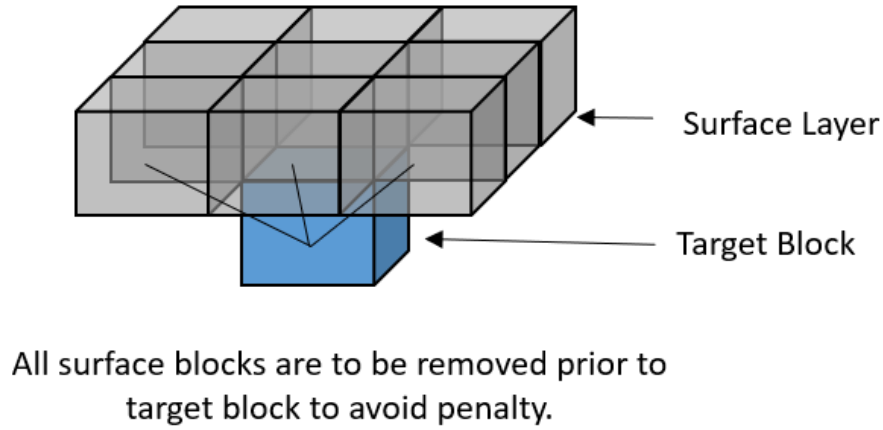
Figure 6.2: Overburden removal precedence.
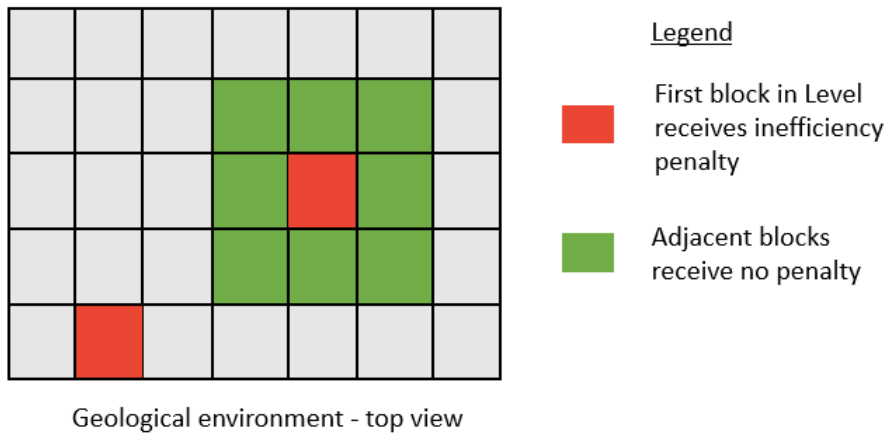
Figure 6.3: Discrete excavator inefficiency penalty.

The question remains to determine the appropriate amount of penalty for these actions. The effect of these penalties will be explored parametrically as shown in results Section 6.4.1.3. The average H_2O concentration of the environment is used as a base case penalty in this chapter. Equation 6.6 shows the agent's reward if the action is determined to be inefficient or impractical. Note the negative sign causing a penalty. The concentration is multiplied by 10 kg for each block to convert to a H_2O product mass. This scaling also helps to distinguish cumulative penalties and rewards more easily on learning curve charts over several steps.

$$Average\ Reward\ \text{(kg)} = -10\ kg \frac{\sum_1^n H_2O_\mu}{n} s \qquad (6.6)$$

Where n is the number of blocks and H_2O_μ is the concentration in kg H_2O per kg regolith for each block and s is a scalar used for tuning. The value for s has been chosen as 1.0 after parametric analysis.

The agent will also be penalized for extracting any material lower than the average concentration. This part of the reward function encourages the agent to focus on high-*grade* regions and takes advantage of geological domains where high concentrations are more common in the same region. This penalty was introduced at a later stage after initial trials demonstrated slow learning progress. The results of this modification are shown in Section 6.4.1.3. The average block H_2O concentration in the environment has been used as a baseline for this penalty. The resulting reward or penalty is determined according to Equation 6.7.

$$Reward\ (kg) = 10kg \times\ H_2O_\mu - Average\ Reward \qquad (6.7)$$

It is important to realise that the reward function is used to train the agent to perform desirable behaviours. It should not be used to directly demonstrate the value of an ISRU operation. For example, the agent will collect rewards and penalties throughout the extraction trajectory. The cumulative value of the reward does not equal the true "value" of the operation or the quantity of resource utilisation. The penalties and baseline within the reward function do not actually represent physical *ore* quantities. To find the true quantities from the ISRU trajectory, a post-processing accumulation step should be carried out, using the extraction trajectory H_2O *grades* and any *cut-off grade*.

6.3.5 Agent Action Mapping and Episode Termination

The Advantage Actor-Critic's (A2C) actor neural network is configured with n^2 action output nodes. Where n is the side length of the geological environment. This represents a 2D plane of n × n possible actions, with each node correlating to a surface location in the block environment. For example, a geological environment with size $7 \times 7 \times 3$ blocks will have a two-dimensional selection plane of $7 \times 7 = 49$ possible actions. A visual example of the action mapping is shown for a $7 \times 7 \times 3$ environment in Figure 6.4. The uppermost available block will be extracted for each of the possible actions. The dependency constraints in Section 6.3.4 will be checked for each action and cause either a reward for extraction or a penalty for violating the constraints. The agent eventually learns the expected state values for each action and choses the highest state-value blocks to extract.

The 2D selection plane method works well for small environments. However, the number of output nodes for the neural network increases with n^2. This greatly increases training time for larger environments due to the number of additional neural network parameters. Alternatively, agent output node configuration could be simplified to only 5 actions for all environments. The 5 actions: North, South, East, West and Extract would allow the agent to traverse through the environment and select the current location for extraction. The downside of this method is that rewards are less common, and more training steps are required to offset the reward sparsity.

Only the 2D selection plane will be applied in this chapter, however further investigations in the future should examine the effectiveness of different agent action mapping techniques.

The default terminal state is reached when the maximum allowable number of steps have been taken. This terminal state serves to ensure large portions of the geological environment are left intact and hence boundary conditions are not likely to be experienced. The maximum number of steps is input as a percentage of the closest integer number of blocks in the geological environment. The default trajectory length in this chapter is equal to 10% of the number blocks in the geological environment. That is 90 valid timesteps
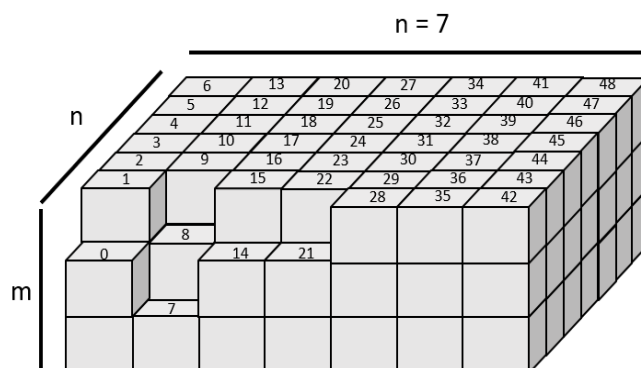
Figure 6.4: Agent action mapping for n x n block environment.

per episode for an environment with dimensions of $15 \times 15 \times 4$. Invalid actions that violate precedence constraints will still count as episode timesteps but no change to the environment or remaining number of "valid" timesteps will occur.

6.3.6 Agent Training

6.3.6.1 Algorithms and Tuning

The RL pipeline proposed in this chapter has been developed iteratively by testing three main learning algorithms. The algorithms, introduced in section 6.2.4, comprise of the following options available in the Stable Baselines [122] package:

- Deep Q-Learning - (DQN);

- Synchronous Actor-Critic - (A2C); and

- Actor-Critic with Experience Replay - (ACER).

The results from these algorithms can be highly sensitive to variations in *hyperparameters* such as the learning rate and discount factor. Tuning of the learning rate and gamma discount factors has been carried out using a grid-search method [173]. Training has been

run for 11.5 hours on the computational cluster Katana supported by Research Technology Services at UNSW Sydney [236]. Grid search training has been conducted with 4 CPUs for the A2C architecture and 1 CPU for the ACER architecture. The *hyperparameter* tuning results can be seen in Section 6.4.1. The trained agents are evaluated on a set of 100 unseen environments throughout training to determine the generalisation effectiveness of the algorithm. Tuning of the environmental penalty for this problem was also conducted using grid-search.

Once final training parameters have been chosen, agent training was conducted using 16 parallel CPU cores. The results can be viewed in Section 6.4.2.

6.3.6.2   Supervised Learning and Evaluation

Comparing a stochastic agent's capabilities while also removing the distorting effect of varied reward concentrations in the evaluation environments is important. Evaluating an agent with randomly generated environments does not efficiently achieve comparative results as some environments will naturally contain more available rewards than others. To remove this variance and help quantify the optimisation ability of agents, a supervised learning approach will be taken.

A large set of randomly generated environments will be saved and divided into training and test sets. Evaluation on the smaller test set can then be carried out to compare agents during training. The test set is made up of 100 randomly generated environments which will remain unchanged. The training set is periodically updated throughout the training with new randomly generated environments and partially completed environments saved from a training episode. This process of regenerating and recycling increases the diversity of agent experiences rather than using a fixed training set.

Any evaluations of the agent outside of the training loop should also be done on specific environments for comparison, not randomly generated ones. For example, specific environments are chosen and saved when comparing the human trajectory to the agent trajectory

or running scenario tests for *cut-off grade* optimisation.

6.3.6.3   Agent Policy Generalisation

Agent policy generalisation is achieved by ensuring the agent receives a sufficiently diverse set of training experiences. The computational cost of generating a new random environment for every episode is high. Hence, it is desirable to minimise the amount of environment generations while still maintaining a sufficiently diverse training set. A type of supervised or "curriculum" reinforcement learning [210] can be applied to update the training set as required. In this research, diverse training experience is enabled by randomly generating a set of 5000 environments, then slowly updating the set throughout training. The training set is shared between several parallel agents and algorithms, hence the work of re-generation of examples is also shared. The set is updated with partially mined environments saved from previous episodes, along with new randomly generated environments. These new and partially extracted environments are initially introduced with a ratio of 1:1 to ensure a stable state is achieved over time. They are updated at a random frequency with probability of 1 update per 50 000 timesteps per agent. During the training process, environment files are randomly chosen and loaded from the training set. The expected concentrations of new environments and partially extracted environments is shown in Figure 6.5. Over time, the concentration of new to partially extracted environments can be modified as shown in Figure 6.5 at $5\text{x}10^8$ timesteps. At this time the concentration is changed to 2:1 partial environment per new random environment. The fresh environment will only be updated every 1 in 100 000 timesteps per agent. The higher concentration of partially mined environments allows the agent to experience advanced states more often rather than the common initial state. This manages one of the expected issues of exploration, where the agent does not see sufficient samples of advanced stage trajectories. There are a greater number of possible combinations for advanced stage trajectories and hence a lower probability of experiencing a representative sample.

Figure 6.6 shows the learning pipeline for an A2C agent from environment generation
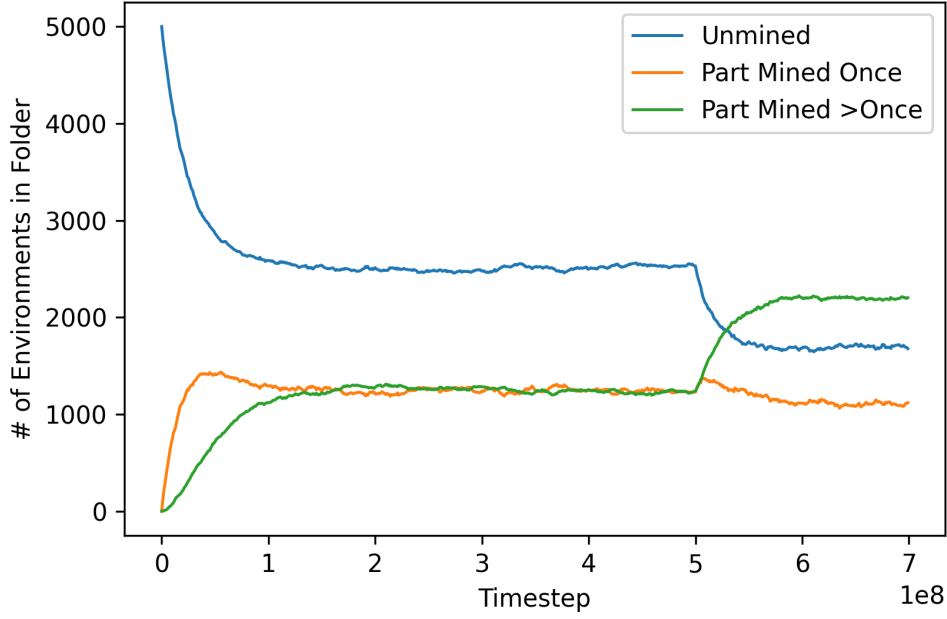
Figure 6.5: Environment types available for training.

through to the policy update training loop. The initial 5000 environment generations are
done independently of the RL training algorithm to fill the storage folder. A further 100
environments are stored separately for evaluation of the agent's generalisation capability.
These 100 environments will never be used for training, only evaluation.
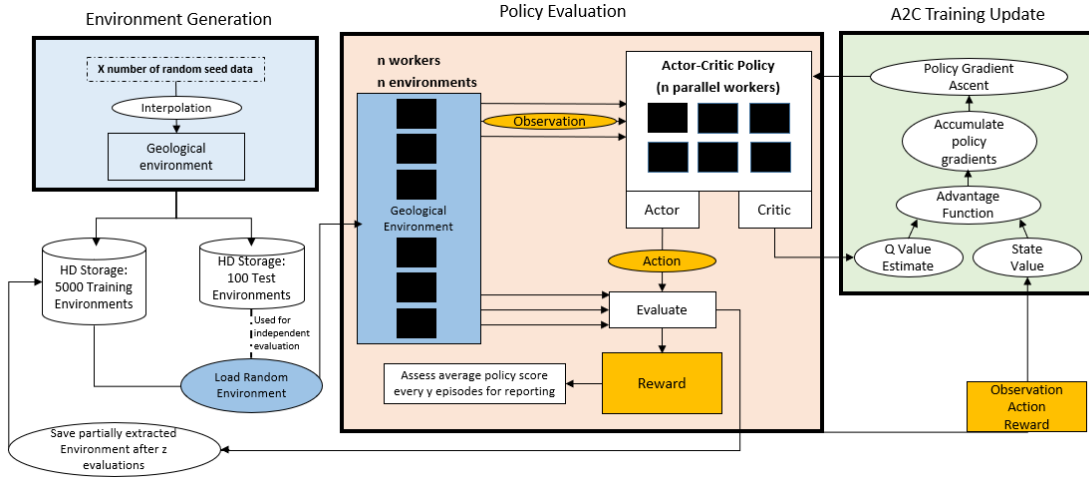
Figure 6.6: Training pipeline for ISRU trajectory optimization with A2C Agents.

A demonstration of the generalisation ability is shown by the agent training evaluations

in results Section 6.4.2.

6.3.7   ISRU Planning Tool Demonstration

6.3.7.1   Human Expert Comparison

It may seem a desirable goal to determine the absolute optimum extraction sequence. However, the "optimum" can only be found for the given inputs. An "optimal" sequence for an inaccurate geological environment is in reality sub-optimal. Hence there is not much additional value to find the mathematical optimum extraction sequence for an ISRU scenario compared to a "near" optimum. It is however important to quantify the performance of the agent against a good baseline. For this purpose, a human expert will be used to provide a trajectory for the agent's performance to be compared. It is possible that the human expert could spend several hours to determine an absolute optimum sequence via educated trial and error. Again, there is not much additional value to find the absolute optimum when inputs are likely to change. In this experiment, the human expert was only allowed one trial at generating a near optimal sequence. The results of the comparison between expert and agent are shown in Section 6.4.3.

6.3.7.2   Risk Adjusted Return

Following the findings of Pelech, Roesler and Saydam [221] and as will be detailed in Chapter 7, the ISRU operation's competitiveness is dependent on the amount of product that can be delivered. It is shown in Chapter 5 that while the processing efficiency and *ore grade* are important factors, the equipment reliability and longevity is key to optimising an ISRU operation. Long life and reliable equipment enables discovery, access and exploitation of higher *grade* material and hence maximise the amount of product that can be delivered. The equipment reliability is therefore an important consideration for the ISRU planning algorithm presented in this chapter.

The lifespan of the equipment is an uncertain quantity which can only be modelled by
a random variable. The agent's discount factor γ already provides the desired effect
and causes imminent rewards to be valued higher than equivalent future rewards. A lower
discount factor encourages the agent to act more greedily and prioritise short-term rewards
over larger long-term rewards. The greedy extraction trajectory must then be truncated
early (terminated) to a sampled equipment lifespan in a post-processing step to determine
the expected return of that ISRU sequence.

A Monte-Carlo Simulation can be run to sample expected returns from the terminated
extraction trajectory. For example, a trajectory is randomly terminated over 10 000 trials
to determine the expected distribution of returns based on the equipment reliability. The
probability of termination on any timestep has been modelled by the equipment failure
random variable shown in Equation 6.8.

$$\Pr\left(Terminal|t\right) = \Pr(X < 0.001t) \tag{6.8}$$

Where t is the timestep and $X \in (0,1)$ a uniform random variable. In this example, the
probability of failure increases linearly as time t goes on to simulate wearing of equip-
ment parts. Any probability function can be applied here in practice to yield the desired
equipment reliability response.

An example distribution of the expected return, or risk adjusted return from a specific
environment is shown in results Section 6.4.4.1.

6.3.7.3 Cut-off grade optimisation

Cut-off grade optimisation is traditionally a multidimensional problem solved to maximise
the value of a mining operation [116]. The *cut-off grade* determines the destination of
the excavated material. For example, a *cut-off grade* may be raised to 10% H_2O meaning
that any material lower than that would be discarded to the waste stream, saving energy

and resources for more productive material. Higher *grades* will still report to the product stream and undertake further beneficiation to produce pure H_2O.

The potential of a system to be optimised in this manner also depends on the capacities and bottlenecks along the production line. It is therefore important to understand the system capacity constraints. For the case studied in this chapter; the production system has three stages: a moderate-capacity excavation stage, a high-capacity transport stage that can undertake extra works and a low-capacity beneficiation stage which acts as the overall limitation of the system. The production flowchart with capacity constraints is shown as part of Figure 6.7 with material flows.
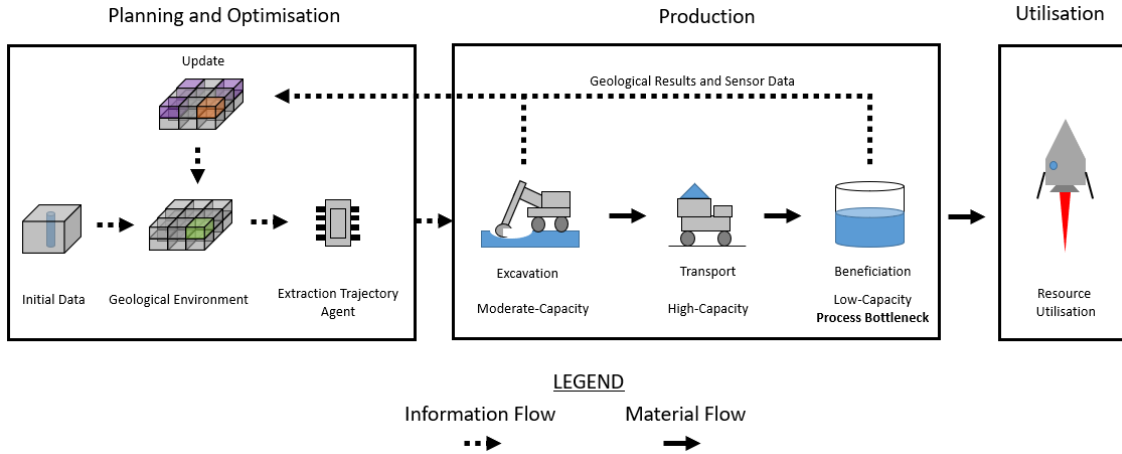
Figure 6.7: Simple lunar ISRU process including planning and information Updates.

The excavation step itself has surplus capacity to enable excavation and discarding of waste material while sustaining a fully utilised beneficiation step. This is analogous to a mill-constrained system in terrestrial mining [116, 161]. In this scenario, it is usually advantageous to increase the *cut-off grade*, maximise throughput *grades* and hence H_2O output from the beneficiation bottleneck. Conversely with a mine-constrained system, the *cut-off grade* should be reduced to maximise overall material throughput and hence H_2O output which is limited by the excavation step.

6.3.7.4 Rapid Environment Updates

An optimal sequence of extraction is required to maximise ISRU value prior to equipment failure. The optimal sequence will deliver the greatest amount of product with the least amount of work by taking advantage of variances in the geology. It is known that estimation errors will occur in generating the environment due to geological uncertainty. As extraction progresses, more geological information will be obtained, and the geological uncertainty will reduce. This may lead to necessary updates of the observable environment.

This issue, the changing understanding of geology has been intentionally decoupled from the ISRU optimisation in this chapter. The solution applied here is to train a general agent to optimise extraction for any foreseeable geological environment. Information will be gained about the geology as ISRU progresses and the modelled environment can be updated accordingly. The general agent will then be given a newly updated environment to generate a new trajectory. The process for information updating is described in Figure 6.7 with the information flow from the extraction process to the planning process and back again.

Updates can be managed by a generalised extraction policy so that the agent can run on any foreseeable geological environment and determine a near-optimum sequence. The ability of a general agent to produce near-optimal extraction trajectories for unseen environments also enables rapid scenario testing and decision making. Scenarios can be carried out based on varying input risk parameters such as geological value and equipment lifespan. A demonstration of the generalisation capability of the agent is shown in Section 6.4.2. Evidence of variable scenario testing is also shown in the *cut-off grade* optimisation results in Section 6.4.4.2.

6.4 Results

6.4.1 Hyperparameter Tuning

6.4.1.1 Learning Rate

The results for the learning rate *hyperparameter* tuning are shown in Figure 6.8 and Figure 6.9. The optimum learning rate for the ACER architecture in this problem is 0.0001 and 0.001 for A2C.
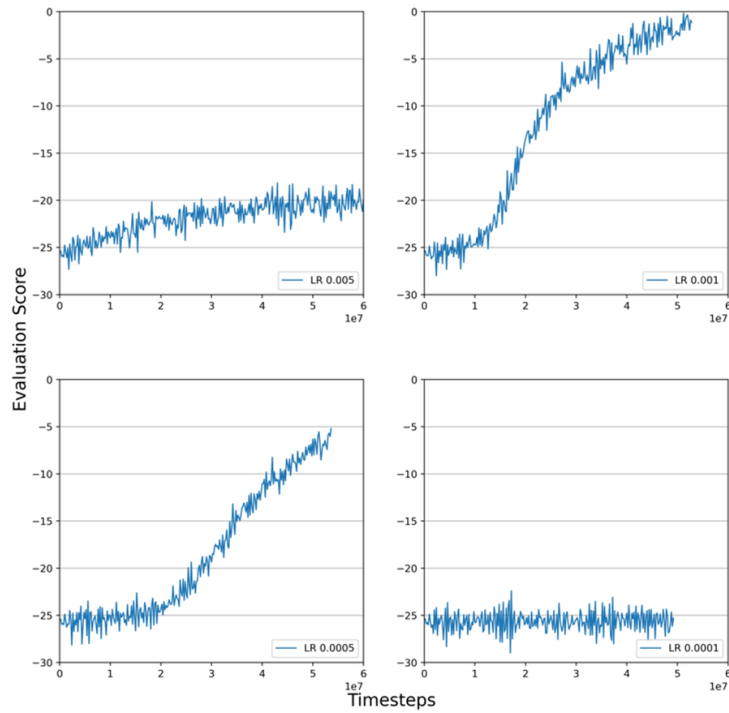
Figure 6.8: A2C learning rate parameter tuning.

6.4.1.2 Gamma Discount Factor

The discount factor γ has also been parametrically tuned between the values of zero and one. The results of this tuning are shown in Figure 6.10 and Figure 6.11 for A2C and ACER, respectively. A gamma value of 0.8 has been selected for the final training of both

161
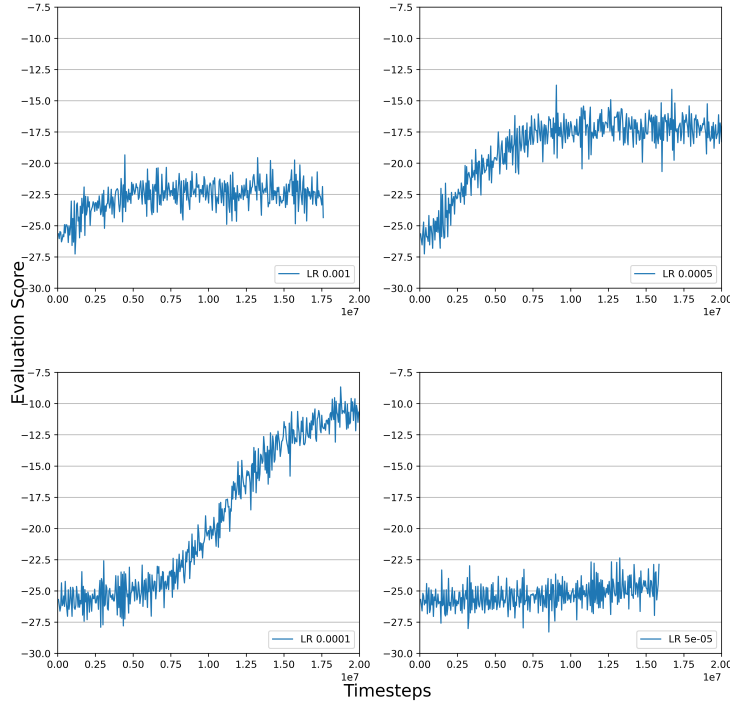
Figure 6.9: ACER learning rate parameter tuning.

algorithms. An extended training session is also carried out for the A2C gamma value of 0.99 to determine if longer training times will affect the result in Figure 6.14.

6.4.1.3 Reward function shaping

The error penalty and reward baseline are shown in Equation 6.6 and 6.7, as the average H_2O concentration of the environment. This is an arbitrary selection of baseline and sensitivity analysis on the magnitude of this baseline is necessary to determine an appropriate value. A scaling factor applied to the average concentration baseline and training was conducted with the scaling value of 0.0, 0.5, 1.0, 2.0, 3.0 and 5.0. The effect of the scaling factor on training effectiveness is shown in Figure 6.12 and Figure 6.13 for A2C and ACER, respectively. A penalty scalar of 1.0 has been chosen for the final training, although a value of 2.0 may improve results with the ACER architecture in particular, the penalty scalar affects the environment rewards, and a standardised value has been chosen to allow better comparison of final generalisation results in Figure 6.14.
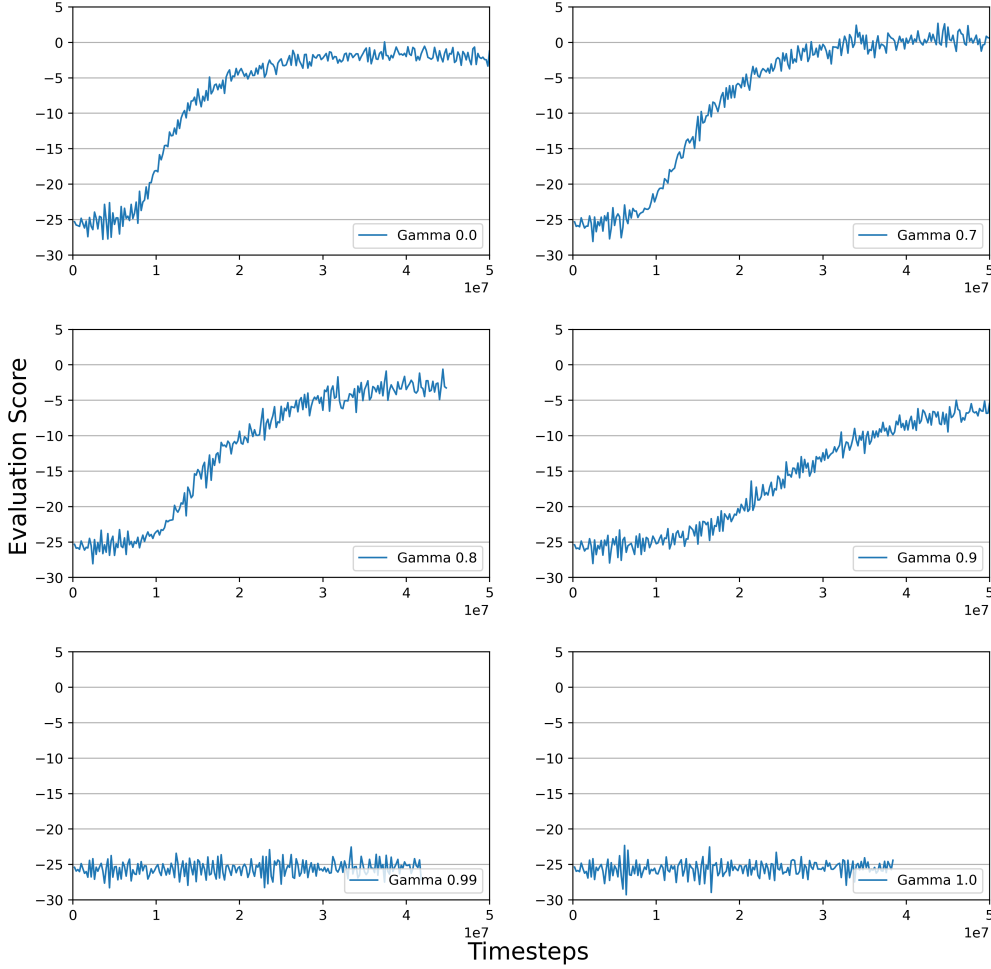
Figure 6.10: A2C gamma parameter tuning.

6.4.2   Architectures and Policy Generalisation

The DQN architecture was trialled and found to be inappropriate for this problem setup. The greedy-epsilon exploration method [196], which uses an occasionally random step dependant on an annealed epsilon factor leads to many repeated steps in the early stages of an episode and little advantageous exploration in the later stages of the training.

Policy gradients maintain a more consistent exploration rate and better targeting of exploration in later stages and hence are the preferred family of algorithms for this problem.

The A2C (Synchronous Actor-Critic) and the ACER (Actor Critic with Experience Re-
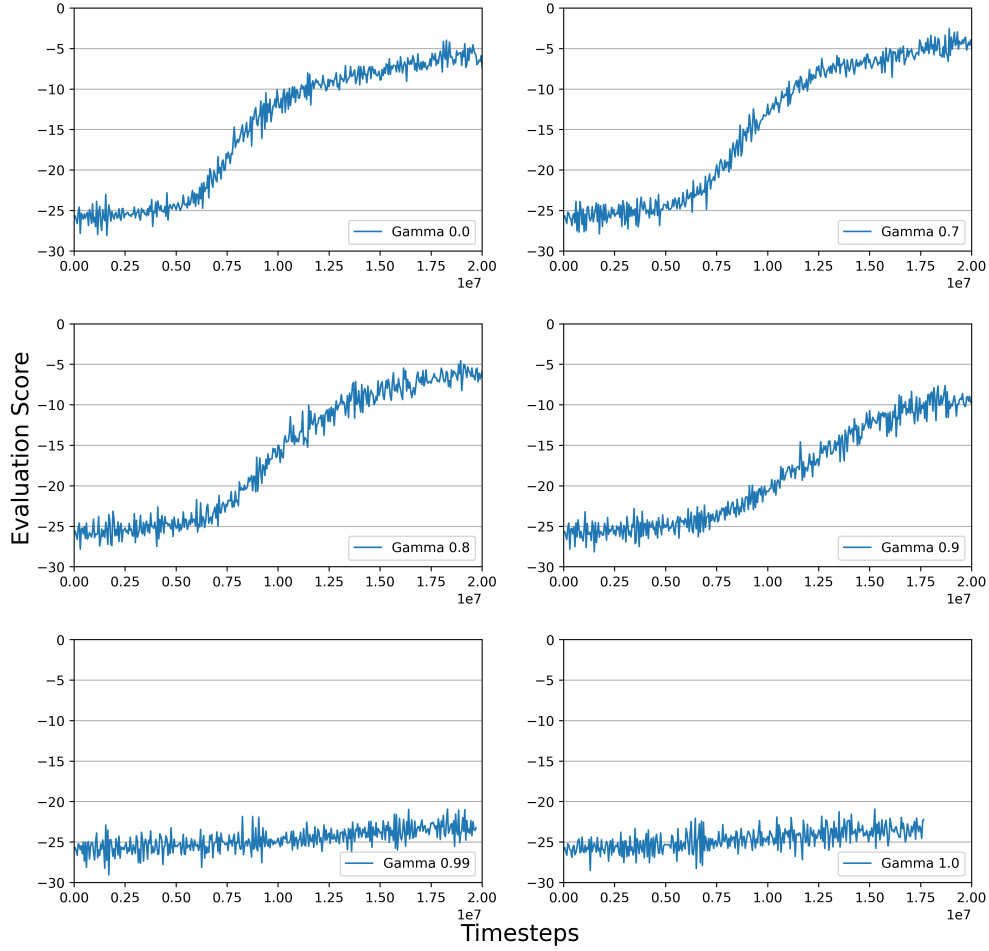
Figure 6.11: ACER gamma parameter tuning.

play) architectures have been trained in parallel to determine the best option.

The agent is evaluated against 100 unseen environments over the course of the training at intervals of 50 000 timesteps. A moving average of the results of these evaluations is plotted in Figure 6.14. The A2C architecture was run with gamma 0.8 and 0.99 and the ACER architecture with gamma 0.8. The ability of the agent to generalise across these 100 unseen environments improves over time and is used as the main indicator of the training success.

It has been found that the ACER architecture does not perform well with the type of CPU resources available. Long training times (in excess of 120 hours) are required to train
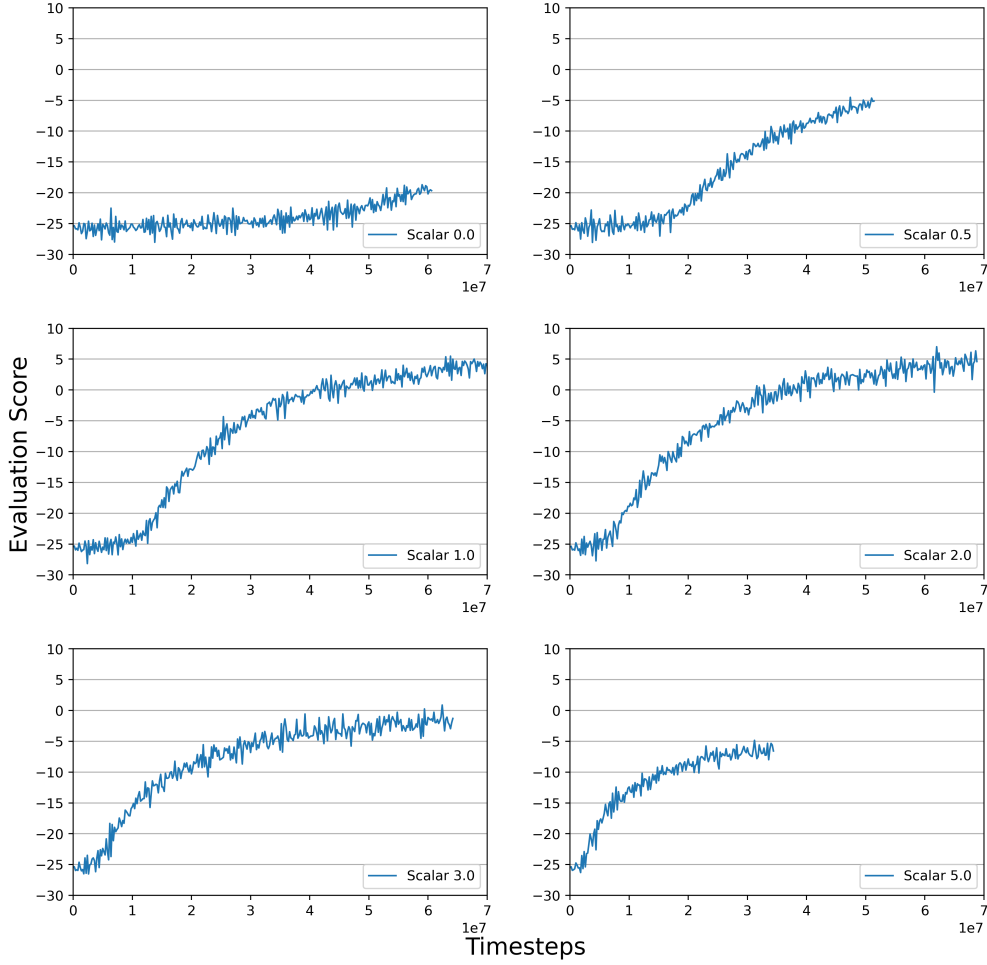
Figure 6.12: A2C penalty scalar parameter tuning.

the architectures proposed in this chapter. Practically, only 12-hour compute sessions are available, and the process must be saved and loaded every 12 hours to enable longer training time. The experience replay buffer has not been saved and reloaded for ACER and results in extended episodes, slow learning, and an unstable plateau on the learning curve. Further training of the ACER agent is not practical without changes to the architecture to limit episode lengths.

The A2C architecture with gamma parameter 0.8 has shown acceptable training performance and will therefore be used exclusively for the results section in this chapter. Note that there is no definitive end point to RL agent training. The A2C training has been
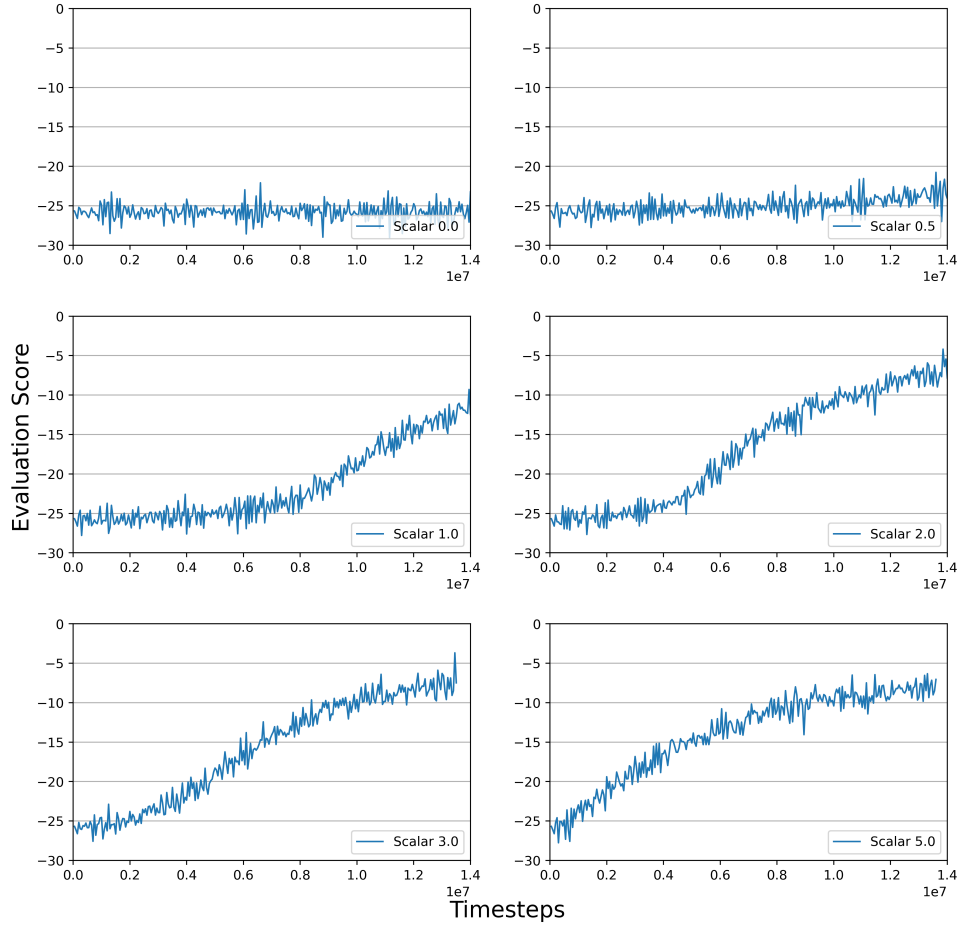
Figure 6.13: ACER penalty scalar parameter tuning.

terminated as a lengthy plateau and slight decline in performance has been experienced.

6.4.3 Human Expert Results

The trained agent has been run against a human mine sequencing expert, the author of this chapter. The comparison was undertaken on two unseen geological environments, the single-seed and two-seed orebody shown in Figure 6.1. The comparison between the agent and human's proposed trajectories for the singe-seed environment can be seen in Figure 6.15.

Quantifying these results in terms of the *ore grade* distribution in the environment is shown
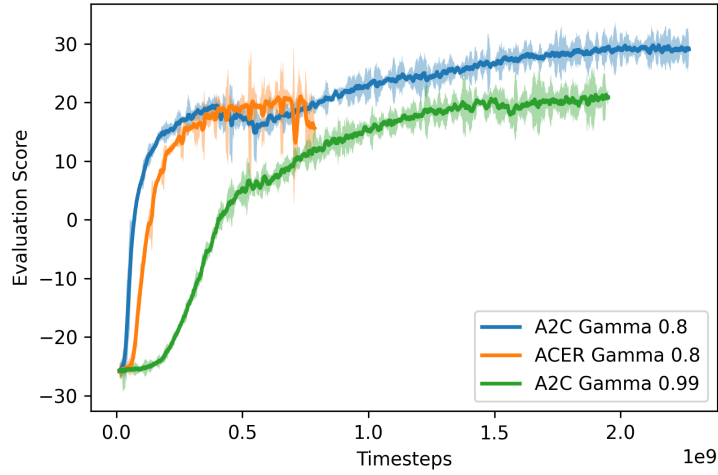
Figure 6.14: General evaluation score of the agent over time.

in Figure 6.16, where it can be seen the agent initially provides a higher-grade sequence from timesteps 0-20 (the mined grade result shown in green on the chart) where the human has planned better for the long term. Figure 6.17 shows a comparison of the quantities delivered over time. The agent performs much better over shorter timeframes. The agent is potentially suffering from insufficient training experience with late-stage trajectories, or
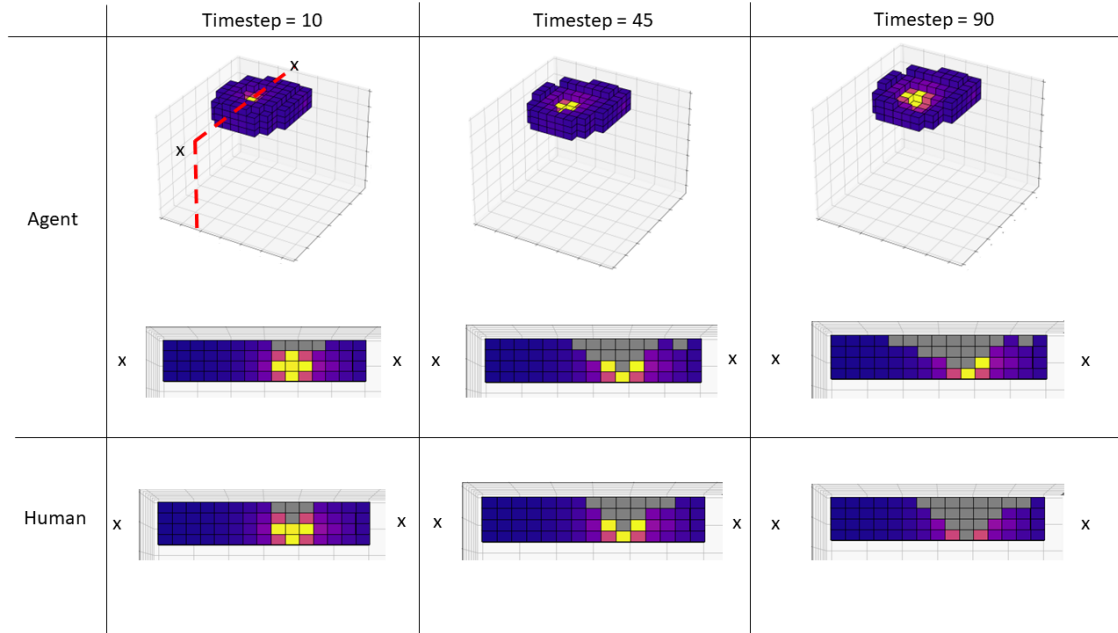
Figure 6.15: Visualisation of agent extraction sequence for a single seed environment.

the greedy nature of the algorithm is discounting future returns sufficiently to cause this
result. To minimise issues with training, Section 6.3.6.2 describes the method to provide
regular experience of advanced trajectories by re-using partially mined environments in
the training pipeline. The results shown in red on the chart represent the average mined
grade from the sequence during timestep 20-40. The result written in black represents the
average mined grade across the entire sequence.
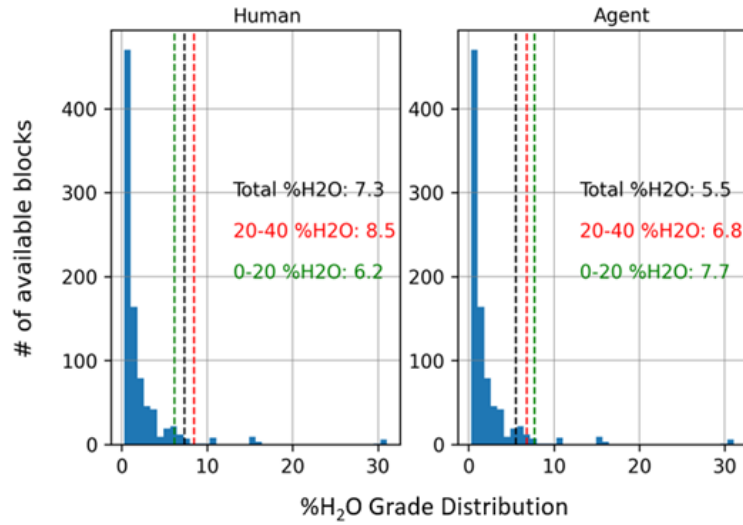
Figure 6.16: Geological distribution and performance comparison for a single-seed envi-
ronment.

The two-seed environment has also been used for comparison. Figure 6.18 shows a visual-
isation of the sequences returned by the agent and human expert. The sequences deviate
in terms of strategy here, as the human has planned two separate pits to extract higher
grades over a longer timeframe while the agent has focussed on just the highest-grade
pit and eventually pushes across to the lower *grade* seed. As can be seen in Figure 6.19
and 6.20, the agent provides superior returns for the 0-20 timeframe and also the 20-40
timeframe. The human expert still manages to produce the most overall, although with
less of a margin in this scenario. It appears that the agent is exhibiting the same issue
with longer term rewards that was exhibited with the single-seed scenario.

It is also clear from both scenarios, that the human expert is not providing an optimal
sequence. The human is not considering the cumulative advantage of small incremental

decisions over the course of the mine life, instead mainly focussing on the end goal. This is an issue with ISRU as previously mentioned in Table 6.1. The time limit of the operation is unknown due to uncertainties around equipment lifespan. Planning to extract the highest amount of product over an arbitrary mine-life is not useful if the equipment does not survive that period. A solution to this problem is shown with the trained agent in the next section.

This problem can also be formulated as mathematical model to compare the true optimality. This approach has not been pursued in this chapter for two main reasons. Firstly, the mathematical optimum is unlikely to be a real optimum that can be practically implemented. Exceedingly complex models and high computational requirements are required to obtain a mathematical optimum that respects all practical rules and constraints in the real world. Secondly, the geological model is unlikely to be 100% accurate, negating any added value from achieving an optimum based upon it. A comparison of the trained RL agent may be compared against a mathematical optimum in future work to further demonstrate the advantages or RL for this task.
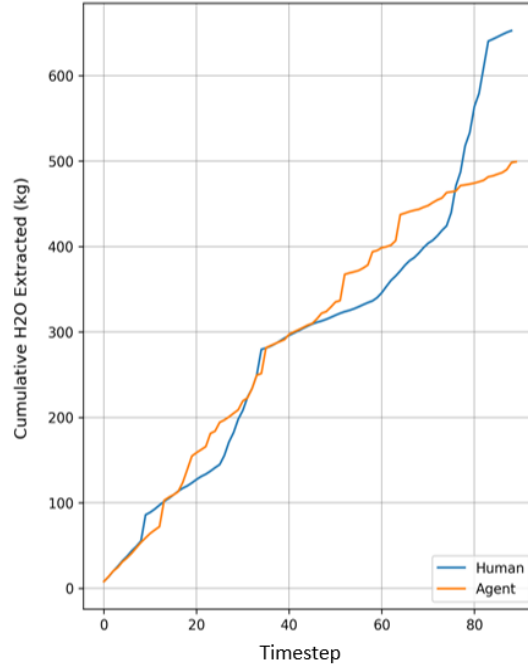
Figure 6.17: Cumulative performance comparison for a single-seed environment.
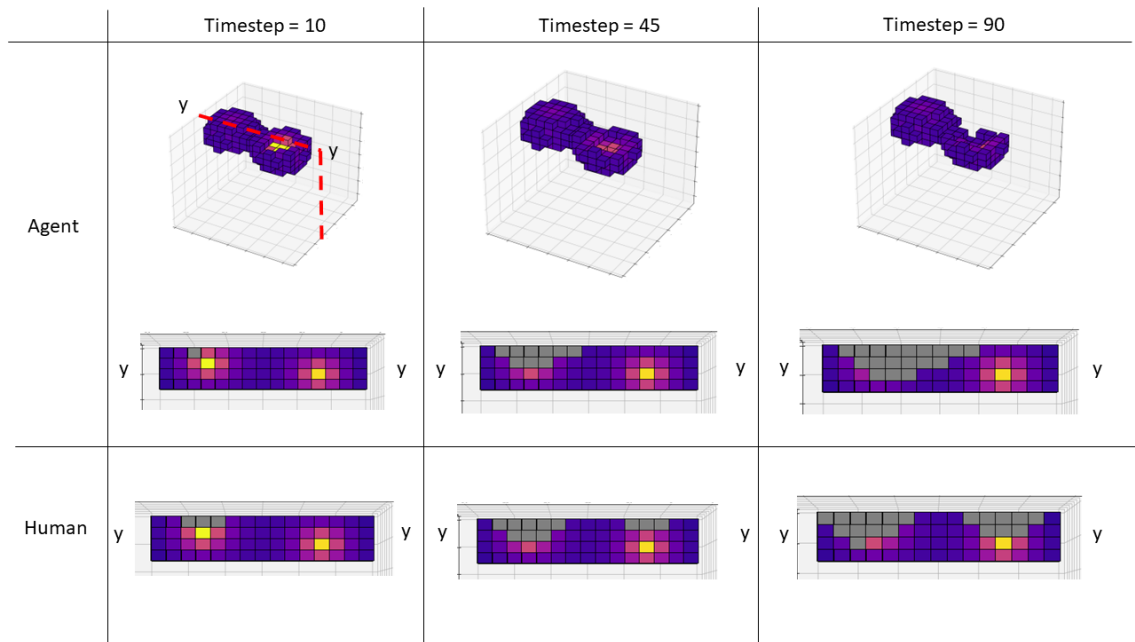
Figure 6.18: Visualisation of agent extraction sequence for a two-seed environment.
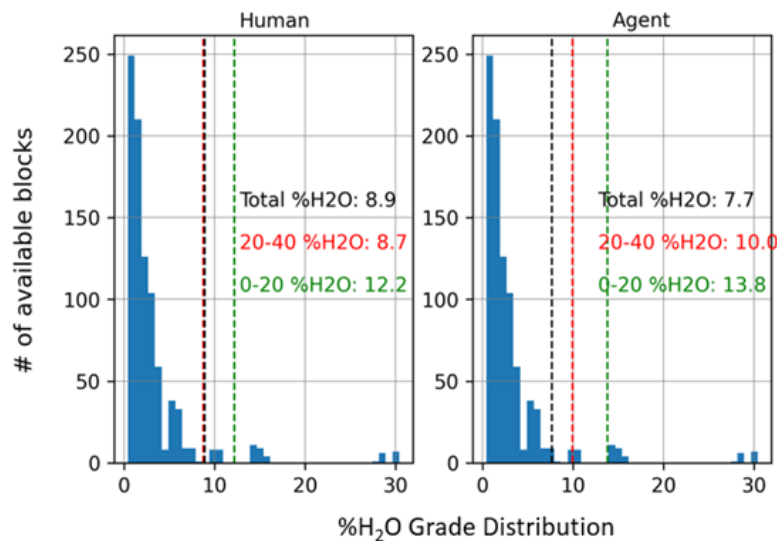
Figure 6.19: Geological distribution and performance comparison for single-seed environment.
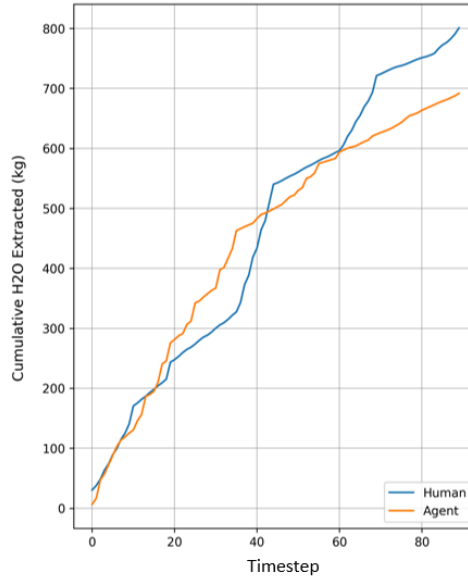
Figure 6.20: Cumulative performance comparison for a two-seed environment.

6.4.4   Novel ISRU Planning Tools

6.4.4.1   Risk Adjusted Return

The Equation 6.8 reliability function has been used to determine the termination length of each of 10 000 extraction scenarios. A probability density of the expected returns can be generated with these results as shown in Figure 6.21a and 6.21b. The human performance expectation is bimodal, as a significant low-*grade* extraction phase is undertaken in the middle of the sequence. The agent performance is more regular with the highest probability of extracting around 300 kg H_2O for the operation lifetime.

Figure 6.21c shows the cumulative probability for expected product of the two sequences over 10 000 Monte Carlo trials. The majority of equipment failures occur while the agent is outperforming the human in this example. For example, reading from the cumulative probability chart there is an 80% probability that the agent will produce less than ~375 kg of H_2O while the human has the same confidence to produce less than ~305 kg H_2O. The human clearly has a longer-term goal in mind and manages to produce the overall highest results with nearly 150 kg more product than the agent. However, according to

171
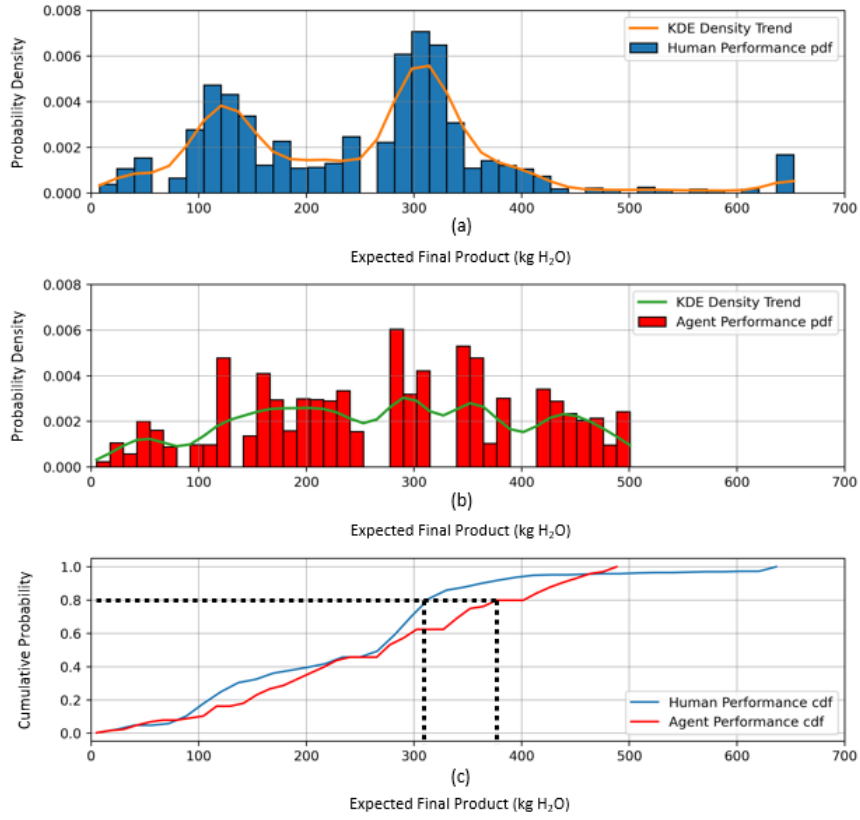
Figure 6.21: Expected returns for human and agent on single-seed environment.

these reliability assumptions there is less than a 0.2% chance of achieving it. This analysis shows that after taking equipment reliability assumptions into account, the agent's greedy sequence is a better choice for ISRU.

6.4.4.2 Cut-off grade optimisation

The ISRU sequencing tool has been run iteratively on a three-seed geological environment subject to various product stream *cut-off grades*. The system is constrained by the beneficiation step as outlined in Figure 6.7. The environment shown in Figure 6.22a and b are the same environment subject to 0% and 10% respective *cut-off grades*.

The results of multiple extraction sequence trials (8 stochastic trials for each *cut-off grade*) are shown in Figure 6.23. The optimal *cut-off grade* is 2% H_2O in this case and will likely

Cut-off grade – 0% H$_2$O   Cut-off grade – 10% H$_2$O

(a)   (b)
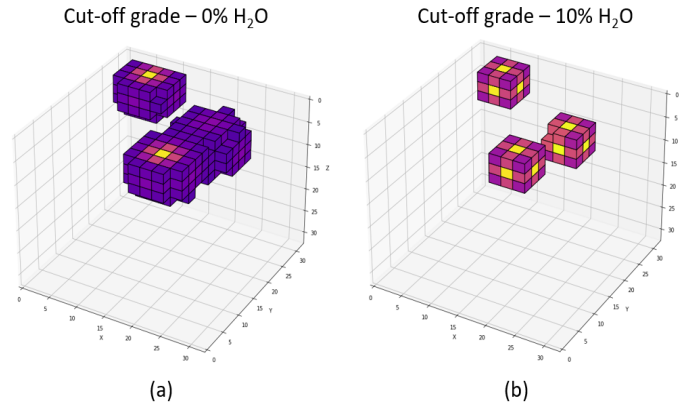
Figure 6.22: Three-seed complex environment subject to different cut-off grades.
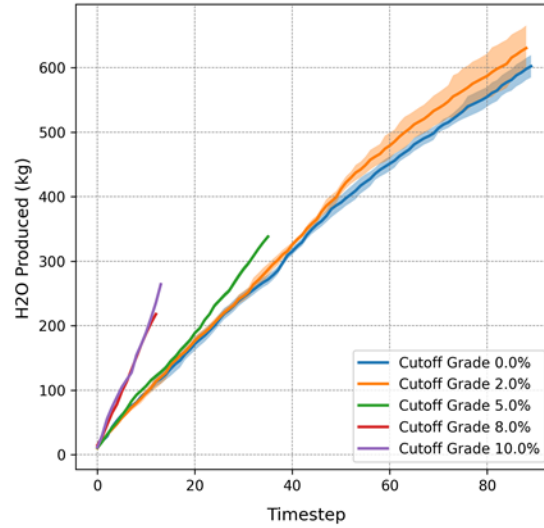
Figure 6.23: Effect of applying a cut-off grade to extraction.

increase the overall production of H$_2$O. Higher *cut-off grades* increase the rate of overall production; however, the *ore reserve* is also exhausted much sooner and the total volume produced is less.

Rapid scenario testing and its extension to *cut-off grade* optimisation demonstrates the usefulness of a trained agent in planning ISRU extraction and maximising the value of the operation. In modern terrestrial mining operations, this type of optimisation study is done by teams of engineers using the much slower traditional methods outlined by Hall [116].

6.5 Discussion

6.5.1 Hyperparameter Tuning

Only the major *hyperparameter*s, the discount factor γ and the learning rate have been parametrically tuned via a grid-search method. The penalty scalar is an environmental modifier, not a learning *hyperparameter*. Each algorithm trialled has several other unique parameters that have been left at their default values in the Stable Baselines package [122]. It is possible that tuning of all these parameters may also increase performance for this specific task, however it becomes impractical to implement grid search as a solution with so many sub-optimal parameters to tune.

One parameter that seems to affect the ACER algorithm is the experience replay buffer size. Periodic spikes can be seen in the ACER learning curve in Figure 6.14. These correspond to saving and re-loading the neural network and consequently flushing the experience replay buffer as training is re-started. This effect seems to be neutral or even positive in early stages as the improvement rate exceeds any negative effects of a refreshed experience buffer. As the improvement rate plateaus, the lost experience buffer takes too long to recover and the limited available training computing resources (12-hour limit) do not allow any real gains to be made. It is thought that changing the size of the experience buffer or extending the available time between saving, loading and buffer refreshing may affect this result.

6.5.2 Agent Optimality

In this chapter, the generalised RL agent has been evaluated against a human expert to determine its effectiveness. The human was deliberately time constrained when searching for the optimum sequence, only one trial was allowed. The human expert's sequence is therefore likely to be sub-optimal.

It may be desirable to evaluate the agent against algorithms that are known to achieve

optimal solutions. However, it has already been identified in this chapter that the traditional mine planning algorithms are not suited to the ISRU problem. They require cost and revenue assumptions which are too uncertain for off-Earth markets and operations among other incompatibilities outlined in Table 6.1. Currently there are no mathematical optimal solutions for the ISRU extraction problem and similar to terrestrial mine sequencing there is limited added value in finding the absolute optimum, especially when practical limitations must be considered.

Due to the inherent sub-optimality of the human expert, it is not possible to quantify how much improvement an RL agent can attain or when to stop training. The advantage of an RL agent over a human expert is specific to each different environment and distribution of *ore grades*. It is not expected that the RL agent will be able to provide a constant and predictable advantage over the human expert. The human expert can also find more effective solutions if more time is allowed for scenario trials. The results of this chapter simply demonstrate that an RL agent can be used to produce an effective ISRU extraction sequence. The optimality of that solution is not known, and more work can be done to improve the solution.

6.5.3   Stochastic Agent Policy

A stochastic actor-critic is required for training in this environment to ensure adequate exploration. It has been necessary in this research to maintain a stochastic agent policy even after training has been completed. It is known that a deterministic policy, taking the maximum value action could yield a higher return [261]. However, in this implementation, the agent selects an action, and a check is run in the environment to ensure the action complies to the precedence constraints. If the action violates these constraints, it is considered invalid, and no change is made to the environment. With a deterministic policy, the agent would enter an infinite loop in this case. The same environmental observation is made repeatedly, and the same action selected. To avoid the infinite loop, a stochastic policy where some random actions are taken is implemented in this chapter.

The high-dimensional action map (225 action outputs) in this work means long train-
ing times are required to approach a deterministic policy limit as mentioned by Silver
et al. [261]. It may be advantageous in future work to investigate lower dimensional ac-
tion architectures to reduce neural network training requirements and potentially enable
deterministic policy evaluations.

Note the stochasticity of the result in Figure 6.23 appears to increase as the number of
timesteps increases. This indicates less appropriate training has been experienced for the
later timesteps, an issue that will be investigated in future works.

6.5.4   Reinforcement Learning Architectures

The DQN algorithm available in the Stable Baselines [122] package is inefficient for this
problem. The greedy-epsilon random exploration method tends to visit many invalid or
low-value states. This causes a significant amount of wasted compute time as progress
is made only when valid states are accepted. The guaranteed convergence of the value
function as iterations approach infinity is, however, a desirable trait of the DQN algorithm.
Future works may examine more advanced DQN implementations such as Information-
Directed Exploration [214] for the mine sequencing problem on a single environment. A
more efficient DQN agent could be trained to converge to the optimal sequence for a single
environment and then be used to compare and quantify the performance of a generalised
policy agent. Although, the training time required to optimise an environment individually
using DQN may not be worth the optimality trade-off for using a generalised agent.

The general ISRU sequencing problem appears to be better suited to policy gradient meth-
ods such as Actor-Critic [301, 304] due size and stochasticity of geological environments.
Off-policy learning techniques such as Prioritised Experience Replay [251] are also use-
ful for learning generalised policies. However, with the rapid progress of Reinforcement
Learning algorithms in recent years it is expected that new and improved RL algorithms
will become available for this problem in the future.

6.5.5   Training Distributions

The RL agent learns underlying distributions and patterns of input data. Although the geological environments in this study are generated using random seeds, some structure and regular variance has been designed into these environments as would be expected in a real geological environment.

It is possible that the agent is learning the broad underlying distribution that these environments are being generated with. It was hypothesised that running the agent on completely different types of geology would lead to poor results, meaning that the agent may need additional training for new deposit types. However, during the experiments there has been no direct evidence of such an occurrence. The *cut-off grade* optimisation performed unexpectedly well. These modified *cut-off grade* environments are very different to the original seed generated environments and cannot be generated with the same underlying distribution. Yet, the general agent still followed similar trajectories, with sensible variations regardless of the *cut-off grade* applied to the input environment.

If any future issues are found with running the agent on environments outside the original training possibilities, a prescribed curriculum learning method [228] can be applied to update the agent with relevant new experiences and reduce training times.

6.5.6   Future Work

Simple geological environments have been used for training the algorithm in this work. The long training times and difficulty in scaling-up this architecture mean that this particular method is only practical for small geological environments. Scaling-up the RL architecture will likely require modifying the action output mapping to reduce dimensionality and potentially implementing a Convolutional Neural Network for pre-processing the environment. These tasks will require significant re-design of the environments and algorithm. This chapter has not quantified the full potential of Reinforcement Learning for ISRU planning, it has only been demonstrating that it can work. Future work should

focus on scaling up the capabilities, increasing efficiency and demonstration on full scale
geological environments.

Extending this ISRU planning tool to different mining systems such as drilling or tunnelling
outlined in Chapter 4 is also possible. That will be required for a quantitative assessment of
the effectiveness of those systems when their respective reliability parameters are known.
Extending the RL tool can be achieved with modifications of the reward function and
environment precedence constraints.

The specific example shown in this chapter is aimed at bridging the gaps between tradi-
tional mine planning and off-Earth In-Situ Resource Utilisation. However, the technique
shown here can also be used for future terrestrial mine planning. This has already been
partly demonstrated by Kumar [155], although that agent was not generalised and did not
have the capacity to modify the long-term schedule as shown by the agent in this chapter.

6.6 Conclusions

Several problems have been detailed in this chapter for the transfer of traditional mine
planning algorithms to ISRU. These problems include the uncertainty of inputs, the dif-
ferent optimisation objectives of ISRU and terrestrial mining and the assumption that all
ore will be recovered within a specified mine life. The reality for early ISRU operations
is that when a piece of equipment fails, replacement parts may take a long time to re-
supply from Earth. This delays resource extraction and invalidates the already uncertain,
time-dependant inputs such as market pricing, costs and NPV discount factors.

A novel method for planning and optimising ISRU has been developed and demonstrated
in this chapter that doesn't need cost, price or discount factor inputs. For this method,
the traditional process is evolved from manual design and schedule iteration to producing
and analysing RL agent trajectories based on variable input risk distributions. Using this
method, mine plans can be easily optimised within the unique constraints and uncertainties
that come with ISRU.

A generalised RL agent has been shown that can produce mine extraction sequences from a range of geological block models for lunar H_2O resources. When comparing the results to an expert human engineer, it has been found that the agent is better at micro-managing short term decisions and sometimes achieve higher results than the human. The generalised agent also enables *cut-off grade* optimisation and risk adjusted return assessments to be conducted and rapidly updated with continuous inflow of new environmental data. The algorithm has been demonstrated using just one simple mining system example, but the agent's capabilities can be modified to optimise the application of any mining system shown in Chapters 4 or 5.

There are still many opportunities for further development of this method, notably around increasing the speed and effectiveness of agent training. The findings of this chapter could also be used as an alternative to traditional mine planning algorithms. This may reduce labour intensity of terrestrial mine planning processes in the future.

Uncertainties around cost and revenue inputs are a weakness of traditional mine planning algorithms when applied to ISRU. However, these inputs are critically important to the traditional methods of understanding economic feasibility of mining projects. The following chapter will investigate this weakness further and develop a new method for determining the economic feasibility of an ISRU project without using these uncertain inputs.

Chapter 7

ISRU Project Appraisal with Uncertain Inputs

7.1 Introduction

The Net Present Value (NPV) has been used to assess the value and economic feasibility of terrestrial and off-Earth mining projects in the past [5, 26, 53, 135, 259, 272, 315]. As per Objective 3, this chapter outlines a deficiency in this method when applied to ISRU. Costs and revenue of an ISRU operation are difficult to estimate for NPV and add an additional order of complexity into the ISRU planning and optimisation process. This chapter demonstrates a novel ISRU project appraisal method that can provide valuable indicators for planning and optimisation engineers even with highly uncertain inputs, fulfilling Objective 4. In this study, the nearest terrestrial competitor is used to determine the competitiveness of an off-Earth mine. The nearest terrestrial competitor can launch water resources directly from Earth instead of in-situ extraction. These competitors can be directly compared in terms of physical, not financial quantities. The physical comparison removes the need for higher-order financial parameters such as the NPV discount factor and is more accurate for engineering optimisation.

The consideration of the geology outlined in Chapter 2, mining systems from Chapters 4 and 5, mining sequences discussed in Chapter 6, space logistics and market demand are all important factors in determining mine feasibility and are key inputs into the appraisal method used in this study. There are still many uncertainties around equipment specifications (e.g. mass, power, mining rate) and geology (e.g. *ore grade*, hardness). Assumptions and simplifications are made in this chapter to allow the demonstration of the appraisal method. Due to the uncertainty of assumptions, a sensitivity analysis has also been undertaken to show the impact of variance in some of these assumed factors. These insights, along with the new ISRU appraisal method, can also be used to identify areas of improvement for future off-Earth mining projects.

A comparative appraisal is also undertaken in parallel for H_2O resource extraction from a dormant comet part of the Near-Earth Object population, demonstrating the flexible usage of this new technique according to Objective 5.

7.2 Literature Review

Net Present Value (NPV) analysis has been employed by various researchers including Sonter [272], Andrews *et al.* [5], Blair *et al.* [26], Craig *et al.* [53], Zacharias *et al.* [315], Jones *et al.* [135], and Shishko *et al.* [259] to determine economic viability of mining projects on asteroids, the Moon or Mars. NPV is a well-known project evaluation tool used in mining and other industries. It is designed to guide investment decisions by accounting for the value of future revenues and costs by assigning a discount factor. The discount factor causes earlier revenues to be valued higher and later costs to be less demanding [305]. It is limited by these same features when used to assess projects with high uncertainty around cost, revenue and timing of investment [1,142,292]. Keller, Collopy and Componation [141] have shown that the predicted cost of research, development and capital for space systems has proven to be highly inaccurate in the past. Off-Earth mining projects are expected to have similar inaccuracies as there are no reference operations for costs or any established market price for revenue estimation. This limits the applicability of NPV analysis to

off-Earth mining. Furthermore, the NPV is designed only for project investment decision making. Terrestrial mine planners use additional measures for production planning and scheduling such as the Net Smelter Return (NSR) in the base metals industry. The NSR is calculated as the undiscounted value of the metal-in-concentrate minus all refining charges and transport costs with metal recovery factors applied [305]. Erdem, Güyagüler and Demirel [87] and Morley, Snowden and Day [198] have previously identified some of the issues around uncertainty with NPV for terrestrial mining projects. They have made use of Monte Carlo simulations to produce probability distributions of the NPV and improve analysis, however this tool is still only an indicator of project viability and not as useful as the NSR for mine planning purposes.

The "mass payback ratio" concept utilized by Sonter [272] illustrates the need to expend mass in the form of propellants, rocket bodies and mining consumables in order to return product mass to the market. This method builds on the NPV evaluation and is not affected by cost, revenue and time uncertainty. However, as pointed out by Blair *et al.* [26], the mass payback ratio does not guarantee economic benefit in the way NPV is designed to do.

The previous off-Earth mining studies mentioned above [135, 259, 272, 315] generally focus on input variables based on orbital mechanics, rocket fuel requirements, product mass returned and time of the return trip. Terrestrial mining feasibility studies also require confident geological resource characterization and extraction methods to be considered. Andrews *et al.* [5] takes the first steps at incorporating a design for the mining and processing system on an M-Type asteroid which is included in the NPV analysis. Blair *et al.* [26] build on this and suggest potential mining systems for the lunar surface which affect the NPV calculation as does Craig *et al.* [53].

Asteroid mining logistics have been examined through NPV and project feasibility by other authors such as Probst *et al.* [231] and Dorrington, Kinkaid, and Olsen [74]. It is evident in these papers that the NPV method of assessing asteroid mining missions has a significant effect on the decision outcome, due to the time dependent discount factor.

7.3 Mining Systems

7.3.1 Lunar Strip Mining

Mining systems proposed for the Moon include traditional excavator and haulage systems shown by Amah *et al.* [4] and in-situ ice sublimation methods shown by Zacny *et al.* [320]. For terrestrial operations, conventional strip mining utilizes equipment such as the dragline and bucket-wheel excavators. It is a common method for mining shallow and flat sedimentary style ore deposits, e.g. coal deposits. The concept of strip mining might also be theoretically applied to the sedimentary ice deposits inside shadowed lunar craters. A procedure for selecting these systems for a given *mineral resource* has been discussed in Chapter 5, the systems described in more detail in this chapter are used to define constraints for the appraisal model.

The lunar bucket wheel excavators in this scenario are based on a small terrestrial model with mass of 4 300 kg as shown in Section 7.3.2 and an excavation rate of 15.5 m^3 per hour. The strip mining system has been modelled as shown in Figure 7.1. The bucket wheel excavator will advance into the page and return along the next strip. All waste will be augered across to the dump. This may create an electrostatic dust hazard as has been experienced on the lunar surface during the Apollo missions [227]. However, Poppe *et al.* [227] have modelled the solar wind at low incidence angles across crater rims and demonstrated a reduced electrostatic potential inside the crater. The hazard of electrostatic dust is therefore expected to be reduced in the chosen shadowed crater mining region. Nevertheless, Kawamoto [139] has also proposed electrostatic shielding as a control to manage the hazard if present. Each bucket wheel excavator will contain a volatile extraction oven powered by concentrated sunlight [146] or microwave beam [326] to reduce the built-in power and mass requirements. A storage tank is included which will be periodically deposited.
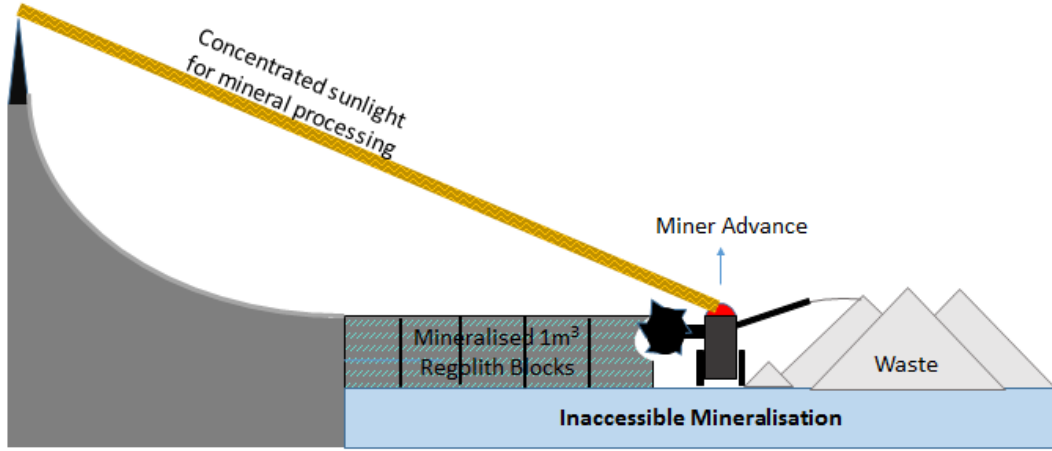
Figure 7.1: Lunar crater strip mining system.

7.3.2 Bucket-Wheel Excavator Parametric Design

The bucket-wheel excavator has been designed using various mechanical assumptions and the empirical off-Earth soil excavation model proposed by Luth and Wismer [181] and utilized by other researchers for off-Earth applications [133] [69] [308]. The parameters for the bucket-wheel design are shown in Table 7.1.

The calculated horizontal friction $(H_{friction})$ and cohesion $(H_{cohesion})$ forces are used to determine the drive torque needed for the bucket wheel, with the assumption that the circular cut made by the excavator will require the same force as the same length of horizontal cut using the empirical model developed by Luth and Wismer in Equations 7.1, 7.2, 7.3 and 7.4 [181, 308]. A vertical force $(V_{friction} + V_{cohesion})$ holds the cutting tools in place, provided by the counterweight, the bucket-wheel and boom. The free body diagram in Figure 7.2 has been used to resolve the reaction forces with Equations 7.5 to 7.7 and assumptions from Table 7.1.

$$H_{friction} = \gamma g w l^{1.5} \beta^{1.73} d^{0.5} \left(\frac{d}{l \sin \beta} \right)^{0.77} \left(1.05 \left(\frac{d}{w} \right)^{1.1} + 1.26 \frac{v^2}{gl} + 3.91 \right) \qquad (7.1)$$

Table 7.1: Parameter table for Bucket-Wheel Excavator design

Parameter	Value
Factor of Safety for counter weight (FOS)	3.0
Length of blade (l)	0.2 m
Depth of cut (d)	0.2 m
Width of blade (w)	0.2 m
Lunar gravity (g_{moon})	1.62m/s^2 [308]
Counterweight length	2m
Number of buckets in contact with soil	3
Cutting Arc of bucket wheel	$\frac{1}{3}$ of circumference
Power Efficiency	50%
$W_{counterweight}/W_{boom}$	3.0
Number of buckets	8
Boom length	3 m
Compacted Regolith Specific mass (γ)	1900 kg/m^3 [308]
Loose Regolith Specific mass	1600 kg/m^3
Rake angle (β)	0.785 rad (45°)
Tool Speed (v)	0.15 m/s
Soil cohesion (c)	170 N/m^2 [308]
Bucket-wheel diameter	2.0 m

$$V_{friction} = \gamma g w l^{1.5} d^{0.5} \left(0.193 - (\beta - 0.714)^2\right) \left(\frac{d}{l \sin \beta}\right)^{0.777}$$
$$\left(1.31 \left(\frac{d}{w}\right)^{0.966} + 1.43 \frac{v^2}{\text{gl}} + 5.60\right) \quad (7.2)$$

$$H_{Cohesion} = \gamma g w l^{1.5} \beta^{1.15} d^{0.5} \left(\frac{d}{l \sin \beta}\right)^{1.21}$$
$$\left(\left(\frac{11.5 c^{1.21}}{\gamma g d}\right) \left(\frac{2v}{3w}\right)^{0.121} \left(0.055 \left(\frac{d}{w}\right)^{0.78} + 0.065\right) + 0.64 \frac{v^2}{\text{gl}}\right) \quad (7.3)$$

$$V_{Cohesion} = \gamma g w l^{1.5} d^{0.5} \left(0.48 - (\beta - 0.70)^3\right) \left(\frac{d}{l \sin \beta}\right)$$
$$\left(\left(\frac{11.5 c^{0.41}}{\gamma g d}\right) \left(\frac{2v}{3w}\right)^{0.041} \left(9.2 \left(\frac{d}{w}\right)^{0.225} - 5.0\right) + 0.24 \frac{v^2}{\text{gl}}\right) \quad (7.4)$$

For ease of calculation, the excavation forces are taken as the average of two buckets. The weight of the wheel itself is assumed to be equal to the expected vertical excavation force and the counterweight will be three times the weight of the boom (Eq. 7.7). The total bucket-wheel excavator mass has been assumed as 4 300 kg when operating, in line with smaller terrestrial excavation equipment.

The bucket wheel Miner Rate (R_{bw}) has been calculated as 15.5 m^3/h regolith and power requirement of 2.4 kW for excavation and material movement with the speed and tool size assumptions in Table 7.1. Power for heating and extracting the volatiles will be provided by concentrated sunlight directed from the crater rims, this will reduce the battery mass required and improve economics and reliability of the system. The assumptions for this simple design are made to fulfill the input requirements of the mining model in this chapter. No engineering optimisation has been undertaken. Results of such a study would affect the modelled results here.
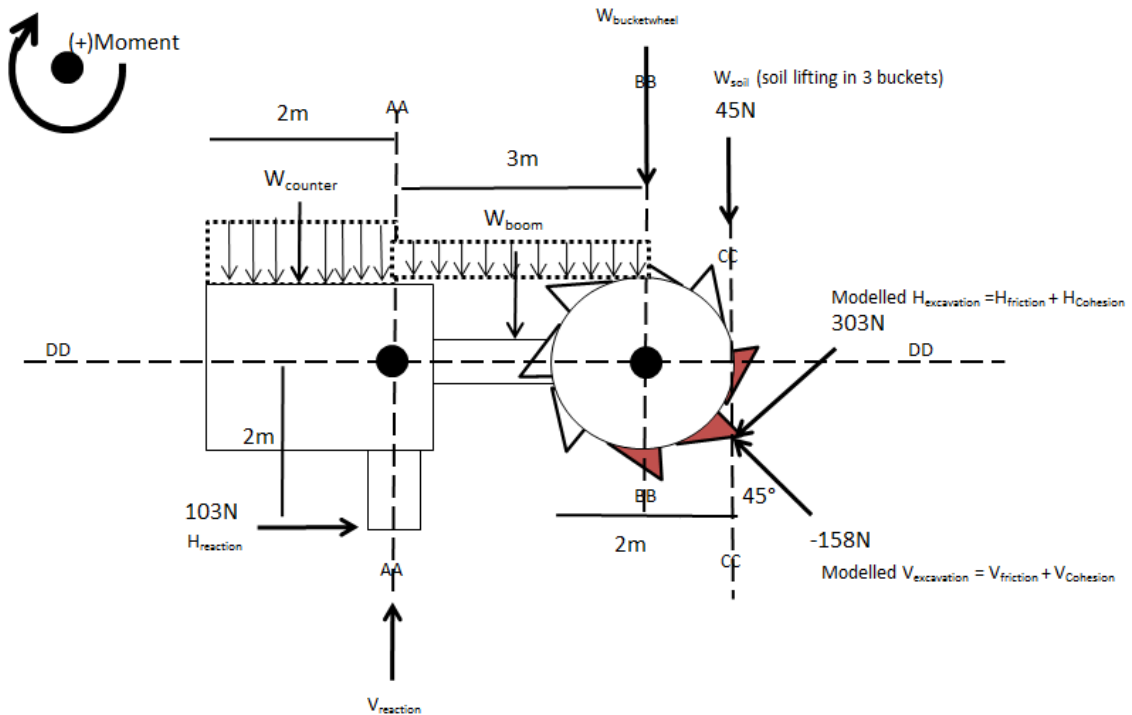
Figure 7.2: Free body diagram of excavator for mass estimation.

$$\frac{W_{bucketwheel} + W_{counter} + W_{boom}}{g_{Moon}} = 4300 \; kg \qquad (7.5)$$

$$W_{bucketwheel} = \; (H_{friction} + H_{cohesion}) \; sin(45°) + (V_{friction} + V_{cohesion}) \; cos(45°) \quad (7.6)$$

$$W_{counter} = \; 3 \times W_{boom} \qquad (7.7)$$

7.3.3   Lunar In-Situ Sublimation

The In-Situ Water Sublimation (ISWS) system relies on technology currently untested in operational conditions. It is based on experiments by Ethridge and Kaukler [90] that demonstrate microwave extraction of ice from lunar regolith simulants. The aim of this method is to drill holes into the regolith and apply microwave radiation to sublimate water from the sediment. This process has been illustrated in Figure 7.3. Water recovery in lab conditions has been measured around 85% [89], however, for the purpose of the model a conservative operational recovery has been assumed at 30% of in-situ material. Zacny *et al.* [319] suggests an alternative system (MISWE) which utilizes conductive heating in order to reduce design complexity and increase efficiency and volatiles recovery. However, the low thermal conductivity of lunar regolith [90] indicates conductive heating systems will be ineffective. Volatile extraction experiments with thermal conductive heating in a vacuum oven style apparatus have also been carried out by Reiß [235] with chemically adsorbed H_2O samples, providing support to heating methodologies for the lunar environment. The microwave sublimation system is described throughout this chapter to demonstrate the model, although conductive heating can also be substituted with the same modelled results until further research is undertaken to prove otherwise.

The water product will also need to be hauled to the depot location where it should be loaded onto the chosen transportation system. This process solves some of the technical

issues with conventional strip mining. For example, the machinery specifications are far less demanding as the bulk regolith will not be moved. Dust can be reduced compared to strip mining and the ore strength is less of a problem as drilling mechanisms have a greater ability to penetrate harder material.
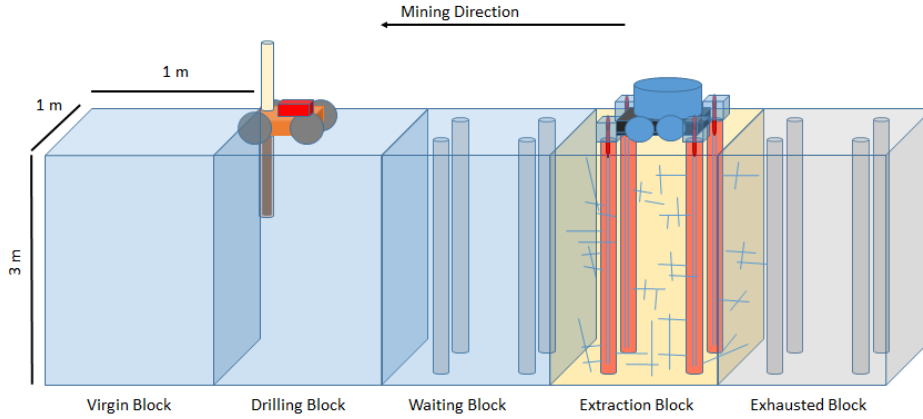
Figure 7.3: Lunar in-situ sublimation method.

7.3.4 In-Situ Sublimation Miners Parametric Design

The In-Situ Sublimation miner has been designed based on the energy requirements to sublimate ice in a lunar shadowed crater environment where temperatures during the daytime have been observed around 120-150 K [218]. Vaporization of ice under low pressure occurs around at around 220 K [108]. Table 7.1 and Table 7.2 show the physical and assumed parameters for the design of the In-Situ Sublimation system in Equations 7.8-7.12.

$$Specific\ Energy\ to\ sublimate\ Ice\ \left(\frac{J}{kg\ H_2O}\right) = E_{H2O} = 1000 \times (\Delta T \times C_{H_2O} + H_s) \tag{7.8}$$

The surrounding regolith will also be heated to the same temperature as the ice, and the energy required will depend on the concentration of ice in regolith.

Table 7.2: In-Situ Sublimation mining parameters.

Parameter	Value
Atmospheric Pressure	Below 100 Pa
Initial Temperature (Solid)	120 K [108, 218]
Final Temperature (Vapor)	220 K [108]
Average Specific heat capacity of H_2O between 120K-220K (C_{H2O})	1.36 J/gK [106]
Approximate H_2O Enthalpy of Sublimation (H_s)	2 800 J/g [92, 106]
Average Specific heat capacity of Regolith between 120K-220K (C_R)	0.5 J/gK [121]
Average Ore Grade (see Section 2.2.2)	50 kg H_2O/m^{3}regolith
Battery Mass % of total	50%
Mining Recovery of resource	30%
Mining Rate required ($R_{sublimation}$)	3 kg/h H_2O
Heating efficiency (assumed)	30%
Time between recharges ($T_{recharge}$)	4 hours
Specific Energy density of Battery	190 Wh/kg [243]
Factor of Safety (FOS) on Power supply	1.2

$$\textit{Specific Energy to heat regolith } \left(\frac{J}{kg \ H_2O} \right) = \ E_R = \frac{\gamma \times 1000 \times (\Delta T \times C_R)}{\textit{Average Ore Grade}} \quad (7.9)$$

ΔT is the change in temperature required to achieve sublimation and C is the average specific heat capacity (J/gK) across the temperature range. H_s is the approximate heat required to transition phases from solid to gas and the bulk density of compacted regolith is γ.

$$\textit{Energy for mining } (J/s) = E_{\text{mining}} = \ \frac{(E_{H_2O} + E_R) \ \times \textit{Mining Rate}}{3600 \ \times \textit{Efficiency}} \quad (7.10)$$

$$\textit{Battery Storage } (\textit{Watt hours}) = \ E_{\text{mining}} \times T_{\text{recharge}} \ \times FOS \quad (7.11)$$

$$\textit{Miner Mass } (kg) = \ \frac{\textit{Battery Storage}}{\textit{Specific Energy of Battery} \times \textit{Battery Mass } \% \textit{ of Total}} \quad (7.12)$$

Using these assumptions and Equations 7.8, 7.9, 7.10 and 7.12, the sublimation miner mass has been calculated as 1210 kg with a 24 kW (E_{mining}) heating element or microwave. A significant unknown in these assumptions is the efficiency of heating for icy lunar regolith. It is hypothesized that the water heating efficiency is related to the thermal conductivity and percentage ice of the regolith. Reiß [235] has investigated the effects of many variables. However, there is not currently sufficient geological data from ice deposits on the Moon to support the efficiency assumption made here. Brisset, Miletich and Metzger [32] have completed modelling on a similar ISWS method and show that extraction efficiency is likely to be well below 50%. The assumptions here only suffice to demonstrate the model and indicate at results only under the circumstances outlined in this chapter. Mass and power could be significantly reduced if new technology could utilize concentrated sunlight more effectively, heating efficiency could be increased or the heating could be targeted at the water more effectively. The unknown properties of regolith in lunar cold traps may also affect these assumptions. Further research must be undertaken on the factors that affect efficiency of heating on the Moon.

The drill design is based on a prototype that has demonstrated drilling 1m depth in icy regolith conditions, using 100 N downforce, 100 W of power in 1 hour [322]. The amount of power required for the drilling function is 70% of the total power of the unit [322]. For the requirements of the In-Situ Sublimation mine in this chapter, three holes will be drilled per hour at maximum depth of 3 m each. Work time before recharging is assumed as four hours and a 500 N (W_{driller}) downforce is required. It has been determined that the battery mass is not the limiting factor, rather it is the requirement for downforce. Acceleration due to gravity (g_{moon}) on the Moon is 1.62 m/s^2, and with a Factor of Safety of 2.5 to ensure stability the driller mass has been calculated as 780 kg with Equation 7.13. No engineering optimisation work has been conducted here and the results of such work would affect the end result of the model used in this chapter.

$$Driller\ mass\ (kg) = \frac{W_{\text{driller}} \times FOS}{g_{\text{moon}}} \qquad (7.13)$$

7.3.5   Comet Single Craft Mining

Asteroid mining research is being conducted by several groups around the world, and many concept designs share similar features to those shown by Zacny *et al.* [318] and Kuck [151]. Dorrington and Olsen [75] have also shown a method for parametric calculation of the energy and time requirements for an asteroid mining mission. Dreyer *et al.* [78] have proposed an optical heating method for mining asteroids for volatiles by surface heating through concentrated solar light. However, this method is not thought to be applicable to dormant comet mining due to the necessity to penetrate the barren regolith crust layer that has been theorized by Brandt and Chapman [30].

A major difficulty with mining a dormant comet is transporting the equipment and ensuring it is operational and independent for long periods. Any complex mechanical parts may need repair before the mining phase has finished. Therefore, mechanical reliability is a key consideration for engineers designing an asteroid mining system. The chosen system depicted in Figure 7.4 after the work of Ethridge and Kaukler [90] is another ISWS method. The only mechanical parts of this system are the anchors, drill and storage tank. The base case design has been assumed to have a mass of 70 000 kg, similar to the empty mass of NASA's Space Shuttle Orbiter [188]. This has not been parametrically designed as early results of this investigation have shown that a lunar mine will be more viable due to its closer proximity and the more time-dependent accessibility of asteroids or dormant comets.

This method requires a mining craft to anchor and then drill through the barren surface layers into a dormant comet. Sublimation and extraction are achieved by irradiation of the holes with microwaves produced by a magnetron device. A similar effect can theoretically be achieved by a conductive heating system [319] [235] [32] or channelling solar energy into the borehole [78]. The inputs into this model do not require exact specification of a heating method. More detail can be added in a future run of the model. Water ice trapped in the mining zone will sublime and exhaust from the boreholes similar to previous experiments [319]. The water vapor is then channelled into a storage tank to

await transportation and processing.

7.3.6 Comet Multi-Craft Mining

The multi-craft miner-hauler system allows for increased flexibility and productivity by improving logistical efficiency and separating the tasks of mining and processing from the task of haulage, similar to most mining systems on Earth. It will also use the In-Situ Sublimation system as shown in Figure 7.4. The mining and processing tasks will be completed by a dedicated robot miner that will transfer to a dormant comet ore body and remain there for its entire operational life.
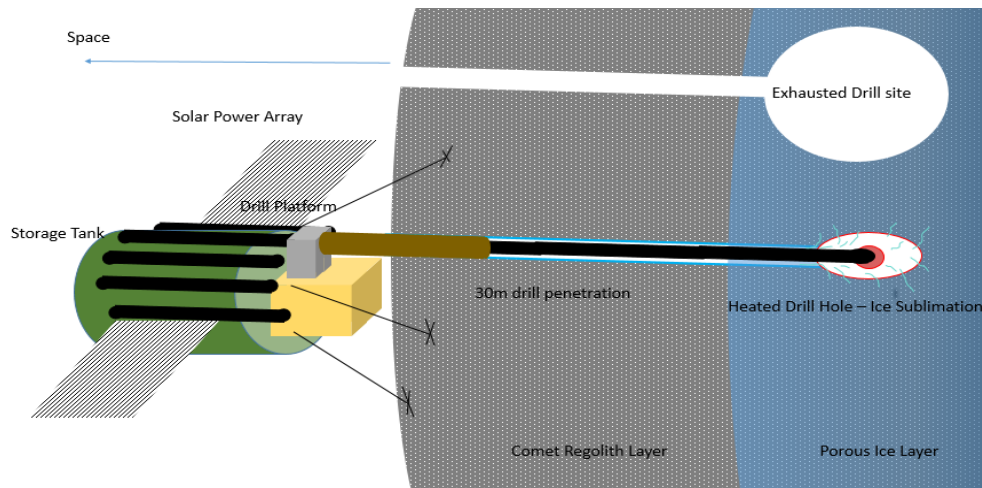
Figure 7.4: In-Situ Water Sublimation on a dormant comet.

The product transport task will then be completed by another class of equipment, the hauler. This will periodically transfer between Low Earth Orbit (LEO) and an optimally selected ore body for a product pickup and return mission. This means that several ore bodies can be mined at once, reducing the waiting time for a craft en-route to pick up. It will also reduce each mission propellant cost, as there will be no need to transport all the mining equipment on every payload trip.

Figure 7.5 shows a mining mission architecture with two dormant comet ore bodies over the period defined between 2020 and 2060. Each level on the y-axis shows a different

location: LEO, and two dormant comet mining targets. The x-axis is a timeline of the mission plan, and the locations of each craft have been plotted to demonstrate the mining and hauling activities and constraints on the missions. Two miner crafts are sent to the orebodies and one hauler moves between them and the LEO market over the operational life. Transits to and from the comet or asteroid targets must optimize ΔV cost (which is related to fuel consumption cost (see Equation 7.21) and journey time to produce the greatest returns on investment for the mining system. This optimisation is included in the following model and greatly affects mission return times and competitiveness.

The equipment in this model has been assumed to produce its own fuel on-site for the payload return mission. That means an ore handling, beneficiation and electrolysis system will be required on board. It also increases the risk that unknown complexities in the ore, such as grain size or breakage could make processing impossible and the mission would be unable to return.
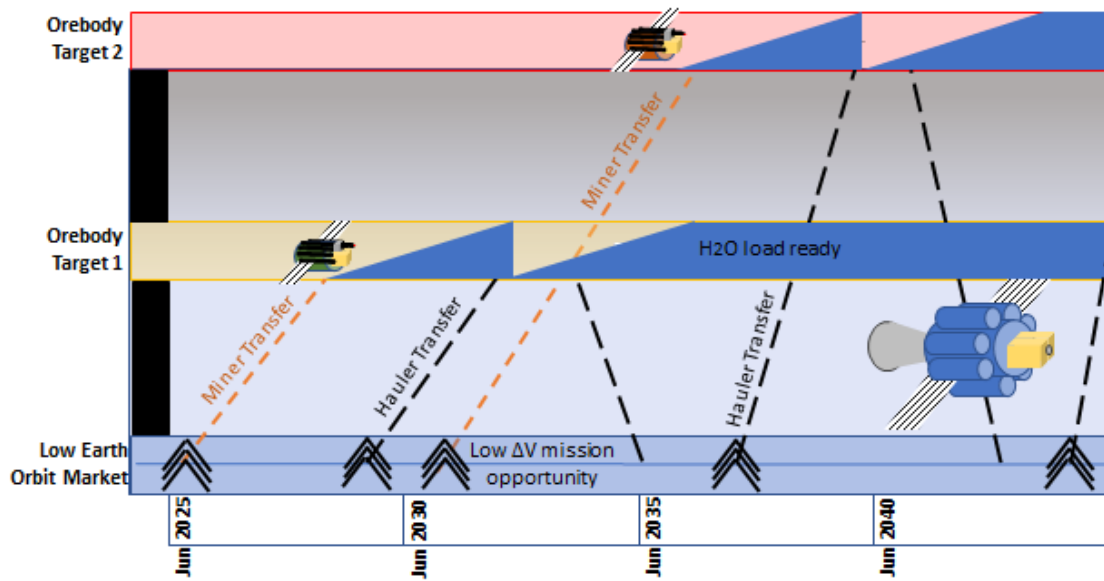
Figure 7.5: Miner-hauler mission schematic.

7.4 Methodology

7.4.1 Infrastructure Assumptions

7.4.1.1 Lunar Mining

The power requirements of each piece of lunar mining equipment are stated in Section 7.3.2 and 7.3.4. It is assumed that solar power installations located on the rims of craters in the southern polar region of the Moon can provide energy continuously [33]. A specific energy per unit mass of solar cell has been referenced at 60 W/kg [107]. Additionally, a 10% mass surcharge has been included in the equipment mass to cover spare parts, equipment and facilities for maintenance and operation. The product transport shuttle will be entirely replaced after every ten years, incurring a 50 000 kg opportunity cost at this interval. It is also expected that a large amount of processed materials sent to the Moon can be re-cycled and repurposed.

One potential piece of infrastructure that would decrease the usage of propellant on the Moon, and hence improve the PPR is the Lunar Resources Launcher (LRL) [238]. The LRL is an electromagnetic rail gun, that would launch the product to an orbital location without needing a rocket. If the LRL is to be employed, it has been calculated by Roesler [238] to require a mass of 40 550 kg to be delivered and constructed on the Moon over a period of 5 years, similar work by other authors support the concept [82,187]. All relevant opportunity costs for the infrastructure are included in the model. High detail has not been included on the infrastructure design and requirements as it is outside the scope of this project.

7.4.1.2 Comet Mining

Minimal in-space infrastructure is required for the comet mining scenario as mining equipment will be designed as self-sufficient. A storage depot at the market location will be advantageous to service the market, although it is not inherently required as the haulers

will spend long times waiting in Earth orbit. A depot has not been included in the current model.

7.4.2   Non-Financial Appraisal Indicators

7.4.2.1   Propellant Payback Ratio

A significant challenge in determining mine feasibility is the assumption of operation and capital expenditure. It has been shown that assumptions of costs in terms of dollars are non-credible for future space operations [141]. For economic appraisal of ISRU in this thesis, alternative indicators have been devised.

Opportunity cost has been defined by Black, Hashimzade and Myles [25] as equal to "*the benefits that could have been obtained by choosing the best alternative*".

Given that most infrastructure and equipment will be launched from the Earth, this launch cost is used as the opportunity cost. For every kilogram of mining equipment and infrastructure launched into LEO, the opportunity to launch a kilogram of propellant has been forgone.

Equation 7.14 shows the assumption that the cost of supplying water from the Earth to LEO is equal to its launch costs. The water launch cost is also equal to the cost of supplying mining equipment to LEO. It is assumed that equipment and water are relatively cheap to acquire once research and development is complete and the large majority of real costs are attributed to launch costs. To extrapolate this concept and use for Near-Earth Objects (NEO's), their specific ΔV (change in velocity) requirements and the Rocket Equation are used as shown in Equation 7.21. For the lunar surface case the ratio shown in Equation 7.15 is used. This equation is based on referenced capabilities of the Falcon Heavy rocket [326] as described in Section 7.4.6.2. It means that for every kilogram of mining equipment put on the Moon, the opportunity cost (Q_{op}) of 7.6 kg of propellant could be sent from Earth to LEO.

$$Cost_{H_2O \ to \ LEO} \approx Cost_{MineEquip \ to \ LEO} \tag{7.14}$$

$$Q_{op} = \ \frac{62000 \ kg}{8300 \ kg} Q_{mass \ delivered \ to \ Lunar \ Surface} \tag{7.15}$$

The Propellant Payback Ratio (PPR) is shown in Equation 7.16. It shows the quantity (Q_s) in kilograms yielded from off-Earth mining on the forgone opportunity to launch the propellant directly from Earth (Q_{op}). A value greater than 1 signifies a mining project can yield more than direct launch of water from Earth. The PPR can therefore be used to determine if an off-Earth water mining project will be viable and competitive.

$$PPR = \ Q_s/Q_{op} \tag{7.16}$$

When examining the PPR on an annual or biannual scale, an issue arises where it is possible that no propellant costs are sunk in accessing the mine during that period. This yields an impossible calculation divided by 0. In reality, there are costs associated with supplying product from the mine but they have been sunk in previous years. It is therefore prudent to depreciate those costs over a number of years so that no product is supplied at zero cost. Linear depreciation of capital is a common economic tool [206] used for this purpose and is applied to the PPR equation for inspection on smaller timescales according to the pseudocode in Algorithm 1. The periods for linear depreciation in this model are: 5 years for the lunar scenarios and 7 years for the comet mining scenarios. This has a smoothing effect on the cumulative PPR graph over time. In effect, parts of the PPR are spread over several years but not changed in absolute value over the whole mine life. Therefore, the final cumulative depreciated PPR and final non-depreciated PPR should be equal when numerical rounding effects are ignored. Q_d is the depreciated Opportunity Cost (Q_{op}) of accessing the mine in kg. It is a vector of length equal to the number of biannual periods in the mine life. Elementwise multiplication is used (Hadamard product $\circ$) to apply linear depreciation factors.

Algorithm 1 Linear Opportunity Depreciation

1: **for** $a \in [1 \ : \ final \ year - 4]$ **do**

2:     $Q_d\,[a : a + 4] = \ Q_d\,[a : a + 4] + [0.36 \quad 0.28 \quad 0.2 \quad 0.12 \quad 0.04] \circ \ Q_{op(a)}$

3: **end for**

4: Then

$$Q_d\,[a + 1 : a + 4] = \ Q_d\,[a + 1 : a + 4] + [0.36 \quad 0.28 \quad 0.2 \quad 0.12\ ] \circ \ Q_{op(a+1)}$$

$$Q_d\,[a + 2 : a + 4] = \ Q_d\,[a + 2 : a + 4] + [0.43 \quad 0.33 \quad 0.24\ ] \circ \ Q_{op(a+2)}$$

$$Q_d\,[a + 3 : a + 4] = \ Q_d\,[a + 3 : a + 4] + [0.56 \quad 0.44\ ] \circ \ Q_{op(a+3)}$$

$$Q_d\,[a + 4 : a + 4] = \ Q_d\,[a + 4 : a + 4] + \ Q_{op(a+4)}$$

After these depreciation factors have been applied, Equation 7.17 should hold true and the cumulative depreciated PPR over the entire mine life can be used as a metric for mine feasibility.

$$\sum_{a=1}^{\text{final year}} Q_{op(a)} = \sum_{a=1}^{\text{final year}} Q_{d(a)} \tag{7.17}$$

7.4.2.2   Substituted Mass Payback Ratio

The PPR appraisal indicator is based on the assumption that the nearest competitor to a lunar ISRU mine is one that launches a product from the Earth's surface. The PPR is only applicable off-Earth for propellant mining operations. It is also possible to compare other resource utilisation operations against any material competitor from Earth using a modified version of the PPR.

The product sent from Earth can be the same material that would be mined off-Earth, or a more efficient substitute. The competitor on Earth is handicapped by the transport costs in comparison to the miner based at the market location on the Moon. There is also an opportunity cost (transport cost of equipment and infrastructure) for a lunar mine to supply a commodity. The opportunity cost is foregone to simply send the commodity instead.

197

The Substituted Mass Payback ratio (SMP ratio) is shown in Equation 7.19. It is similar to the Mass Payback Ratio used by Sonter [272] and the Propellant Payback Ratio used in Equation 7.16. However, the SMP ratio accounts for substitution of commodities and can be used in mining feasibility studies for a range of ISRU projects.

The SMP ratio enables calculation of the relative competitiveness of a mining project compared with an Earth based competitor sending the preferred substitute. For example, instead of using iron sourced from the lunar regolith for manufacturing, a lighter substitute (aluminium) might be sent from Earth instead. Q_s represents the quantity (kg) of a commodity supplied by the lunar mine adjusted to the density of the most preferred Earth substitute, as shown in Equation 7.18. Q_{op} represents the opportunity cost quantity (kg) of mining a commodity on the lunar surface. It is equivalent to the sum of mining equipment and infrastructure mass (kg) required on the Moon to produce the equivalent of the desired commodity.

$$Q_s = Volume \ of \ Mined \ Commodity \times \frac{Density \ of \ Substitute}{Density \ of \ Commodity} \qquad (7.18)$$

$$SMP \ Ratio \ = \frac{Q_s}{Q_{op}} \qquad (7.19)$$

Using this formula in place of the Net Present Value, a mining project assessment demonstration can be carried out in the same way as shown in this chapter for the PPR indicator. Similarly, an SMP value below 1 indicates a non-viable project. Values above one are increasingly more competitive than an Earth based supplier.

7.4.3 Orbital Mechanics Input

Planning a simple spacecraft mission for minimal use of fuel usually means the use of a Hohmann transfer [43]. This method is applied to the dormant comet mining missions to determine the ΔV requirements.

The Hohmann transfer is completed in two stages shown in Figure 7.6, as ΔV_a and ΔV_b:

ΔV_a - Initial rocket burn and ΔV to begin transfer ellipse.

ΔV_b - Final rocket burn to circularize final orbit.
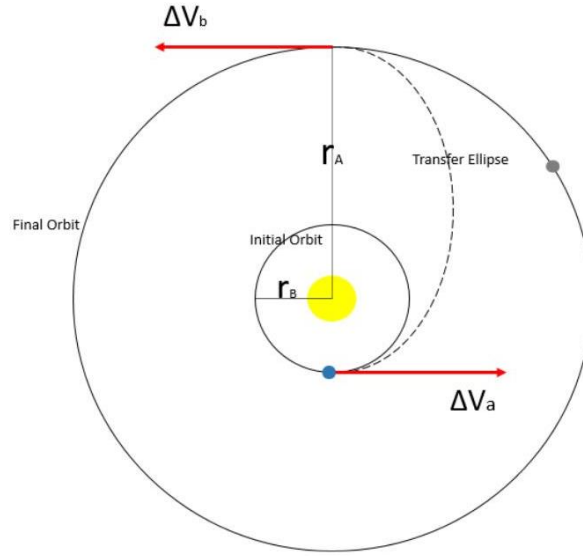
Figure 7.6: A simple Hohmann transfer after Chobotov [43].

To determine the fuel requirements of a transfer, the propellant velocity (V_p) is required. V_p can be determined from the specific impulse (I_{sp}) of a propellant and rocket combination [123]. The I_{sp} for a H_2/LOx chemical rocket is around 420 seconds in a vacuum [42]. Equation 7.20 shows the calculation of V_p in meters per second.

$$V_p = I_{sp} \times g \tag{7.20}$$

Where g is the acceleration due to gravity on Earth's surface, 9.81 m/s^2.

The mass of propellant (kg) required for a specific change in velocity (ΔV) in m/s can be calculated using the rearranged Rocket Equation as shown in Equation 7.21 [43].

$$Propellant\ Mass = m_e/e^{-\Delta V/V_p} - m_e \tag{7.21}$$

199

Where m_e is the empty mass of the rocket in kilograms and the propellant exhaust velocity is V_p. The Rocket Equation (7.21) forms an important part of calculating the PPR in the mining system appraisal shown in this chapter.

7.4.4 Market Input

A demand profile prediction for the period from 2020 to 2060 has been developed as shown in Figure 7.7. It allows the modelling of appropriate mine production rates for this particular profile. Huang, Chang and Chou [125] show a method for forecasting demand in uncertain markets that makes use of historical data and Monte Carlo simulations. However, no historical demand data is available for off-Earth markets and it is accepted that prediction of demand quantities in a high growth market will be unreliable [183]. The demand prediction in this model will only be used to determine mine production rates and the alternative supply that could be brought from Earth. The primary results of this chapter are only applicable in the future market outlined by this demand profile, however they still allow insight into whether a project will be economically competitive. Sensitivity analysis is conducted on the demand profile as shown in Figure 7.17 to test potential changes in the demand profile.
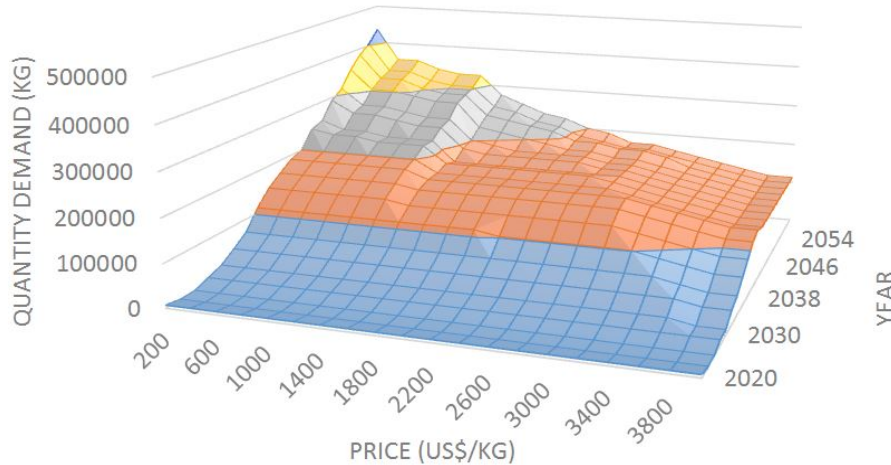
Figure 7.7: H_2O market demand assumptions in LEO.

The approach to develop the market prediction is based on occurrence of events that could

make use of a water supply in orbit. The events include Mars missions [256], circum-lunar tourism [103], satellite service missions [64, 180] and refuelling space stations or hotels for station keeping requirements [132]. Each of these event types has been assigned a quantity of water as shown in Table 7.3. The Dragon Capsule, Falcon 9 and Falcon Heavy rockets have been used as rocket mass benchmarks [291]. The Mars missions are assumed to have rocket and payload mass of 15 000 kg [291], with the circum-lunar mission not requiring a full payload with an assumed mass of 6 000 kg. Demand for large single events such as Mars missions has been smoothed over several years as water can be stockpiled.

Table 7.3: Propellant market events.

Event Type	ΔV Assumption	Single Event Quantity
Space Station Servicing	Atmospheric drag dependent on several re-boosts per year. [312]	800 kg
Circum-lunar Tourism	$\tilde{}$4000 m/s [103, 312]	10 000 kg
Satellite Servicing	$\tilde{}$45 m/s [78]	360 kg
Mars Missions	$\tilde{}$4000 m/s with aero-braking [132, 291, 309]	25 000 kg

Satellite servicing works on a different model; to transit to and refuel other satellites. A direct calculation of propellant is not easily applicable. Instead, an analysis by Long, Richards and Hastings [180] of satellite operations from 1957 to 2000 in Geosynchronous Earth Orbit (GEO) shows the average annual number of servicing opportunities in the past in Table 7.4. This has been used to estimate the future servicing event occurrence. The refuelling of space stations has also been based on a similar paradigm to satellite servicing with additional consideration of atmospheric drag in LEO [64].

Table 7.4: Orbital servicing market after Long, Richards and Hastings [180].

Service type	Average Annual opportunities	Average GEO opportunities
Refuel	20	8.9
Repair	8.2	3.7
Relocation in GEO	13	13
Deployment assistance	0.3	0.1

The date of initial occurrence for each event type is based on assumed timeframes from the literature [64, 103, 132, 180, 256, 291]. An increase in instances of each event type over time

has been assumed to correspond with a reduction in the price of water as per economic theory [186]. The apparent demand insensitivity to price changes in the early stages of the forecast period (2020-2030) is an emergent feature of the forecasting method. The technology to utilize water resources in space is not expected to proliferate until later years and hence quantity demand will not immediately increase due to lower prices. In economic theory this phenomenon is referred to as demand inelasticity [186]. The presence of this feature shows the predicted demand profile follows known economic conventions.

7.4.5 Geological Input

7.4.5.1 Dormant Comet Model

Dormant comets have been chosen as a target ore body due to the higher concentration of water present relative to asteroids. See Chapter 2 for more details about the geological evolution of comets, asteroids and other bodies in the solar system. Alternative mining systems will be required for asteroids due to the geological differences. Only dormant comet mining is considered in this chapter.

The chosen comet ore body 2003 WY25 (D/1891 Blanpain W1) is used as an example in the Near-Earth Object population [67] containing the desired geological characteristics. Fernández, Jewitt and Sheppard [94] imply that 4% of the Near-Earth Objects could be extinct comets. Another candidate Near-Earth dormant comet 2002 CX58 [94] has also been used for analysis. The asteroid Apophis and a fictitious Earth-Trojan asteroid located at Earth Lagrange point L4 (along the Earth's orbital path around the sun) were chosen for analysis due to their low ΔV rendezvous requirements to explore the effects of that parameter.

Assumptions from literature [3, 27, 67, 72, 148, 157, 224, 271, 314] has been used to develop a geological block model of a dormant comet for economic mining analysis. Block models are used in the terrestrial mining industry to plan the economic extraction of resources. They can also be applied to off-Earth Mining scenarios. A 2-D representation of the comet

block model is shown in Figure 7.8. This model is used in the mining system simulation code for this chapter.
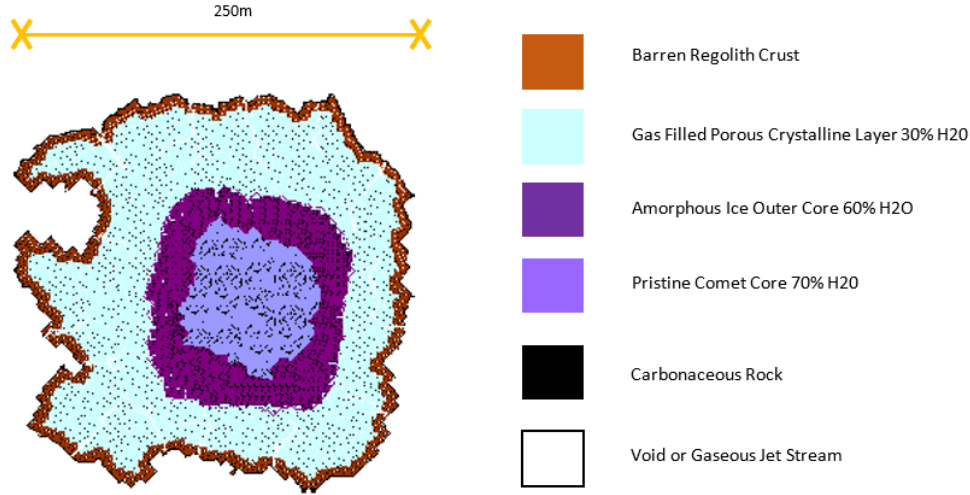
Figure 7.8: Block model representation of dormant comet.

7.4.5.2   Lunar Crater Model

The lunar cratering and impact gardening theory has been employed to create a resource block model for the shadowed lunar polar crater mine analysis. A 2-D representation of the block model is shown in Figure 7.9. Blocks are scaled in this model to represent 1 m^3 of material. The average ore grade in each block is assumed to be 50 kg/m^3 for the base case scenario, in line with the LCROSS mission results [17, 117].

7.4.6   Transport Time and Cost

7.4.6.1   Comet and Asteroid Transport

The ΔV governs how much fuel will be required for a mission, which is an important cost driver in a rocket transport scenario. The launch windows and trip times are also very important from an economic point of view, because they determine how long will be required for a payload to be delivered.
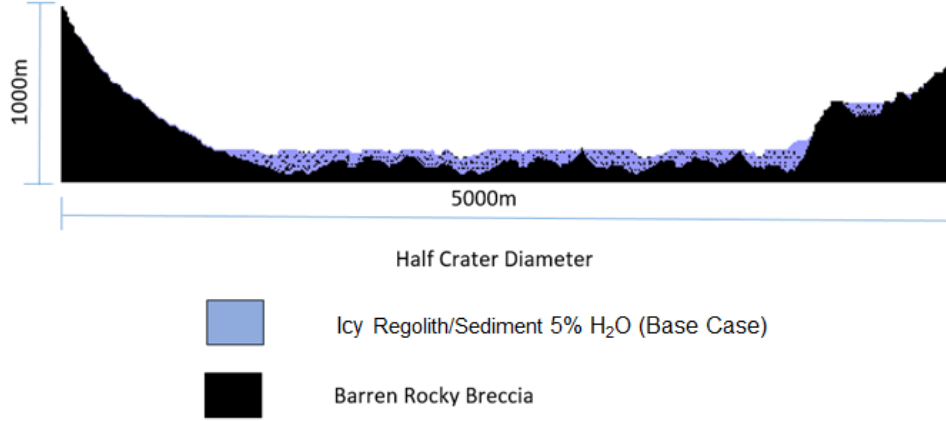
Figure 7.9: Lunar crater block model diagram.

In order to analyse the ΔV, launch windows and transport times for various near Earth mining targets, the Trajectory Planner software was used. A processed example of the output of the Trajectory Planner is shown in Figure 7.10. This grid has been used to determine optimum launch windows and mission times in the analysis model within a maximum tolerance of 300 days idle in LEO, the minimum ΔV within this window is chosen. It is important to note that the Hohmann Transfer (Figure 7.6) requires two rocket burns or changes of velocity (ΔV). The data shown in Figure 7.10 represents the sum of the launch and arrival ΔV for the trajectory towards the dormant comet 2003 WY25. Minimum ΔV launch opportunities are shown in blue and increasing cost is shown in yellow then red. The x-axis launch date will correspond to the respective arrival date on the y-axis where a ΔV is chosen on the plot.

7.4.6.2   Lunar Transport

The Moon is a prospective candidate for an off-Earth mining operation and colony. It is much closer than most of the Near-Earth Asteroids (NEAs), allowing quick re-supply to a permanent human base and reducing the overall risk to a mining operation.

Minimum ΔV launch windows from Earth to the Moon will occur approximately once
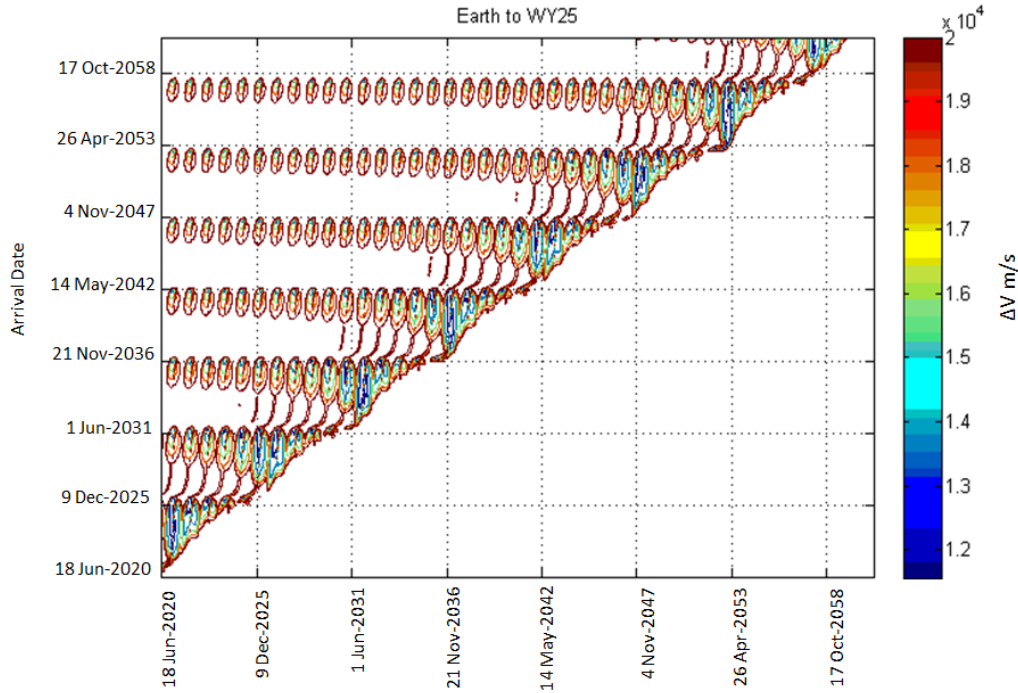
Figure 7.10: Earth to 2003 WY25 travel time and ΔV.

per month, where rockets can be launched from Earth at the lowest cost. Travel time to the Moon is generally just over 3 days [169]. This gives a lot of flexibility compared to NEO missions where the travel time is greater and launch windows are far less common. The ΔV requirement to reach the Moon's surface from LEO have been referenced as approximately 5.9 km/s including inefficiencies in landing and changing orbits [43] [312]. The Falcon Heavy rocket has been referenced as capable of lifting payloads of 62 000 kg to LEO, 26 000 kg to GTO or 8 300 kg to the surface of the Moon [326].

7.4.7   Mining Model Fundamental Equations

7.4.7.1   Lunar Strip Mine

The market demand profile is used in Algorithm 2 to determine the Optimum Biannual Supply (kg) from the mine in order to maximize revenue from the market profile shown in Figure 7.7. Alternative strategies can be considered separately if the model is re-run. The

timescale of the mining model is on the basis of 24 month periods, or biannual periods. This period has been chosen due to the uncertain nature of the market demand input (see Section 7.4.4). Inspection on a smaller timescale such as years would inappropriately increase the resolution of the results.

Algorithm 2 Determining Optimum Biannual Product Supply Quantity

---
1: $H_2O = Biannual\ Supply\ in\ kg\ H_2O$

2: $Return(H_2O) = H_2O \times Unit\ Price(H_2O)$

3: **for** $H_2O > 0$ **do**

4:     **procedure** Maximise($Return(H_2O)$)

5:                 ▷ Supply is optimised by maximising the Return(H_2O) function

6:     $Optimal\ Biannual\ Supply = H_2O\ @\ max(Return(H_2O))$

7:     **end procedure**

The number of biannual product shipments is then calculated with Equation 7.22.

$$N_{shipments} = \frac{Optimum\ Biannual\ Supply}{DP_{mass}} \tag{7.22}$$

Where the Delivery Payload (DP$_{\text{mass}}$) is assumed to be 10 000 kg with a re-usable shuttle craft of 50 000 kg mass, slightly less than the Space Shuttle Orbiter [188].

The Rocket Equation 7.21 is used to determine the Transport Propellant Mass (kg) of delivering a product shipment from the mine to the market location in LEO. Note that the propellant required to supply equipment to the mine is not included in the LEO market profile or the opportunity cost. This is because the equipment launches will originate from Earth's surface, and does not directly affect the LEO market demand.

The total quantity to be mined is therefore according to Equation 7.23.

$$Biannual\ Mine\ Production\ (kg\ H_2O) =$$
$$(\ Transport\ Propellant\ Mass + DP_{mass}\ ) \times N_{shipments} \tag{7.23}$$

The required mining rates can be calculated as in Equations 7.24 and 7.25. Equipment and infrastructure mass follows according to the assumptions in Section 7.4.1. A 24-hour operation has been assumed, as power can be supplied from eternally lit peaks on the crater rims in the southern polar region of the Moon. If this were not the case, production and infrastructure mass requirements would be much higher. The importance of certain real estate locations on the Moon is evident here.

$$Production\ Rate\ (kg\ H_2O/h) = \frac{Biannual\ Mine\ Production}{2 \times 365 \times 24} \tag{7.24}$$

$$Process\ Throughput\ (m^3\ regolith/h) = \frac{Production\ Rate}{Average\ Ore\ Grade} \tag{7.25}$$

The Average Ore Grade for the base case model is 50 kg H_2O/m^3 regolith as in Section 2.2.2.

The amount of minable resource in the block model is tracked as it is depleted according to the Process Throughput. The resource block model is copied into identical strips to numerically represent a 3D version of Figure 7.9. As mining production is carried out, the resource model is depleted by the same amount. This ensures that production does not exceed the limits of the existing resource. If the resource is exhausted, the modelled mine production will terminate. The ore blocks are of uniform grade in this model and are not covered in a waste layer. This is the simplest form of geology possible, and is not likely to benefit greatly from the Extraction Sequencing Algorithm shown in Chapter 6. The extraction sequence has also been kept geometrically minimal for easier computation as the purpose of this chapter is only to demonstrate the appraisal method. Optimal extraction sequences on true geological deposits will likely be more complicated.

The equipment availability is assumed according to Table 7.5. Availability is expected to increase as mining techniques improve over time. A maintenance mass surcharge of 10% in spare parts and support equipment is included in the equipment mass cost for each mining vehicle. Equipment Utilization is planned to be 80%, as some production delays

Table 7.5: Equipment availability.

Year	Availability Factor
2020-30	0.6
2030-60	0.7

will occur. The algorithm is constrained to produce at a constant rate. More miners are required to fill the production gap that exists due to poor availability. This is one of the largest opportunity cost drivers in the model. The mining fleet will be periodically replaced three times over the forty-year mine life. The number of miners required for a particular Process Throughput in any given period is calculated according to Equation 7.26.

$$N_{bucket\ miners} = \frac{Process\ Throughput}{Availability \times Utilization \times R_{bw}} \qquad (7.26)$$

The Miner Rate (R_{bw}) and mass of each miner has been calculated in Section 7.3.2.

Once all equipment requirements are known and the infrastructure assumptions are added according to Section 7.4.1, the Propellant Payback Ratio can be calculated as per Equations 7.15 and 7.16.

7.4.7.2   Lunar In-Situ Sublimation Mine

The equations that constitute the lunar sublimation mine model are similar to the strip mining model. Different factors and constants are applied to reflect the equipment specifications. There are two critical mining activities in this model, drilling and sublimation. The number of sublimation miners based on the parametric equations in Section 7.3.4 can be calculated from the required mine Production Rate (Equation 7.24) and the Number of sublimation miners as shown in Equation 7.27. The sublimation rate ($R_{sublimation}$) is from the assumptions Table 7.2. The Sublimation Throughput is then quantified in Equation 7.28.

$$N_{sublimation\ miners} = \frac{Production\ Rate}{R_{sublimation} \times Availability\ \times Utilisation} \quad (7.27)$$

$$Sublimation\ Throughput\ (m^3\ regolith/h) = \frac{Production\ Rate}{Average\ Ore\ Grade\ \times\ \ Mining\ Recovery}$$
$$(7.28)$$

The Average Ore Grade base case is 50 kg H_2O/m^3 regolith from Section 2.2.2 and the Mining Recovery is from the assumptions Table 7.2.

It has been assumed that the drillers can drill three holes per hour at a maximum depth of 3 m. The Average Depth (m) of the ore body is measured from the block model. An iterative loop is run to determine the extents of each 1 m^2 vertical column in the block model by counting down 1 m^3 blocks until either bedrock or large breccia is encountered, or the maximum depth of 3 m is reached. This loop simulates the drilling process over the entire ore body and averages the results. The average depth of regolith for the lunar block model in this chapter is 2.4 m when limited to the top 3 m. The Area Drilled per Hour (m^2/h) parameter assumes one borehole is required per m^2 surface area of regolith, and three holes are drilled per hour as per Section 7.3.4. These assumptions should be a focus of further research efforts to determine the optimum settings. The number of drillers ($N_{drillers}$) necessary to maintain the mine Production Rate with all assumptions is therefore calculated as in Equation 7.29.

$$N_{drillers} = Round\ up(\frac{Sublimation\ Throughput}{Area\ Drilled\ per\ Hour\ \times\ Average\ Depth}) \quad (7.29)$$

All equipment mass is then multiplied out for each equipment and the associated infrastructure is added as described in Section 7.4.1.

7.4.7.3   Comet Single Miner

The comet mining systems require optimisation of the ΔV (m/s) trips to and from the ore body. Time and propellant cost are taken into consideration. This is a multi-objective optimisation problem and a hierarchical approach has been employed. The first parameter to optimize is the mission return ΔV. A tolerance of acceptable return journeys has been set as no greater than $+50\%$ ΔV of the minimum possible journey within the forty-year period using Equations 7.30 and 7.31. The Near-Earth Object's orbit relative to Earth is usually periodic on a timescale of less than a few years and hence many acceptable return journeys can be found with the $+50\%$ tolerance. Furthermore, the return journey propellant is mined and processed in-situ, and a greater return ΔV will increase that mining requirement exponentially according to the Rocket Equation 7.21 and hence length of mission and risk will be greater. A potential mission list is created which can be used to optimize the final mining plan according to the requirements of the next steps. Departure dates and arrival dates are indexed to the Mission ΔV in an array and extracted when needed.

$$A = min\ ([\Delta V]) \tag{7.30}$$

$$Mission\ \Delta V = [\Delta V < 1.5A] \tag{7.31}$$

The second step in the mission optimisation hierarchy is to allow sufficient time for the miner to complete collection of the resource before the departure window passes. A mining season has been calculated according to Equation 7.32. It has been assumed that setup will take 14 days to land and attach to the comet, drilling the access holes to the orebody will take 28 days. The sublimation time is planned to take 100 days and pack-up will add a further 7 days. Time must also be allowed for the miner to arrive to the ore body. This is calculated from the optimisation of minimum ΔV and the reading the corresponding arrival and departure dates.

Extraction rate is calculated according to Equation 7.33, where the sublimation time is at least 100 days. The overall time of the mission is calculated according to Equation 7.34. The model has been parameterized in this way to allow for sensitivity analysis on each variable as the actual lengths of mining season are currently unknown.

$$Mining\ Season\ (days) = Setup\ Time + Drilling\ Time + Sublimation\ time + Packup\ time$$
$$(7.32)$$

$$Extraction\ Rate\ (\frac{kg}{h}) = \frac{Q_s(i) + Transport\ Propellant\ Mass}{Sublimation\ time \times 24} \qquad (7.33)$$

Each payload or supply Quantity for each mission i ($Q_s(i)$) is assumed to be 50 000 kg H_2O. The Transport Propellant Mass is calculated from the Rocket Equation 7.21. It is important to note that the comet mining systems are inherently unable to maintain constant production according to market demand like the lunar mine due to the long and varying transit and delay times.

$$Mission\ Time\ (days) = Earth\ Arrival - Earth\ Departure \qquad (7.34)$$

It is undesirable to have mining equipment waiting in orbit for extended periods without returning value. Hence a limit on the waiting time for departure from Earth on a new mission has been set at 300 days.

The Rocket Equation 7.21 is used to determine the transport opportunity cost to reach the ore body and once all mission parameters are known for the single craft, the Propellant Payback ratio can be calculated according to Equation 7.15. The propellant Q_{op} required to access the mine includes initial opportunity costs of sending equipment to the dormant comets from Earth and subsequent propellant costs for missions once equipment is already in LEO.

7.4.7.4 Comet Multi-Craft

The multi craft scenario model operates similar to the single craft model, however, the potential mission list is passed to a secondary optimisation algorithm that maximizes the PPR under the constraints of two additional hauler crafts. The pseudocode for this optimisation is shown in Algorithm 3. Where 44 000 and 57 000 is the serial value for: 18 Jun 2020 and 21 Jan 2056 respectively. In a future evolution of this model, more advanced optimisation algorithms may increase the PPR.

Algorithm 3 Mission Selection Optimisation

1: **for** $Hauler \in [1:5]$ **do**

2:     $Start\ Date = 44000$

3:     **while** $Start\ Date < 57000$ **do**

4:         $Start\ Date = Return\ Date$

5:         $Max\ Start\ Date = Return\ Date\ +\ 300$

6:         $i = i + 1$

7:         **procedure** MAXIMIZE($Mission\ PPR(i)$) between [Start Date, Max Start Date]

8:             $Return\ Date(i) =\ Start\ Date(i) +\ Mission\ Time(i)$

9:             [Mission List (i)]=

10:            [Hauler, Destination, Mission PPR(i), Start Date(i), Return Date(i)]

11:        **end procedure**

12:    **end while**

7.5 Results

7.5.1 Lunar Conventional Strip Mine Scenario

Figure 7.11 shows the strip mining scenario has a low Cumulative PPR of 0.08 over a forty-year mine life.

As the mine progresses it will require less equipment and infrastructure deliveries and
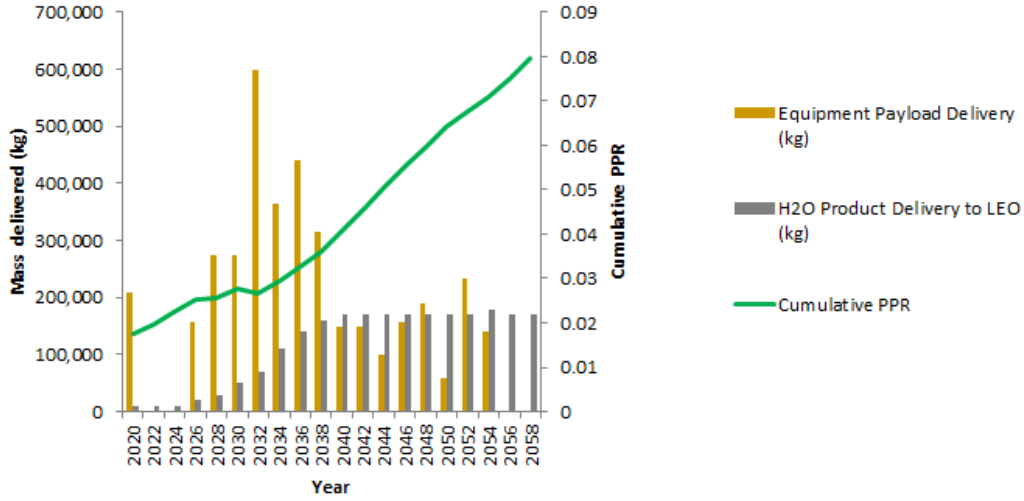
Figure 7.11: Lunar strip mine feasibility.

will be able to supply higher production. However, during the initial production ramp up phase, a large amount of new equipment will be transported to the Moon. This requires fuel usage in Low Earth Orbit, which could be more easily supplied from Earth. The opportunity cost is high for this project and the Cumulative PPR is low.

The effect of changing market location for the strip mine scenario to GEO and introducing new transport technologies is shown in Figure 7.12. For example, the construction of on-site infrastructure to reduce launch costs from the Moon can improve the economics of a lunar strip mine. The Lunar Resources Launcher (LRL) is an electromagnetic rail launcher as described in Section 7.4.1 which reduces the propellant requirement from the Moon's surface to LEO. The amount of mining equipment required to deliver the same amount of propellant to LEO is also reduced and the competitiveness increased, although an increased opportunity cost (~40 550 kg [238]) will be incurred during the five-year construction phase of the LRL. Solar thermal and nuclear thermal rockets are space propulsion technologies in the research and development phase which promise to increase the efficiency of rocket propulsion. The effect of introducing a thermal rocket by increasing the specific impulse to 825s [162] in Equation 7.20 is also shown in Figure 7.12.
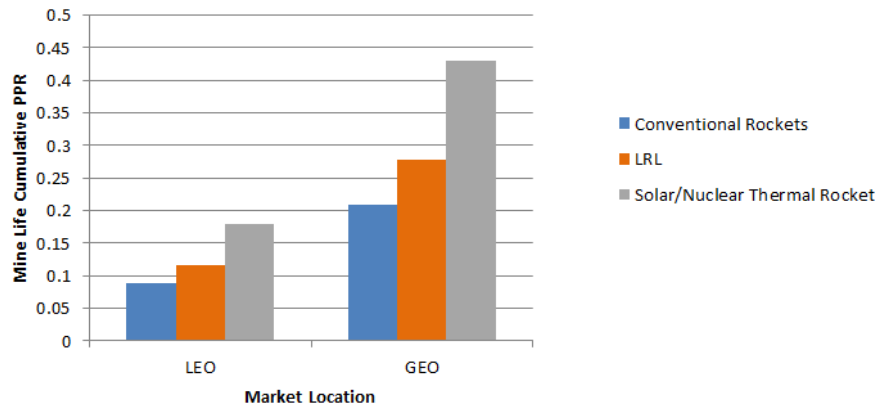
Figure 7.12: Effect of market location and transport technology on lunar strip mine PPR.

7.5.2   Lunar In-Situ Sublimation Mining Scenario

Figure 7.13 shows the base case PPR, equipment mass delivery and product mass for the Lunar Crater In-Situ Sublimation project.
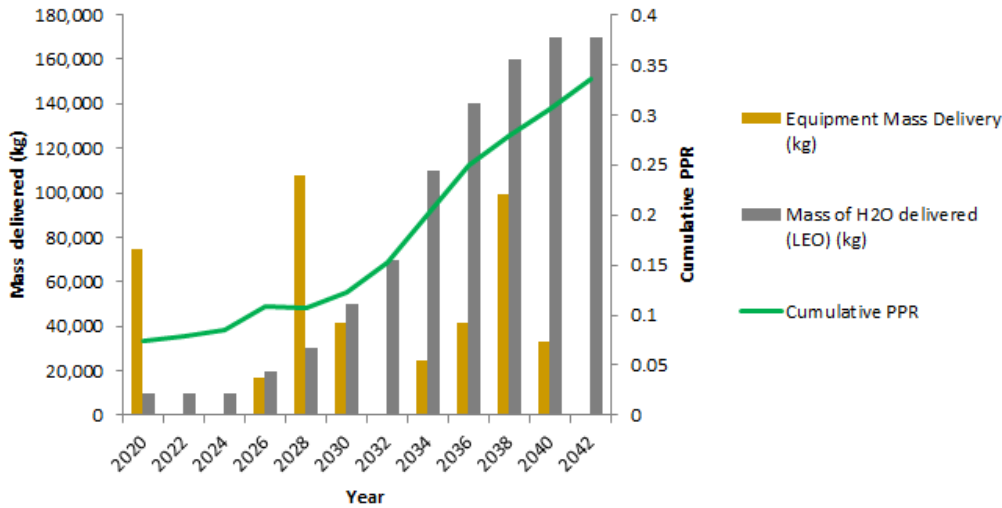
Figure 7.13: Lunar water sublimation base case feasibility.

The ramp up phase of mining operation can be seen in the earlier years with equipment and infrastructure being transported from Earth and little product return. The cumulative mine life PPR is more than four times that of the base case strip mine model, although it only reaches 0.33 over 22 years. Far below parity with the Earth based competitor. Equip-

ment requirements are also less than in the lunar strip mine scenario, as expected. Mine production terminates 18 years earlier in this scenario as the mineral reserve as defined by the block model in Figure 7.9 has been exhausted due to mining system constrains such as drill length and recovery. Note that recovery of the resource is assumed to be lower for the sublimation mining method (30%) compared to the strip mining method (100%).

7.5.3   Comet Single Craft Mining Scenario

This model uses a single craft with In-Situ Sublimation capability. The robot will transit to the object, mine it and return with a payload. This system exhibits a low Propellant Payback Ratio, as the opportunity cost in launching equipment is far greater than the return. This example project will involve two separate missions to two different near Earth comet ore bodies. The result is shown in Figure 7.14.
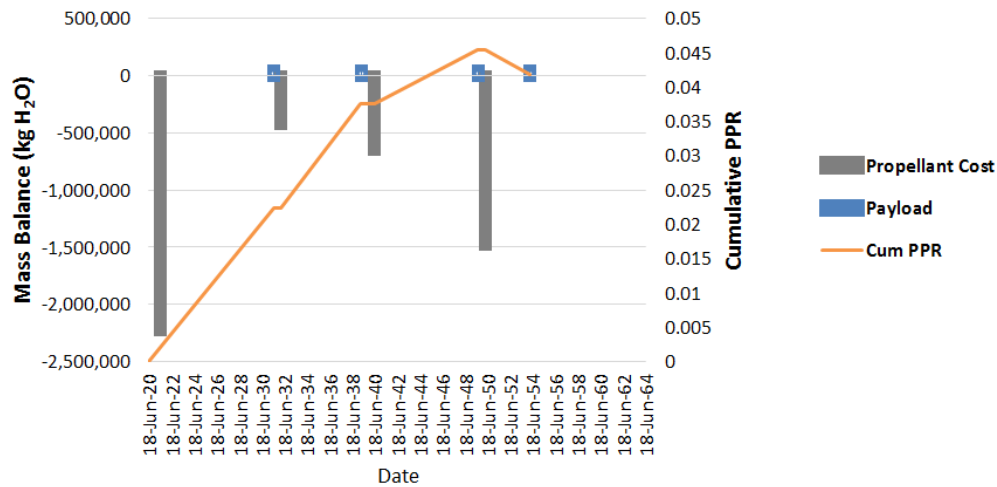
Figure 7.14: Dormant comet single-miner system base case.

Using the four target orebodies and only a single mining craft, four payloads could be delivered in the time between 2020 and 2060, yielding a miserable cumulative Propellant Payback of 0.04. There is a large propellant costs compared to payload with this system. Transport efficiency is very low as the whole equipment and payload are transported with each transfer.

7.5.4 Comet Multi-Craft Mining Scenario

The multi-target miner-hauler system is similar to the single miner system, in that it uses the same In-Situ Sublimation technology. However, it separates haulage from the mining process. This allows an increase in transport efficiency and operational flexibility when selecting missions. The base case for this model is shown in Figure 7.15. Once again, this mining system does not appear to yield enough product to make it a viable operation. The cumulative PPR of this project reaches 0.2. This result is superior to that of the lunar strip mine. However, it is unable to meet market demand changes as easily as the lunar mine. Expansion plans would require capital commitment at least 10 years prior to product return. This is due to the long waiting times for optimal launch windows coupled with long transit times. The miner transport ΔV cost is shown in the early development stage of this system, which can also be seen in Figure 7.15.
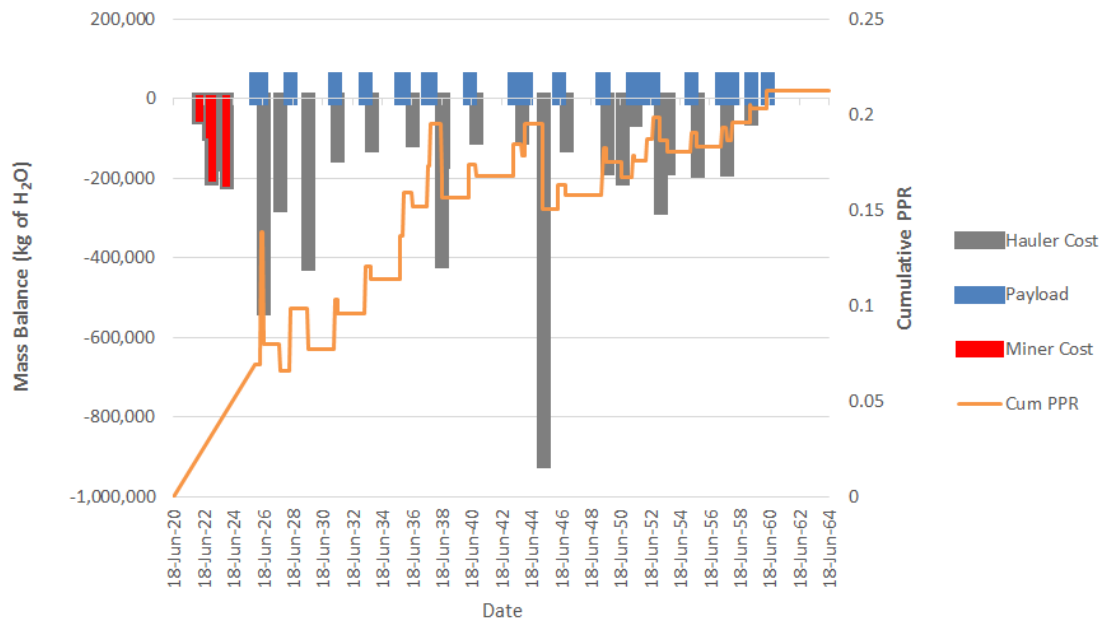
Figure 7.15: Miner-hauler system base case.

7.5.5   Sensitivity Analysis

Sensitivity analysis has been conducted on several aspects of the model. Figure 7.16 shows the effect of improved ore grade in a shadowed lunar crater. It has been indicated from the LCROSS Impactor mission that more than 5% H_2O per m^3 regolith is available [17]. This has been used as the base case assumption for ore grade. Ore grade greatly affects the PPR mostly due to the reduced equipment requirements to produce H_2O at higher grade.
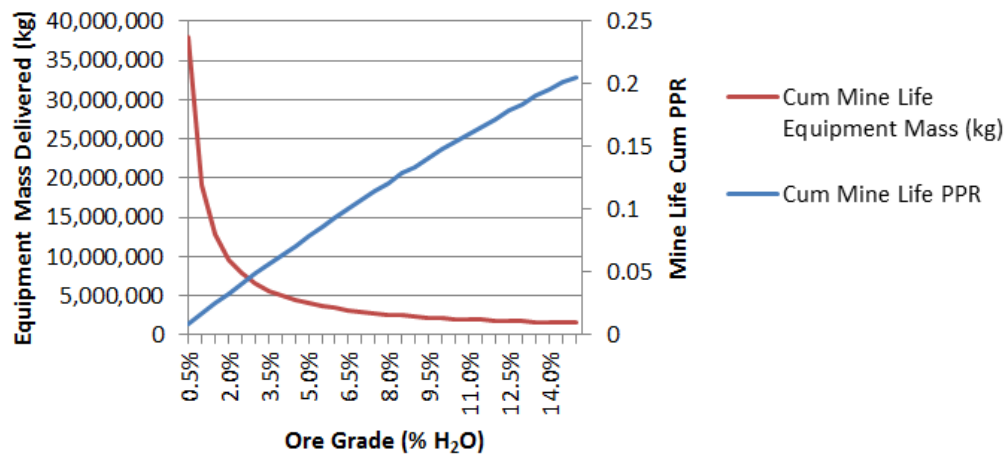
Figure 7.16: Lunar strip mine sensitivity to ore grade.

The analysis of the ore grade parameter was only conducted on the strip mine method in the lunar crater because the physical relationship between ice sublimation and ore recovery is not known. However, the In-Situ Sublimation method PPR is also expected to exhibit a positive correlation to ore grade. The results of the sensitivity analysis on Ore Grade suggest that deposits with below 5% H_2O will have much larger mining costs compared to above 5% grade for this particular mining system.

Market demand has been used to determine the mining rate of this deposit, and hence equipment numbers. The base case market demand is generally increasing each year as shown in Section 7.4.4. The mine production will expand to match this demand.

Figure 7.17 shows the effect of increasing the market demand assumption and using the

same strip mining method. A linear factor was applied to the input demand profile to conduct the analysis. It appears that an increase in market demand will increase the PPR of the project mostly due to the extra capacity in product shuttle infrastructure that will be used more efficiently. The advantage of production on large scale [186] is an emergent feature of this model. However, incremental gains will become smaller as the operation is scaled up.
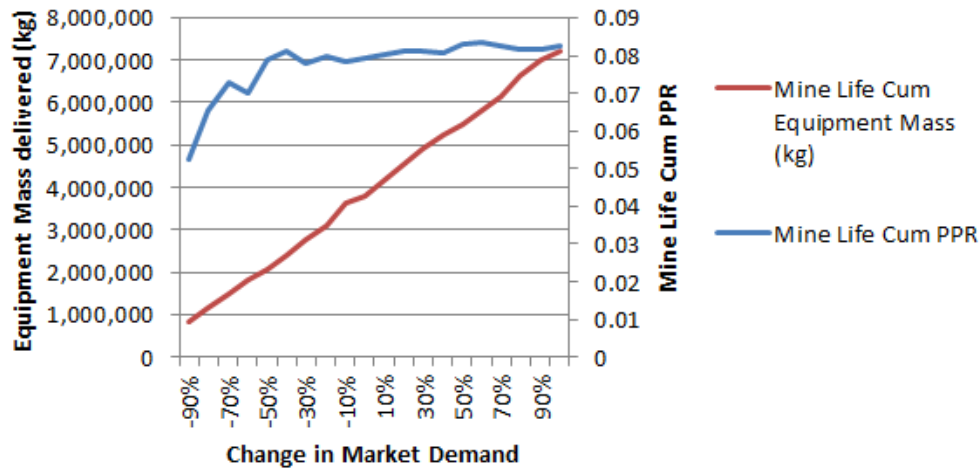
Figure 7.17: Lunar strip mine sensitivity to market demand.

7.6 Discussion

The market profile and geological block model are uncertain inputs in terrestrial and off-Earth mining operations. The market profile in this section is based on predictions of future advancements in technology and space economy as shown in Section 7.4.4. It is a collation of educated assumptions on the path of development that might be followed in the future. The prediction is uncertain, although it uses the best available information and suits the purpose of demonstrating this model.

The geological block models are based on limited scientific data from various space probe missions as outlined in Chapter 2 and Section 7.4.5. They have been constructed by visualizing the relevant formation theory in the same basic way geological models are created

for terrestrial mining. Although this technique is commonly used in the mining industry, it usually suffers from imperfect or insufficient data input. In order to improve the chances of success of an off-Earth mining project, reliable data on the ore body composition, structure and geomechanics is required.

The results are only intended to provide an indication of viability for each of the modelled scenarios and to demonstrate the novel assessment approach using the Propellant Payback Ratio. The inputs are not considered perfect. Similar to terrestrial mining project assessments, assumptions must be made to fill in the gaps where data or knowledge is missing or too expensive to acquire. In particular, the mining systems based on sublimation of in-situ ice require more experimental work, optimisation and proving before deployment. Optimisation of the mass requirements for equipment and infrastructure will also have a positive effect on the PPR as the equipment assumptions made for this appraisal model should be considered conservative.

The dormant comet mining model utilized only four dormant comet ore bodies for the transport optimisation stage. It was discovered that a single Near-Earth Object may only have three or four optimum missions available in a forty-year period. This is an unacceptably small number of mission opportunities as it reduces operational flexibility and ability to respond to market changes. Analysing hundreds of NEOs will give more options for missions, and enable the miner to reduce waiting time for a launch opportunity. It is noted that the majority of NEOs are geologically different to dormant comets, instead they are thought to be hard rock asteroids. Mining methods will need to be completely re-examined for further analysis with a wider selection of NEO ore bodies.

7.7 Conclusions

The use of the Propellant Payback Ratio as a comparison tool has enabled potential off-Earth mining projects to be viewed in a fresh manner, in this case without uncertain financial inputs. It has removed some uncertainty around costs and revenue, and has

allowed comparison of yet-to-be developed technologies. Sensitivity analysis has also been possible for extreme ranges of physical factors, where NPV would have added another layer of potential error with an estimated discount factor. The removal of the NPV discount factor has also enabled comparison of these projects into the more distant future.

From the assumptions and analysis used in this study, the most likely candidate for an off-Earth water mine in the near future is the lunar In-Situ Sublimation mine. However, with the current technology, knowledge and market it is not yet economically viable. Research and development is required to better understand the efficiency of using a sublimation system. The lunar strip mining operation requires an excessive amount of mining equipment. The bucket wheel excavators are also required to move large amounts of regolith, which is likely to lead to unachievable equipment specifications and continuous maintenance in the harsh lunar environment.

An alternative ore source was also considered on some Near-Earth Objects. However, due to transit times, the single craft comet mining system is inefficient and unable to respond to increasing market demand in Low Earth Orbit. The PPR results from this scenario show it is inferior to the miner-hauler system and unlikely to be utilized in the future for mining dormant comets. The comet miner-hauler system is a noteworthy option. It may be the perfect supplier to a deep space market such as another mining operation or a colony. However, it cannot compete at this stage with a lunar mine for Low Earth Orbit market.

The ISRU project appraisal method demonstrated in this chapter can be used in conjunction with the equipment designs, mining method selection procedure and extraction sequence optimisation methods proposed in the previous chapters. Together, these elements form a useful toolkit for undertaking ISRU planning and optimisation studies in the future.

Chapter 8

Conclusions and Future Work

8.1 Thesis Outcomes and Contributions

The objectives of this thesis were set out to rationalise the development of broad and multidisciplinary ISRU planning and optimisation methods. The outcomes of each objective are addressed in the following subsections.

8.1.1 Objective 1 - Develop a rapid and low-cost technique to demonstrate equipment designs and show proof-of-concept.

As mentioned in Chapter 4, many of the equipment designs in literature have seemingly reached a development roadblock around Technology Readiness Level 4. To advance past this level, a demonstration in a relevant environment is required. It is difficult to accurately simulate the lunar environment in a laboratory, and the cost and practicality of testing on the lunar surface is prohibitive. Chapters 3 and 4 show how the Discrete Element Method can be calibrated and used for development of prototype systems in a simulated lunar environment. This technique allows for further optimisations to be undertaken in computer simulation prior to increasing the TRL, saving overall development time and

costs.

8.1.2 Objective 2 - Collate and develop conceptual equipment designs that can be used for subsequent planning and optimisation.

The outcome of this objective has provided a foundation upon which to build other sections of this thesis. The objective is mainly addressed in Chapter 4, where a review of the literature and a categorisation of mining systems is completed so they can be used in the following chapters. Along with this, the mining system design process is demonstrated through the development of three novel mining system concepts. These are also compared with system designs collated from literature.

A collection of conceptual mining equipment on its own is not very useful for mine planning purposes, especially when there is insufficient data to make a quantitative comparison of the effectiveness of each system. For this list to *be used for subsequent planning and optimisation*, a mining system selection procedure is developed in Chapter 5. The systems at TRL 4 or above in Chapter 4 are analysed for their functional requirements and ranked based on their expected capability and reliability in a range of geological deposit types.

8.1.3 Objective 3 - Identify areas of deficiency or improvement when applying traditional mine planning methods to ISRU.

Throughout the thesis, numerous weaknesses or incompatibilities are identified when transferring traditional mining techniques to off-Earth ISRU scenarios. For example Chapter 5 identifies that the mining method selection procedures used on Earth [192, 212] are not suitable for off-Earth mining. They are based on terrestrial operational conditions and equipment and therefore irrelevant.

Chapter 4 identified that most published off-Earth mining equipment designs are not capable of rock breakage. This is an indispensable process in most terrestrial operations,

and usually carried out with explosives [62]. There has been little research and development into rock breakage methods for ISRU, meaning that high grade ice deposits are not currently accessible for bulk excavation. This lack of rock breakage capability limits the ability to achieve optimal resource utilisation by applying *cut-off grade* optimisation as shown in Chapter 6.

Chapter 6 delves deeper into the weaknesses of traditional *cut-off grade* theory and pit optimisation for ISRU. It has been identified that traditional pit optimisation and *cut-off grade* methods are based on the inherent assumption that equipment is almost perpetual and can be replaced without delay, subject to the equipment availability assumptions. Based on this, traditional *cut-off grade* theory and pit optimisation assumes that all *ore*, by definition, will be recovered within a specified mine life. The reality for early ISRU operations is that when a system component or piece of equipment fails, replacement parts may take months or years to deliver from Earth. This delays resource extraction for that unspecified timeframe, invalidating many other time dependant inputs such as market pricing, costs and NPV discount factors. Consequently, ISRU mine planning and appraisal results become invalid. The delays in maintenance and parts replacements delivered from Earth mean that a pre-determined equipment lifespan, and the assumption of a specific, pre-determined mine-life does not work.

There are also several other technical inconsistencies of the traditional planning methods when applied to ISRU, such as uncertainty of costs and other inputs and the move toward data-driven rapid extraction plan iteration [146]. Furthermore, the optimisation objective is different for ISRU. ISRU aims to maximise resource utilisation, while traditional planning methods aim to maximise the Net Present Value or profits. This difference in objective means the traditional processes are not necessarily targeting or even capable of yielding the desired results.

Costs and market price estimations are too uncertain at this stage for use in planning ISRU. These inputs are also critical to traditional appraisal methods such as Net Present Value. This deficiency of traditional economic indicators has been detailed further in Chapter 7.

8.1.4 Objective 4 - Resolve any deficiencies for ISRU planning and optimisation.

The outcome of Objective 3 identified issues when transferring terrestrial mine planning and optimisation techniques to ISRU. Objective 4 yielded solutions to resolve these issues.

The novel mining systems presented in Chapter 4 are capable of mining icy regolith with strength comparable to concrete without using explosives. Two new conceptual examples are shown that can feasibly manage UCS 35 MPa material; the Drill and Pull system and the Regolith Tunneller. These contributions improve the availability of ISRU rock breakage systems in literature and improve the ability of future ISRU planners to optimise their harder resources. The Impact Excavator was intended to improve rock breakage capabilities as well. However, as mentioned in Chapter 4 the experiments were not able to be completed and early indications are that it will not be productive with harder materials. More work is required to define those capabilities.

The mining system selection procedure presented in Chapter 5 resolves the gap in literature found for objective ISRU mining system selection. Instead of using operational examples from terrestrial mines [192, 213], the new procedure uses functional analysis, logical assessment, Axiomatic Design [282] and expected reliability to determine the preferred system for each geological deposit type. This procedure has been intentionally designed to allow for future improvement and expansion when new systems are demonstrated and empirical reliability data is acquired.

The numerous issues identified for the transfer of terrestrial mine *cut-off grade* theory and pit optimisation have been resolved by changing the mine planning paradigm for ISRU. Instead of using the traditional algorithms, with uncertain financial and equipment lifespan inputs, a Reinforcement Learning agent can be trained to optimise an extraction sequence rapidly to help engineers make decisions based on parametric scenarios. The RL agent does not maximise profits as for terrestrial mine planning, instead it maximises the product quantity subject to time and resource constraints as required for ISRU. The uncertain financial inputs are not needed for this objective. The resulting sequence can be

truncated at any length to simulate random equipment failures. The RL agent also removes the labour intensive design and scheduling step required for traditional mine planning. This opens more possibilities for future autonomous off-Earth mining operations, where large amounts of sensory data could be used to update the mine plan in near real-time.

Finally, all these newly proposed systems and methods can be used in conjunction with the Cumulative Propellant Payback Ratio or Substituted Mass Payback Ratio assessment. This has been applied in Chapter 7 to determine the competitiveness of ISRU compared to an Earth based competitor. This method is important as it does not need to employ uncertain inputs identified as the greatest weakness of much of the available literature. For example, financial costs, prices and discount factors as for traditional NPV or Discounted Cash Flow assessments.

8.1.5   Objective 5 - Demonstrate usage of the novel ISRU planning and optimisation methods.

As part of the results section of each chapter, the newly proposed methods, systems and procedures are demonstrated with examples and experiments. The tools developed in each chapter have been or may be used directly as inputs into the methods of the following chapters. The lack of high-resolution geological data and valid resource estimations means that the examples shown are somewhat theoretical. They do require many assumptions to be made that would not be acceptable for terrestrial mine feasibility studies and investment decisions. When sufficient data is eventually collected to replace these assumptions as is intended by NASA [48, 56] and ESA [91] at least, these procedures can be implemented realistically to help plan and optimise ISRU projects.

8.2   Implications for Mining Engineering

The planning and optimisation tools presented in this thesis can be used as elements of an ISRU feasibility study or justification for an operational strategy. Terrestrial mining

engineers use a similarly broad range of tools to plan and optimise their mines on Earth. These elements have equivalent categories in general mine planning and terrestrial feasibility studies as outlined in the *Background* chapter and the SME Mining Engineering Handbook [62]. These new contributions can be categorised within the mining engineering discipline as:

- geomechanics and modelling;

- mining system selection;

- economic decision-making including extraction sequencing; and

- project valuation and appraisal.

There are other traditional elements of mining engineering which have been overlooked in the thesis. This is intentional, due to the lack of relevant data in the case of price forecasting and resource estimation. Complexity and time limitations were the constraint in all other cases. Minor mentions throughout the thesis relating to these additional elements can be categorised as:

- commodity market price forecasting;

- geological exploration and resource estimation;

- infrastructure and services design and construction;

- mineral processing; and

- protection of the environment, societal issues, health and safety.

There is an important implication of the analogy to terrestrial mining engineering. The contribution of this thesis is greater than the individual methods and concepts discussed in each chapter. The thesis identifies and resolves various issues with the transfer of terrestrial mine planning tools to ISRU. The combination of these advancements can be used as an example of the mining engineering discipline being applied to the space resources domain.

8.3 Thesis Placement within Key Literature

The contributions made in this thesis complement the existing literature discussed in Chapter 2. The Commercial Lunar Propellant Architecture [146, 147] is one of the most detailed studies to date on lunar ISRU feasibility. It was undertaken as a collaborative multidisciplinary study with 30 authors from industry, government and academia, including some with mining related expertise. The Commercial Lunar Propellant Architecture [146, 147] has many hallmarks of a terrestrial mine feasibility study and has the same stated aims. It is however, missing some of the important mining engineering aspects that would be the focus of a terrestrial mine feasibility study as discussed in Chapter 2. This thesis develops methods and procedures to address many of these missing elements. Lunar geomechanics have been modelled with the DEM method in Chapters 3 and 4, mining systems can now be objectively selected using the mining system selection procedure in Chapter 5, extraction can be scheduled and optimised using the RL algorithm in Chapter 6 and the project can be appraised without uncertain financial inputs as shown in Chapter 7.

The papers by Gertsch and Gerstch [105] and Cox [51] touch upon these important elements of a mining engineering study and state some assumptions to cover them. Minimal detail is provided on how these methods can be implemented for ISRU. Consequently, they do not identify the relevant issues that have been found when directly transferring mining engineering tools to ISRU. The proposed resolutions to these newly identified issues can enhance the method used in the Commercial Lunar Propellant Architecture paper [146, 147] and the work by Blair *et al.* [26]. This can be done by including the elements of optimisation that are specific to the mining engineering discipline in a way that overcomes the important differences relevant to off-Earth In-Situ Resource Utilisation.

8.4 Limitations and Future Work

Future space resource utilisation research can continue from the platform established here. From each of the chapters in this thesis, various potential future research projects have

been identified. The following lists are separated based on the relevant chapters for ease of reference.

Chapter 2 - *Background* has specifically stated further areas of the mining engineering discipline that were not covered in this thesis, hence opportunities for further research. One area is in hazard identification and mitigation for off-Earth mining systems, and a future research topic could relate to the following objective:

- identify and quantify lunar environmental hazards and mitigate those hazards for ISRU. Examples include micrometeoroids, rocket launch debris, solar radiation, temperature variations, and rockfalls.

The applications of DEM presented in Chapters 3 and 4 can be used to develop and optimise more off-Earth mining equipment in simulation, without necessarily prototyping every component. This should speed up the development process for new equipment.

The Discrete Element Method itself is data dependent, Chapter 4 necessarily replaces a model of icy lunar regolith with a concrete particle model as there is little confidence in the geomechanical properties of icy regolith at this time. Future work mapping out the properties of icy regolith at relevant cryogenic temperatures will enable these DEM models to be calibrated more appropriately for equipment optimisation. Two research topics in this area are suggested below:

- determine the geomechanical behaviour of icy lunar regolith in PSR conditions and implement a DEM calibration; and

- develop more ground engaging tools in simulated icy regolith in PSR conditions.

There are three novel equipment designs presented at a Technology Readiness Level of 3 or less in Chapter 4. To improve these TRLs, a physical prototype should be demonstrated in the lab. Although a lab prototype was demonstrated for the Impact Excavator, there were issues with manufacturing that require remediation and re-trial before TRL

4 is attained. The Regolith Tunneller is at TRL 2 as no modelling or prototyping was undertaken. However, this equipment is based on a heritage terrestrial mining equipment and progress should be rapid once started. The Drill and Pull system also requires a laboratory demonstration as the technology has only been modelled in DEM software. The difficulty with demonstration of this system is selecting an appropriate target material and environment for breakage experiments. A simple concrete target material in standard lab conditions should be used initially, as in the simulation, to avoid the difficulties in setting up cryogenic temperature icy regolith experiments. Although, these more difficult environmental settings will be required to eventually reach TRL 5.

The process of designing three novel mining systems has helped to identify many gaps related to equipment components and requirements that are in need of research and development for these systems to be successful. The following suggestions are listed:

- develop autonomous control systems and infrastructure for robotic mining fleets on the Moon addressing issues such as location tracking without GPS, energy transfers and usage, computation and communications systems design;

- design waste dump construction methods for specific mining systems;

- develop systems for re-purposing ISRU waste by-product materials such as using barren regolith for construction and protection;

- optimise lunar mining equipment movements with respect to environmental hazards, road construction, equipment interaction and energy consumption using the available lunar resource site data and assumptions; and

- demonstrate new and more efficient *mining methods* by suggesting creative applications of a particular *mining system*, increasing redundant options and reducing mission risk for that system. Refer to the definitions of a *mining method* and a *mining system* and Section 4.7.2 of this thesis for an example of this research topic.

The mining system selection procedure proposed in Chapter 5 can be further improved when empirical reliability data becomes available. The procedure has been designed to

easily replace the Axiomatic Design principles and functional mapping with empirical reliability data once available. The procedure is currently used to select from a limited pool of off-Earth mining equipment, this pool of input designs can also be expanded as new equipment designs reach the appropriate TRL for functional analysis and making reliability assumptions. Further research in the following area is required to provide this data:

- test lunar mining system prototypes to gather reliability data for input to the off-Earth mining system selection procedure.

The extraction sequencing algorithm described in Chapter 6 is a proof-of-concept. Its capabilities are limited to small geological environments. Changes can be made to the action mapping function to enable much larger model inputs without excessively slowing down training. Although, increased training time is expected for larger, more realistic geological environments. It is also possible that future developments in Reinforcement Learning may significantly increase the training efficiency of this method, allowing more rapid training for more realistic size environments. The following future research topic encompasses this area:

- improve the extraction sequencing Reinforcement Learning algorithm to enable larger geological environments to be sequenced.

- compare the Reinforcement Learning agent against a mathematically optimal solution and further highlight the advantages of using RL for this task.

The results shown by the project appraisal method in Chapter 7 will become out-dated as time passes due to changes in the technological input assumptions. As with terrestrial mining appraisals, the results here must be updated and optimised as new technology and data becomes available. The specific results of this chapter were also not subjected to a rigorous optimisation process using all the methods now available from the works in other chapters. Once sufficient new geological data becomes available, possibly after the

Artemis' VIPER mission [48], a more realistic *mineral resource* estimate can be made. Then, a new project appraisal can be completed using all the tools demonstrated in this thesis. In addition to this, more work can be done in relation to defining, comparing and improving In-Situ Water Sublimation and bulk mining systems. Suggested follow-up projects for this chapter are stated below:

- explore the effects or advantages of using surplus thermal energy, solar or nuclear, for mining icy regolith or extracting volatiles via softening or sublimating targeted areas;

- develop and test centralised beneficiation and volatile extraction systems for icy regolith in lunar PSR conditions.

- determine the level of scale-up, if any, required for mining activity to change the optimal extraction method from In-Situ Water Sublimation to bulk mining methods such as load and haul with a centralised volatile extraction oven.

- theorise future market prices of various off-Earth commodities at specific locations such as GEO or the south pole of the Moon, based on supply and demand scenarios.

- investigate options for infrastructure that can improve the economics or risk profile of ISRU, taking into account site data such as topography, temperature, solar availability, and any assumptions for potential lunar South Pole resource sites; and

- continue updating technical evaluations of off-Earth mining scenarios, considering various market locations and types, new technology and resource locations, types, sizes and ore grades.

8.5 Final Remarks

The methods demonstrated in the previous chapters can be used to plan and optimise lunar In-Situ Resource Utilisation projects in a similar fashion to the mining engineering done

for terrestrial mine projects. There have been some necessary improvements and novelties proposed in this thesis to enable these methods to overcome the differences identified between terrestrial mining operations and ISRU.

The Discrete Element Method has been shown to be useful in determining stability of regolith excavations in the lunar environment as well as enabling computational modelling of excavation and other ground engaging equipment. These models have been used to show proof-of-concept and enhance the development of lunar mining systems without physical prototyping.

Three new mining system concepts have been proposed to increase rock breakage capabilities. These can be developed for future ISRU projects to extract harder, higher grade ores and achieve a higher level of optimality. Two of these systems have been demonstrated in laboratory or DEM experiments.

Mining system selection is a pre-requisite of ISRU planning and optimisation studies and must be undertaken objectively to produce optimal results. A mining system selection procedure has been proposed in this thesis, to guide the task for ISRU. This is analogous to mining method selection on Earth.

Terrestrial mining projects are significantly enhanced by optimising schedules and extraction sequences, taking into account ore grades, ground stability and practical constraints. The traditional methods used for this task do not easily transfer to ISRU due to several key differences mentioned in Chapter 6. Instead, a Reinforcement Learning agent with the goal of maximising product quantity in a limited time frame has been demonstrated. Finally, the issue of credibility for cost and market price input assumptions has been circumnavigated with a new off-Earth mining project appraisal method.

The broad components of this thesis are part of a multidisciplinary approach to resource extraction planning and optimisation, as is necessarily the case for terrestrial mining. In a sense, the thesis can be considered an expansion of the mining engineering discipline into the space resources domain. It can be used as a foundation for future mining engineers to

further develop ISRU planning and optimisation techniques in ways that have so far not been thoroughly discussed in space related literature.

Appendix A

Supplementary Materials

				DP					
				1	2	3	4	5	6
				Joules per second (J/s)	Arm rotation angle (°)	Drum diameter (m)	Arm length (m)	Wheel diameter (m)	Bucket opening gap (m)
FR	1	Provide energy		x					
	2	Contact drum with material		x	x				
	3	Rotate drum with torque		x		x			
	4	Lift material weight		x	x		x		
	5	Transport material with wheel torque		x				x	
	6	Reverse rotate drum to unload material		x					x

Figure A.1: Design Parameter Mapping for the Bucket Drum Excavator.

			DP	1	2	3	4	5	6	7
				Joules per second (J/s)	Wheel diameter (m)	Bucket Volume (m^3)	Bucket wheel diameter (m)	Auger velocity (rad/s)	Storage volume (m^3)	Actuator extension (m)
FR		1	Provide energy	x						
		2	Transport to site with wheel torque	x	x					
		3	Dig material	x		x				
		4	Rotate bucket wheel with torque	x			x			
		5	Transfer material to storage	x			x	x		
		6	Store material						x	
		7	Unload material with linear actuator tip	x						x

Figure A.2: Design Parameter Mapping for the Continuous Excavator.

				DP												
				1	2	3	4	5	6	7	8	9	10	11	12	13
				Joules per second (J/s)	Chamber volume (m³)	Jaw coordinates (m,m,m)	Actuator extension length (m)	Jaw passing gap size (m)	Chamber volume (m³)	Door close gap (m)	Heating power (J/s)	Gas pressure (Pa)	Pressure differential (Pa)	Condensation surface area (m²)	Waste storage volume (m³)	Waste pass rate (m)
FR	1	Provide energy		x												
	2	Hold material			x											
	3	Feed material			x	x										
	4	Crush material		x			x									
	5	Sort to fine grain material					x	x								
	6	Hold crushed material							x							
	7	Confine chamber		x						x						
	8	Heat material		x	x						x					
	9	Measure chamber pressure			x						x	x				
	10	Remove volatiles at preset pressure		x	x								x			
	11	Condense volatiles									x			x		
	12	Store waste			x										x	
	13	Pass waste to dump		x	x											x

Figure A.3: Design Parameter Mapping for the Crusher Oven.

			DP						
			1	2	3	4	5	6	7
			Joules per second (J/s)	Reaction Mass (kg)	Wheel diameter (m)	Bucket tooth incidence angle (°)	Bucket volume (m³)	Actuator extension (m)	Bucket rotation angle (°)
FR	1	Provide energy	x						
	2	Provide Reaction force		x					
	3	Transport to site with wheel torque	x	x	x				
	4	Loosen Material	x			x			
	5	Dig material	x			x	x		
	6	Extend linear actuator to lift bucket	x				x	x	
	7	Rotate bucket to unload	x				x		x

Figure A.4: Design Parameter Mapping for the Discrete Excavator.

				DP						
				1	2	3	4	5	6	7
				Joules per second (J/s)	Wheel diameter (m)	Extension velocity (m/s)	Rotation velocity (rad/s)	Auger Length (m)	Anchor length (m)	Percussion rate (Hz)
FR		1	Provide energy	x						
		2	Transport to site with wheel torque	x	x					
		3	Extend drill through rock	x		x				
		4	Rotate drill to remove cuttings	x		x	x			
		5	Use auger for anchor hole	x		x	x	x		
		6	Install anchor	x					x	
		7	Use percussion to break rock	x		x	x	x	x	x

Figure A.5: Design Parameter Mapping for the Hammer Drill.

FR				DP					
				1	2	3	4	5	6
				Joules per second (J/s)	Bucket tooth incidence angle (°)	Bucket volume (m³)	Extend actuator (m)	Wheel diameter (m)	Bucket rotation angle (°)
	1	Provide energy		x					
	2	Loosen Material		x	x				
	3	Dig material		x	x	x			
	4	Lift arm with linear actuator		x		x	x		
	5	Transport material with wheel torque		x		x		x	
	6	Unload material		x		x			x

Figure A.6: Design Parameter Mapping for the Load-Haul-Dump Rover.

			DP											
			1	2	3	4	5	6	7	8	9	10	11	12
			Joules per second (J/s)	Wheel diameter (m)	Extension velocity (m)	Percussion rate (Hz)	Rotation velocity (rad/s)	Anchor extension length (m)	Incidence angle (°)	Borer reach length (m)	Brace extension distance (m)	Angular velocity (rad/s)	Cutting head advance distance (m)	Auger speed (rad/s)
FR	1	Provide energy	x											
	2	Move to site with wheel torque	x	x										
	3	Extend drill through rock for anchor	x		x									
	4	Use drill percussion to break rock	x		x	x								
	5	Rotate drill to remove cuttings	x		x	x	x							
	6	Install anchor	x				x	x						
	7	Set up tunnel face	x						x					
	8	Extend borer head to face	x							x				
	9	Brace force on tunnel walls	x								x			
	10	Rotate cutting head with torque	x								x	x		
	11	Apply normal force	x								x	x	x	
	12	Transfer material to access	x								x	x	x	x

Figure A.7: Design Parameter Mapping for the Micro Tunnel Borer.

FR			DP								
			1	2	3	4	5	6	7	8	9
			Joules per second (J/s)	Chamber volume (m^3)	Shutter gap (m)	Heating power (J/s)	Gas pressure (Pa)	Pressure differential (Pa)	Condensation surface area (m^2)	Waste storage volume (m^3)	Waste pass cross sectional area (m^2)
	1	Provide energy	x								
	2	Hold material		x							
	3	Confine chamber	x		x						
	4	Heat material	x	x		x					
	5	Monitor chamber pressure		x		x	x				
	6	Remove volatiles at pre-set pressure		x				x			
	7	Condense volatiles							x		
	8	Store waste								x	
	9	Pass waste to dump									x

Figure A.8: Design Parameter Mapping for the Oven.

			DP								
			1	2	3	4	5	6	7	8	9
			Joules per second (J/s)	Actuator extensions (m)	Storage volume (m^3)	Refill pressure (Pa)	Gas pressure (Pa)	Gas outlet diameter (m)	Intake area (m^2)	Storage volume (m^3)	Wheel diameter (m)
FR	1	Provide energy	x								
	2	Position jets and intake with actuators	x	x							
	3	Store gas			x						
	4	Refill gas store			x	x					
	5	Pressurize jets			x	x	x				
	6	Mobilize material with gas pressure					x	x			
	7	Collect material						x	x		
	8	Store material								x	
	9	Transport material with wheel torque	x							x	x

Figure A.9: Design Parameter Mapping for the Pneumatic Excavator.

			DP			
			1	2	3	4
			Joules per second (J/s)	Tub volume (m³)	Wheel Diameter (m)	Actuator extension length (m)
FR	1	Provide energy	x			
	2	Store material		x		
	3	Transport with wheel torque	x	x	x	
	4	Unload material with actuator arm	x	x		x

Figure A.10: Design Parameter Mapping for the Tip Truck.

References

[1] L. M. Abadie. Valuation of long-term investments in energy assets under uncertainty. *Energies*, 2:738–768, 2009.

[2] R. Aboul Hosn, L. Sibille, N. Benahmed, and B. Chareyre. Discrete numerical modeling of loose soil with spherical particles and interparticle rolling friction. *Granular matter*, 19:1–12, 2017.

[3] Y. Alibert, C. Broeg, W. Benz, G. Wuchterl, O. Grasset, C. Sotin, C. Eiroa, T. Henning, T. Herbst, L. Kaltenegger, A. Léger, R. Liseau, H. Lammer, C. Beichman, W. Danchi, M. Fridlund, J. Lunine, F. Paresce, A. Penny, A. Quirrenbach, H. Röttgering, F. Selsis, J. Schneider, D. Stam, G. Tinetti, and G. White. Origin and formation of planetary systems. *Astrobiology*, 10(1):19–32, 2010.

[4] E. E. Amah, D. G. Andrews, A. Barnard, C. M. Busby, J. Carrol, C. Ciampi, A. L. Freeman, L. A. Gibbons, A. L. Girardeau-Dale, R. W. Gruenenfelder, A. M. Hadaller, C. W. Hjelm, B. M. Hopkins, M. C. Hughes, H. H. Kim, J. E. Lesko, S. W. Rich, N. M. Rodriguez, N. C. Smith, and A. M. Yunusov. Defining a successful commercial lunar mining program. In *Proceedings of AIAA SPACE 2012 Conference and Exposition*, Pasadena, California, 2012. American Institute of Aeronautics and Astronautics.

[5] D. G. Andrews, K. D. Bonner, A. W. Butterworth, H. R. Calvert, B. R. H. Dagang, K. J. Dimond, L. G. Eckenroth, J. M. Erickson, B. A. Gilbertson, N. R. Gompertz, O. J. Igbinosun, T. J. Ip, B. H. Khan, S. L. Marquez, N. M. Neilson, C. O. Parker,

E. H. Ransom, B. W. Reeve, T. L. Robinson, M. Rogers, P. M. Schuh, C. J. Tom, S. E. Wall, N. Watanabe, and C. J. Yoo. Defining a successful commercial asteroid mining program. *Acta Astronautica*, 108:106–118, 2015.

[6] L. Art and H. Mauch. *Dynamic Programming: A Computational Tool.* Springer, Berlin Heidelberg, Berlin, Heidelberg, 2007.

[7] H. Askari-Nasab and K. Awuah-Offei. An agent-based framework for open pit mine planning. *CIM Bulletin*, 3, 2008.

[8] E. Asphaug. Impact origin of the Moon. *Annual Review of Earth and Planetary Sciences*, 42(1):551–578, 2014.

[9] J. Atkinson and K. Zacny. Mechanical properties of icy lunar regolith: Application to ISRU on the Moon and Mars. In *Earth and Space 2018: Engineering for Extreme Environments*, pages 109–120. American Society of Civil Engineers Reston, VA, 2018.

[10] S. Avalos and J. M. Ortiz. *A guide for pit optimization with pseudoflow in python.* Predictive Geometallurgy and Geostatistics Lab, Queen's University, Ontario, Canada.

[11] V. Badescu, editor. *Moon: Prospective energy and material resources.* Springer Science & Business Media, 2012.

[12] D. Bahat, A. Rabinovitch, and V. Frid. *Tensile fracturing in rocks.* Springer, 2005.

[13] B. Bailey, J. Bleacher, S. Lawrence, E. Mahoney, and J. A. Robinson. The Artemis Program: Enabling human exploration of the Moon. *The Impact of Lunar Dust on Human Exploration*, 2020.

[14] C. Balci, M. A. Demircin, H. Copur, and H. Tuncdemir. Estimation of optimum specific energy based on rock properties for assessment of roadheader performance (567bk). *Journal of the Southern African Institute of Mining and Metallurgy*, 104(11):633–641, 2004.

245

[15] I. Ballington, E. Bondi, J. Hudson, G. Lane, and J. Symanowitz. A practical application of an economic optimisation model in an underground mining environment. *Orebody Modelling and Strategic Mine Planning*, 2004.

[16] A. C. Barr. On the origin of Earth's Moon. *Journal of Geophysical Research: Planets*, 121(9):1573–1601, 2016.

[17] A. Basilevsky, T. Abdrakhimov, and V. A. Dorofeeva. Water and other volatiles on the Moon: A review. *Solar System Research*, 46(2):89–107, 2010.

[18] X. Bednarek, S. Martin, A. Ndiaye, V. Peres, and O. Bonnefoy. Calibration of DEM parameters on shear test experiments using kriging method. In *EPJ Web of Conferences*, volume 140, page 15016. EDP Sciences, 2017.

[19] N. J. Bennett, D. Ellender, and A. G. Dempster. Commercial viability of lunar in-situ resource utilization (ISRU). *Planetary and Space Science*, 182:104842, 2020.

[20] W. Bergeson. Review of long drive microtunneling technology for use on large scale projects. *Tunnelling and Underground Space Technology*, 39:66–72, 2014.

[21] J. Bertisen and G. A. Davis. Bias and error in mine project capital cost estimation. *The Engineering Economist*, 53:118–139, 2008.

[22] T. Beysolow II. Applied reinforcement learning with Python, with OpenAI gym, Tensorflow and Keras. 2019.

[23] N. Bilgin, D. Tumac, C. Feridunoglu, A. R. Karakas, and M. Akgul. The performance of a roadheader in high strength rock formations in Küçüksu tunnel. In *Materiały konferencyjne. 31th ITA-AITES World Tunnel Congress, Instanbul*, 2005.

[24] M. R. Bitarafam and M. Ataei. Mining method selection by multiple criteria decision making tools. *The Journal of The South African Institute of Mining and Metallurgy*, 104(9):493–498, 2004.

[25] J. Black, N. Hashimzade, and G. Myles. *A Dictionary of Economics*. Oxford University Press, New York, 2012.

[26] B. R. Blair, J. Diaz, M. Duke, E. Lamassoure, R. Easter, M. Oderman, and M. Vaucher. Space resource economic analysis toolkit: The case for commercial lunar ice mining. *Final report to the NASA Exploration Team*, 2002.

[27] D. Bockelée-Morvan. An overview of comet composition. In *Proceedings International Astronomical Union Synopsium*, volume 280, page 261–274, Meudon, France, 2011. International Astronomical Union.

[28] C. W. Boon, G. T. Houlsby, and S. Utili. Designing tunnel support in jointed rock masses via the DEM. *Rock Mechanics and Rock Engineering*, 48:603–632, 2015.

[29] E. Bozorgebrahimi, R. Hall, and G. Blackwell. Sizing equipment for open pit mining–a review of critical parameters. *Mining Technology*, 112:171–179, 2003.

[30] J. Brandt and R. Chapman. *Introduction to Comets*. Cambridge University Press, 2004.

[31] N. V. Brilliantov, N. Albers, F. Spahn, and T. Pöschel. Collision dynamics of granular particles with adhesion. *Physical Review E*, 76(5):051302, 2007.

[32] J. Brisset, T. Miletich, and P. Metzger. Thermal extraction of water ice from the lunar surface - a 3D numerical model. *Planetary and Space Science*, 193, 2020.

[33] D. B. J. Bussey, P. D. Spudis, and M. S. Robinson. Illumination conditions at the lunar south pole. *Geophysical Research Letters*, 26(9):1187–1190, 1999.

[34] D. E. Cameron. Grade control and mine planning – observations from the front. In *Proceedings of the SME Annual Meeting*, Minneapolis, MN, 2018. Society for Mining, Metallurgy and Exploration.

[35] P. Campbell, R. J. Young, S. Blackburn, A. J. Merchant, and T. J. Veasey. The use of high speed image and stress analysis for the evaluation of tensile based breakage tests. *Minerals engineering*, 14(8):911–915, 2001.

[36] K. M. Cannon and D. T. Britt. A geologic model for lunar ice deposits at mining scales. *Icarus*, 347:113778, 2020.

[37] R. M. Canup and E. Asphaug. Origin of the Moon in a giant impact near the end of the Earth's formation. *Nature*, 412(6848):708–712, 2001.

[38] W. Carrier III. Trafficability of lunar microrovers (part 3). Technical report TR96–01, Lunar Geotechnical Institute, 1996.

[39] W. D. Carrier III, G. R. Olhoeft, and W. Mendell. Chapter 9: Physical properties of the lunar surface. In G. H. Heiken, D. T. Vaniman, and B. M. French, editors, *Lunar Sourcebook: a user's guide to the Moon*. Cambridge University Press, 1991.

[40] S. Cesar. Earning a social license to operate in mining: A case study from Peru. *Resources Policy*, 64:101482, 2019.

[41] M. A. Chavy-Macdonald, K. Oizumi, J. P. Kneib, and K. Aoyama. The cis-lunar ecosystem — a systems model and scenarios of the resource industry and its impact. *Acta Astronautica*, 188:545–558, 2021.

[42] B. Chehroudi, D. Talley, and V. Yang. Liquid propellants and combustion: Fundamentals and classifications. In R. Blockley and W. Shyy, editors, *Encyclopedia of Aerospace Engineering*, page 1–14. John Wiley and Sons, Ltd, 2010.

[43] V. A. Chobotov. *Orbital Mechanics 3rd Edition*. American Institute of Aeronautics and Astronautics, 2002.

[44] J. Cilliers, J. Rasera, and K. Hadler. Estimating the scale of space resource utilisation (SRU) operations to satisfy lunar oxygen demand. *Planetary and Space Science*, 180:104749, 2020.

[45] F. Cocks, P. Klenk, S. Watkins, W. Simmons, J. Cocks, E. Cocks, and J. Sussingham. Lunar ice: Adsorbed water on subsurface polar dust. *Icarus*, 160:386–397, 2002.

[46] C. Coetzee. Particle upscaling: Calibration and validation of the discrete element method. *Powder Technology*, 344:487–503, 2019.

[47] C. J. Coetzee. Calibration of the discrete element method. *Powder Technology*, 310:104–142, 2017.

[48] A. Colaprete. Volatiles Investigating Polar Exploration Rover (VIPER). 2021.

[49] J. E. Colwell, S. Batiste, M. Horányi, S. Robertson, and S. Sture. Lunar surface: Dust dynamics and regolith mechanics. *Reviews of Geophysics*, 45, 2007.

[50] A. J. Cornah. Incremental improvement of grade control models using resource data. In *Proceedings of the Ninth International Mining Geology Conference, The Australasian Institute of Mining and Metallurgy*, page 387–395, Adelaide, SA, 2014.

[51] R. M. Cox. Planning a lunar mine to recover hydrous ore deposits. In *Proceedings of the Eighth International Conference on Engineering, Construction, Operation, and Business In Space*, page 162–169, 2002.

[52] J. Craft, J. Wilson, J. Chu, K. Zacny, and K. Davis. Percussive digging systems for robotic exploration and excavation of planetary and lunar regolith. In *Proceedings of the 2009 IEEE Aerospace conference, IEEE Conference Publications*, page 1–7, 2009.

[53] G. A. Craig, S. Saydam, and A. G. Dempster. Mining off-Earth minerals: A long-term play? In *Proceedings of A Southern African Silver Anniversary Meeting, 2014 SOMP*, Johannesburg, South Africa, 2014. Journal of the South African Institute if Mining and Metallurgy.

[54] I. A. Crawford. Lunar resources: A review. *Progress in Physical Geography*, 39(2):137–167, 2015.

[55] I. A. Crawford, K. H. Joy, and M. Anand. Chapter 25 - lunar exploration. In T. Spohn, D. Breuer, and T. V. Johnson, editors, *Encyclopedia of the Solar System (Third Edition)*, pages 555–579. Elsevier, Boston, 2014.

[56] S. Creech, J. Guidi, and D. Elburn. Artemis: An overview of NASA's activities to return humans to the Moon. In *2022 IEEE Aerospace Conference (AERO)*, pages 1–7, 2022.

[57] J. Cui, X. Hou, G. Wen, and Z. Liang. Thermal simulation of drilling into lunar rock simulant by discrete element method. *Acta Astronautica*, 160:378–387, 2019.

[58] K. Dagdelen. Open pit optimization-strategies for improving economics of mining projects through mine planning. In *Proceedings of the 17th International Mining Congress and Exhibition of Turkey*, page 117–121, 2001.

[59] J. Dallas. *Environmental Considerations of Space Resources Extraction*. Doctoral dissertation, The University of New South Wales, 2021.

[60] J. A. Dallas, S. Raval, J. P. Alvarez Gaitan, S. Saydam, and A. G. Dempster. The environmental impact of emissions from space launches: A comprehensive review. *Journal of Cleaner Production*, 255:120209, 2020.

[61] J. A. Dallas, S. Raval, J. P. A. Gaitan, S. Saydam, and A. G. Dempster. Mining beyond Earth for sustainable development: Will humanity benefit from resource extraction in outer space? *Acta Astronautica*, 167:181–188, 2020.

[62] P. Darling, editor. *SME mining engineering handbook*. SME, Englewood, Colorado, 3rd ed. edition, 2011.

[63] J. De Pue, G. Di Emidio, R. D. V. Flores, A. Bezuijen, and W. M. Cornelis. Calibration of DEM material parameters to simulate stress-strain behaviour of unsaturated soils during uniaxial compression. *Soil and Tillage Research*, 194, 2019.

[64] J. Decoto and P. Loerch. Technique for GEO RSO station keeping characterization and maneuver detection. In *Proceedings of the Advanced Maui Optical and Space Surveillance Technologies Conference*, AMOS, 2015.

[65] T. Degris, M. White, and R. S. Sutton. Off-policy actor-critic, 2012. arXiv preprint arXiv:1205.4839.

[66] H. Dehghani and M. Ataee-Pour. Determination of the effect of operating cost uncertainty on mining project evaluation. *Resources Policy*, 37:109–117, 2012.

[67] F. DeMeo and R. P. Binzel. Comets in the near-Earth object population. *Icarus*, 194(2):436–449, 2008.

[68] S. M. Derakhshani, D. L. Schott, and G. Lodewijks. Micro–macro properties of quartz sand: Experimental investigation and DEM simulation. *Powder Technology*, 269:127–138, 2015.

[69] G. F. Diaz Lankenau, K. Skonieczny, W. L. Whittaker, and D. S. Wettergreen. Effect of bucket-wheel scale on excavation forces and soil motion. *Journal of Terramechanics*, 47:341–348, 2012.

[70] R. Dimitrakopoulos. *Advances in applied strategic mine planning.* Springer, 2018.

[71] H. Q. Do, A. M. Aragón, and D. L. Schott. Automated discrete element method calibration using genetic and optimization algorithms. In *EPJ Web of conferences*, volume 140, page 15011. EDP Sciences, 2017.

[72] B. Donn and G. W. Sears. Planets and comets: Role of crystal growth in their formation. *Science*, 140(3572):1208–1211, 1963.

[73] F. V. Donzé. Impacts on cohesive frictional geomaterials: A DEM analysis applied to concrete. *European Journal of Environmental and Civil Engineering*, 12(7-8):967–985, 2008.

[74] S. Dorrington, N. Kinkaid, and J. Olsen. Trajectory design and economic analysis of asteroid mining missions to asteroid 2014 EK24. In *Proceedings of the Third International Future Mining Conference*, Sydney, Australia, 2015. Australasian Institute of Mining and Metallurgy.

[75] S. Dorrington and J. Olsen. Mining requirements for asteroid ore extraction. In *Proceedings of the 68th International Astronautical Congress*, Adelaide, Australia, 2017. International Astronautical Congress.

[76] C. Dreier. An improved cost analysis of the Apollo program. *Space Policy*, 60:101476, 2022.

[77] J. Drelich and J.-Y. Hwang. *Water in mineral processing.* SME, 2012.

[78] C. B. Dreyer, J. Sercel, L. Gertsch, A. Lampe, T. J. Canney, and A. Abbud-Madrid. Optical mining subscale testing. In *Proceedings of the 15th Biennial International Conference on Engineering Science and Operations in Challenging Environments, Earth and Space 2016*, Orlando, Florida, 2016. American Society of Civil Engineers.

[79] L. R. e Sousa, E. Vargas Jr, M. M. Fernandes, and R. Azevedo. *Innovative numerical modelling in geomechanics*. CRC Press, 2012.

[80] M. Efatmaneshnik and M. J. Ryan. A general framework for measuring system complexity. *Complexity*, 21:533–546, 2016.

[81] B. L. Ehlmann and C. S. Edwards. Mineralogy of the martian surface. *Annual Review of Earth and Planetary Sciences*, 42(1):291–315, 2014.

[82] M. Ehresmann, R. A. Gabrielli, G. Herdrich, and R. Laufer. Lunar based massdriver applications. *Acta Astronautica*, 134:189–196, 2017.

[83] B. Elevli. Open pit mine design and extraction sequencing by use of OR and AI concepts. *International Journal of Surface Mining and Reclamation*, 9:149–453, 1995.

[84] A. Ellery. Sustainable in-situ resource utilization on the Moon. *Planetary and Space Science*, 184:104870, 2020.

[85] E. A. Elsayed. *Reliability engineering*. John Wiley and Sons, 2012.

[86] N. Erarslan, Z. Z. Liang, and D. J. Williams. Experimental and numerical studies on determination of indirect tensile strength of rocks. *Rock Mechanics and Rock Engineering*, 45(5):739–751, 2012.

[87] O. Erdem, T. Güyagüler, and N. Demirel. Uncertainty assessment for the evaluation of net present value: a mining industry perspective. *The Journal of The Southern African Institute of Mining and Metallurgy*, 112:405–412, 2012.

[88] A. S. Erickson. Revisiting the U.S.-Soviet space race: Comparing two systems in their competition to land a man on the Moon. *Acta Astronautica*, 148:376–384, 2018.

[89] E. Ethridge and W. Kaukler. Microwave extraction of water from lunar regolith simulant. In *Proceedings of Space Technology and Applications International Forum – STAIF 2007*. American Institute of Physics, 2007.

[90] E. Ethridge and W. Kaukler. Microwave processing of planetary surfaces for the extraction of volatiles. In *Proceedings of the 49th AIAA Aerospace Sciences Meeting including the New Horizons Forum and Aerospace Exposition*, Orlando, Florida, 2011. American Institute of Aeronautics and Astronautics.

[91] European Space Agency. ESA space resources strategy. 2019.

[92] R. Feistel and W. Wagner. Sublimation pressure and sublimation enthalpy of H_2O ice Ih between 0 and 273.16 K. *Geochimica et Cosmochimica Acta*, 71:36–45, 2007.

[93] T. Fernholz. Rocket billionaires : Elon Musk, Jeff Bezos and the new space race, 2018.

[94] Y. R. Fernández, D. C. Jewitt, and S. S. Sheppard. Albedos of asteroids in comet-like orbits. *The Astronomical Journal*, 130(1):308–318, 2005.

[95] K. E. Fishbaugh, F. Poulet, V. Chevrier, Y. Langevin, and J. P. Bibring. On the origin of gypsum in the Mars north polar region. *Journal of Geophysical Research: Planets*, 112, 2007.

[96] E. A. Fisher, P. G. Lucey, M. Lemelin, B. T. Greenhagen, M. A. Siegler, E. Mazarico, O. Aharonson, J.-P. Williams, P. O. Hayne, G. A. Neumann, et al. Evidence for surface water ice in the lunar polar regions using reflectance measurements from the Lunar Orbiter Laser Altimeter and temperature measurements from the Diviner Lunar Radiometer Experiment. *Icarus*, 292:74–85, 2017.

[97] F. F. Foxborough, P. King, and E. J. Pedroncelli. Tests on the cutting performance of a continuous miner. *Journal of the Southern African Institute of Mining and Metallurgy*, 81(1):9–25, 1981.

[98] V. François-Lavet, P. Henderson, R. Islam, M. G. Bellemare, and J. Pineau. An introduction to deep reinforcement learning, foundations and trends in machine learning, 2018.

[99] D. D. Frey, E. Jahangir, and F. Engelhardt. Computing the information content of decoupled designs. *Research in Engineering Design*, 12:90–102, 2000.

[100] J. Gao, X. Hou, and L. Wang. Solar power satellites research in China. *Online Journal of Space Communication*, 9(16):6, 2021.

[101] K. Gao, L. Wang, C. Du, J. Li, and J. Dong. Research on the effect of dip angle in mining direction on drum loading performance: a discrete element method. *The International Journal of Advanced Manufacturing Technology*, 89(5):2323–2334, 2017.

[102] T. V. Garza-Cruz, M. Pierce, and P. K. Kaiser. Use of 3DEC to study spalling and deformation associated with tunnelling at depth. In *Proceedings of the Seventh International Conference on Deep and High Stress Mining, Australian Centre for Geomechanics*, page 421–434, Perth, 2014.

[103] G. Genta. Private space exploration: A new way for starting a spacefaring society? *Acta Astronautica*, 104:480–486, 2014.

[104] L. Gertsch, R. Gustafson, and R. Gertsch. Effect of water ice content on excavatability of lunar regolith. In *Proceedings of the AIP Conference*, page 1093–1100, AIP, 2006.

[105] L. S. Gertsch and R. E. Gertsch. Surface mine design and planning for lunar regolith production. In *AIP Conference Proceedings*, page 1108–1115. American Institute of Physics, 2003.

[106] W. F. Giauque and J. W. Stout. The entropy of water and the third law of thermodynamics. The heat capacity of ice from 15 to 273° k. *Journal of the American Chemical Society*, 58(7):1144–1150, 1936.

[107] J. Gibb. Lightweight flexible space solar arrays, past, present and future. In *Proceedings of 7th World Conference on Photovoltaic Energy Conversion*, Waikoloa Village, HI, USA, 2018. WCPEC.

[108] L. Glasser. Water, water, everywhere: Phase diagrams of ordinary water substance. *Journal of Chemical Education*, 81(3), 2004.

[109] N. Goswami. *Scramble for the skies : the great power competition to control the resources of outer space.* Lexington Books, Lanham, 2020.

[110] A. Grabowski and M. Nitka. 3D DEM simulations of basic geotechnical tests with early detection of shear localization. *Studia Geotechnica et Mechanica*, 43(1):48–64, 2021.

[111] T. L. Grove and M. J. Krawczynski. Lunar mare volcanism: where did the magmas come from? *Elements*, 5(1):29–34, 2009.

[112] M. Gul and M. F. Ak. A comparative outline for quantifying risk ratings in occupational health and safety risk assessment. *Journal of Cleaner Production*, 196:653–664, 2018.

[113] A. Gupta. *Mineral processing design and operation : an introduction.* Elsevier, Amsterdam ; Boston, 1st ed. edition, 2006.

[114] K. Hadler, D. J. P. Martin, J. Carpenter, J. J. Cilliers, A. Morse, S. Starr, J. N. Rasera, K. Seweryn, P. Reiss, and A. Meurisse. A universal framework for space resource utilisation (SRU). *Planetary and Space Science*, 182:104811, 2020.

[115] G. E. Halkos and A. S. Tsirivis. Effective energy commodity risk management: Econometric modeling of price volatility. *Economic Analysis and Policy*, 63:234–250, 2019.

[116] B. Hall. Cut-off grades and optimising the strategic mine plan. *Australasian Institute of Mining and Metallurgy*, 2014.

[117] E. Hand. Moon mission tackles water question. *Nature*, 459:758–759, 2009.

[118] M. A. Haque, E. Topal, and E. Lilford. Evaluation of a mining project under the joint effect of commodity price and exchange rate uncertainties using real options valuation. *The Engineering Economist*, 62:231–253, 2017.

[119] A. W. Harris, L. Drube, L. A. McFadden, and R. P. Binzel. Chapter 27 - Near-Earth Objects. In *Encyclopedia of the Solar System*, pages 603–623. Elsevier, 2014.

[120] P. O. Hayne, A. Hendrix, E. Sefton-Nash, M. A. Siegler, P. G. Lucey, K. D. Retherford, J.-P. Williams, B. T. Greenhagen, and D. A. Paige. Evidence for exposed water ice in the Moon's south polar regions from lunar reconnaissance orbiter ultraviolet albedo and temperature measurements. *Icarus*, 255:58–69, 2015.

[121] B. Hemingway, R. A. Robie, and W. H. Wilson. Specific heats of lunar soils, basalt, and breccias from the Apollo 14, 15, and 16 landing sites, between 90 and 350°K. *Proceeedings of the Fourth Lunar Science Conference*, Supplement 4:2481–2487, 1973.

[122] A. Hill, A. Raffin, E. Maximilian, A. Gleave, A. Kanervisto, R. Traore, P. Dhariwal, C. Hesse, O. Klimov, A. Nichol, M. Plappert, A. Radford, J. Schulman, S. Sidor, and Y. Wu. Stable baselines, 2018.

[123] G. R. Hintz. *Orbital Mechanics and Astrodynamics Techniques and Tools for Space Missions*. Springer International Publishing, Switzerland, 2015.

[124] M. Hristakeva and D. Shrestha. Different approaches to solve the 0/1 knapsack problem. In *Proceedings of The Midwest Instruction and Computing Symposium*, 2005.

[125] M. G. Huang, P. L. Chang, and Y. C. Chou. Demand forecasting and smoothing capacity planning for products with high random demand volatility. *International Journal of Production Research*, 46(12):3223–3239, 2008.

[126] H. Hughes. Some aspects of rock machining. page 205–211, 1972.

[127] ISRM. *The Complete ISRM Suggested Methods for Rock Characterization, Testing and Monitoring: 1974-2006*. International Society for Rock Mechanics, 2007.

[128] Itasca Consulting Group. PFC - particle flow code, 2018.

[129] R. Jia, Y. Lv, G. Wang, E. Carranza, Y. Chen, C. Wei, and Z. Zhang. A stacking methodology of machine learning for 3D geological modeling with geological-geophysical datasets, Laochang Sn camp, Gejiu (China). *Computers Geosciences*, 151(104754), 2021.

[130] M. Jiang, Z. Shen, and C. Thornton. Microscopic contact model of lunar regolith for high efficiency discrete element analyses. *Computers and Geotechnics*, 54:104–116, 2013.

[131] S. Jianlan. China emphasizes international cooperation in future lunar and deep space exploration. *Bull Chin Acad Sci*, 2:72–79, 2019.

[132] L. Johnson, J. Carroll, R. Estes, E. Lorenzini, B. Gilchrist, M. Martinez-Sanchez, J. Sanmartin, and I. Vas. Electrodynamic tethers for reboost of the International Space Station and spacecraft propulsion. In *Proceedings of the Space Programs and Technologies Conference*. American Intstitute of Aeronautics and Astronautics, 1997.

[133] L. L. Johnson and R. H. King. Measurement of force to excavate extraterrestrial regolith with a small bucket-wheel device. *Journal of Terramechanics*, 47:87–95, 2010.

[134] Joint Ore Reserves Committee. Australasian code for reporting of exploration results, mineral resources and ore reserves. *AusIMM, Melbourne*, 44:320, 2012.

[135] C. A. Jones, J. J. Klovstad, D. R. Komar, and E. L. Judd. Cost breakeven analysis of cis-lunar ISRU for propellant. In *Proceedings of the AIAA SciTech Forum*, San Diego, California, 2019. American Institute of Aeronautics and Astronautics.

[136] G. Just, K. Smith, K. Joy, and M. Roy. Parametric review of existing regolith excavation techniques for lunar in situ resource utilisation (ISRU) and recommendations for future excavation experiments. *Planetary and Space Science*, 180:104746, 2020.

[137] S. J. Kapurch, editor. *NASA systems engineering handbook*. Diane Publishing, 2010.

[138] N. B. Karlsson, L. Schmidt, and C. S. Hvidberg. Volume of martian midlatitude glaciers from radar observations and ice flow modeling. *Geophysical Research Letters*, 42:2627–2633, 2015.

[139] H. Kawamoto. Improved electrostatic shield for lunar dust entering into mechanical seals of equipment used for long-term lunar exploration. In *Proceedings of the 44th International Conference on Environmental Systems*, Tuscon, Arizona, 2014. International Conference on Environmental Systems.

[140] T. Kazerani, Z.-Y. Yang, and J. Zhao. A discrete element model for predicting shear strength and degradation of rock joint by using compressive and tensile test data. *Rock mechanics and rock engineering*, 45(5):695–709, 2012.

[141] S. Keller, P. Collopy, and P. Componation. What is wrong with space system cost models? A survey and assessment of cost estimating approaches. *Acta Astronautica*, 93:345–351, 2014.

[142] H. Kierulff. MIRR: A better measure. *Buisness Horizons*, 51:321–329, 2008.

[143] J. Kim and T. Wilhelm. What is a complex graph? *Physica A: Statistical Mechanics and its Applications*, 387:2637–2652, 2008.

[144] J. E. Kleinhenz and A. Paz. Case studies for lunar ISRU systems utilizing polar water. In *Proceedings of ASCEND 2020*, page 4042. 2020.

[145] J. L. Klosky, S. Sture, H. Y. Ko, and F. Barnes. Mechanical properties of JSC-1 lunar regolith simulant. In *Proceedings of Engineering, Construction, and Operations in Space V*, page 680–688, Albuquerque, New Mexico, 1996.

[146] D. Kornuta, A. Abbud-Madrid, J. Atkinson, J. Barr, G. Barnhard, D. Bienhoff, B. B, V. Clark, J. Cyrus, B. DeWitt, C. Dreyer, B. Finger, J. Goff, K. Ho, L. Kelsey, J. Keravala, B. Kutter, P. Metzger, L. Montgomery, P. Morrison, C. Neal, E. Otto, G. Roesler, J. Schier, B. Seifert, G. Sowers, P. Spudis, M. Sundahl, K. Zacny, and G. Zhu. *Commercial Lunar Propellant Architecture A collaborative Study of Lunar Propellant Production*. United Launch Alliance, 2018.

[147] D. Kornuta, A. Abbud-Madrid, J. Atkinson, J. Barr, G. Barnhard, D. Bienhoff, B. Blair, V. Clark, J. Cyrus, and B. DeWitt. Commercial lunar propellant architecture: a collaborative study of lunar propellant production. *Reach*, page 100026, 2019.

[148] S. J. Kortenkamp and G. W. Wetherill. Terrestrial planet and asteroid formation in the presence of giant planets: I. Relative velocities of planetesimals subject to Jupiter and Saturn perturbations. *Icarus*, 143(1):60–73, 1999.

[149] J. Kozicki, J. Tejchman, and H. B. Mühlhaus. Discrete simulations of a triaxial compression test for sand by DEM. *International Journal for Numerical and Analytical Methods in Geomechanics*, 38, 2014.

[150] N. Krayner and R. Katz. Experimental method for measuring simplicity in mechanical design. *Journal of Engineering Design*, 29:1–19, 2018.

[151] D. L. Kuck. The exploitation of space oases. In *Proceedings Princeton Conference on Space Manufacturing*. Space Studies Institute, 1995.

[152] O. Kulak, S. Cebi, and C. Kahraman. Applications of axiomatic design principles: A literature review. *Expert Systems with Applications*, 37(9):6705–6717, 2010.

[153] O. Kulak and C. Kahraman. Multi-attribute comparison of advanced manufacturing systems using fuzzy vs. crisp axiomatic design approach. *International Journal of Production Economics*, 95:415–424, 2005.

[154] E. Kulu. In-space economy in 2021—statistical overview and classification of commercial entities. In *72nd International Astronautical Congress (IAC 2021), Dubai, United Arab Emirates*, pages 25–29, 2021.

[155] A. Kumar. *Artificial Intelligence Algorithms for Real-Time Production Planning with Incoming New Information in Mining Complexes*. Doctoral dissertation, McGill University, 2020.

[156] A. Kumar and R. Dimitrakopoulos. Production scheduling in industrial mining complexes with incoming new information using tree search and deep reinforcement learning. *Applied Soft Computing*, 110(107644), 2021.

[157] C. Lagerkvist and A. Barucci. Asteroids: Distributions, morphologies, origins and evolution. *Surveys in Geophysics*, 13(2):165–208, 1992.

[158] D. R. Lammlein. Lunar seismicity and tectonics. *Physics of the Earth and Planetary Interiors*, 14:224–273, 1977.

[159] M. E. Landis, S. Byrne, J.-P. Combe, S. Marchi, J. Castillo-Rogez, H. G. Sizemore, N. Schörghofer, T. H. Prettyman, P. O. Hayne, C. A. Raymond, et al. Water vapor contribution to Ceres' exosphere from observed surface ice and postulated ice-exposing impacts. *Journal of Geophysical Research: Planets*, 124(1):61–75, 2019.

[160] J. E. Lane, P. T. Metzger, and R. A. Wilkinson. *A review of discrete element method (DEM) particle shapes and size distributions for lunar soil*. NASA Glenn Research Center, Cleveland, Ohio, 2010.

[161] K. Lane. *The economic definition of Ore, Cutoff grades in theory and practice*. Mining Journal Books Ltd, London, 1988.

[162] T. J. Lawrence. Nuclear-thermal-rocket propulsion systems. In C. Bruno, editor, *Nuclear space power and propulsion systems*, page 31–52. American Institute of Aeronautics and Astronautics, 2016.

[163] Y. LeCun, L. Bottou, Y. Bengio, and P. Haffner. Gradient-based learning applied to document recognition. In *Proceedings of the IEEE*, volume 86, page 2278–2324, 1998.

[164] Y. S. Lee, P. Nandwana, and W. Zhang. Dynamic simulation of powder packing structure for powder bed additive manufacturing. *The International Journal of Advanced Manufacturing Technology*, 96(1):1507–1520, 2018.

[165] A. Lele. *Asian space race: Rhetoric or reality?* Springer Science & Business Media, 2012.

[166] M. Leslie. Space tourism begins to take off. *Engineering*, 10:4–6, 2022.

[167] C. Li, C. Wang, Y. Wei, and Y. Lin. China's present and future lunar exploration program. *Science*, 365(6450):238–239, 2019.

[168] D. Li and L. N. Y. Wong. The brazilian disc test for rock mechanics applications: review and new insights. *Rock mechanics and rock engineering*, 46(2):269–287, 2013.

[169] J. Y. Li, S. P. Gong, X. Wang, and J. X. Li. Launch window for manned Moon to Earth trajectories. *Aircraft Engineering and Aerospace Technology*, 84(5):344–356, 2012.

[170] S. Li, R. Dimitrakopoulos, J. Scott, and D. Dunn. Quantification of geological uncertainty and risk using stochastic simulation and applications in the coal mining industry. In *Proceedings of Orebody and Strategic Mine Planning*, Perth, Australia, 2004.

[171] S. Li, P. G. Lucey, R. E. Milliken, P. O. Hayne, E. Fisher, J.-P. Williams, D. M. Hurley, and R. C. Elphic. Direct evidence of surface exposed water ice in the lunar polar regions. *Proceedings of the National Academy of Sciences*, 115(36):8907–8912, 2018.

[172] S. Liang and J. Wang. *Advanced remote sensing: terrestrial information extraction and applications.* Academic Press, 2019.

[173] P. Liashchynskyi and P. Liashchynskyi. Grid search, random search, genetic algorithm: A big comparison for NAS, 2019. arXiv preprint arXiv:1912.06059.

[174] J. F. Lindsay. *Lunar stratigraphy and sedimentology.* Elsevier Scientific, New York, 1976.

[175] D. Linne, G. Sanders, J. Kleinhenz, and L. Moore. Current NASA in-situ resource utilization (ISRU) strategic vision. In *Space Resources Roundtable and the Planetary & Terrestrial Mining and Sciences Symposium*, number GRC-E-DAA-TN69644, 2019.

[176] D. L. Linne, J. M. Schuler, L. Sibille, J. E. Kleinhenz, A. J. Colozza, H. J. Fincannon, S. R. Oleson, N. H. Suzuki, and L. Moore. Lunar production system for extracting oxygen from regolith. *Journal of Aerospace Engineering*, 34(4):04021043, 2021.

[177] F. Liu, S. Li, L. Zhang, C. Zhou, R. Ye, Y. Wang, and J. Lu. 3DCNN-DQN-RNN: A deep reinforcement learning framework for semantic parsing of large-scale 3D point clouds. In *Proceedings of the IEEE International Conference on Computer Vision*, page 5678–5687, 2017.

[178] T. Liu, C. Wei, L. Liang, J. Zhang, and Y. Zhao. Simulation and analysis of the lunar regolith sampling process based on the discrete element method. *Transactions of the Japan Society for Aeronautical and Space Sciences*, 57:309–316, 2014.

[179] D. Loizeau, C. Quantin-Nataf, J. Carter, J. Flahaut, P. Thollot, L. Lozac'h, and C. Millot. Quantifying widespread aqueous surface weathering on Mars: The plateaus south of coprates chasma. *Icarus*, 302:451–469, 2018.

[180] A. Long, M. Richards, and D. E. Hastings. On-orbit servicing: A new value proposition for satellite design and operation. *Journal of Spacecraft and Rockets*, 44(4):964–976, 2007.

[181] H. J. Luth and R. D. Wismer. Performance of plane soil cutting blades in sand. *Transactions of the ASAE*, 14:255–62, 1971.

[182] Luxembourg Space Agency. Opportunities for space resources utilization future markets and value chains. 2018.

[183] J. M. Lyneis. System dynamics for market forecasting and structural analysis. *System Dynamics Review: The Journal of the System Dynamics Society*, 16(1):3–25, 2000.

[184] A. López-Delgado, S. López-Andrés, I. Padilla, M. Alvarez, R. Galindo, and A. Vázquez. Dehydration of gypsum rock by solar energy: Preliminary study. *Geomaterials*, 4:82–91, 2014.

[185] A. K. Manshad, H. Jalalifar, and M. Aslannejad. Analysis of vertical, horizontal and deviated wellbores stability by analytical and numerical methods. *Journal of Petroleum Exploration and Production Technology*, 4:359–369, 2014.

[186] A. Marshall. *Principles of Economics. Palgrave Classics in Economics.* Palgrave Macmillan, London, 2013.

[187] L. Mascolo and A. Stoica. Electro-magnetic launchers on the Moon. In *Proceedings of the 2018 NASA/ESA Conference on Adaptive Hardware and Systems.* IEEE, 2018.

[188] G. L. Matloff. *Deep Space Probes: To the Outer Solar System and Beyond Second Edition.* Springer Praxis Publishing, Chichester, 2005.

[189] M. R. McLean and M. A. Addis. Wellbore stability analysis: A review of current methods of analysis and their field application. In *Proceedings of the IADC/SPE Drilling Conference*, Houston, Texas, 1990.

[190] C. Meagher, R. Dimitrakopoulos, and D. Avis. Optimized open pit mine design, pushbacks and the gap problem—a review. *Journal of Mining Science*, 50:508–526, 2014.

[191] A. Meurisse and J. Carpenter. Past, present and future rationale for space resource utilisation. *Planetary and Space Science*, 182:104853, 2020.

[192] L. Miller-Tait, L. Panalkis, and R. Poulin. UBC mining method selection. In *Proceeding of the Mine Planning and Equipment Selection Symposium*, page 163–168, 1995.

[193] R. Milliken, R. C. Ewing, W. Fischer, and J. Hurowitz. Wind blown sandstones cemented by sulfate and clay minerals in gale crater, Mars. *Geophysical Research Letters*, 41:1149–1154, 2014.

[194] I. Mitrofanov, M. Litvak, A. Sanin, R. Starr, D. Lisov, R. Kuzmin, A. Behar, W. Boynton, C. Hardgrove, and K. Harshman. Water and chlorine content in the martian soil along the first 1900 m of the curiosity rover traverse as estimated by the DAN instrument. *Journal of Geophysical Research: Planets*, 119:1579–1596, 2014.

[195] V. Mnih, A. Badia, M. Mirza, A. Graves, T. Lillicrap, T. Harley, D. Silver, and K. Kavukcuoglu. Asynchronous methods for deep reinforcement learning. In *Proceedings of The 33rd International Conference on Machine Learning, PMLR*, volume 48, pages 1928–1937, 2016.

[196] V. Mnih, K. Kavukcuoglu, D. Silver, A. Graves, I. Antonoglou, D. Wierstra, and M. Riedmiller. Playing atari with deep reinforcement learning, 2013. arXiv preprint arXiv:1312.5602.

[197] N. Morales, S. Seguel, A. Cáceres, E. Jélvez, and M. Alarcón. Incorporation of geometallurgical attributes and geological uncertainty into long-term open-pit mine planning. *Minerals*, 9:108, 2019.

[198] C. Morley, V. Snowden, and D. Day. Financial impact of resource/reserve uncertainty. *The Journal of The Southern African Institute of Mining and Metallurgy*, 99:299–302, 1999.

[199] A. Mowshowitz and M. Dehmer. Entropy and the complexity of graphs revisited. *Entropy*, 14:559–570, 2012.

[200] R. Mueller and P. Van Susante. A review of lunar regolith excavation robotic device prototypes. In *Proceedings of the AIAA SPACE 2011 Conference and Exposition*, page 7234, 2011.

[201] R. P. Mueller, R. E. Cox, T. Ebert, J. D. Smith, J. M. Schuler, and A. J. Nick. Regolith advanced surface systems operations robot (RASSOR). In *Proceedings of the 2013 IEEE Aerospace Conference*, page 1–12. IEEE, 2013.

[202] R. P. Mueller, J. D. Smith, J. M. Schuler, A. J. Nick, N. J. Gelino, K. W. Leucht, I. I. Townsend, and A. G. Dokos. Design of an excavation robot: regolith advanced surface systems operations robot (RASSOR) 2.0. In *ASCE Earth & Space Conference*, number STI NO. 25616, 2016.

[203] R. Munos, T. Stepleton, A. Harutyunyan, and M. G. Bellemare. Safe and efficient off-policy reinforcement learning. *Advances in Neural Information Processing Systems*, 29, 2016.

[204] A. Mwangi, Z. Jianhua, H. Gang, R. Kasomo, and M. Innocent. Ultimate pit limit optimization methods in open pit mines. *A Review, Journal of Mining Science*, 56:588–602, 2020.

[205] A. Myers. *Complex system reliability.* Springer, 2010.

[206] S. Müller. *Capital stock approximation with the perpetual inventory method: An upyear.* Institute for Employment Research, Nuremberg, Germany, 2017.

[207] M. Nachon, S. Clegg, N. Mangold, S. Schröder, L. Kah, G. Dromart, A. Ollila, J. Johnson, D. Oehler, and J. Bridges. Calcium sulfate veins characterized by Chem-Cam/Curiosity at Gale crater, Mars. *Journal of Geophysical Research: Planets*, 119, 2014.

[208] T. Nakamura and C. Senior. Solar thermal power for lunar materials processing. *Journal of Aerospace Engineering*, 21:91–101, 2008.

[209] H. Nakashima, Y. Shioji, K. Tateyama, S. Aoki, H. Kanamori, and T. Yokoyama. Specific cutting resistance of lunar regolith simulant under low gravity conditions. *Journal of Space Engineering*, 1:58–68, 2008.

[210] S. Narvekar, B. Peng, M. Leonetti, J. Sinapov, M. E. Taylor, and P. Stone. Curriculum learning for reinforcement learning domains: A framework and survey. *Journal of Machine Learning Research*, 21:1–50, 2020.

[211] P. L. Nelson. *Space Capitalism : How Humans will Colonize Planets, Moons, and Asteroids.* Palgrave studies in classical liberalism. Springer International Publishing : Imprint: Palgrave Macmillan, Cham, 1st ed 2018. edition, 2018.

[212] D. E. Nicholas. *Method Selection-A Numerical Approach, Design and operation of caving and sublevel stoping mines.* AIME, 1981.

[213] D. E. Nicholas. *Selection procedure, Mining engineering handbook, Hartman H*. SME, New York, 1993.

[214] N. Nikolov, J. Kirschner, F. Berkenkamp, and A. Krause. Information-directed exploration for deep reinforcement learning, 2018. arXiv preprint arXiv:1812.07544.

[215] J. J. Y. Ofori and D. R. Ofori. Earning a social license to operate: Perspectives of mining communities in Ghana. *The Extractive Industries and Society*, 6(2):531–541, 2019.

[216] M. Owusu-Tweneboah, V. Temeng, and K. Awuah-Offei. Agent-based optimization for truck dispatching in open-pit mines. In *Proceedings of the 2019 SME Annual Conference and Expo and CMA 121st National Western Mining Conference*, Denver, CO, 2019. Society for Mining, Metallurgy and Exploration (SME).

[217] T. O'Callaghan and G. Graetz. *Mining in the Asia-Pacific : Risks, Challenges and Opportunities*. The Political Economy of the Asia Pacific. Springer International Publishing, Cham, 2017.

[218] D. A. Paige, M. A. Siegler, J. A. Zhang, P. O. Hayne, E. J. Foote, K. A. Bennet, A. R. Vasavada, B. T. Greenhagen, J. T. Schofield, D. J. McCleese, M. C. Foote, E. DeJong, B. G. Bills, W. Hartford, B. C. Murray, C. C. Allen, K. Snook, L. A. Soderblom, S. Calcutt, F. W. Taylor, N. E. Bowles, J. L. Bandfield, R. Elphic, R. Ghent, T. D. Glotch, M. B. Wyatt, and P. G. Lucey. Diviner lunar radiometer observations of cold traps in the Moon's south polar region. *Science*, 330:479–482, 2010.

[219] G. J. Park. *Analytic methods for design practice*. Springer Science and Business Media, 2007.

[220] T. M. Pelech, A. Demptster, and S. Saydam. Developing the case for mining resources on the Moon. In *Proceedings of the Future Mining 2019*, AusIMM, Sydney, 2019.

[221] T. M. Pelech, G. Roesler, and S. Saydam. Technical evaluation of off-Earth ice mining scenarios through an opportunity cost approach. *Acta Astronautica*, 162:388–404, 2019.

[222] T. M. Pelech, L. Sibille, A. Dempster, and S. Saydam. A framework for off-Earth mining method selection. *Acta Astronautica*, 181:552–568, 2021.

[223] J. N. Pelton. Space-based solar power satellite systems. In *Space 2.0*, pages 103–114. Springer, 2019.

[224] M. Peplow. Deep impact: sifting through the debris. *Nature*, 436(7048), 2005.

[225] C. Pitcher, N. Kömle, O. Leibniz, O. Morales-Calderon, Y. Gao, and L. Richter. Investigation of the properties of icy lunar polar regolith simulants. *Advances in Space Research*, 57:1197–1208, 2016.

[226] J. J. Plaut, A. Safaeinili, J. Holt, R. J. Phillips, J. Head, R. Seu, N. E. Putzig, and A. Frigeri. Radar evidence for ice in lobate debris aprons in the mid-northern latitudes of Mars. *Geophysical Research Letters*, 36, 2009.

[227] A. R. Poppe, M. Piquette, A. Likhanskii, and M. Horányi. The effect of surface topography on the lunar photoelectron sheath and electrostatic dust transport. *Icarus*, 221:135–146, 2012.

[228] R. Portelas, C. Colas, L. Weng, K. Hofmann, and P. Y. Oudeyer. Automatic curriculum learning for deep RL: A short survey, 2020. arXiv preprint arXiv:2003.04664.

[229] D. O. Potyondy and P. A. Cundall. A bonded-particle model for rock. *International Journal of Rock Mechanics and Mining Sciences*, 41(8):1329–1364, 2004.

[230] F. Poulet, J. Carter, J. Bishop, D. Loizeau, and S. Murchie. Mineral abundances at the final four curiosity study sites and implications for their formation. *Icarus*, 231:65–76, 2014.

[231] A. Probst, G. González Peytaví, B. Eissfeller, and R. Förstner. Mission concept selection for an asteroid mining mission. *Aircraft Engineering and Aerospace Technology: An International Journal*, 88(3):458–470, 2016.

[232] A. Puzrin. *Constitutive Modelling in Geomechanics : Introduction.* Springer, Berlin, 2012.

[233] D. Rapp. *Use of Extraterrestrial Resources for Human Space Missions to Moon or Mars.* Astronautical Engineering. Springer International Publishing : Imprint: Springer, Cham, 2nd ed 2018. edition, 2018.

[234] E. Rauch, D. T. Matt, and P. Dallasega. Application of axiomatic design in manufacturing system design: a literature review. *Procedia CIRP*, 53:1–7, 2016.

[235] P. M. Reiß. *In-Situ Thermal Extraction of Volatiles from Lunar Regolith.* Doctoral dissertation, Technische Universität München, 2018.

[236] Research Technology Services. *Katana.* UNSW, Sydney, 2021.

[237] J. R. Rinderle and N. P. Suh. Measures of functional coupling in design. *Journal of Engineering for Industry*, 104(4):383–388, 1982.

[238] G. Roesler. Mass estimate for a lunar resource launcher based on existing terrestrial electromagnetic launcher. *Machines*, 2013(1):50–62, 2013.

[239] M. E. Rossi. *Mineral Resource Estimation.* Springer Netherlands : Imprint: Springer, Dordrecht, 2014.

[240] L. Rubanenko, J. Venkatraman, and D. A. Paige. Thick ice deposits in shallow simple craters on the Moon and mercury. *Nature Geoscience*, 12(8):597–601, 2019.

[241] G. Ryder. Lunar samples, lunar accretion and the early bombardment of the Moon. *Eos, Transactions American Geophysical Union*, 71(10):313–323, 1990.

[242] K. Sacksteder and G. Sanders. In-situ resource utilization for lunar and Mars exploration. In *Proceedings of the 45th AIAA Aerospace Sciences Meeting and Exhibit*, page 345, 2007.

[243] B. Samaniego, E. Carla, L. O'Neill, and M. Nestoridi. High specific energy lithium sulfur cell for space application. In *E3S Web of Conferences 16*. ESPC 2016, 2017.

[244] F. Samimi Namin, K. Shahriar, M. Ataee-pour, and H. Dehghani. A new model for mining method selection of mineral deposit based on fuzzy decision making. *The Journal of The Southern African Institute of Mining and Metallurgy*, 108:385–395, 2008.

[245] G. Sanders. NASA lunar ISRU strategy. In *"What next for space resource utilisation?" workshop*, number JSC-E-DAA-TN73162, 2019.

[246] G. Sanders and J. Kleinhenz. In situ resource utilization (ISRU) envisioned future priorities. In *Luxembourg Space Week*, 2022.

[247] H. Satish, J. Ouellet, V. Raghavan, and P. Radziszewski. Investigating microwave assisted rock breakage for possible space mining applications. *Mining technology*, 115(1):34–40, 2006.

[248] S. J. Sawaryn, P. Bustin, M. G. Cain, I. A. Crawford, S. Lim, A. Linossier, and D. J. Smith. Lunar drilling-challenges and opportunities. In *Proceedings of the SPE Annual Technical Conference and Exhibition*. Society of Petroleum Engineers, 2018.

[249] S. Saydam, R. Mitra, and C. Russell. A four dimensional interactive learning system approach to mining engineering education. In *Proceedings of the Second International Future Mining Conference*, page 279–286, 2011.

[250] M. A. Sayeed, K. Suzuki, and M. M. Rahman. Strength and deformation characteristics of granular materials under extremely low to high confining pressures in triaxial compression. *International Journal of Civil and Environmental Engineering*, 11(4), 2011.

[251] T. Schaul, J. Quan, I. Antonoglou, and D. Silver. Prioritized experience replay, 2015. arXiv preprint arXiv:1511.05952.

[252] L. Scholtès and F.-V. Donzé. A DEM model for soft and hard rocks: role of grain interlocking on strength. *Journal of the Mechanics and Physics of Solids*, 61(2):352–369, 2013.

[253] J. Schrittwieser, T. Hubert, A. Mandhane, M. Barekatain, I. Antonoglou, and D. Silver. Online and offline reinforcement learning by planning with a learned model. In *Proceedings of the 35th Conference on Neural Information Processing Systems (NeurIPS 2021)*, 2021.

[254] D. Schrunk, B. Sharpe, B. L. Cooper, and M. Thangavelu. *The Moon: Resources, future development and settlement.* Springer Science & Business Media, 2007.

[255] J. Schulman, S. Levine, P. Abbeel, M. Jordan, and P. Moritz. Trust region policy optimization. In *Proceedings of the 32nd International Conference on Machine Learning, PMLR*, volume 37, page 1889–1897, 2015.

[256] E. Seedhouse. *Martian Outpost The Challenges of Establishing a Human Settlement on Mars.* Chichester, Praxis Publishing, 2009.

[257] T. Sgobba. *Space Safety and Human Performance.* Butterworth-Heinemann, 2017.

[258] A. Shaheen and A. Sleit. Comparing between different approaches to solve the 0/1 knapsack problem. *International Journal of Computer Science and Network Security*, 16:1, 2016.

[259] R. Shishko, R. Fradet, S. Do, S. Saydam, C. Tapia-Cortez, A. G. Dempster, and J. Coulton. Mars colony in situ resource utilization: An integrated architecture and economics model. *Acta Astronautica*, 138:53–67, 2017.

[260] L. Sibille and J. Dominguez. Joule-heated molten regolith electrolysis reactor concepts for oxygen and metals production on the Moon and Mars. In *50th AIAA Aerospace Sciences Meeting including the New Horizons Forum and Aerospace Exposition*, page 639, 2012.

[261] D. Silver, G. Lever, N. Heess, T. Degris, D. Wierstra, and M. Riedmiller. Deterministic policy gradient algorithms. *Proceedings of the 31st International Conference on Machine Learning, PMLR*, 32(1):387–395, 2014.

[262] G. Singh, S. Balaji, J. J. Shah, D. Corman, R. Howard, R. Mattikalli, and D. Stuart. Evaluation of network measures as complexity metrics. In *Proceedings of the*

ASME 2012 International Design Engineering Technical Conferences and Computers and Information in Engineering Conference, page 1065–1076. American Society of Mechanical Engineers, 2012.

[263] K. Skonieczny. *Lightweight Robotic Excavation*. Doctoral dissertation, Carnegie Mellon University, 2013.

[264] K. Skonieczny, M. Delaney, D. S. Wettergreen, and W. L. Whittaker. Productive lightweight robotic excavation for the Moon and Mars. *Journal of Aerospace Engineering*, 27:04014002, 2013.

[265] K. Skonieczny, D. Wettergreen, and W. R. Whittaker. Advantages of continuous excavation in lightweight planetary robotic operations. *The International Journal of Robotics Research*, 35:1121–1139, 2016.

[266] E. N. Slyuta. Physical and mechanical properties of the lunar soil (a review). *Solar System Research*, 48:330–353, 2014.

[267] V. Šmilauer. *Cohesive particle model using discrete element method on the Yade platform*. Doctoral dissertation, Czech Technical University, 2010.

[268] V. Šmilauer, V. Angelidakis, E. Catalano, R. Caulk, B. Chareyre, W. Chèvremont, S. Dorofeenko, J. Duriez, N. Dyck, J. Eliáš, B. Er, A. Eulitz, A. Gladky, N. Guo, C. Jakob, F. Kneib, J. Kozicki, D. Marzougui, R. Maurin, C. Modenese, G. Pekmezi, L. Scholtès, L. Sibille, J. Stránsknský, T. Sweijen, K. Thoeni, and C. Yuan. The YADE Project, 2021.

[269] J. D. Smith, R. P. Mueller, A. J. Nick, and B. C. Buckles. RASSOR excavator for ISRU lunar mining. In *Proceedings of the Space Resources Roundtable*, Golden, Colorado, 2019.

[270] M. Smith, D. Craig, N. Herrmann, E. Mahoney, J. Krezel, N. McIntyre, and K. Goodliff. The Artemis Program: an overview of NASA's activities to return humans to the Moon. In *2020 IEEE Aerospace Conference*, pages 1–10. IEEE, 2020.

[271] L. A. Soderblom, T. L. Becker, G. Bennett, D. C. Boice, D. T. Britt, R. H. Brown, B. J. Buratti, C. Isbell, B. Giese, T. Hare, M. D. Hicks, E. Howington-Kraus, R. L. Kirk, M. Lee, R. M. Nelson, J. Oberst, T. C. Owen, M. D. Rayman, B. R. Sandel, S. A. Stern, N. Thomas, and R. V. Yelle. Observations of comet 19P/Borrelly by the Miniature Integrated Camera and Spectrometer aboard Deep Space 1. *Science*, 296(5570):1087–1091, 2002.

[272] M. J. Sonter. The technical and economic feasibility of mining the near-Earth asteroids. *Acta Astronautica*, 41:637–647, 1997.

[273] G. F. Sowers and C. B. Dreyer. Ice mining in lunar permanently shadowed regions. *New Space*, 7(4):235–244, 2019.

[274] U. Sruthi and P. S. Kumar. Volcanism on farside of the Moon: New evidence from antoniadi in South Pole Aitken basin. *Icarus*, 242:249–268, 2014.

[275] L. Starukhina. Water on the Moon: What is derived from the observations. In V. ed, editor, *Moon: Prospective Energy and Material Resources*, page 56–70. Berlin, Springer Berlin Heidelberg, 2012.

[276] H. Steinhaus. *Mathematical Snapshots.* Dover, New York, 3rd edition, 1999.

[277] B. D. Stewart, E. Pierazzo, D. B. Goldstein, P. L. Varghese, and L. M. Trafton. Simulations of a comet impact on the Moon and associated ice deposition in polar cold traps. *Icarus*, 215(1):1–16, 2011.

[278] D. Stuart and R. Mattikalli. *META II complexity and adaptability.* Boeing Co, St Louis, MO, 2011.

[279] O. Su and N. A. Akcin. Numerical simulation of rock cutting using the discrete element method. *International journal of rock mechanics and mining sciences*, 48(3):434–442, 2011.

[280] N. Suh. *The principles of design.* Oxford University Press on Demand, 1990.

[281] N. P. Suh. Axiomatic Design of Mechanical Systems. *Journal of Mechanical Design*, 117(B):2–10, 06 1995.

[282] N. P. Suh. Axiomatic design theory for systems. *Research in engineering design*, 10(4):189–209, 1998.

[283] N. P. Suh. A theory of complexity, periodicity and the design axioms. *Research in Engineering Design*, 11(2):116–132, 1999.

[284] T. A. Sullivan, E. Koenig, C. W. Knudsen, and M. A. Gibson. Pneumatic conveying of materials at partial gravity. *Journal of Aerospace Engineering*, 7:199–208, 1994.

[285] J. D. Summers and J. J. Shah. Mechanical engineering design complexity metrics: size, coupling, and solvability. *Journal of Mechanical Design*, 132:021004, 2010.

[286] R. S. Sutton. Reinforcement learning architectures. *Proceedings ISKIT*, 92, 1992.

[287] R. S. Sutton and A. G. Barto. *Reinforcement Learning : An Introduction*. MIT Press, 1998.

[288] L. P. Suwal and R. Kuwano. Statically and dynamically measured poisson's ratio of granular soils on triaxial laboratory specimens. *Geotechnical Testing Journal*, 36(4):493–505, 2013.

[289] W. Swick and J. Perumpral. A model for predicting soil-tool interaction. *Journal of Terramechanics*, 25:43–56, 1988.

[290] V. Tang and V. Salminen. Towards a theory of complicatedness: framework for complex systems analysis and design. In *Proceedings of the 13th International Conference on Engineering Design*. Professional Engineering for The Institution of Mechanical Engineers, 2001.

[291] D. A. Tito, G. Anderson, J. P. Carrico, J. Clark, B. Finger, G. A. Lantz, M. E. Loucks, T. MacCallum, J. Poynter, T. H. Squire, and S. P. Worden. Feasibility analysis for a manned Mars free-return mission in 2018. In *Proceedings of the Aerospace Conference, 2013 IEEE*. IEEE, 2013.

[292] T. F. Torries. NPV or IRR? Why not both? In *Proceedings of SME Annual Meeting 1997*, Denver, Colorado, 1997. Society for Mining, Metallurgy, and Exploration.

[293] V. T. Tran, F.-V. Donzé, and P. Marin. A discrete element model of concrete under high triaxial loading. *Cement and Concrete Composites*, 33(9):936–948, 2011.

[294] A. Tubis, S. Werbińska-Wojciechowska, and A. Wroblewski. Risk assessment methods in mining industry—a systematic review. *Applied Sciences*, 10(15):5172, 2020.

[295] M. Ucgul, J. M. Fielke, and C. Saunders. Three-dimensional discrete element modelling of tillage: Determination of a suitable contact model and parameters for a cohesionless soil. *Biosystems Engineering*, 121:105–117, 2014.

[296] A. Van As and R. G. Jeffrey. Hydraulic fracturing as a cave inducement technique at northparkes mines. *Proceedings of the MassMin Conference*, pages 165–172, 2000.

[297] A. Vernile. *The rise of private actors in the Space Sector*. Springer, 2018.

[298] H.-J. Volk. Wirtgen drives the development of surface mining. *Procedia Engineering*, 138:30–39, 2016.

[299] C.-C. Vu, O. Plé, J. Weiss, and D. Amitrano. Revisiting the concept of characteristic compressive strength of concrete. *Construction and Building Materials*, 263:120126, 2020.

[300] H. Wang. Underground mine planning optimization process to improve values and reduce risks. In *Mining Goes Digital*, page 335–343. CRC Press, 2019.

[301] J. X. Wang, Z. Kurth-Nelson, D. Tirumala, H. Soyer, J. Z. Leibo, R. Munos, C. Blundell, D. Kumaran, and M. Botvinick. Learning to reinforcement learn, 2016. arXiv preprint arXiv:1611.05763.

[302] X. E. Wang, J. Yang, Q. F. Liu, Y. M. Zhang, and C. Zhao. A comparative study of numerical modelling techniques for the fracture of brittle materials with specific reference to glass. *Engineering Structures*, 152:493–505, 2017.

[303] Y. Wang and F. Tonon. Calibration of a discrete element model for intact rock up to its peak strength. *International journal for numerical and analytical methods in geomechanics*, 34(5):447–469, 2010.

[304] Z. Wang, V. Bapst, N. Heess, V. Mnih, R. Munos, K. Kavukcuoglu, and N. de Freitas. Sample efficient actor-critic with experience replay, 2016. arXiv preprint arXiv:1611.01224.

[305] F. W. Wellmer, M. Dalheimer, and M. Wagner. *Economic Evaluations in Exploration Second Edition.* Springer-Verlag, Berlin, 2008.

[306] D. Wettergreen, S. Moreland, K. Skonieczny, D. Jonak, D. Kohanbash, and J. Teza. Design and field experimentation of a prototype lunar prospector. *The International Journal of Robotics Research*, 29:1550–1564, 2010.

[307] M. A. Wieczorek, B. P. Weiss, and S. T. Stewart. An impactor origin for lunar magnetic anomalies. *Science*, 335(6073):1212–1215, 2012.

[308] A. Wilkinson and A. DeGennaro. Digging and pushing lunar regolith: Classical soil mechanics and the forces needed for excavation and traction. *Journal of Terramechanics*, 44:133–152, 2007.

[309] P. D. Wooster, R. D. Braun, J. Ahn, and Z. R. Putnam. Trajectory options for human Mars missions. In *Proceedings of the AIAA/AAS Astrodynamics Specialist Conference and Exhibit*, Keystone, Colorado, 2006. American Institute of Aeronautics and Astronautics.

[310] R. Yarahmadi, R. Bagherpour, A. Khademian, L. M. O. Sousa, S. N. Almasi, and M. M. Esfahani. Determining the optimum cutting direction in granite quarries through experimental studies: a case study of a granite quarry. *Bulletin of Engineering Geology and the Environment*, 78(1):459–467, 2019.

[311] M. Yavuz. The application of the analytic hierarchy process (AHP) and Yager's method in underground mining method selection problem. *International Journal of Mining, Reclamation and Environment*, 29(6):453–475, 2015.

[312] K. Yazdi and E. Messerschmid. Analysis of parking orbits and transfer trajectories for mission design of cis-lunar space stations. *Acta Astronautica*, 55:759–771, 2004.

[313] X. Yingzhuo. China's planning for deep space exploration and lunar exploration before 2030. *Chin. J. Space Sci.*, 38(5):591–592, 2018.

[314] T. Yoshino, M. J. Walter, and T. Katsura. Core formation in planetesimals triggered by permeable flow. *Nature*, 422(6928), 2003.

[315] M. Zacharias, L. Gertsch, A. Abbud-Madrid, B. Blair, and K. Zacny. Real-world mining feasibility studies applied to asteroids, the Moon and Mars. In *Proceedings of the AIAA SPACE 2011 Conference and Exposition*, Long Beach, California, 2011. American Institute of Aeronautics and Astronautics.

[316] K. Zacny. Lunar drilling, excavation and mining in support of science, exploration, construction, and in situ resource utilization (ISRU). In V. Badescu, editor, *Moon: Prospective Energy and Material Resources*, page 235–265. Springer, 2012.

[317] K. Zacny, B. Betts, M. Hedlund, P. Long, M. Gramlich, K. Tura, P. Chu, A. Jacob, and A. Garcia. PlanetVac: Pneumatic regolith sampling system. In *Proceedings of the Aerospace Conference*, page 1–8. IEEE, 2014.

[318] K. Zacny, P. Chu, J. Craf, M. M. Cohen, W. W. James, and B. Hilscher. Asteroid mining. In *Proceedings of the AIAA SPACE Forum*, San Diego, California, 2013. American Institute of Aeronautics and Astronautics.

[319] K. Zacny, P. Chu, G. Paulsen, A. Avanesyan, J. Craft, and L. Osborne. Mobile In-Situ Water Extractor (MISWE) for Mars, Moon, and asteroids in-situ resource utilization. In *Proceedings of the AIAA SPACE 2012 Conference and Exposition*, Pasadena, California, 2014. American Institute of Aeronautics and Astronautics.

[320] K. Zacny, K. Luczek, A. Paz, and M. Hedlund. Planetary Volatiles Extractor (PVEx for in situ resource utilisation (ISRU). In *Proceedings of the 15th Biennial ASCE Converence on Engineering, Science, Construction and Operations in Challenging Environments*, Pasadena, California, 2016. American Society of Civil Engineers.

[321] K. Zacny, G. Mungas, C. Mungas, D. Fisher, and M. Hedlund. Pneumatic excavator and regolith transport system for lunar ISRU and construction. In *Proceedings of the AIAA SPACE 2008 conference and exposition*, page 7824, 2008.

[322] K. Zacny, G. Paulsen, C. P. McKay, B. Glass, A. Dave, A. F. Davila, M. Marinova, B. Mellerowicz, J. Heldmann, C. Stoker, N. Cabrol, M. Hedlund, and J. Craft. Reaching 1m deep on Mars: The icebreaker drill. *Astrobiology*, 13(12), 2013.

[323] K. A. Zacny, M. Quayle, and G. Cooper. Enhancing cuttings removal with gas blasts while drilling on Mars. *Journal of Geophysical Research: Planets*, 110, 2005.

[324] Q. Zhang, Z. Han, M. Zhang, and J. Zhang. New model for predicting instantaneous cutting rate of axial-type roadheaders. *KSCE Journal of Civil Engineering*, 21(1):168–177, 2017.

[325] T. Zhao. Introduction to discrete element method. In *Coupled DEM-CFD Analyses of Landslide-Induced Debris Flows*. Springer, 2017.

[326] R. Zubrin. Moon direct: A new cost-effective plan for a lunar base. In *Proceedings of the AIAA SPACE Forum*, Orlando, Florida, 2018. American Institute of Aeronautics and Astronautics.